Assessment of atmospheric trace metals and water soluble ionic species at two regional background sites

A.D. Venter

20049544

Thesis submitted in fulfilment of the requirements for the degree *Philosophia Doctor* in Environmental Sciences at the Potchefstroom Campus of the North-West University

Promoter: Dr P.G. van Zyl

Co-promoter: Prof J.P. Beukes

November 2015

Gen1v1:Rev22v21

2Tim3v16-17

Acknowledgements

I wish to express my extreme gratitude to those who made the completion of this thesis possible:

- First and foremost, to Jesus Christ for the capacity, inspiration, grace and blessings received.
- My wife Marcell, thank you for your understanding and loving support.
- To my parents, Kobus and Rosemary, who have always inspired and supported me – the best role models.
- Dr Pieter van Zyl and Prof Paul Beukes for all the long hours of tutoring, reading and discussions.
- All my friends, family and colleagues for their support and encouragement.
- This research would not have been possible without the necessary funding and support from the Atmospheric Chemistry Research Group of the North-West University.
- The financial assistance of the National Research Foundation (NRF) towards this research is hereby acknowledged. Opinions expressed and conclusions arrived at, are those of the author and are not necessarily to be attributed to the NRF.

Preface

This thesis is submitted in article format, as allowed by the North-West University (NWU). This entails that articles are added into the thesis as they were published, submitted, or prepared for submission to the specific journals. Therefore the conventional "Results and discussions chapter" was replaced by the various articles. Separate background and motivation (Chapter 1), literature (Chapter 2), experimental (Chapter 3) and project evaluation chapters (Chapter 9) were included in the thesis, even though some of this information had already been summarised in the articles. This will result in some repetition of ideas/similar text in some of the chapters and articles. The fonts, numbering and layout of Chapters 4 – 8 (containing the articles) are also not consistent with the rest of the thesis, since they were added in the formats published, submitted, or prepared for submission as required by the journals.

Rationale for submitting thesis in article format

Currently it is a prerequisite for handing in a PhD at the NWU that one article be submitted to a journal. Many draft articles prepared by post-graduate students are never submitted to internationally accredited peer-reviewed journals. Therefore, the candidate decided to submit this PhD thesis in article format to ensure that the bulk of the work is published. At the time completing this thesis two articles had already been published, one accepted and two more prepared for submission to ISI-accredited journals. Therefore, the prerequisite of the NWU was exceeded.

Contextualising the articles in the overall storyline

The topic of this PhD was associated with atmospheric trace metals and water-soluble ionic species. Five articles are presented in this thesis, each focusing on a different aspect related to the topic. In the first two articles (Chapters 4 and 5), specific trace metals species, i.e. mercury and hexavalent chromium, which are of particular importance within the South African context were considered. Thereafter two articles on general trace metal concentrations (Chapter 6) and water soluble inorganic ionic concentrations (Chapter 7) are presented. In the last article (Chapter 8) trace metal and water soluble ionic concentrations, together with many other species/parameters in the plume of a typical South African braai is discussed as a case study.

Status of the articles:

- Article 1 (Statistical exploration of gaseous elemental mercury (GEM) measured at Cape Point from 2007 to 2011) was published in *Atmospheric Chemistry and Physics*, a journal of the European Geosciences Union. The article is presented as the final published version.
- Article 2 (Regional atmospheric Cr(VI) pollution from the Bushveld Complex, South Africa) was accepted (in press) in *Atmospheric Pollution Research*, an Elsevier journal. The article was formatted according to the journal's author guidelines.
- Article 3 (Measurement of atmospheric trace metals at a regional background site (Welgegund) in South Africa) was prepared for *Atmospheric Chemistry and Physics*, a journal of the European Geosciences Union. The article was formatted according to the journal's author guidelines.
- Article 4 (Measurement of atmospheric inorganic ionic species at Welgegund, South Africa) was prepared for *Atmospheric Chemistry and Physics*, a journal of the European Geosciences Union. The article was formatted according to the journal's author guidelines.
- Article 5 (Plume characterization of a typical South African braai) was published in the *South African Journal of Chemistry*. The article is presented as the final published version.

Other articles, to which the candidate contributed as co-author, published during the duration of this study, but not included for examination purposes are:

1. Vakkari, Petri Tiitta, Kerneels Jaars, Philip Croteau, Johan Paul Beukes, Miroslav Josipovic, Veli-Matti Kerminen, Markku Kulmala, **Andrew D. Venter**, Pieter G. van Zyl, Douglas R. Worsnop, and Lauri Laakso. Re-evaluating the contribution of sulfuric acid and the origin of organic compounds in atmospheric nanoparticle growth. Geophysical Research letters. 2015
2. Sundström, A.-M., Nikandrova, A., Atlaskina, K., Nieminen, T., Vakkari, V., Laakso, L., Beukes, J. P., Arola, A., Van Zyl, P. G., Josipovic, M., **Venter, A. D.**, Jaars, K., Pienaar, J. J., Piketh, S., Wiedensohler, A., Chiloane, E. K., De Leeuw,

G., and Kulmala, M. Characterization of satellite-based proxies for estimating nucleation mode particles over South Africa. Atmospheric Chemistry and Physics, 15, 4983–4996, 2015. doi:10.5194/acp-15-4983-2015

3. Jaars, K., Beukes, J.P., van Zyl, P.G., **Venter, A.D.**, Josipovic, M. Pienaar, J.J., Vakkari, V., Aaltonen, H., Laakso, H., Kulmala, M., Tiitta, P., Guenther A., Hellen, H., Laakso, L., Hakola, H., Ambient aromatic hydrocarbon measurements at Welgegund, South Africa. Atmospheric Chemistry and Physics 07/2014; 14:7075–7089
4. Vakkari, V., Kerminen, V-M., Beukes, J.P., Tiitta, P., van Zyl, P.G., Josipovic, M., **Venter, A.D.**, Jaars, K., Worsnop, D.R., Kulmala, M., Laakso, L., Rapid changes in biomass burning aerosols by atmospheric oxidation. Geophysical Research Letters 03/2014
5. Tiitta, P., Vakkari, V., Croteau, P., Beukes, J.P., van Zyl, P.G., Josipovic, M., **Venter, A.D.**, Jaars, K., Pienaar, J.J., Ng, N.L., Canagaratna, M.R., Jayne, J.T., Kerminen, V-M., Kokkola, H., Kulmala, M., Laaksonen, A., Worsnop, D.R., Laakso, L., Chemical composition, main sources and temporal variability of PM1 aerosols in southern African grassland. Atmospheric Chemistry & Physics 02/2014; 14(6):1909-1927
6. **Venter, A.D.**, Vakkari, V., Beukes, J.P., van Zyl, P.G., Laakso, H., Mabaso, D., Tiitta, P., Josipovic, M., Kulmala, M., Pienaar, J.J., Laakso, L., An air quality assessment in the industrialised western Bushveld Igneous Complex, South Africa, South African Journal of Science, 108, No 9/10, 2012

Book chapters to which the candidate contributed as co-author, published during the duration of this study, but not included for examination purposes are:

1. Beukes, J.P., **Venter, A.D.**, Josipovic, M., Van Zyl, P.G., Vakkari, V., Jaars, K., Dunn, M. and Laakso, L. Automated continuous air monitoring, In: Monitoring Of Air Pollutants – Sampling, Sample, Preparation And Analytical Techniques, editor P Forbes, Elsevier, 2015 (ISBN: 9780444635532)
2. Lauri Laakso, Johan Paul Beukes, Pieter Gideon Van Zyl, Jacobus Pienaar, Miroslav Josipovic, **Andrew Venter**, Kerneels Jaars, Ville Vakkari, Casper Labuschagne, Kgaugelo Chiloane, and Juha-Pekka Tuovinen. Ozone concentrations and their potential impacts on vegetation in southern Africa,

Developments in Environmental Science, Chapter 20, Vol. 13. Elsevier Ltd. 2013, http://dx.doi.org/10.1016/B978-0-08-098349-3.00020-7

Abstract

In this study, atmospheric trace metals and water soluble ionic species were investigated. Five research articles are presented. In the first two articles specific trace metals species, i.e. mercury and hexavalent chromium, which are of particular importance within the South African context, are considered. Thereafter two articles on general trace metal concentrations and water soluble inorganic ionic concentrations measured at a regional background site are presented. In the last article trace metal and water soluble ionic concentrations, together with many other species/parameters determined in the plume of a typical South African braai are discussed as a case study.

In article one, the continuous high-resolution gaseous elemental mercury (GEM) data from the Cape Point Global Atmosphere Watch (CPT GAW) station between 2007 and 2011 were evaluated with different statistical analysis techniques. GEM data were evaluated by cluster analysis and the results indicated that two clusters, separated at 0.904 ngm^{-3}, existed. The two-cluster solution was investigated by means of back-trajectory analysis to determine the air mass history. The net result indicated that not all low GEM concentrations are of marine origin, and similarly, not all high GEM concentrations have a terrestrial origin. Equations were developed by means of multi-linear regression (MLR) analysis that allowed for the estimation and/or prediction of atmospheric GEM concentrations from other atmospheric parameters measured at the CPT GAW station. These equations also provided insight into the relation and interaction of GEM with other atmospheric parameters. Both measured and MLR calculated data confirm a decline in GEM concentrations at CPT GAW over the period evaluated.

In article two, hexavalent chromium, Cr(VI), was investigated and the regional atmospheric pollution of Cr(VI) from the ferrochromium and other related industries located in the western Bushveld Complex (wBC) of South Africa was determined. Particulate matter was sampled for an entire calendar year at a regional background site, which is situated downwind of the wBC on the dominant anti-cyclonic recirculation route of air mass over the South African interior. Results indicated that

Cr(VI) concentrations in air masses that had passed over the regional background were below the detection limit of the analytical technique applied. However, Cr(VI) in air masses that had passed over the wBC were elevated and had a median concentration of 4.6 ngm^{-3}. The majority of Cr(VI) was found to be in the finer size fraction ($PM_{2.5}$), which could be explained by the properties of Cr(VI)-containing PM being emitted by the sources in the wBC and the atmospheric lifetimes of different PM size fractions. The results also indicated that it is possible that not only pyrometallurgical sources in the wBC, but also other combustion sources outside the wBC contributed to the observed atmospheric Cr(VI) concentrations.

In article three, aerosol sampling was performed at Welgegund in South Africa, which is a regionally representative background site. PM_1, $PM_{1-2.5}$ and $PM_{2.5-10}$ samples were collected for thirteen months and 32 atmospheric trace metal species were detected. Atmospheric Fe had the highest concentrations in all three size fractions, while Ca was the second most abundant species. Cr and Na concentrations were the third and fourth most abundant species respectively. Trace metal concentrations determined at Welgegund were compared to levels thereof in the wBC. Similar trace metals were detected and both indicated that Fe was the most abundant species. However, concentrations of trace metal species in the wBC were significantly higher compared to levels thereof at Welgegund. With the exception of Ni, none of the trace metals measured at Welgegund exceeded local and international standard limit values. No distinct seasonal pattern was observed in the $PM_{2.5-10}$ size fraction, while the PM_1 and $PM_{1-2.5}$ size fractions indicated elevated trace metal concentrations coinciding with the end of the dry season, which could partially be attributed to decreased wet removal and increases in wind generation of particulates. Principal Component Factor Analysis (PCFA) analysis was successfully applied and revealed three meaningful factors in the PM_1 size fraction, i.e. fly ash, pyrometallurgical-related and crustal. No meaningful factors were determined for the $PM_{1-2.5}$ and $PM_{2.5-10}$ size fractions. Pollution roses confirmed this impact of wind-blown dust on trace metal concentrations, while the influence of industrial activities was also substantiated.

In article four, PM_1, $PM_{1\text{-}2.5}$ and $PM_{2.5\text{-}10}$ samples were collected for thirteen months at Welgegund and analysed in order to determine the concentrations of the major inorganic ionic species. Results indicated that SO_4^{2-} concentrations in the PM_1 size fraction were significantly higher compared to the other species in all three size fractions. SO_4^{2-} and NH_4^+ dominated the PM_1 size fraction, while SO_4^{2-} and NO_3^- were the predominant species in the $PM_{1\text{-}2.5}$ and $PM_{2.5\text{-}10}$ size fractions. SO_4^{2-} had the highest contribution in the two smaller size fractions, while NO_3^- had the highest contribution in the $PM_{2.5\text{-}10}$ size fraction. SO_4^{2-} levels could be attributed to the impacts of aged air masses passing over source regions, while marine air masses were considered to be the major source of NO_3^-. The reaction of SO_4^{2-} with gas-phase NH_3 was considered to be the major source of NH_4^+ in the PM_1 size fraction. The PM at Welgegund was determined to be acidic, mainly due to excess concentrations of SO_4^{2-}. Comparison of Welgegund inorganic ion measurements to measurements thereof at Marikana indicated that the concentrations of almost all the inorganic ion species were higher at Marikana. At Welgegund PM_1 and $PM_{1\text{-}2.5}$ fractions revealed a seasonal pattern with higher inorganic ion concentrations measured from May – September. Higher concentrations could be attributed to decreased wet removal of these species, since these months coincide with the dry season in this part of South Africa. Increases in pollutants concentrations due to more pronounced inversion layers trapping pollutants near the surface, as well as increases household combustion and wild fires during these months were also considered to contribute to elevated levels of inorganic ions. Back trajectory analysis of each of the sampling months was also performed, which revealed higher concentrations of inorganic ionic species corresponding to air mass movements over source regions.

In article five, a case study, a comprehensive analysis of atmospheric gaseous and aerosol species within a plume originating from a typical South African braai (barbeque) at Welgegund was conducted. Five distinct phases were identified during the braai. The highest trace metal concentrations were associated with species typically present in ash. High Pb concentrations were detected. SO_4^{2-}, Ca^{2+} and Mg^{2+} were the dominant water-soluble species present in the aerosols. The largest number of organic aerosol compounds was in the$PM_{1\text{-}2.5}$ fraction, which also had the highest semi-quantified concentration. It was indicated that PM_{10} concentrations were problematic

during the meat grilling phase. From a climatic point of view, a relatively high single scattering albedo (ω_o) indicated a cooling aerosol direct effect, while periods with lower ω_o coincided with peak black carbon (BC) emissions. SO_2, NO_x and CO increased significantly, while O_3 did not notably change. Aromatic and alkane volatile organic compounds were determined, and high benzene levels were observed. The results indicated that a recreational braai does not pose significant health risks. However, the longer exposure periods that are experienced by occupational vendors will significantly increase health risks.

Keywords: Trace metals, gaseous elemental mercury, inorganic ions, hexavalent chromium, braai plume, Welgegund atmospheric measurement site

Table of Contents

List of Tables

Chapter 2

Chapter 3

Chapter 4

Chapter 6

Chapter 8

List of Figures

Chapter 2

Chapter 3

Chapter 4

Chapter 5

Chapter 6

Chapter 7

Chapter 8

Chapter 1

Project description and objectives

1.1 Introduction

In this chapter, the relevance of the current investigation in terms of air quality is briefly discussed. Chapter 1 also presents the scientific gap that was identified and the objectives that were set to address this gap.

1.1.1 Background and motivation

Accurate and complete emission inventories for atmospheric trace metals are required on regional and global scales for modellers and policy makers in order to assess the current level of environmental contamination by these pollutants, major emission sources, and the contribution of the atmospheric pathway to the contamination of terrestrial and aquatic environments (Pacyna & Pacyna, 2001). The presence of trace transition metal species in the atmosphere can be attributed to the emission of particulate matter (PM) into the atmosphere by anthropogenic activities, as well as from natural sources. Anthropogenic activities that lead to emission of trace metals are usually related to high temperature processes such as smelting, fuel combustion, or waste incineration (Galloway *et al.*, 1982). Stationary fossil fuel combustion, such as from coal, is considered to be a major source of chromium (Cr), mercury (Hg), manganese (Mn), antimony (Sb), selenium (Se), tin (Sn), and thallium (Tl), while oil combustion is a major source of nickel (Ni) and vanadium (V) emissions. Another major source of trace metals is ferrous and non-ferrous metal production that typically emits iron (Fe), Cr, Ni, Mn and V, while also being the largest source of atmospheric arsenic (As), cadmium (Cd), copper (Cu), indium (In), and zinc (Zn) (Pacyna & Pacyna, 2001). In such processes metals are mostly emitted in gaseous forms that rapidly condense on the surfaces of particles having a high surface area leading to their likely presence in relatively fine PM (typically with aerodynamic diameter <1 µm) (Galloway *et al.*, 1982). Trace metals in coarse particles (typically with aerodynamic diameter >1 µm) are mostly attributed to mechanical processes such as rock weathering, soil erosion,

volcanic eruptions, or bubble bursting (sea salt elements such as potassium (K), calcium (Ca), sodium (Na), chloride (Cl)). Coarse particles are deposited faster and have relatively short atmospheric lifetimes, while finer particles may attain lifetimes longer than six days under dry conditions with lower frequencies of wet deposition (Lawler *et al.*, 2009). Therefore, emissions from anthropogenic activities may have a significant influence on the atmospheric trace metal budget on a regional scale. At present, limited data exist for atmospheric trace metal concentrations in South Africa.

Trace metals emitted into the atmosphere can cause a variety of health-related and environmental problems; depending on the extent and time of exposure (Jacobson *et al.*, 2000). Certain trace metals (e.g. Mn, Fe, Cu, Zn, Se, V, Cr, lead (Pb) and Ni) have interactive influences with biological processes. Many external influences such as climatology and meteorology influence the behaviour and chemistry of atmospheric trace metal species, which results in atmospheric changes such as cloud composition and –lifetime, as well as toxic effects on ecosystems. Atmospheric deposition of some trace metals (e.g. Fe, Mn, Cu, Cd, and Zn) is essential for marine productivity (Morel *et al.*, 2003).

Several atmospheric trace metals are important within the South African context, but in this study specifically atmospheric mercury (Hg) and hexavalent Cr, i.e. Cr(VI), were considered. Hg is a volatile trace metal emitted into the atmosphere, which can be transported over large distances in the atmosphere due to its low reactivity and solubility. After oxidation of Hg to less volatile and more soluble compounds, Hg is mainly removed from the atmosphere through wet deposition (Lin *et al.*, 2006). The aqueous Hg compounds deposited are then converted into more toxic methylated Hg, which bio-accumulates in the aquatic food chain. The high concentration of methyl Hg in predatory fish poses a serious health risk for people and animals that depend on a fish diet (Mergler *et al.,* 2007). This has led to an increase in research on atmospheric Hg (Brunke *et al.,* 2012, Lindberg *et al.,* 2007, Slemr *et al.,* 2013). Coal combustion in industrial activities, which includes electricity generation, petrochemical plants and gasification processes, is considered to be the major source of atmospheric Hg (Laudal *et al.*, 2000; Wagner, 2001). South Africa is considered to be the 6th largest emitter of Hg and is also a signatory of the Minamata Convention (global legally binding

agreement). Therefore, inclusion of Hg in the South African National Ambient Air Quality Standards (NAAQS) is imminent. Hg is monitored extensively in the Northern Hemisphere (NH). However, according to the knowledge of the candidate only a few long-term studies on Hg have been reported for the southern hemisphere (SH). The German Antarctic research station measured total gaseous Hg (TGM) from January 2000 to January 2001 (Slemr *et al.* 2008). Slemr *et al.* (2008) reported the long-term monitoring results of TGM at the Cape Point Global Atmospheric Watch (CP GAW) atmospheric monitoring station in South Africa covering the period between September 1995 and December 2004.

Cr is a redox active metal that persists either as Cr(III) or Cr(VI) in the environment. These two oxidation states have opposing toxicity and mobility. Cr(III) is an essential micro-nutrient and is mostly insoluble in water, while Cr(VI) is very toxic and readily transported (Rai *et al.*, 1989). Cr(VI) is strongly associated with human carcinogenicity. South Africa holds the majority of the world's viable Cr ore (chromite) resources and is the second largest producer of ferrochromium (crude alloy that is the precursor to stainless steel) (Beukes *et al.,* 2010). Cr in the mined chromite is in the Cr(III) oxidation state, but the high temperatures involved in industrial process can result in oxidation to the hexavalent state. Cr(VI) emissions can also occur from hazardous waste incinerators, municipal waste combustors, sewage sludge incinerators, boilers and other industrial furnaces. The production of ferrochromium and stainless steel has been mentioned among the greatest contributors to atmospheric emission of Cr that can threat the environment (Mukherjee, 1998). Source apportionment and extent of ambient Cr(VI) transport in the South African environment needs thorough examination.

Apart from atmospheric trace metals found in aerosols, many other chemical compounds are present as particulate matter. Water-soluble inorganic ions are an important group of compounds present in atmospheric aerosols (Jacobson *et al.*, 2000; Bourotte *et al.*, 2007). Many studies have been conducted on the deposition of anions (acidic) and cations (basic) on terrestrial and aquatic ecosystems and their buffering effect. Major water-soluble inorganic ions are associated with atmospheric visibility degradation, adverse human health effects and acidity of precipitation (Dockery &

Pope, 1996). Determining the complete chemical composition of aerosols is important to gain insight into sources and their toxicity, as well as to evaluate effectiveness of abatement strategies for relevant emission sectors (Mkoma *et al.*, 2014).

1.1.2 Objectives

The general aim of this study was to assess atmospheric trace metals measured at two background sites in South Africa, as well as water-soluble ionic species at one of these sites. Although various trace metal species were investigated in general, specific emphasis was placed on atmospheric Hg and Cr(VI) due to their importance within the South African context. The specific objectives of this study were to:

- Statistically assess gaseous elemental mercury (GEM) measured at Cape Point for at least a five-year period;
- Evaluate the extent of regional atmospheric Cr(VI) pollution from the western Bushveld Complex, which is likely to be a source region with elevated atmospheric Cr(VI) levels;
- Conduct characterisation of general trace metal concentrations at a regional background site and identify possible sources/source areas;
- Evaluate the most prominent water-soluble inorganic ionic species at the same regional background site that was considered in the general trace metal study;
- Conduct an assessment of trace metal and water-soluble inorganic ionic species concentrations, as well as levels of other parameters/species in the plume of a typical South African braai as a special case study;

By completing the above objectives, it is anticipated that the accumulation of knowledge will contribute to:

- Expanding the knowledge base, including chemical characterisation of atmospheric aerosols in the South African environment;
- Supplementing air quality policy and management structures, considering the potential significance of Cr(VI) and GEM;
- Directing future studies, allowing researchers to reach beyond the current scope.

Chapter 2

Literature survey

2.1 Introduction

In this chapter, background information for this study is presented with particular reference to air pollution, classification and mitigation, aerosols, trace metals, inorganic ionic species and, as a case study, the constituents of a typical South African braai (barbeque).

2.2 Air pollution

Air pollution, i.e. emission of species beyond their natural average levels, is an age-old phenomenon. Natural pollution from erupting volcanoes, natural fires and desert dust has existed since before mankind. Human activities have led to air pollution from the start of the first fire and the clearing of land for the first agricultural activities (windblown dust).

During the industrial revolution (18th and 19th centuries) large-scale mechanisation occurred, allowing humans to greatly transform and benefit from natural resources. Unfortunately, environmental concerns increased in accordance. As an example, the use of coal during the industrial revolution reduced land constraints (e.g. in terms of wood for fuel) and contributed to an increase in agricultural production (e.g. crop rotation and food imports), which lowered the direct load on nature. However, uncontrolled emissions from coal combustion led to thickening black smog and soot that aggravated sociological and environmental problems (infections, respiratory problems, poisoning, workplace accidents, etc.) (Kasa, 2008).

Currently, urban smog is still prevalent in many cities around the world. Urban smog is caused by the build-up of gases and particles (aerosols) being emitted form industries, vehicles and other human activities or formed chemically from precursor species (Jacobson, 2002). Similar to smog, other anthropogenic activities have led to acid rain, water pollution, soil pollution, increased greenhouse gas concentrations with

associated climate change, as well as socio-economic impacts related to the afore-mentioned occurrences. In order to alleviate these socio-economic and environmental problems since the industrial revolution up until the present, authorities have introduced laws to curb emissions (Kasa, 2008). Atmospheric pollution is not just of local concern, but due to the dramatic increase in the world population, urbanisation and industrialisation, and the significant spatial areas and temporal time scales that can be influenced by atmospheric pollution, it is of global importance.

2.2.1 Classification and mitigation

Atmospheric pollutants are generally classified as gases or particulates (aerosols) that were emitted directly into the atmosphere (primary pollutants) or formed through transformation in the atmosphere (secondary pollutants), which originated from natural of anthropogenic sources.

Jacobson (2002) distinguishes a gas from a particle in two ways. In a gas the atoms or molecules are separated whereas in particulate form atoms and molecules form aggregates. Secondly, particles may contain liquids or solids. He states that the particulates may be further separated in aerosol particles and hydrometeor particles. Aerosol particles are discussed in more detail in Section 2.3. Although air consists of gases and particles, the mass of air is dominated by gases. Of all gas molecules in the lower atmosphere, which is commonly referred to as the troposphere, more than 99% are molecular nitrogen and oxygen. The primary/secondary and natural/secondary nature of the atmospheric species relevant to this study will be discussed later in this literature review.

Leading authorities and/or international bodies (e.g. such as the World Health Organisation, United States Environmental Protection Agency and European Environment Agency) have compiled lists of so-called criteria pollutants, for which the tolerable levels in ambient- and/or indoor conditions were determined (EEA, 2015; WHO, 2015; USEPA, 2015). Typically, criteria pollutant species include specific trace gases, aerosols, organic and inorganic constituents. Species specific limits and standards have been set which should not be exceeded, or only exceeded a set amount of times in order to minimise associated health and/or environmental impacts. The

limits, standards and number of criteria species are revised by authorities periodically as technology advances and circumstances change.

In South Africa the National Environmental Management: Air Quality Act, 2004 (Act No. 39 of 2004) details the criteria for atmospheric pollutants, their individual standards and permissible limits. The legislation in South Africa is in accordance with that of international authorities, but adjusted to local circumstances. The ambient criteria pollutants governed by South African legislation include: Gaseous species (SO_2, NO_2, O_3, Benzene and CO), aerosol mass (PM_{10} and $PM_{2.5}$) and a trace metal species (lead (Pb)) (SA, 2009; SA, 2012b). Table 2.1 summarizes these species in accordance with the national standards, their ambient concentrations and the permissible exceedances for the time interval measured.

Table 2.1.: South African ambient air quality criteria pollutants are assessed against the national standards in this table. Concentrations are in μgm^{-3} and values in brackets are the tolerable frequency of exceedances.

	SO_2	**NO_2**	**O_3**	**CO**	**Benzene**	**PM_{10}**	**$PM_{2.5}$**	**Pb**
10 minutes	500 (526)							
1 hour	350 (88)	200 (88)		30# (88)				
8 hour			120 (11)	10# (11)				
24 hour	125 (4)	40 (0)				75 (4)		
1 year	50 (0)				5 (0)	40 (0)	25 (0) 20* (0)	0.5 (0)

CO national standards are in mgm-3

* PM2.5 national standard will be 20 µg.m-3 from January 2016 – December 2029

2.2.2 Meteorology

The atmosphere consists of four layers, i.e. the troposphere (up to ~10 to 16 km above the surface), stratosphere (above the troposphere up ~50 km above the surface), the

mesosphere (above the stratosphere up ~85 km above the surface), and the thermosphere (above the mesosphere up ~500 km above the surface), in which temperatures change with altitude. Contained in the troposphere, the boundary layer extends from the surface to between 500 and 3 000 m altitude (Jacobson, 2002; Lenschow, 2003).

Pollutants emitted near the ground accumulate in the boundary layer, and result in concern, since it is this region of the atmosphere in which all humans live. When pollutants escape the boundary layer, they may travel long distances before they are removed from the atmosphere. The bottom 10 % of the boundary layer is known as the surface layer and is characterised by turbulence produced by wind shear and convection (Lenschow, 2003).

The convective mixed layer is the region of air just above the surface layer. This encompasses the bulk of the planetary boundary layer and becomes mixed due to the sun heating the ground, resulting in energy being transferred to the air and thermal mixing taking place. The thermal mixing increases the efficiency of transport of atmospheric constituents. The top of the mixed layer is often bounded by a temperature inversion, which is a decrease in temperature with increasing height (Jacobson, 2002). The inversion inhibits thermal turbulence originating from the surface layer or the mixed layer. Pollutants are generally trapped beneath or within an inversion. Therefore, the closer the inversion is to the ground, the higher pollutant concentrations become, since the mixing volume is less. The mixed layer grows during the day through the input of heat at the surface, entraining air from above the inversion as it does so (Denmead *et al.*, 1999; Lenschow, 2003).

The meteorology in South Africa is characterised by strong seasonal variability. Above the eastern interior of South Africa, the atmospheric circulation pattern is dominated by anti-cyclonic circulation during the winter months and experiences frequent easterly disturbances during the summer. The influx of westerly disturbances occur approximately 20% of the time throughout the year (Garstang *et al.*, 1996). Similarly, the precipitation in South Africa typically starts in October and ends in March (wet season), contributing to the strong seasonal variation. The precipitation cycle strongly affects the atmospheric scrubbing of local pollutant concentrations originating as

primary emissions from wild fires during the dry season, as well as wet scavenging by precipitation and clouds during the wet season (Laakso *et al.*, 2012). The cloud cover over the interior of South Africa, especially the Highveld region, is often limited due to a dominant high pressure system, created by the high altitude and the subtropical subsidence (Tyson & Preston-Whyte, 2000). The high pressure system, combined with low heat capacity of the soil, creates frequent atmospheric inversion layers that significantly reduce the vertical mixing (Garstang *et al.*, 1996). These inversions are most pronounced just before sunrise. In the presence of sunlight, the inversions begin to break down through convective heating and consequently the height of the mixed layer is increased (Tyson *et al.,* 1996). The afore-mentioned meteorological conditions modulate the pollutant levels above the Highveld. With the high incidence of anti-cyclonic circulations, pollutants can be trapped over southern Africa for several days before exiting the subcontinent, primarily towards the east coast via a well-defined plume (Garstang *et al.*, 1996; Freiman & Piketh, 2002; Laakso *et al.*, 2012).

2.3 Aerosols

2.3.1 Emissions, formation and effects

An aerosol is a collective term that refers to solid, liquid, or mixed-phase particles suspended in air (Jacobson, 2002). Combustion and other high-temperature processes are largely responsible for primary emissions of fine-mode particles, while mechanical processes such as grinding, entrainment of dust and soil, or droplet formation by waves generate coarse-mode particles (Turner & Colbeck, 2008). Formation of aerosols may furthermore occur through homogeneous or heterogeneous condensation. During homogeneous condensation, gases can nucleate to form new particles, while heterogeneous condensation favours uptake of vapour by pre-existing particles. Gas-to-particle-conversion (new particle formation, i.e. NPF) followed by condensational growth of the freshly-formed nanoparticles is a frequently observed phenomenon in the atmosphere (Kulmala *et al.*, 2004).

According to the USEPA, particle size is directly linked to health problems, since smaller particles penetrate deeper into the respiratory system, and may even be absorbed by the bloodstream. Susceptible groups with pre-existing lung or heart

disease, as well as elderly people and children, are particularly vulnerable. The health effects of PM with different chemical compositions or emanating from various sources may vary as well.

Atmospheric aerosol particles affect the Earth's climate in two ways. Firstly, there is a direct effect on the earth's radiative balance by scattering and absorbing the solar radiation. Secondly as an indirect effect, aerosol particles can act as cloud condensation nuclei (CCN) and determine optical properties of the clouds and affect the cloud life time (Sundström *et al.*, 2015). The condensational growth rate (GR) of aerosol particles formed during atmospheric NPF events is an important factor influencing the lifetime of these particles and their ability to become climatically relevant (Yli-Juuti *et al.*, 2011).

Aerosols are removed from the atmosphere by wet or dry deposition. The removal may occur within minutes or may take weeks after release or physiochemical formation of the aerosols, during which time the aerosols may travel metres if removal is fast, or thousands of kilometres if removal is slow (Turner & Colbeck, 2008). Aerosols may further be distinguished by their size and number concentration, and chemical composition as discussed in the subsequent section.

2.3.2 Size and number concentration

Aerosols or particulate matter (PM) can be sampled without considering size ranges. Such sampling would typically be termed as total suspended PM. However, it is much more common to sample aerosols in a size fraction correlating to the aerodynamic diameter less than 10, 2.5 or 1 µm, which are termed PM_{10}, $PM_{2.5}$ and PM_1 with an instrument fitted with a single inlet with a fixed aerosol cut-off size. Alternatively, fractions within the afore-mentioned size ranges can be sampled with instruments fitted with two or more cut-off inlets fitted in series to obtain for instance PM with aerodynamic diameters smaller than 1 µm (PM_1), between 1 and 2.5 µm ($PM_{1\text{-}2.5}$) and between 2.5 and 10 µm ($PM_{2.5\text{-}10}$) (Booyens *et al.*, 2015).

If additional sizing of PM_1 needs to be considered, more sophisticated sampling techniques are usually applied. A Differential Mobility Particle Sizer (DMPS), a Balanced Scanning Mobility Analyzer (BSMA) and an Air Ion Spectrometer (AIS) are

instruments typically used in sizing PM_1 aerosols, whereas a Condensation Particle Counter (CPC) can be used to determine the number concentration (total number concentration, or size resolved number concentration if the CPC is paired with a DMPS, AIS or BSMA) (Yli-Juuti *et al.*, 2011). The number concentration of aerosol particles decreases with increasing particle size, i.e., particles at the small end of the size distribution can be abundant in number and since mass depends upon the diameter cubed, such particles may contribute only a small amount of the total mass (Turner & Colbeck, 2008).

Distinct peaks (modes) in concentration occur when the size spectrum (in diameter space) of PM_1 aerosols are investigated. The size distributions of atmospheric aerosols, their composition, sources, and sinks are key elements to understand and manage their effects on health, visibility, and climate. PM_1 accounts for 50–70% of PM_{10} (Yue *et al.*, 2009). Atmospheric fine particles can be classified to ultrafine (PM<100 nm) and accumulation mode (100 nm<PM<1µm) particles. The ultrafine particles can be further divided into nucleation (<30 nm) and Aitken mode particles (30 nm<PM<100 nm).

2.3.2.1 Composition

As mentioned in previous sections, aerosols may originate from natural or anthropogenic sources. The NPF is strongly connected to the presence of sulphuric acid and other vapours of very low volatility, as well as the magnitude of solar radiation (Sundström *et al.*, 2015). Yli-Juuti *et al.* (2011) and references therein explain that a substantial fraction of atmospheric PM_1 aerosol particle mass is found to consist of organic compounds. In addition to sulphuric acid (from SO_2 oxidation), these vapours would be the most probable candidates responsible for nucleation mode growth. Certain anthropogenic activities might escalate the natural emissions, e.g. dust from open cast mining and SO_2 from pyrometallurgical industries that contribute to NPF events. The typical origin and composition of aerosols, as well as gas species relevant to aerosol formation and growth are discussed below in Sections 2.2.3.1 and 2.2.3.2.

2.3.2.2 Natural

The gases and aerosols resulting from the natural environment are presented in Table 2.2.

Table 2.2: Sources and emissions of naturally occurring aerosols in the atmosphere, as well as gas species that can serve as precursors to secondary aerosols being formed

Source	Emissions
Dust	Mineral aerosols are produced by wind erosion and resuspension in arid and semi-arid regions. Dust contributes ~45 % to the total atmospheric aerosol load, calculated as the sum of the main oxides of various metals, i.e. aluminium (Al), silicon (Si), iron (Fe), titanium (Ti) and non-sea-salt calcium (Ca), sodium (Na), magnesium (Mg) and potassium (K) (Marconi *et al.*, 2014).
Sea spray	Produced by wind, waves and bubble bursting, these ionic species in order of importance are: Cl^-, Na^+, SO_4^{2-} and Mg^{2+} (Grythe *et al.*, 2014).
Volcanism	Although not a constant, vast amounts of mainly of ash, sulphate and carbonaceous compounds are ejected into the atmosphere around the world in sporadic locations (Andersson *et al.*, 2013).
Biomatter respiration and decay	A variety of compounds are emitted from both natural and crop plants. Isoprene (C_5H_8), monoterpenes ($C_{10}H_{16}$) and sesquiterpenes ($C_{15}H_{24}$) form the majority of these emissions (Griffin *et al.*, 1999). Biogas produced during anaerobic digestion is primarily composed of methane (CH_4) and carbon dioxide (CO_2), with smaller amounts of hydrogen sulphide (H_2S) and ammonia (NH_3). Typically, the mixed gas is saturated with water vapour and may contain dust particles and siloxanes (Monnet, 2003).
Farming	The agricultural aerosols are almost equally composed of organic particles and dust (inorganic particles). The dust particles (as discussed above) constitute silica and clay minerals, while organic particles are a mixture of fungal spores, bacteria, pollens, fragments of plants, etc. (Telloli *et al.*, 2014).
Fires	The smoke emitted by natural fires is characterised by the composition of the fuel and by the physical and chemical processes during combustion. Andreae and Metlet (2001) explain that open vegetation fires are typically dynamic fires, i.e. a moving fire front passes through a fuel bed, such as a savannah or forest. As a result, different combustion fuel types are present at any given time, and their combined emissions are released into the smoke plume. Plant biomass consists of cellulose and hemicelluloses (typically 50-70% dry matter), lignin (15-35%), proteins, amino acids, and other metabolites, including volatile substances (alcohols, aldehydes, terpenes, etc.). In addition, it contains minerals (up to 10%) and water (up to 60%). Thermal degradation begins with a drying/distillation step, in which water and volatiles are released, followed by pyrolysis, during which thermal cracking of the fuel molecules occurs (Andreae & Metlet, 2001).

2.3.2.3 Anthropogenic

The sources and composition of typical anthropogenic aerosols are presented in Table 2.3:

Table 2.3: Sources and emissions of aerosols in the atmosphere resulting from anthropogenic activities, as well as gas species that can serve as precursors to secondary aerosols being formed

Source	Emissions
Fires	Fires in the natural environment i.e. open vegetation fires may also be considered anthropogenic, since these fires are started intentionally or as a consequence of human behaviour. The emissions are the same as for natural fires, as discussed above.
Industrial combustion	In the petrochemical and electricity generation industries, production is usually achieved by the pyrogenic processing of fossil fuels. Emissions from these sources include: volatile organic compounds (VOCs), polycyclic aromatic hydrocarbons, NO_x, SO_x, PM_{10}, CO_2, soot (black carbon and organic matter), sulfate (SO_4^{2-}), metals, and fly ash. The fly ash consists of trace metals and oxygenated compounds in the form of quartz, hematite, gypsum, and clays (Jacobson, 2002).
Mining	Large quantities of dust are produced and released in the working atmosphere during mining (crushing, drilling, and cutting) and handling of mineral ores. Dust from coal mines contain silica, naphthalene and about thirteen poly-nuclear aromatic hydrocarbons (Banerjee *et al.*, 2001).
Pyro-metallurgical processes	The pyrometallurgical processes are potential sources of dust (transport of raw materials, bag filter dust, ash, slag and residues). The smelting processes produce off-gases from the furnaces and may contain dust, metals, volatile organic components and other gaseous species (NO_x, CO_x, SO_x) (Apostolovski-Trujic *et al.*, 2007).
Automobile emissions	Motor vehicles are a major source of particulate matter, CO, NO_2, hydrocarbons, SO_2, lead (Pb – historically before the abolishment of Pb based fuels), and ozone (as a secondary emission). An estimated 86% of the world's vehicles are found in industrialized countries (Schwela *et al.*, 1997).
Domestic heating	A wide range of persistent organic pollutants (POPs) polycyclic aromatic hydrocarbons, PM, trace metals and gasses (e.g. NO_x and CO) are prevalent when using coal or wood for domestic cooking and space heating (Lee *et al.*, 2005).

2.4 Trace metals

Since trace metals in PM were specifically considered in this study, additional background with regard to atmospheric trace metals is presented in subsequent sections.

Trace metals are ubiquitous throughout the environment. Some trace metals are essential for life (e.g. Fe), others are micro-nutrients (e.g., selenium (Se)) and some are considered as toxic elements (e.g., mercury (Hg)). Levels of these elements in the environment are determined by the local geochemistry and anthropogenic emissions (Barbante *et al.*, 2011). Atmospheric pollution of trace metals is global, reaching even the most remote areas of our planet. (Boutron *et al.*, 2011).

The study of trace metals in successive dated snow and ice layers (preserved in the Antarctic and Greenland ice caps) has been a reliable method in explaining historic atmospheric concentrations and events. For example, Greenland snow dated from the mid-1960s indicated that Pb concentrations were two orders of magnitude higher than in Greenland ice about 3 000 yrs old (Murozumi *et al.*, 1969). The widespread use of Pb additives in gasoline starting in the 1930s, which accounted for the spike from the mid-1960s and correlated with the decreasing trend from the 1970s onward with the abolition of Pb additives in gasoline (Nriagu, 1990). Similarly, atmospheric pollution linked with Pb and silver (Ag) production activities in ancient Greece and Rome could be determined (Boutron *et al.*, 2011).

2.4.1 Sources and composition

The most common trace metals emanating from the various natural sources are presented below as a continuation of the natural aerosol sources discussion in Section 2.3.2.2, Table 2.2.

Table 2.4: Sources and emissions of natural occurring trace metal species in the atmosphere

Source	Emissions
Vegetation	Low concentrations of metals, including titanium (Ti), manganese (Mn), Zn, Pb, Cd, Cu, cobalt (Co), antimony (Sb), arsenic (As), nickel (Ni), and Cr are present in vegetation. These substances vaporize during burning, and then quickly recondense onto soot or ash particles (Jacobson, 2002).
Dust	More than 50% of atmospheric Cr, Mn and V, and more than 20% of Cu, Mo, Ni, Pb, Sb and Zn are from dust (Pacyna, 1998).
Volcanism	Volcanic eruptions generate about 20% of natural atmospheric Cd, Hg, As, Cr, Cu, Ni, Pb and Sb (Pacyna, 1998).
Sea-salt	Aerosols generated by spray and wave action may contribute to about 10% of total natural trace metal emissions (Nriagu, 1989).

Anthropogenic high-temperature processes result in the release of volatile metals as vapours forming particles by condensation or gas-to-particle reactions (Pacyna, 1998). Of all the trace metals emitted into the air industrially, Fe is by far the most abundant (Jacobson, 2002). Although atmospheric Pb pollution has now declined, snow samples indicate a new group of trace metals with elevated levels, i.e. Pt, Pd and Rh. These metals are linked to their use especially as catalysts in automobiles. Snow samples prior to 1969–1975 and since 1976−1995, associated with the use of catalytic converters on automobiles, confirm this trend (Barbante & Cescon, 2000). A series of snow samples covering the period from 1834 to 1990, collected in Antarctica, indicates an increase in V, Cr, Cu, Zn, Ag, Cd, bismuth (Bi) and uranium (U) species (Planchon *et al.*, 2002). These elevated levels are attributed to emissions of heavy metals to the atmosphere from human activities in the Southern Hemisphere especially non-ferrous metal mining and smelting in Chile, Peru, Zaire, Zambia and Australia (Boutron *et al.*, 2011).

The most common trace metals emanating from the various anthropogenic sources, as presented by Jacobson (2002) and references therein are presented below in Table 2.5 as a continuation of the above-mentioned discussion and discussions in Section 2.3.2.3., Table 2.3.

Table 2.5: Anthropogenic sources of trace metals and their associated emissions

Source	Trace metal emission species
Oil-fired power plants	V, Ni, Fe
Smelters	Fe, Cd, Zn, Cr, Ni, V, Mn, Si
Open-hearth furnaces at steel mills	Fe, Zn, Cr, Cu, Mn, Ni, Pb
Municipal waste incineration	Zn, Fe, Hg, Pb, Sn, As, Cd, Co, Cu, Mn, Ni, Sb
Coal-fired power plants	Fe, Zn, Pb, V, Mn, Cr, Cu, Ni, As, Co, Cd, Sb, Hg
Vehicular	Pb, Fe, Cu, Zn, Ni, Cd, Zn, Pt, Pd, Rh

2.4.2 Health impacts

Elevated concentrations of atmospheric aerosol particles have been associated with adverse effects on human health (Schwartz *et al.*, 1996, Laden *et al.*, 2006). Particle size and shape are key factors that control the extent of penetration of particles into the human respiratory tract. In addition, the potential health effects depend on many other factors, such as chemical and physical characteristics of aerosols, the amount of toxic substances, their solubility in biological fluids, etc. Nevertheless, it was found that PM_{10} toxicity can be related to soluble components (especially soluble trace metals) (Voutsa & Samara, 2002), which are an important factor in lung inflammation, most likely because of their bioavailability (Dreher *et al.*, 1997). Trace metal species, such as Pb, Hg and Cr, have proven impacts on human health (Fenger, 2009).

2.4.3 General chemistry

The importance of sulphuric acid or sulphate in secondary aerosol formation during NPF has already been discussed (Section 2.3.1.). Additionally, sulphuric acid is the

inorganic acid contributing most to acid rain. Combustion of fuel containing sulphur produces SO_2, which can then be oxidised to sulphuric acid according to Equation 2.1:

$$2SO_2 + 2H_2O + O_2 \rightarrow 2H_2SO_4 \quad (2.1)$$

The atmospheric oxidation of SO_2 (Equation 2.1) is strongly influenced by the relative humidity (RH). Little oxidation occurs at RH below 70%, but at higher RH relatively rapid oxidation and conversion to sulphuric acid occurs. Equation 2.1 can be rewritten to indicate only the oxidation state of S, as indicated in Equation 2.2.

$$S(IV) + \tfrac{1}{2}O_2 \rightarrow S(VI) \quad (2.2)$$

S(VI) oxidation in the atmospheric aqueous phase is known to be catalysed by Fe(III) and Mn(II). Iron in cloud water exists both in the Fe(II) and Fe(III) states and there is a series of cycling reactions between these two forms (Stumm & Morgan, 1996; Seinfeld & Pandis, 2006):

$$Fe^{3+} + H_2O \leftrightarrow FeOH^{2+} + H^+ \quad (2.3)$$

$$FeOH^{2+} + H_2O \leftrightarrow Fe(OH)^+ + H^+ \quad (2.4)$$

$$Fe(OH)_2^+ + H_2O \leftrightarrow Fe(OH)_3\,(s) + H^+ \quad (2.5)$$

Fe(II) appears not to directly catalyse the reaction indicated in Equation 2.2, but is first oxidised to Fe(III) before S(IV) oxidation can begin (Huss *et al.,* 1982; Seinfeld & Pandis, 2006).

$$Fe(OH)_3\,(s) + 3H^+ \leftrightarrow Fe^{3+} + 3H_2O \quad (2.6)$$

More uncertainty exist for the mechanism of Mn(II) catalysed oxidation of S(VI) (Seinfeld & Pandis, 2006). There also seems to be a synergism when both Fe(III) and Mn(II) occur (Seinfeld & Pandis, 2006).

2.5 Atmospheric mercury

Atmospheric gaseous elemental Hg (GEM) and Cr(VI) were two specific trace metals species considered in the study, therefore additional attention is given to these trace metal species.

As in the case with gaseous pollutants and trace metal species, the amount of Hg mobilised and released into the atmosphere has increased since the beginning of the industrial revolution (Kasa, 2008; Boutron *et al.*, 2011; Keating *et al.*, 1997). The atmosphere plays a crucial role in the global biogeochemical cycle of Hg. Atmospheric Hg generally exhibits strong regional and temporal distribution patterns depending on emission sources, physicochemical properties, as well as meteorological, geographical, and atmospheric chemical conditions (Fu *et al.*, 2011).

Mercury can exist in three oxidation states: Hg^0 (elemental), Hg^{2+} (mercurous), and Hg_2^{2+} (mercuric-Hg(II)). The properties and chemical behaviour of mercury strongly depend on the oxidation state. Hg^{2+} and Hg_2^{2+} can form numerous inorganic and organic chemical compounds, however, Hg^{2+} is rarely stable under ordinary environmental conditions (Rice *et al.*, 1997). Gaseous elemental mercury (GEM), however, is the most stable persistent species and may have a residence time in the atmosphere of up to one year. Therefore, GEM is on the priority lists of a large number of international agreements and conventions (Brunke *et al.*, 2010).

2.5.1 Sources and composition

Atmospheric mercury exists in vapour and particulate forms. The vapour form (in totality) is known as total gaseous mercury (TGM), and consists of the stable dominant GEM and short-lived reactive gaseous mercury (RGM) species. As is the case with the particulate mercury in the atmosphere, mercury in water, soil, plants and animals is in the form of inorganic mercury salts and organic forms such as methylated mercury (Keating *et al.*, 1997). Hg is readily removed from the atmosphere by either wet or dry deposition. Keating *et al.* (1997) explain that even after Hg is deposited; it is frequently released back into the atmosphere either as a gas or in association with particles, to be re-deposited elsewhere. Considering the above, GEM may circulate in the atmosphere for up to a year, and hence can be widely dispersed and transported thousands of kilometres from emission sources. Natural (Rice *et al.*, 1997) and anthropogenic sources (Keating *et al.*, 1997) of atmospheric mercury are presented in Table 2.6.

Table 2.6: Natural and anthropogenic sources of atmospheric mercury in the atmosphere

Natural sources	Anthropogenic sources
Volatilization of mercury in marine and aquatic environments	Combustion sources – waste combustion and fossil fuels processes
Volatilization from vegetation	Electrical industry – fluorescent lamps, thermostats and batteries
Degassing of geologic materials	Dental – amalgam in repairing dental caries
Volcanic emissions	Manufacturing – production of chlorine and caustic soda
	Wood processing – anti-fungal agent
	Metallurgy – solvent for precious metals and catalyst
	Pharmaceutical – preservative

For each of the anthropogenic operations, the Hg is present as a trace contaminant. Because of its relatively low boiling point, Hg is volatilized during high temperature operations and discharged to the atmosphere. Mercury deposition is mainly in the Hg(II) state from either emitted Hg(II) or from conversion of emitted Hg^0 to Hg(II) through ozone-mediated oxidation. This process results in regional/global transport, followed by deposition (Rice *et al.*, 1997).

As Hg cycles between the atmosphere, land, and water, mercury undergoes a series of complex chemical and physical transformations, accumulating most efficiently in the aquatic food web. Methyl mercury is accumulated in predatory fish tissue, however, inorganic mercury, which is less efficiently absorbed and more readily eliminated from the body, does not tend to bio-accumulate. Fish consumption dominates the pathway for human and wildlife exposure to methyl mercury (Keating *et al.*, 1997).

2.5.2 Atmospheric Hg chemistry

One of the most prominent reactions concerning atmospheric Hg, is the photochemical driven oxidation of Hg(0) to Hg(II) during midday when solar radiation, O_3 levels and atmospheric halogens produced by sea spray are the most intense (Figure 2.1.). As

discussed in Lau *et al.* (2012) and the references therein, GEM may be oxidised by ·OH, nitrate (NO_3·) or halogen (X·) radicals. The reactive Hg(II) may then be removed from the atmosphere much more easily. Considering the short lifespan of Hg(II) and its reactivity, many further reactions may occur, i.e. reduction back to Hg(0) or methylation (MeHg).

Atmospheric Hg(II), when deposited, is converted to MeHg, which is a potent neurotoxic compound, especially when it bio-accumulates in the food chain. MeHg manifests its toxicity in a variety of symptoms ranging from mild numbness of the extremities, blindness, impaired development of language, attention and memory skills (Krummel *et al.*, 2005), In temperate zones, microbial activities critically impact on MeHg accumulation by carrying out biochemical transformations. Formation of MeHg has been documented in wetland soils, streams, snow, freshwater ponds, marine water column, lakes and tundra watersheds (Barkay *et al.*, 2011 and references therein).

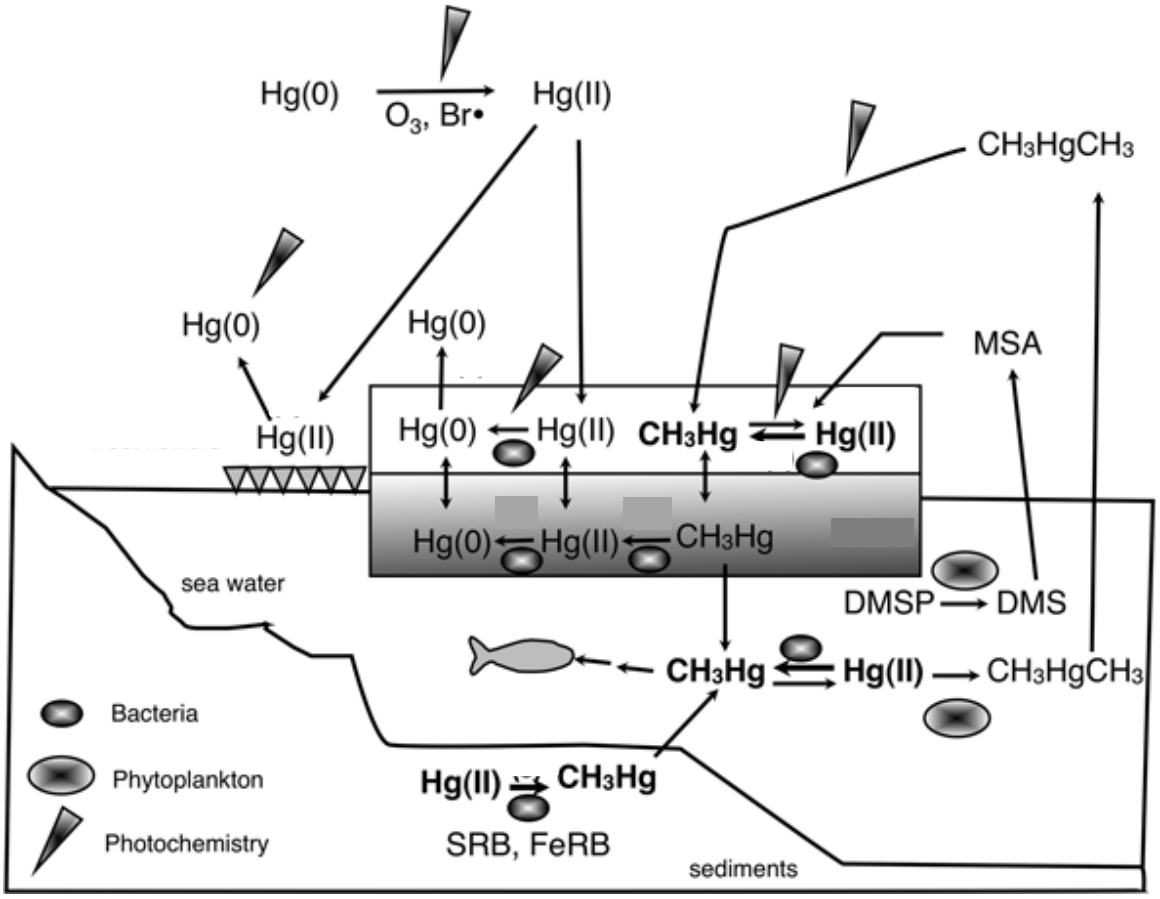

Figure 2.1: The biogeochemical cycle of mercury, major reactions and transport pathways are presented (Barkay *et al.*, 2011).

2.5.3 Atmospheric mercury in South Africa

The Cape Point Global Atmospheric Watch (CPT GAW) station is one of the longest operating background measurement stations in the southern hemisphere. Grab-samples of atmospheric Hg have been collected at CPT GAW since September 1995 and automated measurements with a resolution of 15 min were initiated in March 2007, replacing the manual sampling (Baker *et al.*, 2002; Brunke *et al.*, 2010). Ebinghaus *et al.* (2002) measured TGM at the German Antarctic research station from January 2000 to January 2001, the only other long-term systematic atmospheric Hg measurements reported on in the southern hemisphere.

In South Africa, potential anthropogenic sources of Hg include coal combustion, ferrous and non-ferrous metals production, and artisanal gold mining (Masekoameng *et al.*, 2010). Older emission inventories estimate South African industries to emit 257 tonnes of Hg yr^{-1}. with coal combustion emitting 82.6 tonnes and other industries contributing 174 tonnes, ranking South Africa as the world's second largest emitter of mercury (Trüe, 2010), which are now considered to be wrong. Brunke *et al.* (2012) reported total elemental mercury emissions of 13.1, 15.2, and 16.1 t Hg yr^{-1}, estimated independently using the GEM/CO, GEM/CO_2, and GEM/CH_4 emission ratios and the annual mean CO, CO_2, and CH_4 emissions, respectively, in South Africa for 2007 and 2008. The average of these independent estimates of 14.8 t GEM yr^{-1} is much less than the total of 257 t Hg yr^{-1} reported earlier. Other atmospheric Hg inventories for South Africa have reported 40 t Hg yr^{-1} in 2004 (Leaner *et al.*, 2009) and 50 t Hg yr^{-1} in 2006 (Masekoameng *et al.*, 2010).

2.6 Hexavalent chromium

Chromium is produced from chromite, the only commercially-recoverable source since its discovery in 1798 (Cowey, 1994; Niagru, 1998). South-Africa is considered to hold at least 75 % of the world's viable chromite reserves (Cowey, 1994; Riekkola-Vanhanen, 1999; Murthy *et al.*, 2011). These reserves are concentrated within the Bushveld Complex, located in the central and western parts of the South African Highveld (Glastonbury *et al.*, 2010). Chromium in the environment generally exists in two stable oxidation states, i.e. Cr(III) and Cr(VI). Cr(III) is considered an essential micro-

nutrient for protein, carbohydrate and lipid metabolism in animals and humans (Berner *et al.*, 2004). Hexavalent chromium, i.e. Cr(VI) is regarded as a carcinogenic and mutagenic and severely impacts the respiratory tract when becomes air bone (Proctor *et al.*, 2002). Most Cr(VI) compounds are water soluble, adding to the possibilities of atmospheric chemistry, transport and deposition (Ashley *et al.*, 2003).

2.6.1 Sources and composition

Cr(VI) chemicals in themselves can be a significant source, e.g. chromate and dichromate manufacturing, since the intended product is Cr(VI). Hexavalent chromium compounds that are commonly manufactured include sodium chromate, potassium chromate, potassium dichromate, ammonium dichromate and chromium trioxide (IARC, 1990). Commercial production of chromium trioxide in Japan commenced before 1940 and by 1977, three companies produced a total of 8 300 tonnes, of which 120 tonnes were exported. In the USA, chromium trioxide production, in 1977, was in the range of 26 000 tonnes (Hartford, 1979; IARC, 1990).

There are various coal-combustion industries in South Africa, e.g. coal-fired power stations, coal-to-liquid production, boilers, etc. As discussed by Van Der Merwe *et al.* (2012), chromium is part of the trace minerals occurring naturally in coal and therefore present in most waste material associated with coal combustion. Industries associated with coal combustion also produce fly ash and clinker containing chromium (Nel *et al.*, 2011; Wagner & Laplante, 2005). Although most wastes contain Cr(III), high temperatures and physical abrasion may result in the formation of Cr(VI) that can be released into the atmosphere.

Potgieter *et al.* (2003) indicated that between 30% and 80% of the total chromium in South African cement clinkers are Cr(VI) compounds. Various sources could add chromium to cements, such as the raw materials, refractory bricks lining the kiln, mineral admixtures or the grinding media (normally high-chromium white cast iron) in the final finishing mills.

Panichev *et al.* (2008) demonstrated that Cr(VI) is formed by Cr(III) oxidation with atmospheric oxygen at high temperature during bush fires. They showed that Cr(VI)

concentrations in grass increased from an initial 2.5 to 23.2% in ash at 500 ◦C and up to 58.1% at 900 ◦C.

In addition to the above-mentioned sources, Cr(VI) may be generated or released into the environment by any one of the following processes:

- Electroplating (Cui *et al.*, 2011)
- Leather tanning (Apte *et al.*, 2005)
- Paint industries (Kassem, 2010)
- Stainless steel welding (Scheepers *et al.*, 208)

There are currently fourteen separate FeCr smelters in South Africa (Beukes *et al.*, 2012). The pyro-metallurgical carbo-thermic reduction of chromite yields ferrochrome (FeCr), a crude alloy of iron and chromium (Riekkola-Vanhanen, 1999). Ferrochrome is mostly applied in the manufacturing of stainless steel, a vital alloy in modern day living (Glastonbury *et al.*, 2010). Cr(VI) is formed in small quantities as an unintended by-product during FeCr production (Glastonbury *et al.*, 2010; Beukes *et al.*, 2010; Du Preez *et al.*, 2014). The formation, treatment and stabilisation of South African metallurgical wastes have been reported on and hold true for the FeCr industry (Ma & Garbers-Craig, 2006). A number of different methods to deal with these wastes include:

- Treatment and land filling
- Stabilisation methods such as cementation and vitrification
- Utilisation as a raw material in a separate product
- Recycling of materials to the furnace
- Improved recovery processes, which include hydrometallurgical and pyrometallurgical methods
- Optimised operational parameters may minimise wastes at the source

According to Beukes *et al.* (2012) and references therein, most of the above-mentioned waste treatment options are used to at least some level in the SA FeCr industry on possible Cr(VI)-containing wastes, since the minimisation of wastes implies higher profitability. However the recovery of valuable Cr units from wastes is currently limited to coarser materials such as slags (Mashanyare & Guest, 1997).

Since the emphasis of this chapter is on the ambient levels of Cr(VI), only fine particles are considered. Beukes *et al.* (2010) explain that with regards to Cr(VI) content, the fine particulate matter originating from the off-gas of high temperature processes can be regarded as the most significant source of Cr(VI) containing waste material generated by the FeCr industry. Furthermore, exposure to airborne Cr(VI) by inhalation is more hazardous than other exposure routes (Proctor *et al.*, 2002), indicating the importance of these fine waste materials.

2.6.2 Atmospheric chromium chemistry

Atmospheric chromium exists in either the solid or aqueous phase and it is estimated that anthropogenic sources account for 60-70% of total emissions. Chemical reactions can convert Cr(III) to Cr(VI) and *vice versa*. This conversion, however, must take place in the aqueous phase. In Figure 2.2., the typical solid states (emissions and sinks) and aqueous oxidation and reduction pathways are presented.

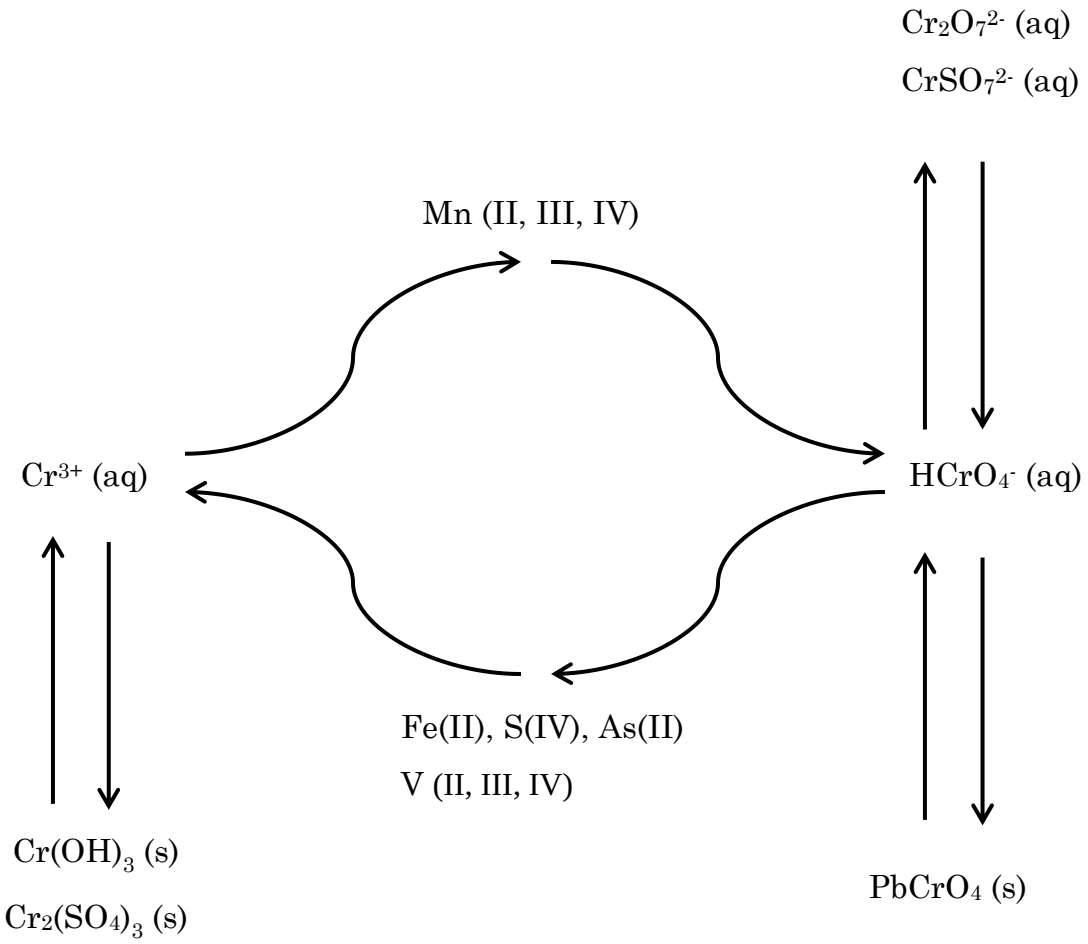

Figure 2.2: A simplified depiction of chromium chemistry in the atmosphere (Seigneur & Constantinou, 1995).

2.7 Water-soluble inorganic ionic species

Major water-soluble inorganic ions are associated with atmospheric visibility degradation, adverse human health effects, and acidity of precipitation, apart from affecting climate change (Dockery & Pope, 1994).

2.7.1 Sources and composition

Aerosols contain a significant fraction of water-soluble ionic components. In Table 2.7 the most common species and their emission sources are discussed.

Table 2.7: Sources and emissions of typical water-soluble inorganic ionic species in the atmosphere

Species	Emissions
Fluoride	Emitted from Al smelters and coal combustion. However, SiF_4 from coal combustion is typically non-soluble and therefore concentrations are typically very low (Xiu *et al.*, 2004).
Chloride	Mostly associated with sea spray and in the coarse particle mode. Chlorine in coal can be emitted in the form of chloride during the combustion (industry and biomass burning) and condensed into fine particle or through photochemical reactions on the fine particle surface (Xiu *et al.*, 2004).
Sulphate	Sulfate in ambient air mainly comes from oxidation of sulphur containing precursors such as SO_2, H_2S, and a large fraction of sulfate in flue gas from coal, heavy oil burning and biomass burning. PM_{10} related sulfate may be attributed to both soil particle and sea salt. In addition, the heterogeneous reaction of ammonia and sulfuric acid on PM_{10} particle surface can also form ammonium sulfate (Wall *et al.*, 1988).
Nitrate	May be of sea salt origin ($NaNO_3$) in the coarse particle fraction at coastal locations or from the deposition of nitric acid (HNO_3) on alkaline minerals or salt particles; however, fine mode NO_3^- may be observed as NH_4NO_3 when associated with coal burning pollution (Xiu *et al.*, 2004). Similarly to fossil fuel combustion, biomass burning is also considered a source.
Ammonium	NH_4 is more similar to SO_4^{2-} than NO_3^-, since SO_4^{2-} and NH_4^+ both have low vapour pressure and are easier to condensate (by reaction of gaseous ammonia) on fine particles (Zhuang *et al.*, 1999). As discussed above, local industrial pollution, biomass burning and sea spray are the important sources of the ions.
Cations (Na^+, K^+, Mg^{2+}, and Ca^{2+})	May account for 24% of the total water-soluble aerosol mass (Karthikeyan & Balasubramanian, 2006). The distribution of cationic species like Mg may vary in both coarse and fine particles and even at measurement sites ~200 km from the sea, water-soluble compounds of Mg such as $MgCl_2$ are attributable to sea-salt sprays (Dos Santos *et al.*, 2009). Further from the coast, these species are closely associated with wind-blown dust and other crustal origins, even volcanic emissions.

2.7.2 General chemistry related to water-soluble species

The two major anionic inorganic water soluble compounds that play a key role in aerosol properties are sulfate and nitrate (Harrison *et al.*, 2004). The formation of these water-soluble compounds *via* oxidation depends on the oxidation capacity of the atmosphere, which is largely due to three species, i.e. O_3, the hydroxyl radical ($OH^{\bullet}$) and the nitrate radical ($NO_3^{\bullet}$).

As discussed by Cornell (2005), O_3 is a product of photochemical air pollution, but also exists in trace amounts in relatively clean, unpolluted air. In the troposphere, O_3 concentrations increase with altitude, i.e. stratospheric source. Photolysis of NO_2 is the only other known way by which tropospheric O_3 can be produced. This reaction is presented below:

$$NO_2 + h\upsilon \rightarrow NO + O \qquad (2.7)$$

$$O + O_2 + M \rightarrow O_3 + M \qquad (2.8)$$

Where M is a third chemical species such as N_2 or O_2 that participate in the reaction.

The $NO_3^{\bullet}$ is formed from the oxidation of NO_2 by O_3 and is an important reactive intermediate in the troposphere. The formation is given by equation 2.9.:

$$NO_2 + O_3 \rightarrow NO_3^{\bullet} + O_2 \qquad (2.9)$$

In the presence of visible light (day time), $NO_3^{\bullet}$ is broken down. This reaction is indicated below:

$$NO_3^{\bullet} + h\upsilon \rightarrow NO + O_2 \text{ (or } NO_2 \text{ and O)} \qquad (2.10)$$

Considering the dependence on light, $NO_3^{\bullet}$ is most abundant at night. It is said that even at night, it may be consumed by NO and produce N_2O_5. N_2O_5 reacts with water and forms nitric acid, therefore $NO_3^{\bullet}$ is rarely observed when relative humidities are over 50% (Connell, 2005).

As discussed above, the atmospheric oxidation of SO_2 (Equation 2.1) in the formation of sulphate, is strongly influenced by the relative humidity (RH). Little oxidation occurs

at RH below 70%, but at higher RH relatively rapid oxidation and conversion to sulphuric acid occurs.

$$2SO_2 + 2H_2O + O_2 \rightarrow 2H_2SO_4 \quad (2.1)$$

$$S(IV) + \tfrac{1}{2}O_2 \rightarrow S(VI) \quad (2.2)$$

Chapter 3

Measurement locations, techniques and data analysis

3.1 Introduction

In this study the trace metal and water soluble inorganic ions present in atmospheric aerosols were investigated, together with ancillary data. In this chapter the measurement locations where sampling was conducted and the methods applied are presented.

3.2 Measurement locations

The three measurement sites, each with its own set of instrumentation, were considered in this study. A brief description of each site is presented in subsequent sections.

3.2.1 Cape Point

The Cape Point (CPT) station (34.21 S, 18.29 E) is managed by the South African Weather Service. It is part of the World Meteorological Organization's (WMO) Global Atmosphere Watch (GAW) network and is therefore of major importance to the international atmospheric and climate change research communities (Brunke *et al.*, 2010; Slemr *et al.*, 2011). The CPT GAW station has the longest atmospheric Hg measurement record in southern Africa. In this thesis, five years of continuous atmospheric Hg measurements at CPT GAW were analysed statistically. The station is located at the southern tip of the Cape Peninsula within the Cape Point National Park on top of a peak 230 m above sea level and about 60 km south of Cape Town. The station has been in operation since the end of the 1970s (Slemr *et al.*, 2008). The measurement site experiences moderate temperatures, dry summers with occasional biomass burning episodes in the surrounding area and increased precipitation during austral winter (Brunke *et al.*, 2010).

The dominant wind direction is from the south-eastern sector which is representative of clean maritime air from the Southern Ocean (Brunke *et al.*, 2004). CPT is, however, occasionally also subjected to air from the northern to north-eastern sector (mainly during the austral winter), which is influenced by anthropogenic emissions from the greater Cape Town area and/or by other continental sources (Brunke *et al.*, 2010). A picture of the CPT GAW measurement site facing in a northerly direction is presented in Figure 3.1.

Figure 3.1.: The Cape Point measurement station and mast at the southern tip of the Cape Peninsula within the Cape Point National Park in the background

3.2.2 Welgegund

The general characterisation of atmospheric trace metal and water soluble inorganic ions was studied at a regional background site, i.e. Welgegund. The Welgegund measurement station (26.341123 S, 26.562144 E, 1480m above mean sea level) is approximately 100 km southwest of Johannesburg. There are no major local pollution sources close to the measurement site. However, it is frequently impacted by air masses with pollution plumes from the Johannesburg-Pretoria megacity, the industrialised

western and eastern Bushveld Igneous Complex, the Vaal Triangle and the industrialised Mpumalanga Highveld (Tiitta *et al.*, 2014; Beukes *et al.*, 2013). No significant point sources exist to the west of Welgegund, therefore in addition to the source regions above, clean background air masses frequently arrive at the measurement station.

As discussed by Tiitta *et al.* (2014) and references therein, the large-scale meteorology in the region is characterised by an anti-cyclonic circulation pattern with a layered atmosphere due to limited vertical mixing (especially during winter months). Under specific synoptic conditions, air re-circulates over the sub-continent for up to 20 days (Tyson *et al.*, 1996).

Atmospheric hexavalent chromium, i.e. Cr(VI), was measured specifically at Welgegund, since this measurement site lies downwind on the dominant re-circulation path of air masses from the western Bushveld Complex, where numerous ferrochrome, base metal and platinum smelters are located. In Figure 3.2 a photo of the Welgegund measurement station and its general surroundings is presented.

Figure 3.2: The Welgegund atmospheric measurement station (www.welgegund.org)

3.2.3 Marikana

In order to contextualise the water-soluble inorganic ions measure at Welgegund (a regional background site) the same species were also measured at Marikana (25.69845 S, 27.48056 E, 1170 m above mean sea level), between Rustenburg and Brits in the North West Province. A mobile atmospheric measurement station was deployed here.

The measurement site was situated on the property of the Marikana Municipal clinic, which provided access to an electrical supply and also ensured the safekeeping of equipment. There were no mining and/or industrial activities within a 1 km radius of the site. The immediate surroundings included informal and semi-formal settlements, a formal residential area with a small commercial region, as well as untarred and tarred roads connecting the communities in this area. Geographically, Marikana is almost in the centre (east to west) of the southern section of the western Bushveld Igneous

Complex , south of the Pilanesberg crater. The western Bushveld Igneous Complex is well known as a highly industrialised area with numerous mining and metallurgical operations. Pyrometallurgical smelters were a major point source with other potential sources of air pollutants from the wind-blown dust from slimes or tailings dams, landfills, haul roads used by mining and large transport vehicles, and fugitive emissions (Venter *et al.*, 2012). A picture taken at dusk at the Marikana measurement station is presented in Figure 3.3, which clearly indicates a plume originating from household combustion travelling toward the measurement site.

Figure 3.3: The Marikana measurement station at dusk. A plume resulting from domestic heating and cooking can be seen as it disperses towards the measurement station

3.3 Measurement instrumentation

Sampling equipment utilised in this study and measurement instrumentation used to obtain ancillary data at each measurement location are subsequently discussed.

3.3.1 Cape Point

Continuous Hg measurements were conducted with a Tekran 2537A vapour-phase mercury analyser (Tekran Inc., Toronto, Canada) with a 15 minute time resolution. A description of the instrument, as well as its calibration and maintenance was presented by Slemr *et al.* (2008, 2013). The analyser is capable of measuring low Hg concentrations typically measured at background locations (Ebinghaus *et al.*, 1999), with a TGM detection limit of ~ 0.05 ngm^{-3}. Under the prevailing atmospheric conditions at the CPT GAW station, and due to the presence of hygroscopic sea salt aerosols, it can be assumed that the reactive gaseous mercury (RGM) will be adsorbed by the inlet tubing and the aerosol filter allowing for the exclusive measurement of atmospheric GEM (Brunke *et al.,* 2010). The 15-minute GEM data were converted to 30-minute averages in order to correlate the results with other trace gas and meteorological measurements at CPT GAW. As described by Brunke *et al.* (2004), the ^{222}Rn detector was designed by the Australian Nuclear Scientific & Technology Organisation (ANSTO) and was partially constructed locally. Trace gas measurements are drawn from the top of a 30m high mast located on the instrument deck of the laboratory. Several trace gases, i.e. carbon monoxide (CO), carbon dioxide (CO_2), methane (CH_4), ozone (O_3), nitrogen dioxide (NO_2) and halocarbons are measured at CPT GAW on a continuous basis. Of these, CO, CO_2, CH_4 and O_3 were used in this study. Detailed instrumental descriptions of these instruments and meteorological parameters measured can be found in previous publications (Brunke *et al.,* 1990, 2004, 2010). Ancillary measurements conducted at CP GAW are indicated in Table 3.1.

Table 3.1: Ancillary atmospheric measurements conducted at CPT GAW

Measured Property	Range
Meteorology	Temperature, relative humidity, wind speed and direction, ambient pressure, vertical temperature gradient and precipitation
Solar radiation	UV - A, UV - B, global (total & diffuse)
Trace gas concentrations	SO_2, CO, CO_2, CH_4, O_3, O_2 and N_2
Mercury	Total gaseous mercury, Gaseous elemental mercury
Tracer species	Rn^{222}, C^{13}, SF_6
Aerosol Mass	$PM_{2.5}$, PM_{10}
Light scattering of aerosol particles	3 - wavelength nephelometer
Light absorption of aerosol particles	Particle Soot Absorption Photometer

3.3.2 Welgegund

Aerosol particles were sampled from 24 November 2010 to 28 December 2011 and analysed to determine the composition of 32 trace metal species and nine water-soluble inorganic ionic species. A Dekati (Dekati Ltd., Finland) PM_{10} cascade impactor (ISO23210) equipped with PTFE filters was used to collect different size fractions ($PM_{2.5-10}$, $PM_{1-2.5}$ and PM_1). The flow rate at the pump was set to 30 $L.min^{-1}$. The sampling duration was one week. In total 54 weeks of samples were collected for all three size ranges. The filters were divided into two equal parts by a specially designed punching system, to enable analysis of both trace metals and inorganic ions using a single set of samples.

Samples collected for the analysis of hexavalent chromium were conducted by using a Partisol (Thermo Rupprecht Patashnick Model 2025) sequential air sampler for measurements of $PM_{2.5-10}$ and $PM_{2.5}$. The measurement campaign was from 1 June 2012 to 31 May 2013. Filter changes were done on a 24h basis. The flowrate was set to

14 L.min^{-1} and 1.67 L.min^{-1} for the PM_{10} and $PM_{2.5}$ size ranges, respectively. Ancillary measurements conducted at Welgegund are indicated in Table 3.2.

Table 3.2: Ancillary atmospheric measurements conducted at Welgegund

Measured Property	Range
Meteorology	Temperature, relative humidity, wind speed and direction, ambient pressure, vertical temperature gradient and precipitation
Solar radiation	Direct and reflected PPFD (PAR), global radiation and net radiation
Aerosol number size distribution	DMPS 10 - 840 nm
Air ion size distribution	AIS 0.4 - 40 nm
Aerosol Mass	PM_{10}
Trace gas concentrations	SO_2, NO, NO_x, O_3, CO
Light absorption of aerosol particles	Multi-angle aerosol absorption photometer
Light scattering of aerosol particles	3 - wavelength nephelometer
Vertical aerosol profile	Vaisala ceilometer
Flux measurements	H_2O, CO_2, SO_2, NO_2 and sensible heat fluxes
Soil measurements	Soil moisture and temperature at different depths, soil heat flux

In addition to the continuous measurements there have been short-term (one year or less) measurements of biogenic and anthropogenic VOCs, aerosol chemical composition and column concentrations of atmospheric trace gases.

3.3.3 Marikana

For the analysis of inorganic aerosol species, an Airmetrics MiniVol™ portable air sampler was used for sample collection. The MiniVol sampler collects simultaneously both PM_{10} and $PM_{2.5}$ samples (Airmetrics, 2011). A programmable timer controlled the pump in order to achieve a sample collection of twelve hours per day for six days, beginning at 06h00 for daytime, or at 18h00 for night time sampling. The exact sampling time was taken into account in concentration calculations. The filters were divided into two equal parts by a specially designed punching system, to be able to analyse both trace metals (Van Zyl *et al.*, 2014) and inorganic ions using a single set of samples. Ancillary measurements conducted at Marikana are indicated in Table 3.3.

Table 3.3: Ancillary air quality measurements conducted at Marikana

Measured Property	Range
Meteorology	Temperature, relative humidity, wind speed and direction, ambient pressure and precipitation
Solar radiation	Direct PPFD (PAR)
Aerosol number size distribution	DMPS 10 - 840 nm
Air ion size distribution	AIS 0.4 - 40 nm
Aerosol Mass	PM_{10}
Trace gas concentrations	SO_2, NO, NO_x, O_3, CO
Light absorption of aerosol particles	Multi-angle aerosol absorption photometer

3.4 Sample preparation and analysis

The analytical methods used in this study are presented in subsequent sections.

3.4.1 Trace metals

Aerosol samples collected for trace metal analysis were extracted by means of hot acid leaching from the filters for ICP-MS analysis (Mouli *et al.*, 2006). The method is summarised in the following bullet points:

- Place filter in a 100 mL Erlenmeyer flask
- Add 20 mL concentrated HNO_3 and 40 mL deionised water
- Boil for five minutes
- Reflux for three hours while stirring continuously
- Transfer cooled extract into a 100 mL volumetric flask
- Fill volumetric flask with deionised water up to the 100 ml mark

The filter material and Erlenmeyer flask were washed twice with deionised water to ensure that all extracted material was collected. As indicated by Van Zyl *et al.* (2014), ICP-MS analysis (Agilent 7500c) was conducted with the US EPA compendium method IO-3.5. Spectral interferences are effectively removed with the Octopole Reaction System (ORS) with an off-axis reaction cell. For ICP-MS analysis, 10 mL of the extraction solution was used. The radio frequency power was 1500 W, sample depth was 8 mm and the flow rate of the carrier gas was 1.05 $L.min^{-1}$. The following 32 trace metal species were analysed: Be, B, Na, Mg, Al, P, K, Ca, Ti, V, Cr, Mn, Fe, Co, Ni, Cu, Zn, As, Se, Sr, Mo, Pd, Ag, Cd, Sb, Ba, Pt, Au, Hg, Tl, Pb and U.

Metal concentrations that were below the detection limit of the ICP-MS were considered to have concentrations of half the detection limit of the specific metal species considered. This assumption is precautionary and is frequently made in health-related environmental studies (Polissar *et al.*, 1998).

3.4.2 Inorganic ions

The collected samples were leached in 5 ml of deionised water and placed in an ultrasonic bath for 30 minutes to achieve optimum sample availability. All dilutions and leaching were made up and done using deionised water (18mΩ). A Dionex ICS3000 ion chromatograph (IC) was used to analyse the samples from both Marikana and Welgegund. The IC was equipped with a 2mm×50mm IonPac AG18 guard column and

a 2 mm×250 mm IonPac AS18 analytical column. It was also equipped with ASRS 2 mm suppressor and 100 µL injection loop. The column temperature was kept at 30°C and the current at 18 mA. Potassium hydroxide was used as eluent and the flow rate was set to 0.250 mL.min^{-1}.

3.4.3 Gaseous elemental mercury

A Tekran 2537A vapour-phase mercury analyser manufactured by Tekran Inc., Toronto, Canada was used to measure gaseous mercury. The Tekran analyser is a continuous analyser that utilises two gold cartridges in parallel, with alternating operation modes (sampling and desorbing /analysing) on a predefined time base of 15-minutes. Due to the fact that Cape Point experiences high temperatures and air humidity, in addition to hygroscopic sea salt aerosols, it was taken that reactive gaseous mercury (RGM) was adsorbed by the inlet tubing and aerosol filter, and that the measured atmospheric mercury concentration thus represents exclusively gaseous elemental mercury (GEM) (Brunke *et al.*, 2010).

The analyser was operated in an air-conditioned laboratory and run with a sampling air flow rate of 1 l.p.m. at 15-minute sampling intervals. The air sample intake was attached to a 30-m high aluminium sampling mast at a height of approximately 5 m above the rocky surface and about 235 m above sea level. A Teflon filter (pore size 0.2 µm; ID = 45 mm) upstream of the instrument protected the analyser against contamination by particulate matter (Brunke *et al.*, 2012). The pre-filtered sample air stream is passed through gold cartridges where the mercury is collected. The trapped methylethyl mercury is thermally desorbed from the Carbotrap® trap into an inert (argon) gas stream that carries the released methylethyl mercury first through a pyrolytic decomposition column, which converts organo-mercury forms to elemental mercury (Hg^0), and then into the cell of a cold-vapour atomic fluorescence spectrometer (CVAFS) for detection (Tekran, 1998).

The mercury detection limit under these conditions is about 0.05 ng.m^{-3} and the span of the analyser is checked by an internal permeation source once every 25 h. The filter was replaced once every two weeks. All mercury data concentrations are given as ng.m^{-3} (STP) at a standard temperature of 273.16 K and pressure of 1013 mbar

(Brunke *et al.*, 2012). The accuracy and precision of this instrument has recently been assessed in measurements inter-comparisons performed at various locations (Ebinghaus *et al.*, 1999).

The 15 min mercury data have been converted to 30-min averages so that comparisons with other trace gas and meteorological data being measured simultaneously at Cape Point could be made

3.4.4 Hexavalent chromium

All chemicals used in this study were of analytical grade. Chemical species used in preparation, extraction and calibration were:

- A reference standard (Spectroscan) for calibration of the Cr(VI) analytical instrument (certified concentration of 1009 ± 5 $\mu g.mL^{-1}$ CrO_4^{2-}),
- Eluent consisting of ammonium sulphate (Merck) and a 25 % ammonia solution (Ace),
- Post-column reagent using 1,5-diphenylcarbazide (Fluka Analytical), 98 % sulphuric acid (Rochelle Chemicals), and HPLC grade methanol (Ace)
- Buffer (Na_2CO_3 – NaOH) for extracting Cr(VI) from samples, prepared from sodium hydroxide (Promark chemicals) and sodium carbonate (Minema),
- Dilution/cleaning was done with deionized water (resistivity 18.2 $M\Omega.cm^{-1}$) produced by a Milli-Q water purification system,
- Pure nitrogen (N_2) (99.999 %, AFROX) was used to purge all Cr(VI) extraction solutions and the headspace of extraction containers during leaching procedures.

As described by Du Preez *et al.* (2014) and references therein, total Cr(VI) was extracted from the filters into an aqueous phase without causing any inter-conversions between Cr(VI) and Cr(III). Both water soluble and water insoluble Cr(VI) compounds were extracted by conducting hotplate digestion extraction with a buffer solution (Ashley *et al.*, 2003). Ambient air in the hot alkaline extraction solution could potentially lead to in situ formation of Cr(VI) in the presence of Cr(III). Therefore, in order to prevent the unwanted oxidation of Cr(III), extraction solutions and the headspace of the extraction container were purged with N_2 prior to, during, and after Cr(VI) extraction (Ashley *et al.*, 2003; Du Preez *et al.*, 2014).

The analytical method utilized in this study was adapted from DIONEX Application updates 144 and 179, (Dionex, 2003; Dionex, 2011). The Cr(VI) content of extracted solutions was determined using a Thermo Scientific DIONEX ICS-3000 ion chromatograph (IC) with a post-column 1,5-diphenylcarbazide (DPC) colorant delivery system (AXP pump) coupled to a UV–visible absorbance detector, a Dionex IonPac AG7 4x50 mm guard column, Dionex IonPac AS7 4x250 mm analytic column, a 1000 µL injection coil, and two 375 µL reaction coils fitted in series with an isocratic pump that allowed for transport of injected samples through the system with the eluent (Du Preez *et al.*, 2014). To minimize the baseline noise of the chromatograms, additional polyetherketone tubing was installed between the AXP pump and the back pressure tubing, resulting in more accurate analyses, especially for lower Cr(VI) concentrations. A six-point calibration line (between 5 and 75 $\mu g.L^{-1}$) was used, which had a relative standard deviation <=1.8 pct and a correlation coefficient >=98.7 %. The detection limit was 0.9 $\mu g.L^{-1}$, which was determined from the baseline amplitude and the calibration sensitivity (slope of the calibration curve) according to the method described by Skoog *et al.* (2014) from a confidence factor that correlated with a 98.3% confidence level. By considering the volume of air sampled, the afore-mentioned detection limit in aqueous solution related to an atmospheric Cr(VI) detection limit of 0.84 $ng.m^{-3}$.

3.4.5 VOC analysis

VOCs were collected on 20 stainless steel adsorbent tubes (6.3 mm ED × 90 mm, 5.5 mm ID, Tenax-TA packing material) during the different phases of the braai experiment (Article 5, Chapter 8).

The first 1.25 m of the adsorbent tube inlet (made from stainless steel) was heated to 120 °C to remove O_3 that leads to sample degradation (Hellen *et al.*, 2012). A constant flow-type automated programmable pump sampler was used at a flow rate of 10 mL min^{-1}. After sampling, the tubes were removed and closed with Swagelok caps. Each tube was separately wrapped in aluminium foil and transported to the laboratory, where it was stored in a freezer.

The analyses and preparation of the adsorbent tubes were done by the Finnish Meteorological Institute as described by Jaars *et al.* (2014). The analysis was performed

with a thermal desorption (TD) system (Perkin-Elmer TurboMatrix™ 650, Waltham, USA) coupled to a gas chromatograph (GC) (Perkin-Elmer® Clarus® 600, Waltham, USA) with a mass spectrometer (MS) detector (Perkin-Elmer® Clarus® 600T,Waltham, USA).

Actual concentrations of all compounds reported in this paper were significantly higher than blank values and also well above the detection limits. Blank values were subtracted from exposed samples. The O_3 removal efficiency, leak tests and general quality assurance of the data has been previously described (Jaars *et al.*, 2014).

3.4.6 Organic compound analysis

A Dekati PM_{10} cascade impactor (ISO23210) equipped with quartz filters was used to collect particulates at a flow rate of 30 $L.min^{-1}$ in different size ranges during the braai experiment (Article 5, Chapter 8). After sampling, the filters were kept in a freezer until analysis. These filters were used to characterize and semi-quantify organic compounds.

As described by Booyens *et al*. (2015), each filter was extracted with a 1:1 mixture of methanol and acetone by utilizing dynamic ultrasonic assisted extraction. The extraction of the organic compounds present in the aerosol particles was completed within 40 min at a flow rate of 1 mL min^{-1}. The analysis was performed with a LECO Pegasus 4D and Agilent 7890 A two dimensional gas chromatograph coupled with a time-of-flight mass spectrometer (GCxGC-TOFMS) system.

The organic compounds were identified with LECO ChromaTOF and Guineu software according to mass spectral matches (similarity fits 700/1000) and retention indices *(I)* (*I* confidence intervals fewer than 150 units). Thereafter, the compounds were categorized according to their functional groups, i.e. hydrocarbons (alkanes, alkenes, alkynes, aromatics), oxygenated species (alcohols, ethers, aldehydes, ketones, carboxylic acids, esters), halogenated compounds (chloride (Cl), bromide (Br), iodine (I), fluorine (F)), as well as N and S-containing organic compounds. The organic compounds were semi-quantified, which is an approximation of the concentration of the organic compounds. In this study, 1-1'binaphthyl was used as an internal standard and the relative concentrations of the organic compounds were expressed as the sum of the normalized

response factors (SNRF), which is a measure of the detector response of an analyte compared to the internal standard. The calculation of these SNRF values is described in Booyens *et al*. (2015).

3.4.7 Additional material analysis during the braai plume characterisation

Similar to the procedures described by Kleynhans *et al*. (2012) randomly selected charcoal briquettes were pulverized to obtain a homogeneous composition for subsequent material characterization (based on ISO 13909-4:2001). Proximate analysis (air-dried basis) was performed to obtain moisture (SANS 5925:2007), ash (ISO 1171:2010) and volatile matter contents (ISO 562:2010), while ultimate analysis determined the total carbon (C), hydrogen (H), nitrogen (N), oxygen (O) (ISO 29541:2010) and sulphur (S) contents (ISO 19579:2006).

Representative samples of raw meat, i.e. one lamb chop and one beef sausage, were chemically analysed according to the guidelines of the association of official analytical chemists (AOAC) to determine the moisture (AOAC 950.46), ash (AOAC 923.03), total fat (AOAC 996.06), protein (Dumas Combustion Method), N (Dumas Combustion Method) and sodium (Na) (AOAC Method 984.27) contents.

3.5 Data analysis

Various statistical toolboxes included in the Matlab software package were used during data analyses. These are discussed in subsequent sections.

3.5.1 Cluster analysis

During cluster analysis, GEM data were processed in MATLAB by making use of the *k*-means function from the clustering toolbox. *K*-means clustering is an iterative partitioning method that uses squared Euclidean distances to partition a data matrix into *k* clusters. The centroid of each cluster is the mean of the points in that cluster. *K*-means uses a two-phase iterative algorithm to minimise the sum of point-to-centroid distances, summed over all *k* clusters. All GEM data considered, i.e. 41 499 measurements, were subjected to five consecutive iterations using cluster analysis.

Silhouette numbers obtained from the clustering were further considered to quantify the separation of the clusters. Silhouette numbers are a measure of how close individual points in a specific cluster are to points in the neighbouring clusters. The silhouette numbers range from +1, indicating points that are very distant from neighbouring clusters, through 0, indicating points that are not distinctly in one cluster or another, to -1, indicating points that are probably assigned to the wrong cluster.

3.5.2 Multi-linear regression

Multi-linear regression (MLR) analysis models the relationship between two or more explanatory independent variables and a dependent variable by fitting a linear equation to the observed data. The MLR equation obtained can be utilised to calculate values for the dependent variable. In this study, GEM values were considered the dependent variable, while 27 other ancillary data parameters (such as gaseous species concentrations and meteorological data) were considered the explanatory independent variables. MLR was used to determine the optimum combination of independent variables to derive an equation that could be used to predict GEM concentrations, while root mean square error (RMSE) was used to compare the calculated values with the measured values.

3.5.3 Principal Component / Factor Analysis

A combination of Principal Component Analysis (PCA) and Exploratory Factor Analysis (EFA) was used to determine the latent structure of the trace metal concentrations by discovering common factors. In this study PCA was computed as an approximation of EFA. Although PCA does not discriminate between common variance and unique variance (as in EFA), the percentage of explained variance in PCA was an immediate index of goodness of fit (Lorenzo-Seva, 2013). PCFA operates on sample-to-sample fluctuations of the transformed concentrations, and although PCFA does not directly yield concentrations of species from various sources, it identifies a minimum number of common factors (Van Zyl *et al.*, 2014).

The trace metal concentrations of the $PM_{2.5-10}$, $PM_{1-2.5}$ and PM_1 size fractions for samples collected at Welgegund were subject to Box-Cox transformation followed by subsequent principal component factor analysis PCFA with Varimax rotation (Kaiser,

1958). Values below the detection limit of the ICP-MS were considered to have concentrations half the detection limit of the species considered (Kulkarni *et al.*, 2007; Al-Momani *et al.*, 2005).

3.5.4 Air mass back trajectories

The origin of air masses arriving at CPT GAW was determined by making use of NCEP (National Centres for Environmental Prediction) GDAS (Global Data Assimilation System) data obtained from NOAA ARL (Air Resources Laboratory of National Oceanic and Atmospheric Administration, ftp://arlftp.arlhq.noaa.gov/pub/archives/gdas1/). Individual eight-day back trajectories with hourly arrival times at an arrival height of 100m were calculated with the Hybrid Single Particle Lagrangian Integrated Trajectory Model (HYSPLIT) 4.820. An arrival height of 100m was chosen since the orography in HYSPLIT is not very well-defined, and therefore lower arrival heights could result in increased error margins on individual trajectory calculations. Considering the above, 24 back trajectories for each day were obtained for the entire sampling period. Individual back trajectories generated in HYSPLIT (24 day^{-1} x 365 days x ~5 years) were superimposed and further analysed in MATLAB to form overlay back trajectory maps. In these overlay back trajectory maps, a colour code indicates the percentage of trajectories passing over 0.2^{o} x 0.2^{o} grid cells, with red being the highest percentage. Similar overlay back trajectory analyses have previously been conducted, e.g. Venter *et al.* (2012), Lourens *et al.* (2011) and Vakkari *et al.* (2013).

Chapter 4

Statistical exploration of gaseous elemental mercury (GEM) measured at Cape Point from 2007 to 2011

Author list and contributions

A. D. Venter[1], J. P. Beukes[1], P. G. van Zyl[*1], E.-G. Brunke[2], C. Labuschagne[2], F. Slemr[3], R. Ebinghaus[4], and H. Kock[4]

1 Unit for Environmental Sciences and Management, North-West University, Potchefstroom, South Africa

2 South African Weather Service, P.O. Box 320, Stellenbosch 7599, South Africa

3 Max-Planck-Institut für Chemie, Hahn-Meitner-Weg 1, 55128 Mainz, Germany

4 Helmholtz-Zentrum Geesthacht, Institute of Coastal Research, Max-Planck-Strasse, 21502 Geesthacht, Germany

Contributions of the various co-authors were as follows. The bulk of the work was done by the candidate A. D. Venter (including sample analysis, data processing, research and writing of the scientific article), with conceptual ideas and recommendations by the promoters P.G. van Zyl and J.P. Beukes. E.-G. Brunke and C. Labuschagne did the data collection while F. Slemr, R. Ebinghaus and H. Kock helped secure infrastructure and logistics at Cape Point for the mercury analyser.

Formatting and current status of article

The article is presented as published in *Atmospheric Chemistry and Physics*, a European Geosciences Union journal. The journal detail can be found at http://www.atmospheric-chemistry-and-physics.net (Date of access: 1 December 2015). The article was published on 16 September 2015.

Consent by co-authors

All the co-authors on the article have been informed that the PhD will be submitted in article format and have given their consent.

Atmos. Chem. Phys., 15, 10271–10280, 2015
www.atmos-chem-phys.net/15/10271/2015/
doi:10.5194/acp-15-10271-2015

Atmospheric Chemistry and Physics Open Access

Statistical exploration of gaseous elemental mercury (GEM) measured at Cape Point from 2007 to 2011

A. D. Venter[1], J. P. Beukes[1], P. G. van Zyl[1], E.-G. Brunke[2], C. Labuschagne[2], F. Slemr[3], R. Ebinghaus[4], and H. Kock[4]

[1]Unit for Environmental Sciences and Management, North-West University, Potchefstroom, South Africa
[2]South African Weather Service, P.O. Box 320, Stellenbosch 7599, South Africa
[3]Max-Planck-Institut für Chemie, Hahn-Meitner-Weg 1, 55128 Mainz, Germany
[4]Helmholtz-Zentrum Geesthacht, Institute of Coastal Research, Max-Planck-Strasse, 21502 Geesthacht, Germany

Correspondence to: P. G. van Zyl (pieter.vanzyl@nwu.ac.za)

Received: 8 December 2014 – Published in Atmos. Chem. Phys. Discuss.: 12 February 2015
Revised: 12 June 2015 – Accepted: 26 August 2015 – Published: 16 September 2015

Abstract. The authors evaluated continuous high-resolution gaseous elemental mercury (GEM) data from the Cape Point Global Atmosphere Watch (CPT GAW) station with different statistical analysis techniques. GEM data were evaluated by cluster analysis and the results indicated that two clusters, separated at 0.904 ng m^{-3}, existed. The air mass history for the two-cluster solution was investigated by means of back-trajectory analysis. The air mass back-trajectory net result showed lower GEM concentrations originating from the sparsely populated semi-arid interior of South Africa and the marine environment, whereas higher GEM concentrations originated predominately along the coast of South Africa that most likely coincide with trade routes and industrial activities in urban areas along the coast. Considering the net result from the air mass back-trajectories, it is evident that not all low GEM concentrations are from marine origin, and similarly, not all high GEM concentrations have a terrestrial origin. Equations were developed by means of multi-linear regression (MLR) analysis that allowed for the estimation and/or prediction of atmospheric GEM concentrations from other atmospheric parameters measured at the CPT GAW station. These equations also provided some insight into the relation and interaction of GEM with other atmospheric parameters. Both measured and MLR calculated data confirm a decline in GEM concentrations at CPT GAW over the period evaluated.

1 Introduction

Mercury (Hg) is a volatile metal emitted into the atmosphere, naturally or through anthropogenic activities, such as the combustion and processing of fossil fuels (Pirrone et al., 2010). It can be transported over large distances in the atmosphere due to its low reactivity and solubility. The removal of Hg from the atmosphere is facilitated mainly through wet deposition. This occurs when Hg is oxidised to less volatile and more soluble compounds (Lin et al., 2006). The deposited aqueous Hg compounds can then be converted into methylated Hg, which is a potent toxin for humans and animals. Methylated Hg bio-accumulates in the aquatic food chain and may lead to the build-up of high concentrations in predatory fish that can pose serious health risks to people and animals that depend on a fish diet (Mergler et al., 2007). These negative environmental impacts of Hg have led to an increase in atmospheric Hg research (Lindberg et al., 2007).

Current emission inventories and models indicate that anthropogenic emissions are the largest source of atmospheric Hg (2880 t yr^{-1}), followed by marine (2680 t yr^{-1}) and terrestrial (1850 t yr^{-1}) sources (Mason, 2009; Pirrone et al., 2010). Industrial coal combustion processes, which include electricity generation, petrochemical plants and gasification processes, are considered to be the major anthropogenic sources of atmospheric Hg (Laudal et al., 2000; Wagner, 2001). It is estimated that coal combustion accounts for approximately a third of anthropogenic Hg emissions in the United States of America (USA) (Laudal et al., 2000). Other main sources of anthropogenic Hg emissions include

non-ferrous metal production, gold refining, cement production and other combustion sources. The United States Environmental Protection Agency (US-EPA) introduced the Clean Air Mercury Rule in March 2005 enforcing the capping of mercury emissions from new and existing coal-fired power plants. The USA and European Union (EU) were among the first to regulate Hg pollution, and it is widely expected that this could significantly influence the way in which South Africa adopts Hg control legislation. In 2013, the Minamata Treaty was signed by South Africa and 98 other countries to protect human health and the environment from anthropogenic emissions and releases of elemental Hg and Hg compounds. It is expected that the Minamata Treaty will have far-reaching implications for South Africa, since it is globally considered to be the 6th largest emitter of mercury, emitting $\sim 50\,\mathrm{t\,yr^{-1}}$ due to the reliance on fossil fuels (Scott and Mdluli, 2012).

The global uncertainty associated with anthropogenic Hg emissions is considered to be $\pm 30\,\%$, while the uncertainties associated with emissions from oceans and terrestrial surfaces are $\pm 50\,\%$ (Lin et al., 2006; Lindberg et al., 2007). Long-term monitoring of Hg is important to reduce these uncertainties associated with Hg emissions from different sources, as well as to provide important information relating to the oxidation mechanism of atmospheric Hg (Slemr et al., 2008, 2013). Although atmospheric Hg is monitored extensively in the Northern Hemisphere, few studies have been published in peer-reviewed literature for the Southern Hemisphere (Ebinghaus et al., 2002; Slemr et al., 2011, 2015; Angot et al., 2014). The German Antarctic research station measured total gaseous Hg (TGM) from January 2000 to January 2001 (Ebinghaus et al., 2002). Gaseous elemental Hg (GEM) measurements have been conducted at the Cape Point Global Atmosphere Watch (CPT GAW) atmospheric monitoring station in South Africa since 1995 and have yielded several publications on long-term trends, depletion events, seasonal cycles and flux rates (Baker et al., 2002; Slemr et al., 2008; Brunke et al., 2010a, b). From 1995 until 2004, approximately 200 3-hour GEM samples have been collected each year with a manual double amalgamation technique (Slemr et al., 2008) at the CPT GAW station, while continuous high-resolution Hg measurements commenced in 2007.

In this paper, a combination of different statistical techniques was applied to continuous high-resolution Hg data collected between March 2007 and December 2011, as well as back-trajectory analyses that were performed in order to provide greater insight into the source regions of GEM at the CPT GAW station. This approach is different from previous studies of GEM measured at the CPT GAW station, where measurements of the most stable radon isotope (^{222}Rn) were used to determine the origin of air masses, i.e. maritime or continental (Brunke et al., 2004; Slemr et al., 2013). The relationship between GEM and other atmospheric parameters measured at the CPT GAW station was also determined statistically in order to establish whether GEM levels could be estimated or predicted from these parameters.

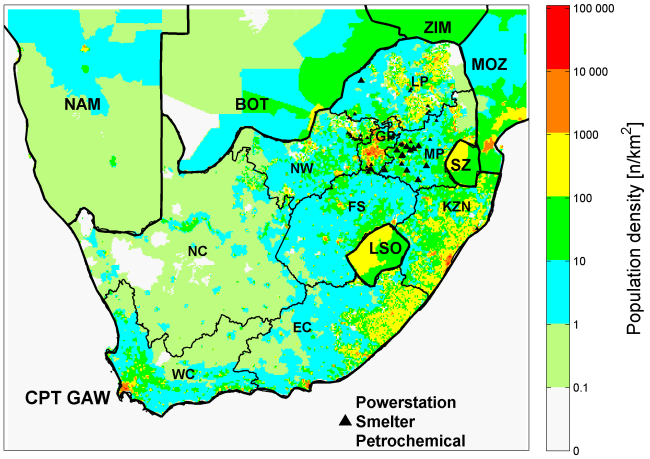

Figure 1. Position of CPT GAW within a regional context. The population density (people per km^2) provides an indication of the possible location of anthropogenic pollution sources, while the location of large anthropogenic point sources (e.g. coal-fired power stations, metallurgical smelters and petrochemical plants, adapted from Venter et al., 2012 and Lourens et al., 2011, 2012) is also indicated. NAM = Namibia, BOT = Botswana, ZIM = Zimbabwe, MOZ = Mozambique, SZ = Swaziland, LSO = Lesotho, WC = Western Cape, EC = Eastern Cape, NC = Northern Cape, NW = North West, FS = Free State, KZN = KwaZulu-Natal, GP = Gauteng, MP = Mpumalanga and LP = Limpopo.

2 Experimental

2.1 Site description

The CPT GAW station (34°21′ S, 18°29′ E) is located in a nature reserve approximately 60 km south of Cape Town at the southernmost tip of the Cape Peninsula on the top of a coastal cliff at 230 m above sea level. Its location within a regional context is indicated in Fig. 1. The site experiences moderate temperatures with dry summers during which occasional biomass burning events in the surrounding area occur and increased precipitation during the winter (Slemr et al., 2013). Figure 1 is a composite map indicating population density and major point sources (Lourens et al., 2011, 2012; Venter et al., 2012) in South Africa. Population density data were obtained from the Socioeconomic Data and Applications Center (SEDAC) – a data centre in the Earth Observing System Data and Information System (EOSDIS) of the National Aeronautics and Space Administration (NASA). As is evident from Fig. 1, the industrial hub of South Africa that is concentrated around the Johannesburg–Pretoria megacity conurbation (in the Gauteng Province (GP)) and a relatively high density of large point sources (e.g. coal-fired power plant, petrochemical operations, metallurgical

smelters) located in parts of the Mpumalanga (MP), North West (NW) and Free State (FS) provinces that border on GP, are somewhat remote from the CPT GAW station. The nearest large anthropogenic point or area sources that could impact the CPT GAW station directly include the Cape Town metropolitan area, industries associated with the conurbation and an iron smelter on the west coast at Saldanha.

2.2 Sampling

Continuous Hg measurements were conducted with a Tekran 2537A vapour-phase mercury analyzer (Tekran Inc., Toronto, Canada) with a 15-min time resolution. A description of the instrument, as well as its calibration and maintenance were presented by Slemr et al. (2008, 2013). The analyser is capable of measuring low Hg concentrations typically measured at background locations (Ebinghaus et al., 1999), with a TGM detection limit of $\sim 0.05\,\mathrm{ng\,m^{-3}}$. Under the prevailing atmospheric conditions at the CPT GAW station, and due to the presence of hygroscopic sea salt aerosols, it can be assumed that the reactive gaseous mercury (RGM) will be adsorbed by the inlet tubing and the aerosol filter allowing for the exclusive measurement of atmospheric GEM (Brunke et al., 2010b). The 15 min GEM data have been converted to 30 min averages in order to correlate the results with other trace gas and meteorological measurements at CPT GAW. As described by Brunke et al. (2004), the ^{222}Rn detector was designed by the Australian Nuclear Scientific, and Technology Organisation (ANSTO) and was partially constructed locally. Trace gas measurements are drawn from the top of a 30 m high mast located on the instrument deck of the laboratory. Several trace gases (carbon monoxide (CO); carbon dioxide (CO_2); methane (CH_4); ozone (O_3); nitrogen dioxide (NO_2)), and halocarbons are measured at CPT GAW on a continuous basis. Of these, CO, CO_2, CH_4 and O_3 are used in this paper. Detailed instrumental descriptions of these instruments and meteorological parameters measured can be found in previous publications (Brunke et al., 1990, 2004, 2010).

2.3 Statistical analysis

In contrast to previously published atmospheric measurements of the CPT GAW station, the data set used in this paper was not de-trended (Brunke et al., 2004). The complete data set (March 2007 to December 2011) was evaluated statistically in order to determine the influence and interaction of GEM and other atmospheric species on a temporal and spatial basis. The statistical techniques applied are subsequently discussed.

During cluster analysis, GEM data were processed in MATLAB® by making use of the *k*-means function from the clustering toolbox. *K*-means clustering is an iterative partitioning method that uses squared Euclidean distances to partition a data matrix into *k* clusters. The centroid of each cluster is the mean of the points in that cluster. *K*-means uses a two-phase iterative algorithm to minimise the sum of point-to-centroid distances, summed over all *k* clusters. All GEM data considered, i.e. 41 499 measurements, were subjected to five consecutive iterations using cluster analysis. Silhouette numbers obtained from the clustering were further considered to quantify the separation of the clusters. Silhouette numbers are a measure of how close individual points in a specific cluster are to points in the neighbouring clusters. The silhouette numbers range from $+1$, indicating points that are very distant from neighbouring clusters, through 0, indicating points that are not distinctly in one cluster or another, to -1, indicating points that are probably assigned to the wrong cluster.

Multi-linear regression (MLR) analysis models the relationship between two or more explanatory independent variables and a dependant variable by fitting a linear equation to the observed data. The MLR equation obtained can be utilised to calculate values for the dependent variable. In this study, GEM values were considered the dependent variable, while 27 other ancillary data parameters (such as gaseous species concentrations and meteorological data) were considered the explanatory independent variables. MLR was used to determine the optimum combination of independent variables to derive an equation that could be used to predict GEM concentrations, while root mean square error (RMSE) was used to compare the calculated values with the measured values.

2.4 Back-trajectory analysis

The origin of air masses arriving at CPT GAW was determined by making use of NCEP (National Centers for Environmental Prediction) GDAS (Global Data Assimilation System) data obtained from NOAA ARL (Air Resources Laboratory of National Oceanic and Atmospheric Administration, ftp://arlftp.arlhq.noaa.gov/pub/archives/gdas1/). Individual 8-day back trajectories with hourly arrival times at an arrival height of 100 m (above ground level) were calculated with the Hybrid Single Particle Lagrangian Integrated Trajectory Model (HYSPLIT) 4.820. An arrival height of 100 m was chosen since the orography in HYSPLIT is not very well defined, and therefore lower arrival heights could result in increased error margins on individual trajectory calculations. Considering the above, 24 back trajectories for each day were obtained for the entire sampling period. Individual back trajectories generated in HYSPLIT (24/day $\times$ 365 days $\times \sim 5$ years) were superimposed and further analysed in MATLAB® to form overlay back trajectory maps. In these overlay back trajectory maps, a colour code indicates the percentage of trajectories passing over $0.2^\circ \times 0.2^\circ$ grid cells, with red being the highest percentage. Therefore, such images indicate the main areas over which air masses arriving at CPT GAW had passed. Similar overlay back trajectory analyses have previously been used in other non-GEM

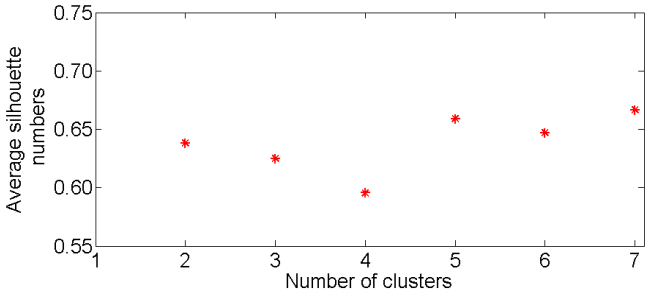

Figure 2. Average silhouette numbers for the various cluster solutions. An increase in silhouette numbers indicates that individual sub-clusters are better separated.

Table 1. The percentage GEM data distribution observed for each cluster solution.

	% GEM distribution in each cluster						
Cluster solutions	1	2	3	4	5	6	7
2	36.79	49.07					
3	3.35	41.34	41.18				
4	1.78	28.54	16.02	39.52			
5	18.37	0.05	27.27	38.47	1.70		
6	11.43	31.36	1.36	27.29	0.05	14.37	
7	1.51	1.23	29.62	11.34	16.76	25.38	0.02

related atmospheric studies, e.g. Venter et al. (2012), Lourens et al. (2011) and Vakkari et al. (2013).

3 Results

3.1 Cluster analysis

Cluster analysis of GEM data was performed to statistically determine the optimal number of clusters that the data could be divided into. The cluster analysis results were assessed by calculating the average silhouette numbers of each cluster solution. Figure 2 shows the average silhouette numbers for the various cluster solutions. According to these results, dividing the GEM data into two clusters yielded an average silhouette number of 0.638, while three or four cluster divisions yielded lower average silhouette numbers. The division of the GEM data into five to ten clusters yielded higher average silhouette numbers, which indicate better separation between clusters. In Table 1, the percentage GEM data distribution (columns) of each cluster solution (rows) is presented, and indicates that cluster solutions containing more than four clusters did not contain statistically significant amounts of GEM data in each cluster, e.g. the five-, six- and seven-cluster solutions all had clusters with $\leq 0.05\,\%$ of the data. Therefore, the two-cluster solution was chosen as the optimal representation for this study. The GEM data distribution in the two clusters for the entire sampling period is presented in

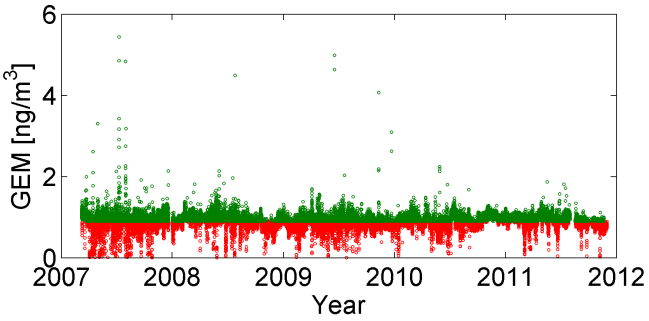

Figure 3. A scatter plot of GEM concentrations over the entire sampling period indicating the two main clusters. According to the clustering applied, division between the two clusters was at a GEM concentration of $0.904\,\mathrm{ng\,m^{-3}}$.

Fig. 3. According to the clustering approach applied, separation between the two clusters was at a GEM concentration of $0.904\,\mathrm{ng\,m^{-3}}$. Figure 3 also indicates a small number of data points with GEM concentrations $> \sim 2\,\mathrm{ng\,m^{-3}}$ that could be investigated as possible plume events, or special case studies. However, these possible higher concentration case studies were not considered in this paper, but may be an important topic to consider in future studies.

3.2 Source region analysis

In order to identify possible sources and/or source regions, the two clusters identified were further investigated by means of associating the arrival times of calculated back trajectories with the GEM data in the two different clusters. This was performed by correlating the GEM concentrations measured during the half hour before and the half hour after the hourly arrival time of the calculated back trajectory. Therefore, all the calculated back trajectories could be divided as being associated with one of the two GEM data clusters. The normalised (to 100 %) overlay back trajectory analysis map associated with GEM data cluster one, i.e. GEM concentration $> 0.904\,\mathrm{ng\,m^{-3}}$, is presented in Fig. 4a, while the overlay back trajectory analysis associated with cluster two, i.e. GEM concentration $< 0.904\,\mathrm{ng\,m^{-3}}$, is shown in Fig. 4b. From both of these overlay back trajectory maps, it is evident that CPT GAW is mainly influenced by air masses from the south west that had passed mainly over the marine background. It also seems as if the air masses associated with GEM concentrations < 0.904 ng $\mathrm{m^{-3}}$ (cluster two, Fig. 4b) have a slightly larger fetch region over the ocean than the air masses associated with GEM concentrations $> 0.904\,\mathrm{ng\,m^{-3}}$ (cluster one, Fig. 4a). However, significant differences between these two overlay trajectory maps, which could indicate possible differences in sources/source regions for the two GEM clusters, are not that evident. Therefore, a third overlay trajectory map (Fig. 4c) was drawn, which represents the difference between the two individual maps, i.e. subtracting the percentage of trajectories passing

over each correlating $0.2° \times 0.2°$ grid cell in Fig. 4b from the percentage of trajectories passing over each $0.2° \times 0.2°$ grid cell in Fig. 4a. In Fig. 4c, positive values (red) correspond with areas over which cluster one's ($> 0.904\,\mathrm{ng\,m^{-3}}$) air masses dominated, whereas negative values (dark blue) indicate areas over which air mass movement of cluster two ($< 0.904\,\mathrm{ng\,m^{-3}}$) were dominant. From this map (Fig. 4c), two observations can be made. Firstly, oceanic regions along both the east- and west coast around CPT GAW correspond with air masses mostly related to cluster one (higher GEM values), which could potentially indicate the influence of shipping routes on GEM measured at CPT GAW. Secondly, air masses that had passed over the very sparsely populated semi-arid Karoo region, almost directly to the north of CPT GAW, were mostly associated with cluster two (lower GEM values). The aforementioned differences in source regions for GEM did not seem to be associated with back trajectory heights, e.g. subsiding air masses from the free troposphere. It was found that the mean height of trajectories resulting in low and high GEM concentrations were almost identical, i.e. 1178 and 1104 m, respectively. A slight difference was observed for the mean air mass back trajectory maximum height, with the lower and higher GEM concentrations peaking at 2785 m and 2654 m, respectively. Similarly, the heights of trajectories passing over land (5 hours or more) were investigated. The mean heights of continental trajectories from cluster one (high GEM) and cluster two (low GEM) were 1490 and 1632 m, and the mean maximum heights of continental trajectories were 3352 and 3599 m, respectively.

The possibility of shipping routes contributing to the high GEM concentrations observed around the coast of South Africa was further investigated. From the Automated Mutual-Assistance Vessel Rescue System (AMVER) website, sponsored by the United States Coast Guard, Fig. 5 was obtained. In Fig. 5, the daily ship locations, derived from an average of 4634 ships per day, for July 2011 are presented in a density plot. The July 2011 timeframe was chosen since it was within the GEM data analysis period. The shipping route density plot indicated in Fig. 5 also closely correlates with NO_x shipping tracks characterised by satellite observations (Skjølsvik et al., 2000; Richter et al., 2011). The similarities of shipping route densities and NO_x shipping tracks, with the areas indicating additional contributions to higher GEM values (as indicated in Fig. 4c), provide credibility to the postulation that shipping around South Africa contributes meaningfully to GEM measured at CPT GAW.

Slemr et al. (2013) and Brunke et al. (2004) demonstrated how ^{222}Rn could be used to identify lower GEM concentrations that were associated with air masses passing over the marine background and higher GEM levels that were associated with a continental influence. In an effort to gain further insight into the difference between continental and marine background GEM concentrations at CPT GAW, the hourly arriving back trajectories calculated for the entire sampling period were divided into groups according to the time that

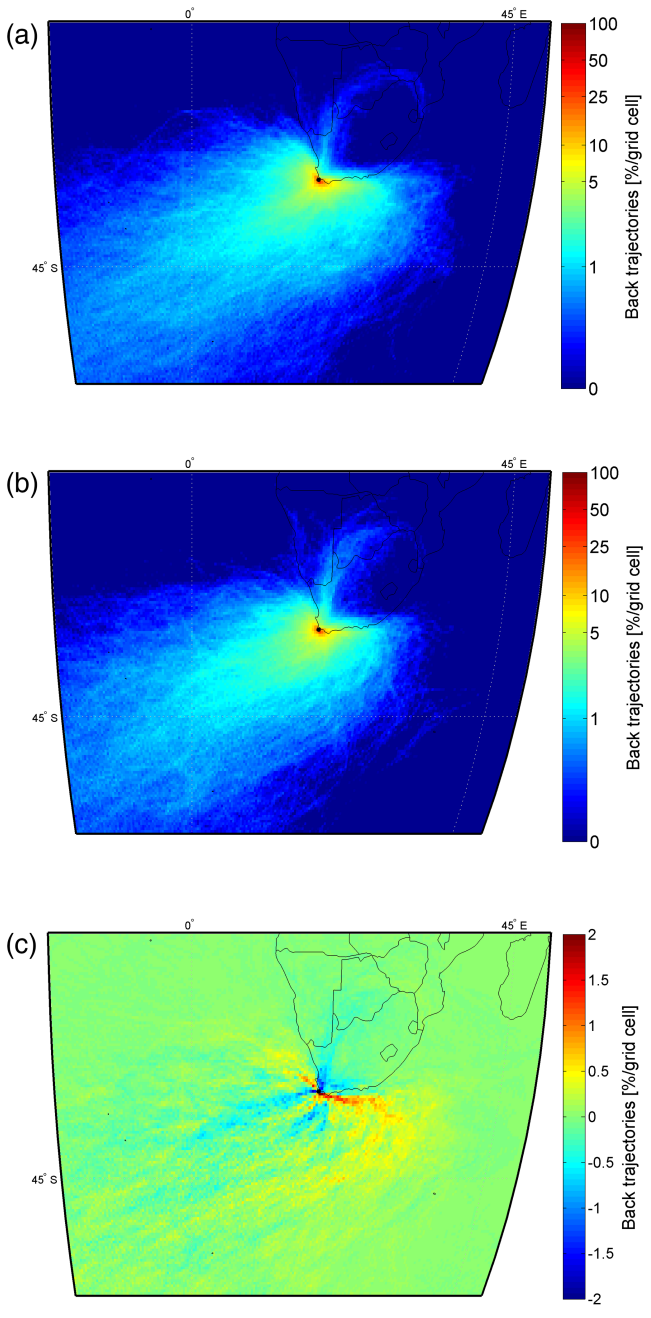

Figure 4. Normalised back trajectory analysis map, i.e. hourly arriving 8-day back trajectories with 100 m arrival height overlaid with MATLAB and normalised to percentage for the entire sampling period for, **(a)** cluster one, i.e. GEM concentration $> 0.904\,\mathrm{ng\,m^{-3}}$, **(b)** for cluster two, i.e. GEM concentration $< 0.904\,\mathrm{ng\,m^{-3}}$ and **(c)** the difference between the two individual maps, i.e. percentage of trajectories passing over each correlating $0.2° \times 0.2°$ grid cells in **(b)** subtracted from the percentage of trajectories passing over each $0.2° \times 0.2°$ grid cell in **(a)**. The colour bar indicates the percentage of trajectories passing over each grid cell.

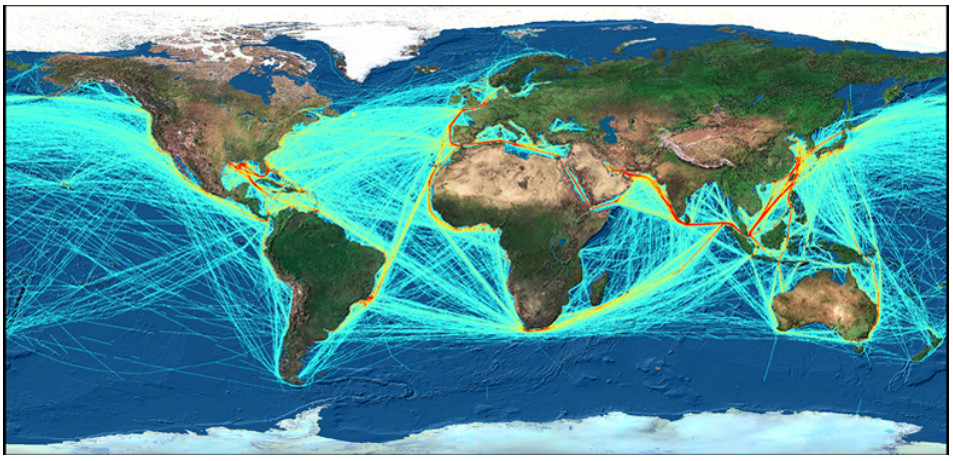

Figure 5. Monthly density plot for the total number of ships registered with Automated Mutual-Assistance Vessel Rescue System (AMVER) for July 2011. AMVER is sponsored by the United States Coast Guard and makes use of the global ship reporting system used worldwide by search and rescue authorities. The ship density plot is compiled from a 2011 average of 4634 ships per day (United States Coast Guard, 2014).

these air masses had spent over the African continent. The statistical distribution of GEM concentrations and the time that air masses spent over the continent are presented in Fig. 6a, while in Fig. 6b ^{222}Rn distribution as a function of time air masses spent over the continent is shown.

An evident trend is observed in Fig. 6a, i.e. an increase of GEM concentrations for air masses that spent more time over the continent. As expected, back trajectories of air masses spending shorter times over the continent were on average associated with the lowest GEM concentrations. However, these groups also had the largest spread in GEM concentrations ($\pm 0.6\,\mathrm{ng\,m^{-3}}$). This can at least partially be explained by uncertainties in the back trajectory calculations. During these calculations, a single hourly position of the air mass was determined for each of its 8-day backward positions. This relatively weak temporal resolution implies that an air mass could, for instance, have passed over the relatively nearby Cape Town conurbation, without being registered as spending any time over the continent. Additionally, the accuracy of trajectories depends on the quality of the underlying meteorological data used during the calculations. Considering the afore-mentioned limitations, the errors accompanying a single trajectory are currently estimated to be 15 to 30 % of the trajectory distance travelled (Vakkari et al., 2013; Stohl, 1998; Riddle et al., 2006). It is therefore possible that a trajectory could have spent a short period over the continent, without being calculated as such. Notwithstanding the possible errors associated with the calculation of individual back trajectories, the large number of trajectories calculated in this study (24/day $\times$ 365 days $\times \sim$ 5 years) ensures that the data obtained is statistically representative. The average marine background GEM concentration for the entire sampling period according to the ^{222}Rn level classification ($< 100\,\mathrm{mBq\,m^{-3}}$ – as proposed by Brunke et al., 2004) was $0.89 \pm 0.106\,\mathrm{ng\,m^{-3}}$, while the average GEM level for air masses that spent 1 hour or less over the continent (Fig. 6a) was $0.92 \pm 0.300\,\mathrm{ng\,m^{-3}}$. This indicates that the classification of air masses arriving at the CPT GAW station with back trajectory analysis correlates well with air mass classification according to ^{222}Rn levels. However, the ^{222}Rn classification method only allows for the separation of the CPT GAW GEM data into relatively few classes, i.e. marine background, mixed and continentally influenced, while the back trajectory analysis methods provide a more quantified classification based on the length of time that air masses spent over the continent resulting in increased GEM concentrations. It is evident from comparison between Fig. 6a and b that back trajectory analysis provides a more sensitive method of characterising GEM according to time that air masses spent over the continent up to 11 h (where GEM concentrations reached a plateau), while ^{222}Rn classification only allows separation within 3 hours that air masses spent over the continent. The difference in average GEM concentrations between air masses that had spent 1 hour or less over the continent, i.e. $0.92\,\mathrm{ng\,m^{-3}}$ and air masses that had spent more than 11 hours on the continent, i.e. $1.09 \pm 0.150\,\mathrm{ng\,m^{-3}}$, therefore provides some quantified indication of the possible continental contribution of GEM at CPT GAW. When GEM concentrations were classified according to ^{222}Rn levels, i.e. ^{222}Rn levels $> 1000\,\mathrm{mBq\,m^{-3}}$ indicating continentally influenced air masses (Slemr et al., 2013), 50 % of the data was greater than $0.92\,\mathrm{ng\,m^{-3}}$. This value is somewhat lower than the average concentration value determined for air masses spending more than 11 h over the continent, i.e. $1.09\,\mathrm{ng\,m^{-3}}$.

According to Jacob et al. (1997), the assumption of a uniform ^{222}Rn emission rate of $1\,\mathrm{atom\,cm^{-2}\,s^{-1}}$ is accurate to roughly 25 % globally, or by a factor of 2 regionally. Therefore the 15–30 % error associated with back trajectory

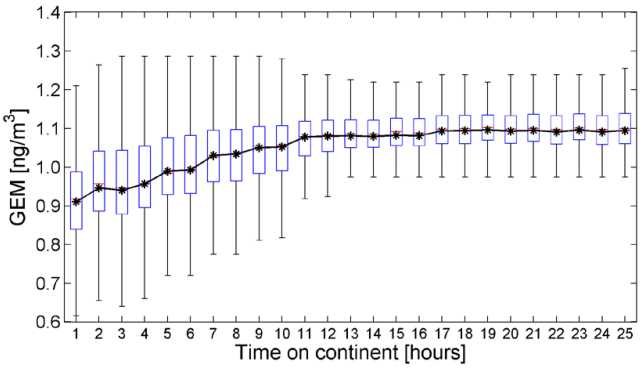

(a)

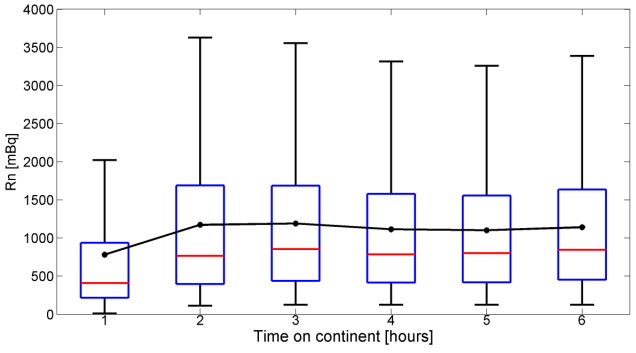

(b)

Figure 6. (a) The statistical distribution of GEM concentrations as a function of time spent over the continent and **(b)** ^{222}Rn distribution as a function time air masses spent over the continent. The mean is indicated by the black stars, the median by the red line, the 25- and 50 percentile by the blue box and the whiskers indicating 99.3 % data coverage (if a normal distribution is assumed), while the black line connects the mean values to provide an indication of the trend observed.

analysis is in the same range as the uncertainties associated with ^{222}Rn as tracer.

3.3 Relationship of GEM with other parameters

In an effort to determine relationships between atmospheric GEM concentrations and other atmospheric parameters measured at the CPT GAW station, as well as to establish whether GEM levels could be estimated or predicted from these parameters, multi-linear regression (MLR) analysis was conducted. In Fig. 7, the RMSE difference between the calculated and measured GEM values, as a function of the number of independent variables included in the optimum MLR solution, is presented. The linear equation containing only a single optimum independent variable, which was determined as absolute humidity, had an RMSE of $\sim$0.1250, while the RMSE was lowered to $\sim$0.1231 if an MLR equation containing the optimum combination of two independent variables, i.e. absolute humidity and O_3, was calculated. The RMSE

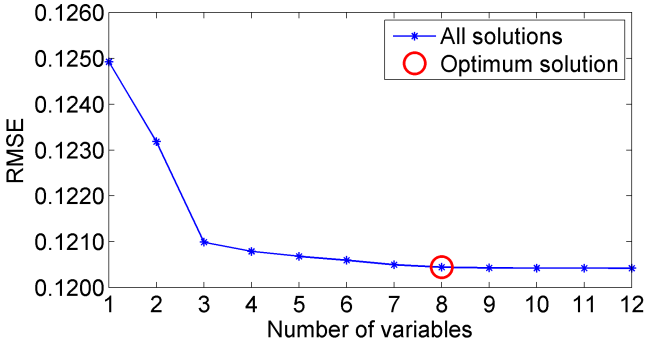

Figure 7. Determination of the optimum combination of independent variables to include in the MLR equation to calculate the dependant variable, i.e. GEM concentration (2007–2011). The root mean square error (RMSE) difference between the calculated and actual GEM concentrations indicated that the inclusion of eight parameters in the MLR solution was the optimum.

Table 2. The overall identity of independent variables during the determination of the optimum combination of independent variables for GEM calculation utilising the entire data set.

No of independent variables	MLR solutions for all GEM values							
1	AbsH							
2	AbsH	O_3						
3	AbsH	O_3	CO					
4	AbsH	O_3	CO	*P*				
5	AbsH	O_3	CO	*P*	*T*			
6	AbsH	O_3	CO	*P*	*T*	CH_4		
7	AbsH	O_3	CO	*P*	*T*	CH_4	Rn	
8	AbsH	O_3	CO	*P*	*T*	CH_4	Rn	WGS

difference between the experimental and calculated GEM values could further be reduced if the optimum MLR solution contained more independent variables. The optimised RMSE was attained when the number of independent variables included in the optimum solution of the equation was increased to eight, and had an RMSE of 0.1205. The measure of optimisation was taken as at least 1 % contribution to the overall reduction of RMSE. Table 2 indicates the identity of the independent parameters determined for each of the optimum MLR solutions.

The inclusion of more independent variables in the MLR solution did not significantly reduce the RMSE, and this can be seen in Fig. 7. A new MLR equation was determined with every addition of independent variables to determine the optimum variable combinations. This implies that new constants were calculated for all independent variables in each new optimum variable combination. Therefore, the afore-mentioned reductions in RMSE observed with an increase in the number of independent variables included in the optimum solution was an overall reduction of RMSE resulting from the increased number of independent variables included in the

combination and not due to the contribution of a single (or two) independent variable(s). The identity and constants associated with the independent variables in the identified optimum MLR solution to predict GEM, i.e. the dependant variable, are provided in Eq. (1):

$$\begin{aligned}\mathrm{GEM} = &-1.2308 + 1.492\times10^{-3}\mathrm{AbsH} - 3.790\times10^{-3}\\ &\mathrm{O_3} + 6.220\times10^{-4}\mathrm{CO} + 1.3630\times10^{-3}P\\ &+ 6.280\times10^{-3}T + 2.180\times10^{-4}\\ &\mathrm{CH_4} - 5.530\times10^{-6}\mathrm{Rn} - 1.110\times10^{-3}\mathrm{WGS},\end{aligned} \quad (1)$$

with GEM in ng m^{-3}, gaseous species (CO, CH_4, O_3 and CO_2) in ppb, T in °C, WGS indicating wind gust speed in km h^{-1}, AbsH the absolute humidity in g m^{-3} and P the ambient pressure in hectopascal (hPa). In Eq. (1), independent variables associated with positive constants indicate that an increase in these parameters would statistically lead to an increase in atmospheric GEM, whereas the increase in independent variables associated with negative constants would statistically lead to lower GEM. Although the MLR equations cannot be used to explicitly derive the origin and/or reaction mechanistic information about GEM at CPT GAW, it could be used to provide some insight.

The positive constants associated with CO and CH_4 could indicate that higher GEM can be attributed to anthropogenic emissions such as fossil fuel (e.g. shipping) and household combustion, as well as natural biomass burning observed during pollution events (Brunke et al., 2010a). Higher O_3 leads to higher hydroxyl (•OH) radical concentrations, therefore the possible negative constant associated with O_3. As discussed in Lan et al. (2012) and the references therein, GEM may be oxidised by •OH, nitrate (NO_3•) or halogen (X•) radicals. Gierens et al. (2014) recently indicated that •OH concentrations reach a peak around midday in the interior of SA, and since •OH has a lifetime of ∼ 1 s, its diurnal variation will therefore follow the diurnal variation of the UV radiation with wavelength capable to photolyse O_3 to O^1D, and therefore achieving peak GEM oxidation during midday. Additionally, the negative constant associated with O_3 in Eq. (2) could also indicate aged air masses, in which GEM decreased (e.g. by oxidation and deposition). The photochemically driven oxidation of GEM results in the formation of gaseous oxidised mercury (GOM). Particulate bound mercury (PBM) and GOM typically reach diurnal minima before sunrise and maxima in the afternoon (Lan et al., 2012). It has been suggested that an abundant halogen radical (X•) concentration present in the marine environment may lead to higher GOM concentrations (Mao and Talbot, 2012). The photochemically driven oxidation of GEM to GOM in summer depletes GEM levels during midday when solar radiation, O_3 levels and atmospheric halogens produced by sea spray are the most intense and would therefore explain negative constants in Eq. (1). This signifies the complex nature of the interaction between chemical species and the physical environment in the atmosphere.

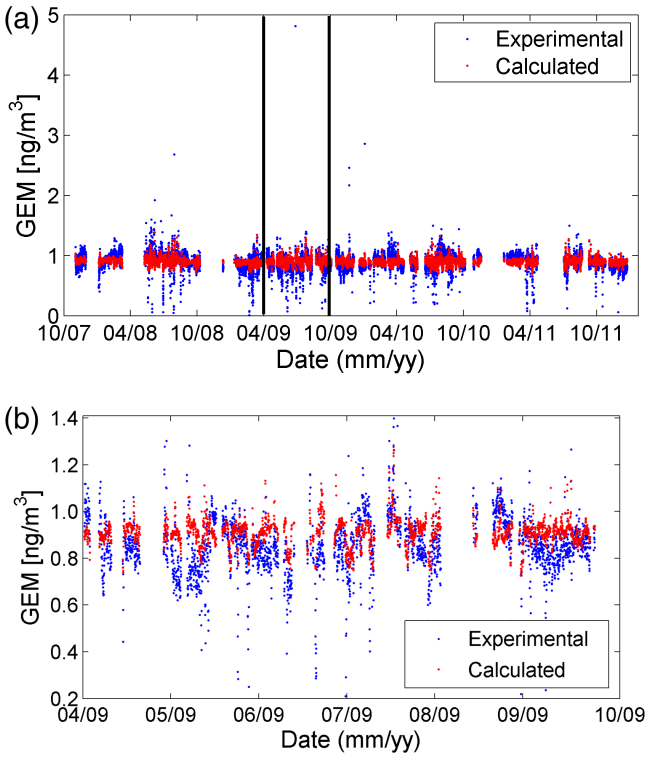

Figure 8. (a) Measured GEM (blue) and calculated GEM concentrations using the MLR Eq. (1) (red) for the entire sampling period. The two vertical black lines in **(a)** indicate a period that was enlarged in **(b)** to indicate more detailed differences between the measured and calculated GEM concentrations.

In addition to providing some insight into the origin and/or reactions of GEM at CPT GAW, it would also be useful to predict GEM at this site with the MLR Eq. (1). In Fig. 8, the measured time series for atmospheric GEM at CPT GAW are presented (blue markers) and compared to the GEM values calculated with Eq. (1) (red markers). Although slight differences are observed, the MLR equation predicts atmospheric GEM concentrations relatively well, with the exception of very high and low levels. Therefore, the MLR Eq. (1) could be used to predict GEM concentrations at CPT GAW if actual measurements thereof are not available.

Although not indicated in Fig. 8 (to prevent cluttering of the graph), linear fitting of the actual continuous measured and calculated (with Eq. 1) GEM concentrations indicated negative slopes of -5.579×10^{-6} and -1.391×10^{-5}, respectively. This indicates a slight decrease of GEM concentrations at CPT GAW over the evaluated period. Brunke et al. (2010a) previously also reported a decrease in GEM at CPT GAW from 1995 to 2009, but this reported decline only included approximately 2 years of continuous measurement. The decline observed for the longer time series reported here provides additional support to the observed decline. In con-

trast, Slemr et al. (2015) reported an increase in GEM concentration at CPT GAW. However, this increase was calculated by utilising pre-processed, i.e. de-trended and deseasonalised data, which was not the case in this study. Therefore these different approaches cannot be directly compared.

4 Conclusions

As far as the authors could assess, this is the first study that has evaluated continuous high-resolution GEM data of CPT GAW with different statistical analysis techniques. Cluster analysis on the data set indicated that the GEM data could be divided into two clusters, separated at atmospheric concentrations of 0.904 ng m^3. Trajectory analyses of the individual clusters, as well as the differences between these clusters, indicated that shipping around Cape Point could be a significant source of GEM. In contrast, low GEM concentrations originated from the southern oceanic background and terrestrial areas with very low anthropogenic activities/population density. Correlation of the time that back trajectories spent over the African continent and GEM concentration, proved that such analyses could be used as an alternative tool to distinguish between continental and marine GEM contributions.

It was also demonstrated that MLR analysis could be used to determine an equation that can be used to predict GEM at CPT GAW. Moreover, this equation provided some insight into the complex nature of GEM chemistry. Lastly, the evaluation of both continuously measured and calculated (with the determined MLR Eq. 1) GEM concentrations seem to indicate a decline in GEM concentrations over the period evaluated in this paper. It remains to be seen whether this decline continues, which would reflect a positive response to global Hg emission reductions, or if it is only part of a longer-term cycle with a temporary decline.

From this statistical study of continuous GEM measurement at Cape Point additional research questions and/or perspectives were identified. Data indicated as extreme events, as indicated by 5, 6 and 7 cluster solutions should be investigated as special case studies. Further research quantifying the contribution of shipping should be undertaken, not only for the southern African region, but also for other busy shipping routes. In addition, source apportionment should be conducted in order quantify the contribution of specific sources.

Acknowledgements. The authors would like to thank the South African Weather Service for making available the GEM data measured at CPT GAW. The financial assistance of the National Research Foundation (NRF) towards this research is hereby acknowledged. Opinions expressed and conclusions arrived at are those of the authors and are not necessarily to be attributed to the NRF.

Edited by: C. Barbante

References

Angot, H., Barret, M., Magand, O., Ramonet, M., and Dommergue, A.: A 2-year record of atmospheric mercury species at a background Southern Hemisphere station on Amsterdam Island, Atmos. Chem. Phys., 14, 11461–11473, doi:10.5194/acp-14-11461-2014, 2014.

Baker, P. G. L., Brunke, E.-G., Slemr, F., and Crouch, A. M.: Atmospheric mercury measurements at Cape Point, South Africa, Atmos. Environ., 36, 2459–2465, 2002.

Brunke, E.-G., Scheel, H. E., and Seiler, W.: Trends of tropospheric CO, N_2O and CH_4 as observed at Cape Point, South Africa, Atmos. Environ., 24A, 585–595, 1990.

Brunke, E.-G., Labuschagne, C., Parker, B., Scheel, H. E., and Whittlestone, S.: Baseline airmass selection at Cape Point, South Africa: application of ^{222}Rn and other filter criteria to CO_2, Atmos. Environ., 38, 5693–5702, doi:10.1016/j.atmosenv.2004.04.024, 2004.

Brunke, E.-G., Slemr, F., Ebinghaus, R., and Kock, H.: Atmospheric Mercury Measurements at Cape Point, South Africa, Clean Air J., 18, 17–21, 2010a.

Brunke, E.-G., Labuschagne, C., Ebinghaus, R., Kock, H. H., and Slemr, F.: Gaseous elemental mercury depletion events observed at Cape Point during 2007–2008, Atmos. Chem. Phys., 10, 1121–1131, doi:10.5194/acp-10-1121-2010, 2010b.

Ebinghaus, R., Jennings, S. G., Schroeder, W. H., Berg, T., Donaghy, T., Guentzel, J., Kenny, C., Kock, H. H., Kvietkus, K., Landing, W., Muhleck, T., Munthe, J., Prestbo, E. M., Schneeberger, D., Slemr, F., Sommar, J., Urba, A., Wallschlager, D., and Xiao, Z.: International field intercomparison measurements of atmospheric mercury species at Mace Head, Ireland, Atmos. Environ., 33, 3063–3073, 1999.

Ebinghaus, R., Kock, H. H., Temme, C., Einax, J. W., Lowe, A. G., Richter, A., Burrows, J. P., and Schroeder, W. H.: Antarctic springtime depletion of atmospheric mercury, Environ. Sci. Technol., 36, 1238–1244, 2002.

Gierens, R. T., Laakso, L., Mogensen, D., Vakkari, V., Beukes, J. P., Van Zyl, P. G., Hakola, H., Guenther, A., Pienaar, J. J., and Boy, M.: Modelling new particle formation events in the South African savannah, S. Afr. J. Sci., 110, 2013-0108, doi:10.1590/sajs.2014/20130108, 2014.

Jacob, D. J., Prather, M. J., Rasch, P. J., Shia, R.-L., Balkanski, Y. J., Beagley, S. R., Bergmann, D. J., Blackshear, W. T., Brown, M., Chiba, M., Chipperfield, M. P., de Grandpáe, J., Dignon, J. E., Feichter, J., Genthon, Ch., Grose, W. L., Kasibhatla, P. S., Kohler, I., Kritz, M. A., Law, K., Penner, J. E., Ramonet, M., Reeves, C. E., Rotman, D. A., Stockwell, D. Z., van Velthoven, P. F. J., Verver, G., Wild, O., Yang, H., and Zimmermann, P.: Evaluation and intercomparison of global atmospheric transport models using 222Rn and other short-lived tracers, J. Geophys. Res., 102, 5953–5970, 1997.

Lan, X., Talbot, R., Castro, M., Perry, K., and Luke, W.: Seasonal and diurnal variations of atmospheric mercury across the US determined from AMNet monitoring data, Atmos. Chem. Phys., 12, 10569–10582, doi:10.5194/acp-12-10569-2012, 2012.

Laudal, D. L., Pavlish, J. H., Graves, J., and Stockdill, D.: Mercury mass balances: A case study of two North Dakota Power Plants, J. Air Waste Manage. Assoc., 50, 1798–1804, 2000.

Lin, C.-J., Pongprueksa, P., Lindberg, S. E., Pehkonen, S. O., Byun, D., and Jang, C.: Scientific uncertainties in atmospheric mercury

models I: Model science evaluation, Atmos. Environ., 40, 2911–2928, 2006.

Lindberg, S., Bullock, R., Ebinghaus, R., Engstrom, D., Feng, X., Fitzgerald, W., Pirrone, N., Prestbo, E., and Seigneur, C.: A synthesis of progress and uncertainties in attributing the sources of mercury in deposition, Ambio, 36, 19–32, 2007.

Lourens, A. S. M., Beukes, J. P., van Zyl, P. G., Fourie, G. D., Burger, J. W., Pienaar, J. J., Read, C. E., and Jordaan, J. H.: Spatial and Temporal assessment of Gaseous Pollutants in the Mpumalanga Highveld of South Africa, S. Afr. J. Sci., 107, 269, doi:10.4102/sajs.v107i1/2.269, 2011.

Lourens, A. S. M., Butler, T. M., Beukes, J. P., van Zyl, P. G., Beirle, S., and Wagner, T.: Re-evaluating the NO_2 hotspot over the South African Highveld, S. Afr. J. Sci., 108, 1146, doi:10.4102/sajs.v108i11/12.1146, 2012.

Mao, H. and Talbot, R.: Speciated mercury at marine, coastal, and inland sites in New England – Part 1: Temporal variability, Atmos. Chem. Phys., 12, 5099–5112, doi:10.5194/acp-12-5099-2012, 2012.

Mason, R. P.: Mercury emissions from natural processes and their importance in the global mercury cycle, Springer, New York, USA, 2009.

Mergler, D., Anderson, H. A., Chan, L. H. M., Mahaffey, K. R., Murray, M., Sakamoto, M., and Stern, A. H.: Methylmercury exposure and health effects in humans: A worldwide concern, Ambio, 36, 3–11, 2007.

Pirrone, N., Cinnirella, S., Feng, X., Finkelman, R. B., Friedli, H. R., Leaner, J., Mason, R., Mukherjee, A. B., Stracher, G. B., Streets, D. G., and Telmer, K.: Global mercury emissions to the atmosphere from anthropogenic and natural sources, Atmos. Chem. Phys., 10, 5951–5964, doi:10.5194/acp-10-5951-2010, 2010.

Richter, A., Begoin, M., Hilboll, A., and Burrows, J. P.: An improved NO_2 retrieval for the GOME-2 satellite instrument, Atmos. Meas. Tech., 4, 1147–1159, doi:10.5194/amt-4-1147-2011, 2011.

Riddle, E. E., Voss, P. B., Stohl, A., Holcomb, D., Maczka, D., Washburn, K., and Talbot, R. W.: Trajectory model validation using newly developed altitude-controlled balloons during the International Consortium for Atmospheric Research on Transport and Transformations 2004 campaign, J. Geophys. Res., 111, D23S57, doi:10.1029/2006JD007456, 2006.

Scott, G. M. and Mdluli, T. N.: The Minamata Treaty/Protocol: Potential Implications for South Africa, Clean Air J., 22, 17–19, 2012.

Skjølsvik, K. O., Andersen, A. B., Corbett, J. J., and Skjelvik, J. M.: Study of Greenhouse Gas Emissions from Ships, 2nd Edn., Norwegian Marine Technology Research Institute, Trondheim, 2000.

Slemr, F., Brunke, E.-G., Labuschagne, C., and Ebinghaus, R.: Total gaseous mercury concentrations at the Cape Point GAW station and their seasonality, Geophys. Res. Lett., 35, L11807, doi:10.1029/2008GL033741, 2008.

Slemr, F., Brunke, E.-G., Ebinghaus, R., and Kuss, J.: Worldwide trend of atmospheric mercury since 1995, Atmos. Chem. Phys., 11, 4779–4787, doi:10.5194/acp-11-4779-2011, 2011.

Slemr, F., Brunke, E.-G., Whittlestone, S., Zahorowski, W., Ebinghaus, R., Kock, H. H., and Labuschagne, C.: ^{222}Rn-calibrated mercury fluxes from terrestrial surface of southern Africa, Atmos. Chem. Phys., 13, 6421–6428, doi:10.5194/acp-13-6421-2013, 2013.

Slemr, F., Angot, H., Dommergue, A., Magand, O., Barret, M., Weigelt, A., Ebinghaus, R., Brunke, E.-G., Pfaffhuber, K. A., Edwards, G., Howard, D., Powell, J., Keywood, M., and Wang, F.: Comparison of mercury concentrations measured at several sites in the Southern Hemisphere, Atmos. Chem. Phys., 15, 3125–3133, doi:10.5194/acp-15-3125-2015, 2015.

Stohl, A.: Computation, accuracy and application of trajectories – a review and bibliography, Atmos. Environ., 32, 947–966, 1998.

United States Coast Guard: AMVER, available at: http://www.amver.com/, last access: 17 November 2014.

Vakkari, V., Beukes, J. P., Laakso, H., Mabaso, D., Pienaar, J. J., Kulmala, M., and Laakso, L.: Long-term observations of aerosol size distributions in semi-clean and polluted savannah in South Africa, Atmos. Chem. Phys., 13, 1751–1770, doi:10.5194/acp-13-1751-2013, 2013.

Venter, A. D., Vakkari, V., Beukes, J. P., van Zyl, P. G., Laakso, H., Mabaso, D., Tiitta, P., Josipovic, M., Kulmala, M., Pienaar, J. J., and Laakso, L.: An air quality assessment in the industrialized western Bushveld Igneous Complex, South Africa, S. Afr. J. Sci., 108, 1059, doi:10.4102/sajs.v108i9/10.1059, 2012.

Wagner, N. J.: Trace Elements in coal, their analysis and environmental impact, Literature Survey, SASOL R&D, Sasolburg, 2001.

Chapter 5

Regional atmospheric Cr(VI) pollution from the Bushveld Complex, South Africa

Author list and contributions

Andrew Derick Venter[1], Johan Paul Beukes[1*], Pieter Gideon van Zyl[1], Miroslav Josipovic[1], Kerneels Jaars[1] and Ville Vakkari[2]

1 Unit for Environmental Sciences and Management, North-West University, Potchefstroom, South Africa

2 Finnish Meteorological Institute, Research and Development, FI-00101 Helsinki, Finland

Contributions of the various co-authors were as follows. The bulk of the work was done by the candidate A. D. Venter (including sample analysis, data processing, research and writing of the scientific article), with conceptual ideas and recommendations by the promoters J.P. Beukes and P.G. van Zyl. The candidate (A.D. Venter), M. Josipovic and K. Jaars helped gather data at the Welgegund measurement station, while V. Vakkari helped create the infrastructure at Welgegund and made conceptual contributions.

Formatting and current status of article

The article is presented as published in *Atmospheric Pollution Research*, an Elsevier journal. The journal detail can be found at http://www.journals.elsevier.com/atmospheric-pollution-research/ (Date of access: 4 May 2016). The article was accepted on 31 March 2016 and presented as "in press".

Consent by co-authors

All the co-authors on the article have been informed that the PhD will be submitted in article format and have given their consent.

Atmospheric Pollution Research xxx (2016) 1–6

HOSTED BY

ELSEVIER

Contents lists available at ScienceDirect

Atmospheric Pollution Research

journal homepage: http://www.journals.elsevier.com/locate/apr

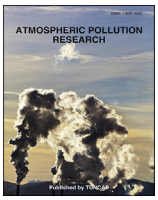

Short communication

Regional atmospheric Cr(VI) pollution from the Bushveld Complex, South Africa

Andrew Derick Venter [a], Johan Paul Beukes [a, *], Pieter Gideon van Zyl [a], Miroslav Josipovic [a], Kerneels Jaars [a], Ville Vakkari [b]

[a] Unit for Environmental Sciences and Management, North-West University, Potchefstroom, South Africa
[b] Finnish Meteorological Institute, Research and Development, FI-00101, Helsinki, Finland

ARTICLE INFO

Article history:
Received 20 November 2015
Received in revised form
28 February 2016
Accepted 31 March 2016
Available online xxx

Keywords:
Hexavalent chromium
Cr(VI)
Welgegund atmospheric research station
Atmospheric transport
Ferrochromium

ABSTRACT

Hexavalent chromium, Cr(VI), is a proven human carcinogen. Of interest in this paper was the regional atmospheric pollution of Cr(VI) from the ferrochromium and related industries located in the western Bushveld Complex (wBC) of South Africa. A significant fraction of the world's ferrochromium and platinum group metals is produced in this region. Particulate matter (PM), in two size fractions, i.e. $PM_{2.5}$ ($\leq$2.5 μm) and $PM_{2.5-10}$ (2.5–10 μm), was sampled for a full calendar year at a regional background site, which is situated downwind of the wBC on the dominant anti-cyclonic recirculation route of air mass over the South African interior. Results indicated that Cr(VI) concentrations in air masses that had passed over the regional background were below the detection limit of the analytical technique applied, but that Cr(VI) in air masses that had passed over the wBC were elevated and had a median concentration of 4.6 ng/m^3. The majority of Cr(VI) was found to be in the finer size fraction ($PM_{2.5}$), which could be explained by the nature of Cr(VI)-containing PM being emitted by the sources in the wBC and the atmospheric lifetimes of different PM size fractions. The results further indicated that it is possible that not only pyrometallurgical sources in the wBC, but also other combustion sources outside the wBC contributed to the observed atmospheric Cr(VI) concentrations.

1. Introduction

Hexavalent chromium, i.e. Cr(VI), is a proven human carcinogen, particularly affecting the respiratory system (Beaver et al., 2009). Cr(VI) pollution is of international interest, since many countries are affected, e.g. the United States of America (Oze et al., 2004), New Caledonia (Oze et al., 2004), Mexico (Robles-Camacho and Armienta, 2000), India (Dubey et al., 2001) and South Africa (Loock et al., 2014).

Various anthropogenic (e.g. Loock et al., 2014; Du Preez et al., 2015; Mandiwana et al., 2007) and natural (e.g. Panichev et al., 2008; Oze et al., 2004, 2007; Steinpress et al., 2004; Robles-Camacho and Armienta, 2000) activities can lead to Cr(VI) pollution. Of particular interest in this paper is the regional atmospheric pollution of Cr(VI) associated with the ferrochromium (FeCr) and related industries in South Africa. FeCr is a relatively crude alloy, consisting principally of Cr and iron (Fe). It is used mainly for the production of stainless steel that is a vital modern alloy. FeCr is mainly produced by the carbo-thermic reduction of chromite ore, mostly in submerged arch furnaces (SAFs) or direct current furnaces (DCFs) (Beukes et al., 2010). Chromite, a mineral with a spinel crystal structure, is the only commercially viable source of new Cr units. South Africa holds a significant portion of the world's viable chromite ore resources (Kleynhans et al., 2012 and references therein) and is the second largest FeCr-producing country (Beukes et al., 2012 and references therein). In South Africa, there are 14 separate FeCr-producing smelters, each with two to six large SAFs and/or DCFs (Beukes et al., 2012). Most of the afore-mentioned smelters are concentrated in or close to the Bushveld Complex (name of the geological structure), wherein the South African chromite deposits occur. The Bushveld Complex is the world's largest chromium and platinum group metals deposit, also with significant reserves of other metals such as vanadium (Xiao and

* Corresponding author.
E-mail address: paul.beukes@nwu.ac.za (J.P. Beukes).

Peer review under responsibility of Turkish National Committee for Air Pollution Research and Control.

http://dx.doi.org/10.1016/j.apr.2016.03.009

Please cite this article in press as: Venter, A.D., et al., Regional atmospheric Cr(VI) pollution from the Bushveld Complex, South Africa, Atmospheric Pollution Research (2016), http://dx.doi.org/10.1016/j.apr.2016.03.009

Laplante, 2004; Moskalyk and Alfantazi, 2003). The production of FeCr is a reducing process, during which Cr(III) in the ore is reduced to Cr(0). However, small amounts of Cr(VI) are unintentionally generated by various processing steps applied by the FeCr industry (Du Preez et al., 2015; Beukes et al., 2010, 2012; Mandiwana et al., 2007; Beukes and Guest, 2001). South Africa is also one of the largest platinum group metals (PGMs) producers (Xiao and Laplante, 2004). Apart from the FeCr industry, the PGM mining and metallurgical refining industries in South Africa also consume significant volumes of chromite ore (Xiao and Laplante, 2004; Cramer et al., 2004). Considering that PGMs are primarily used in the manufacturing of automotive catalytic converters to improve air quality reinforces the notion that the Bushveld Complex is not only of national, but also of international importance.

The western limb of the Bushveld Complex (wBC) is the most exploited, with 11 pyrometallurgical smelters occurring within an approximate 55 km radius (Venter et al., 2012; Hirsikko et al., 2012). Venter et al. (2012) indicated that air quality in the wBC is problematic, with ozone (O_3) and particulate matter (PM) with aerodynamic diameter less than 10 μm (PM_{10}) regularly exceeding the limits prescribed by the South African national ambient air quality standards (NAAQS). Hirsikko et al. (2012) indicated that high amounts of Aitken (20–100 nm in diameter) and accumulation (100–840 nm in diameter) mode particles in the morning and evening originate from household combustion for space heating and cooking from the numerous semi- and informal settlements that are in the wBC, while, during daytime, SO_2-based nucleation followed by condensational growth by vapours from anthropogenic and natural sources resulted in a large number of concentrations of nucleation (1–20 nm in diameter) and Aitken mode particles. Relatively recently, the wBC was also included in a declared air pollution hotspot in terms of the South African National Environmental Management Act (NEMA): Air Quality, termed the Waterberg Priority Area (www.environment.gov.za/sites/default/files/gazetted_notices/nemaqa_waterberg_declaration_g35435gen495.pdf, accessed 28 February 2016). The proclamation of such a priority area indicates that the South African government recognises that air quality standards in this area are regularly exceeded and that improvement in air quality is required.

Notwithstanding the national and international importance of the wBC, the known air quality issues therein and the potential for atmospheric Cr(VI) pollution from there, an assessment of regional atmospheric Cr(VI) pollution from the wBC has not yet been undertaken. In order to at least partially address this knowledge gap, sampling and Cr(VI) analyses were performed at the Welgegund atmospheric research station (www.welgegund.org).

2. Measurement site and methods

2.1. Sampling

In the atmosphere, Cr(VI) is associated with PM, since the vapour pressure of all Cr compounds at ambient conditions is negligible (Kimbrough et al., 1999; Seigneur and Constantinou, 1995). All inter-conversion reactions leading to possible Cr(VI) formation and reduction to Cr(III) are water phase reactions (Kimbrough et al., 1999; Seigneur and Constantinou, 1995). Wet deposition of atmospheric Cr(VI) was not specifically considered in this work, although it is likely that solubilised Cr(VI) will be reduced to Cr(III) (Kimbrough et al., 1999; Seigneur and Constantinou, 1995). Considering the afore-mentioned, only Cr(VI) occurring in PM was evaluated, since the dispersion of PM would be the principal mode of regional Cr(VI) distribution.

Starting at 00:00 am local South African time, daily 24-h $PM_{2.5}$ (≤2.5 μm) and $PM_{2.5-10}$ (2.5–10 μm) samples were automatically collected on 47 mm PTFE filters (GIC Scientific) with a Dichotomous Partisol sampler (Rupprecht & Patashnick Co., Inc.) for a full calendar year, i.e. 1 June 2012–31 May 2013. The flows through the afore-mentioned size fractions were, 10.0 and 6.7 L/min, respectively, with the overall flow being 16.7 L/min. Sampling was conducted without a denuder, which implies that reactive gases that could lead to Cr(III) oxidation was not removed. Previously published results indicated that sampling without a denuder could lead to conversion of Cr(III) in excess of 10% (Mennen et al., 1998). The results reported in this paper should therefore be considered within the limitations of the sampling method applied. However, as will be indicated in subsequent sections, adequate preventative measures were applied during sampling extraction to prevent any inter-conversions between Cr(VI) and Cr(III).

Sampling was conducted at the Welgegund atmospheric research station (latitude 26°34′10″S, longitude 26°56′21″E, 1480 m AMSL), which is situated approximately 100 km west from Johannesburg on a commercial farm. Numerous authors have previously described this research station, its surroundings and the measurements conducted (Booyens et al., 2015; Jaars et al., 2014; Tiitta et al., 2014; Vakkari et al., 2014). For this investigation, Welgegund was a particularly good measurement site for two reasons. Firstly, Welgegund is situated approximately 105 km downwind of the nearest pyrometallurgical smelter in the wBC on the dominant anti-cyclonic recirculation route of air mass over the interior of South Africa (Garstang et al., 1996). This implies that the site is ideally positioned to determine the regional effect of air masses that had passed over the wBC. Secondly, Welgegund is considered to be a regionally representative background site with no direct impacts from pollution sources in close proximity.

Fig. 1 indicates the location of Welgegund within a regional southern African context and the extent of the Bushveld Complex ore deposits (greyscale areas on the southern African map). Additionally, in the zoomed-in map, the locations of large pyrometallurgical smelters in the wBC, the Johannesburg-Pretoria (Jhb-Pta) megacity (Lourens et al., 2012) and large atmospheric point sources (e.g. coal-fired power stations, petrochemical operations and pyrometallurgical smelters) in the interior of South Africa are indicated.

2.2. Cr(VI) extraction and analysis

Ultra-pure water (resistivity 18.2 MΩ cm^{-1}), produced by a Milli-Q water purification system, was used during all procedures requiring dilution, as well as to clean all glassware used. A buffer solution (Na_2CO_3–NaOH) to extract Cr(VI) from samples was prepared from sodium hydroxide (Promark chemicals) and sodium carbonate (Minema). Nitrogen (N_2) (99.999% pure, from AFROX) was used to purge all Cr(VI) extraction solutions and the headspace of extraction containers during leaching procedures. Diphenylcarbazide (DPC) (Fluka), high pressure liquid chromatography (HPLC) grade methanol (Sigma Aldrich) and 98% analytical grade sulphuric acid (Rochelle Chemicals) were used during the Cr(VI) analysis.

Total Cr(VI) was extracted from the filters into the aqueous phase with appropriate precautions taken to prevent any inter-conversions between Cr(VI) and Cr(III) (Ashley et al., 2003). Both water-soluble and water-insoluble Cr(VI) compounds were extracted by conducting hotplate digestion extraction with a buffer solution (Ashley et al., 2003). Ambient air in the hot alkaline extraction solution could potentially lead to the in situ formation of Cr(VI) in the presence of Cr(III). Therefore, in order to prevent the unwanted oxidation of Cr(III), the extraction solutions and the headspace of the extraction containers were purged with N_2 prior to, during, and after Cr(VI) extraction (Ashley et al., 2003; Du Preez

Please cite this article in press as: Venter, A.D., et al., Regional atmospheric Cr(VI) pollution from the Bushveld Complex, South Africa, Atmospheric Pollution Research (2016), http://dx.doi.org/10.1016/j.apr.2016.03.009

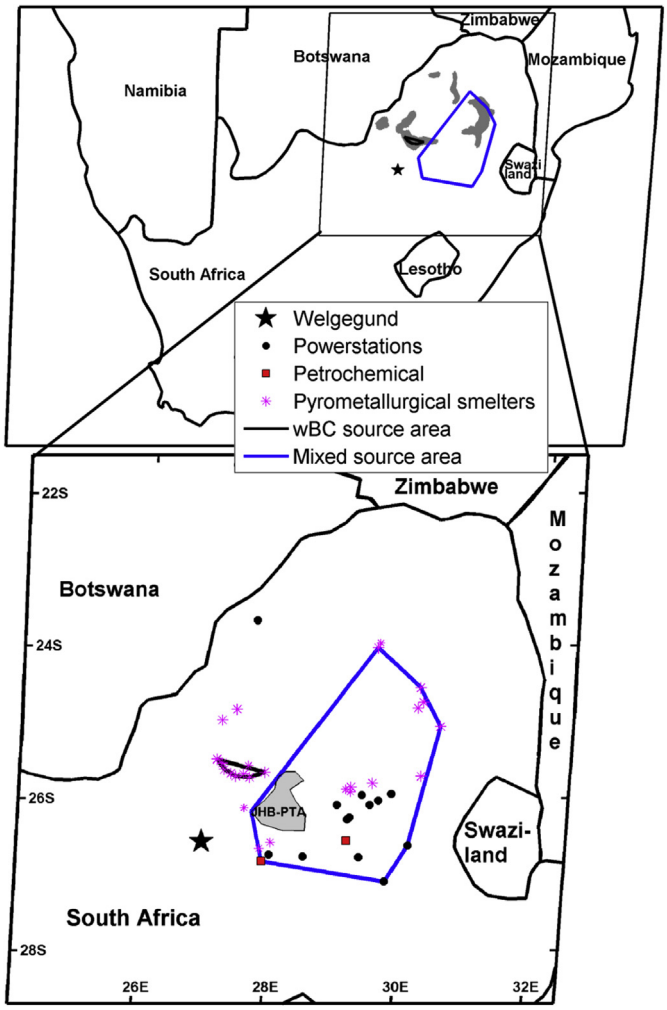

Fig. 1. The location of Welgegund within a regional southern African context and the extent of the Bushveld Complex ore deposits (greyscale areas in the southern African map). Additionally, in the zoomed-in map, the locations of large pyrometallurgical smelters in the wBC, the Johannesburg-Pretoria megacity (greyscale area in the zoomed-in map) and large atmospheric point sources in the interior of South Africa are indicated.

et al., 2015). Both samples and blanks were prepared, extracted and analysed with the same methods.

Various methods can be used to quantify Cr(VI) (Broadhurst and Maidza, 2006; Gómez and Calloa, 2006; Jacobs et al., 2004). The Cr(VI) analytical method applied in this study was adapted from Dionex Application updates 144 and 179 (2003 and 2011), as well as Thomas et al. (2002), as indicated by Loock et al. (2014). Cr(VI) analyses were conducted with an ion chromatograph (IC) (Thermo Scientific Dionex ICS-3000) with a post-column DPC colorant delivery system (AXP pump) coupled to an ultraviolet–visible (UV–vis) absorbance detector. The guard and analytical columns were Dionex IonPac AG7 4 × 50 mm and Dionex IonPac AS7 4 × 250 mm, respectively. A 1000 μℓ injection loop was used, as well as two 375 μℓ knitted reaction coils fitted in series. The post-column colorant reagent and eluent was prepared as previously described (Loock et al., 2014). An eluent flow rate of 1.00 mℓ/min was used, while the post-column colorant reagent was delivered at a flow rate of 0.5 mℓ/min.

Cr(VI) standard solutions for the calibration of the analytical instrument were prepared from a Spectrascan chromate reference standard with a specified concentration of 1009 ± 5 μg/mℓ CrO_4^{-2}. According to literature, the Cr(VI) detection limit for this method was 1 μg/ℓ (Dionex Application update 144, 2003). However, additional PEEK tubing was installed between the AXP pump and the back pressure tubing in order to reduce the pulse caused by the AXP pump that resulted in noise on the baseline of the chromatograms. This modification ensured a smoother baseline that improved the detection limit to 0.9 μg/ℓ, which was determined from the baseline amplitude and the calibration sensitivity (slope of the calibration curve over a Cr(VI) concentration range that gave linear response) according to the method described by Skoog et al. (2014) from a confidence factor that correlated with a 98.3% confidence level. By considering the volume of air sampled, the aforementioned detection limit in aqueous solution related to an atmospheric Cr(VI) detection limit of 0.84 ng/m^3. The accuracy of the combined extraction and analysis method was verified by analysis of a Community Bureau of Reference (former reference materials programme of the European Commission) BCR N° 545 welding dust filter certified reference material (individual identification N° B7-36, purchased on 25 January 2013). After considering dilution factors, a value of 39.7 mg/g Cr(VI) was obtained, which was within the uncertainty of the reference material that was defined as the half width of the 95% confidence interval of the mean of 40.2 mg/g Cr(VI) and 39.5 mg/g total leachable Cr. Due to cost considerations, only one such certified reference material filter was analysed and precisions could not be calculated from it. Every filter obtained via sampling at the Welgegund research station in the study was analysed three times, with the mean used in further data processing. The standard deviation for each such set of three analyses was determined. As a measure of precision the average of all the afore-mentioned standard deviations were found to be 0.4 ng/m^3.

2.3. Air mass histories and association with Cr(VI) analyses

Air mass history was determined by calculating back trajectories with the Hybrid Single-Particle Lagrangian Integrated Trajectory (HYSPLIT) model (version 4.8), developed by the National Oceanic and Atmospheric Administration (NOAA) Air Resources Laboratory (ARL) (Draxler and Hess, 2004). This model was run with meteorological data of the GDAS archive of the National Centre for Environmental Prediction (NCEP) of the United States National Weather Service and archived by the Air Resources Laboratory (ARL) (www.arl.noaa.gov/archives.php, accessed 11 November 2015). All back trajectories were calculated for 96 h, arriving every hour for the entire measurement period, at a height of 100 m. An arrival height of 100 m was chosen since the orography in HYSPLIT is not very well defined, and therefore lower arrival heights could result in increased error margins on individually calculated trajectories.

In order to link sampled PM with air mass history, two source regions were defined. The first source region (indicated as the black polygon in the zoomed-in portion of Fig. 1, as well as Fig. 2a, b and c) comprised a relatively small area in the wBC wherein nine pyrometallurgical smelters occurred. The second source region (indicated as the blue polygon in the zoomed-in portion of Fig. 1, as well as Fig. 2a, b and c) encompassed the Jhb-Pta megacity, as well as the area where most of the very large atmospheric point sources (e.g. coal-fired power stations, petrochemical operations and other pyrometallurgical smelters) occur in the South African interior. Individually calculated hourly-arriving back trajectories for each 24-h sample period were then overlaid on a map that was divided into 0.2° × 0.2° grid cells. On these maps, a colour code indicated the number of trajectories passing over each 0.2° × 0.2° grid cell, with red being the highest number. These 24-h sampling period overlay back trajectory maps were then visualised and sorted into four categories:

Please cite this article in press as: Venter, A.D., et al., Regional atmospheric Cr(VI) pollution from the Bushveld Complex, South Africa, Atmospheric Pollution Research (2016), http://dx.doi.org/10.1016/j.apr.2016.03.009

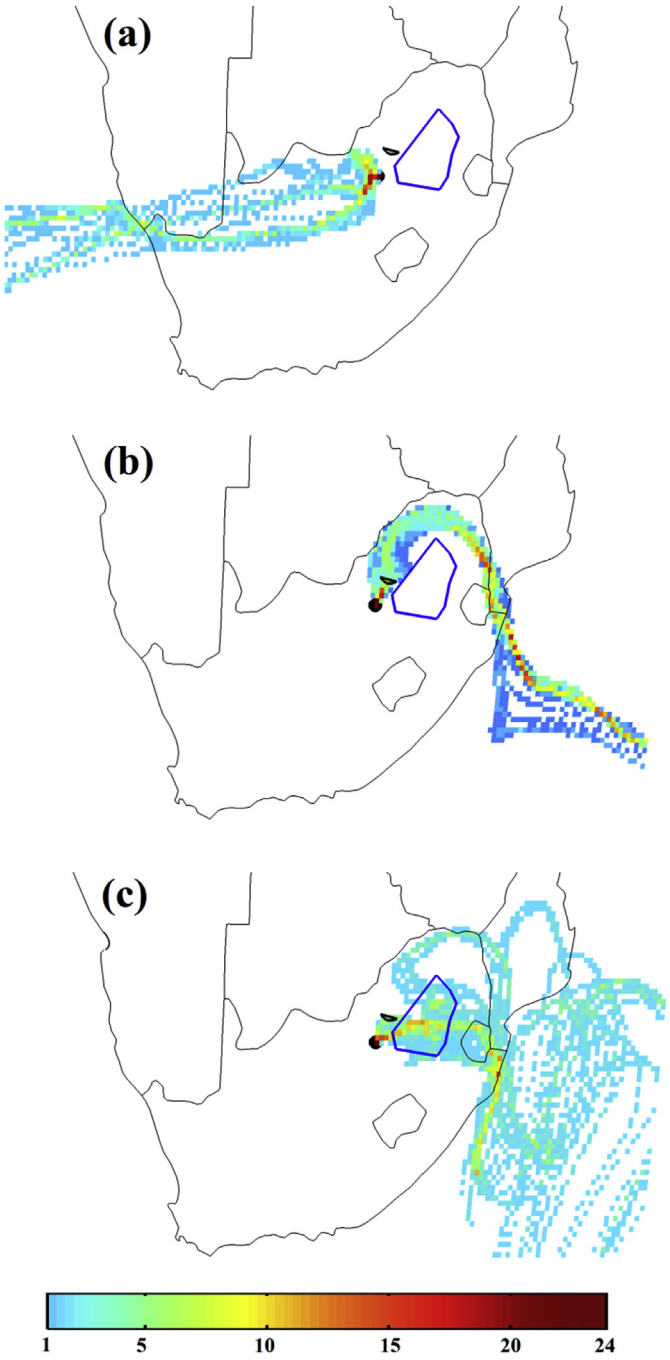

Fig. 2. Examples of air masses calculated for a specific 24-h sample that had passed over the regional background (a), air masses that had spent at least 2 h over the wBC source region (b) and air masses that had spent at least 2 h over the wBC source region, as well as five or more hours over the large mixed source region (c). The colour bar indicates the frequency of hourly-arriving back trajectories calculated for a day passing over 0.2° × 0.2° grid cells.

1) Air masses that had passed over the regional background mainly between north and south, to the west of Welgegund, but not over the two source regions defined in Fig. 1 (Fig. 2a as an example);
2) Air masses that had spent at least 2 h over the source region defined in the wBC (black polygon in Fig. 1) where nine pyrometallurgical smelters are (Fig. 2b as an example);
3) Air masses that had spent at least 2 h over the source region defined in the wBC (black polygon in Fig. 1), as well as five or more hours over the large mixed source region defined in Fig. 1 (blue polygon) (Fig. 2c as an example). These samples were referred to as mixed overpass; and
4) Air masses that did not represent the regional background (category 1), but also did not qualify for category 2 or 3. Samples collected on these days were not considered further.

3. Results and discussions

According to the air mass history selection criteria applied (Section 2.3), 24 samples (each corresponding to 24 h of sampling) could be identified within the year of sampling for which the air history was classified as passing over the wBC source region (category 2, Fig. 2b). Additionally, 23 sample periods were identified for which the air mass history was classified as mixed (category 3, Fig. 2c), while the air mass history for 53 sample periods was classified as passing over the regional background (category 1, Fig. 2a).

Atmospheric Cr(VI) concentrations in the $PM_{2.5}$ and $PM_{2.5-10}$ samples associated with air masses that were classified as passing over the regional background were below the detection limit of the procedure applied. This does not imply that no Cr(VI) occurs in the PM associated with such air mass history, it merely indicates that the concentrations of Cr(VI) were low and could not be detected with the analytical technique applied.

In contrast to the above-mentioned, Cr(VI) in samples associated with air masses passing over the wBC source region (category 2, Fig. 2b) or the mixed region (category 3, Fig. 2c) was substantially higher. Fig. 3 presents the statistical distribution (median, 25 and 75th percentiles and ±2.7 standard deviation) of Cr(VI) in both the $PM_{2.5}$ and $PM_{2.5-10}$ size fractions, as well as the combined PM_{10} fractions, which include both of the afore-mentioned fractions. From these results, it is evident that the majority of the Cr(VI) is present in the $PM_{2.5}$ fraction and to a lesser extent in the coarser $PM_{2.5-10}$ size fraction. Some of the Cr(VI) concentrations determined in the $PM_{2.5-10}$ size fraction were even below the detection limit. This concentration distribution is attributed to two reasons, i.e.: 1) Most of the pyrometallurgical processes potentially releasing PM-containing Cr(VI) will emit very fine PM. The Cr(VI)-containing particles in the off-gas from open and semi-closed SAFs, or from closed SAFs and DCFs, are removed with bag filters and wet venturi scrubbers, respectively (Beukes et al., 2012; Niemelä et al., 2004). These systems remove 99.9% of PM from the off-gas, but are not very effective in capturing PM_1 (Niemelä et al., 2004). Additionally, Cr(III) in the PM_1 that passes through the flare of the CO-rich off-gas

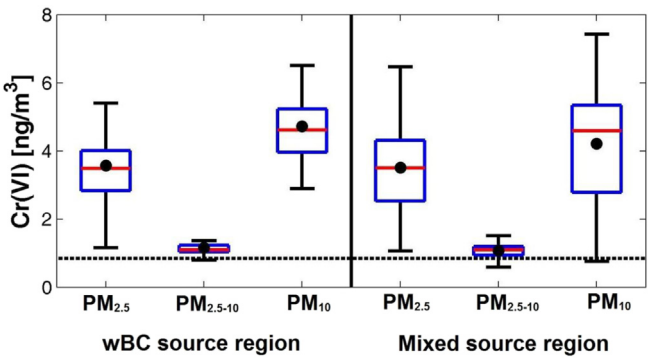

Fig. 3. Cr(VI) concentrations in $PM_{2.5}$ (≤2.5 μm), $PM_{2.5-10}$ (2.5–10 μm) and PM_{10} (sum of $PM_{2.5}$ and $PM_{2.5-10}$) associated with air masses that had passed over the wBC- and mixed source regions. The red line indicates the median, the black dot the mean, the blue rectangle the 25th and 75th percentiles, the whiskers ±2.7 times the standard deviation and the horizontal black dashed line the detection limit.

Please cite this article in press as: Venter, A.D., et al., Regional atmospheric Cr(VI) pollution from the Bushveld Complex, South Africa, Atmospheric Pollution Research (2016), http://dx.doi.org/10.1016/j.apr.2016.03.009

originating from closed SAFs or DCFs being burned may be oxidised resulting in the formation of Cr(VI) (Du Preez et al., 2015). 2) Finer particles have longer atmospheric lifetimes than coarser particles. Therefore, even if coarser Cr(VI)-containing particles are released by mining and metallurgical activities in the wBC, these particles will be removed from the atmosphere relatively quickly, preventing their transport to the Welgegund research station. For instance, Beukes and Guest (2001) reported that the dry milling of chromite ore could lead to the generation of Cr(VI)-containing particles. However, the two most commonly applied FeCr production processes applied by the South African FeCr industry, i.e. pelletised oxidative sintering and pelletised pre-reduction, have ore milling size specifications of d_{90} (indicating the size for which 90% of particles are smaller) of 75 (Kleynhans et al., 2012) and 108 μm (Glastonbury et al., 2015), respectively. Such relatively coarse particles will not have a very long atmospheric lifetime and will therefore mostly only have a local influence within the wBC.

Apart from the above-mentioned deductions, the spread of Cr(VI) concentrations in air masses that had passed over the wBC source region (category 1, Fig. 2b) were much smaller than that of the mixed region. This smaller spread for the wBC source region is indicative of the similar types of sources within this area. Air masses that had passed over the mixed source region (category 3, Fig. 2c) occasionally had higher Cr(VI) concentrations than that of the wBC source region, indicating the existence of other potential sources of Cr(VI) in the mixed region. It is well known that relatively low grade coal with reasonably high ash content (Jeffrey, 2005) is consumed in South Africa for both industrial activities and for household space heating in semi- and informal settlements (Hersey et al., 2015; Venter et al., 2012). These sources could potentially also emit atmospheric Cr(VI) in the mixed source region.

It is also important to contextualise the atmospheric Cr(VI) concentrations reported here within a global context. As stated earlier, Cr(VI) concentrations of air masses that had passed mainly over the regional background (category 1, Fig. 2a) were below the detection limit of 0.84 ng/m^3. The PM_{10} of air masses that had passed over both the wBC source region (category 2, Fig. 2b) and those that had passed over the mixed region (category 3, Fig. 2c) had median Cr(VI) concentrations of 4.6 ng/m^3. This is higher than the average of 0.044 ng/m^3 for Washington DC (Tirez et al., 2011 and references therein) and the range reported for Vienna, i.e. 0.04–0.23 ng/m^3 (Hagendorfer and Uhl, 2007). However, the concentrations were in the same order as atmospheric Cr(VI) reported for a site in Northern Italy and at an industrial site in Tunis that had concentrations ranging between 0.68 and 3.68, and 5.4 and 7.8 ng/m^3 (Catrambone et al., 2013), respectively, as well as at two sites near a stainless steel production facility in Belgium that reported 90th percentiles of 3.5 and 14 ng/m^3 (Tirez et al., 2011).

4. Conclusions

As far as the authors could assess, this is the first scientific report on ambient atmospheric Cr(VI) concentrations for South Africa. Ambient Cr(VI) concentrations in air masses that had passed over the regional background were below the detection limit (0.84 ng/m^3). In contrast, air masses that had passed over the wBC and/or the mixed source regions had elevated Cr(VI) concentrations with an average of 4.6 ng/m^3. The majority of Cr(VI) was found to be in the finer size fraction ($PM_{2.5}$), which could be explained by the nature of Cr(VI)-containing PM being emitted by the sources in the wBC source region and the atmospheric lifetimes of different PM size fractions. The results further indicated that not only pyrometallurgical sources in the wBC, but also other combustion sources outside the wBC could have contributed to the measured atmospheric Cr(VI). Current estimates of the atmospheric half-life of Cr(VI) range from 16 h to 4.8 days (Kimbrough et al., 1999 and references therein). However, simultaneous measurements of atmospheric Cr(VI) concentrations in both the wBC and also at Welgegund could be carried out in future to quantify the range of atmospheric Cr(VI) half-life more precisely. Since numerous meteorological parameters are measured at Welgegund, multivariate data analysis methods could be applied to such a dataset to determine the effect of for instance relative humidity and temperature on the atmospheric half-life of Cr(VI). This would enable a better assessment and prediction of the regional dispersion of Cr(VI) from hotspots, such as the wBC in South Africa and similar areas internationally.

Conflict of interest

The authors of this study do not have any personal/financial conflicts of interest that could interfere with the objectivity of this work.

Acknowledgements

The financial assistance of the National Research Foundation (NRF), South Africa, towards the support of the post-graduate studies of AD Venter is hereby acknowledged. Opinions expressed and conclusions arrived at are those of the author and are not necessarily to be attributed to the NRF. The authors also acknowledge financial support by the Academy of Finland Centre of Excellence (grant no. 272041).

References

Ashley, K., Howe, A.M., Demangec, M., Nygren, O., 2003. Sampling and analysis considerations for the determination of hexavalent chromium in workplace air. J. Environ. Monit. 5, 707–716. http://dx.doi.org/10.1039/b306105c.

Beaver, L.M., Stemmy, E.J., Constant, S.L., Schwartz, A., Little, L.G., Gigley, J.P., Chun, G., Sugden, K.D., Ceryak, S.M., Patierno, S.R., 2009. Lung injury, inflammation and Akt signaling following inhalation of particulate hexavalent chromium. Toxicol. Appl. Pharmacol. 235, 47–56. http://dx.doi.org/10.1016/j.taap.2008.11.018.

Beukes, J.P., Guest, R.N., 2001. Cr(VI) generation during milling. Min. Eng. 14 (4), 423–426. http://dx.doi.org/10.1016/S0892-6875(01)00022-X.

Beukes, J.P., Dawson, N.F., Van Zyl, P.G., 2010. Theoretical and practical aspects of Cr(VI) in the South African ferrochrome industry. J. S. Afr. Inst. Min. Metall. 110, 743–750.

Beukes, J.P., Van Zyl, P.G., Ras, M., 2012. Treatment of Cr(VI)-containing wastes in the South African ferrochrome industry – a review of currently applied methods. J. S. Afr. Inst. Min. Metall. 112, 413–418.

Booyens, W., Van Zyl, P.G., Beukes, J.P., Ruiz-Jimenez, J., Kopperi, M., Riekkola, M.-L., Josipovic, M., Venter, A.D., Jaars, K., Laakso, L., Vakkari, V., Kulmala, M., Pienaar, J.J., 2015. Size-resolved characterisation of organic compounds in atmospheric aerosols collected at Welgegund, South Africa. J. Atm. Chem. 72, 43–64. http://dx.doi.org/10.1007/s10874-015-9304-6.

Broadhurst, J.L., Maidza, T., 2006. Analytical methods for the determination of chromium in the environment. ICDA (International Chromium Development Association), The chromium file no°15. http://www.icdachromium.com/pdf/publications/CHROMIUM_FILE_N_15.pdf (accessed 09.09.09.).

Catrambone, M., Canepari, S., Perrino, C., 2013. Determination of Cr(III), Cr(VI) and total chromium in atmospheric aerosol samples. In: E3S Web of Conferences 1. http://dx.doi.org/10.1051/e3sconf/20130107005.

Cramer, L.A., Basson, J., Nelson, L.R., 2004. The impact of platinum production from UG2 ore on ferrochrome production in South Africa. J. S. Afr. Inst. Min. Metall. 517–527. October 2004.

DIONEX Corporation, 2003. Determination of Hexavalent Chromium in Drinking Water Using Ion Chromatography. Application Update 144, LPN 1495 (Sunnyvale, CA).

DIONEX Corporation, 2011. Sensitivity Determination of Hexavalent Chromium in Drinking Water. Application Update 179 (Sunnyvale, CA).

Draxler, R.R., Hess, G.D., 2004. Description of the HYSPLIT 4 Modelling System, NOAA Technical Memorandum ERL ARL–224.

Dubey, C.S., Sahoo, B.K., Nayak, N.R., 2001. Chromium (VI) in waters in parts of Sukinda Chromite Valley and health hazards, Orissa, India. Bull. Environ. Contam. Toxicol. 67, 541–548. http://dx.doi.org/10.1007/s00128-001-0157-0.

Du Preez, S.P., Beukes, J.P., Van Zyl, P.G., 2015. Cr(VI) generation during flaring of CO-rich off-gas from closed ferrochromium submerged arc furnaces. Metall. Mater. Trans. 46B, 1002–1010. http://dx.doi.org/10.1007/s11663-014-0244-3.

Garstang, M., Tyson, M., Swap, R., Edwards, M., Kållberg, P., Lindesay, J.A., 1996. Horizontal and vertical transport of air over southern Africa. J. Geophys. Res. 101, 23721–23736.

Glastonbury, R.I., Beukes, J.P., Van Zyl, P.G., Sadiki, L.N., Jordaan, A., Campbell, Q.P., Stewart, H.M., Dawson, N.F., 2015. Comparison of physical properties of oxidative sintered pellets produced with UG2 or metallurgical grade South African chromite: a case study. J. S. Afr. Inst. Min. Metall. 115, 699–706. http://dx.doi.org/10.17159/2411-9717/2015/v115n8a6.

Gómez, V., Calloa, M.P., 2006. Chromium determination and speciation since 2000. Trend Anal. Chem. 25, 1006–1015. http://dx.doi.org/10.1016/j.trac.2006.06.010.

Hagendorfer, H., Uhl, M., 2007. Speciation of Chromium in Particulate Matter (PM_{10}): Development of a Routine Procedure, Impact of Transport and Toxicological Relevance. Umweltbundesamt, Vienna, p. 29. REP-0111.

Hersey, S.P., Garland, R.M., Crosbie, E., Shingler, T., Sorooshian, A., Piketh, S., Burger, R., 2015. An overview of regional and local characteristics of aerosols in South Africa using satellite, ground, and modeling data. Atmos. Chem. Phys. 15, 4259–4278. http://dx.doi.org/10.5194/acp-15-4259-2015.

Hirsikko, A., Vakkari, V., Tiitta, P., Manninen, H.E., Gagné, S., Laakso, H., Kulmala, M., Mirme, A., Mirme, S., Mabaso, D., Beukes, J.P., Laakso, L., 2012. Characterisation of sub-micron particle number concentrations and formation events in the western Bushveld Igneous Complex, South Africa. Atmos. Chem. Phys. 12, 3951–3967. http://dx.doi.org/10.5194/acp-12-3951-2012.

Jaars, K., Beukes, J.P., Van Zyl, P.G., Venter, A.D., Josipovic, M., Pienaar, J.J., Vakkari, V., Aaltonen, H., Laakso, H., Kulmala, M., Tiitta, P., Guenther, A., Hellén, H., Laakso, L., Hakola, H., 2014. Ambient aromatic hydrocarbon measurements at Welgegund, South Africa. Atmos. Chem. Phys. 14, 7075–7089. http://dx.doi.org/10.5194/acp-14-7075-2014.

Jacobs, J.A., Motzer, W.E., Abbott, D.W., Guetin, J., 2004. Chromium sampling and analysis. In: Guetin, J., Jacobs, J.A., Avakian, C.P. (Eds.), Chromium(VI) Handbook. CRC Press, USA, pp. 93–142.

Jeffrey, L.S., 2005. Characterization of the coal resources of South Africa. J. S. Afr. Inst. Min. Metall. 95–102.

Kimbrough, D.E., Cohen, Y., Winer, A.M., Creelman, L., Mabuni, C., 1999. A critical assessment of chromium in the environment. Crit. Rev. Environ. Sci. Technol. 29, 1–46. http://dx.doi.org/10.1080/10643389991259164.

Kleynhans, E.L.J., Beukes, J.P., Van Zyl, P.G., Kestens, P.H.I., Langa, J.M., 2012. Unique challenges of clay binders in a pelletised chromite pre-reduction process. Min. Eng. 34, 55–62. http://dx.doi.org/10.1016/j.mineng.2012.03.021.

Loock, M.M., Beukes, J.P., Van Zyl, P.G., 2014. A survey of Cr(VI) contamination of surface water in the proximity of ferrochromium smelters in South Africa. Water SA 40, 709–716. http://dx.doi.org/10.4314/wsa.v40i4.16.

Lourens, A.S.M., Butler, T.M., Beukes, J.P., Van Zyl, P.G., Beirle, S., Wagner, T., Heue, K.-P., Pienaar, J.J., Fourie, G.D., Lawrence, M.G., 2012. Re-evaluating the NO_2 hotspot over the South African Highveld. S. Afr. J. Sci. 108 http://dx.doi.org/10.4102/sajs.v108i11/12.1146. Art. #1146.

Mandiwana, K.L., Panichev, N., Ngobeni, P., 2007. Electrothermal atomic absorption spectrometric determination of Cr(VI) during ferrochrome. J. Hazard. Mater. 145, 511–514. http://dx.doi.org/10.1016/j.jhazmat.2007.01.077.

Mennen, M.G., Koot, W., Putten, E.M., Ritsma, R., Piso, S., Knol, T., Fortezza, F., Kliest, J.J.G., 1998. Hexavalent Chromium in Ambient Air in the Netherlands. Results of Measurements Near Word Preservation Plants and at a Regional Site. RIVM report no. 723101031.

Moskalyk, R.R., Alfantazi, A.M., 2003. Processing of vanadium: a review. Min. Eng. 16, 793–805. http://dx.doi.org/10.1016/S0892-6875(03)00213-9.

Niemelä, P., Krogerus, H., Oikarinen, P., 2004. Proceedings of 10th International Ferroalloys Congress, Cape Town, South Africa, February 2004, pp. 68–77.

Oze, C., Fendorf, S., Bird, D.K., Coleman, R.G., 2004. Chromium geochemistry of serpentine soils. Int. Geol. Rev. 46, 97–126.

Oze, C., Bird, D.K., Fendorf, S., 2007. Genesis of hexavalent chromium from natural sources in soil and groundwater. PNAS 104, 6544–6549, 10.1073_pnas.0701085104.

Panichev, N., Mabasa, W., Ngobeni, P., Mandiwana, K., Panicheva, S., 2008. The oxidation of Cr(III) to Cr(VI) in the environment by atmospheric oxygen during the bush fires. J. Hazard. Mater. 153, 937–941. http://dx.doi.org/10.1016/j.jhazmat.2007.09.044.

Robles-Camacho, J., Armienta, M.A., 2000. Natural chromium contamination of groundwater at León Valley, Mexico. J. Geochem. Exp. 68, 167–181.

Seigneur, C., Constantinou, E., 1995. Chemical kinetic mechanism for atmospheric chromium. Environ. Sci. Technol. 29, 222–231.

Skoog, D.A., West, D.M., Holler, F.J., Crouch, S.R., 2014. Fundamentals of Analytical Chemistry. International Edition, ninth ed. Brooks/Cole, Cengage Learning, Belmont, p. 985.

Steinpress, M.G., Henri, T.D., Simion, V., Auckly, C., Weber, J.V., 2004. Naturally occurring chromium(VI) in groundwater. In: Guetin, J., Jacobs, J.A., Avakian, C.P. (Eds.), Chromium(VI) Handbook. CRC Press, USA, pp. 93–142.

Thomas, D.H., Rohrer, J.S., Jackson, P.E., Pak, T., Scott, J.N., 2002. Determination of hexavalent chromium at the level of the California Public Health Goal by ion chromatography. J. Chromatogr. A956, 255–259.

Tiitta, P., Vakkari, V., Croteau, P., Beukes, J.P., Van Zyl, P.G., Josipovic, M., Venter, A.D., Jaars, K., Pienaar, J.J., Ng, N.L., Canagaratna, M.R., Jayne, J.T., Kerminen, V.-M., Kokkola, H., Kulmala, M., Laaksonen, A., Worsnop, D.R., Laakso, L., 2014. Chemical composition, main sources and temporal variability of PM_1 aerosols in southern African grassland. Atmos. Chem. Phys. 14, 1909–1927. http://dx.doi.org/10.5194/acp-14-1909-2014.

Tirez, K., Silversmit, G., Bleux, N., Adriaensens, E., Roekens, E., Servaes, K., Vanhoof, C., Vincze, L., Berghmans, P., 2011. Determination of hexavalent chromium in ambient air: a story of method induced Cr(III) oxidation. Atmos. Environ. 45 (2011), 5332–5341. http://dx.doi.org/10.1016/j.atmosenv.2011.06.043.

Venter, A.D., Vakkari, V., Beukes, J.P., van Zyl, P.G., Laakso, H., Mabaso, D., Tiitta, P., Josipovic, M., Kulmala, M., Pienaar, J.J., Laakso, L., 2012. An air quality assessment in the industrialised western Bushveld Igneous Complex, South Africa. S. Afr. J. Sci. 108 http://dx.doi.org/10.4102/sajs.v108i9/10.1059. Art. #1059.

Vakkari, V., Kerminen, V.-M., Beukes, J.P., Tiitta, P., Van Zyl, P.G., Josipovic, M., Venter, A.D., Jaars, K., Worsnop, D.R., Kulmala, M., Laakso, L., 2014. Rapid changes in biomass burning aerosols by atmospheric oxidation. Geophys. Res. Lett. 41, 2644–2651. http://dx.doi.org/10.1002/2014GL059396.

Xiao, Z., Laplante, A.R., 2004. Characterizing and recovering the platinum group minerals – a review. Min. Eng. 17, 961–979. http://dx.doi.org/10.1016/j.mineng.2004.04.001.

Please cite this article in press as: Venter, A.D., et al., Regional atmospheric Cr(VI) pollution from the Bushveld Complex, South Africa, Atmospheric Pollution Research (2016), http://dx.doi.org/10.1016/j.apr.2016.03.009

Chapter 6

Measurement of atmospheric trace metals at a regional background site (Welgegund) in South Africa

Author list and contributions

A. D. Venter[1], P.G. van Zyl[1], J. P. Beukes[1], M. Josipovic[1], K. Jaars[1], J. Hendriks[1], W. Booyens[1]

1 Unit for Environmental Sciences and Management, North-West University, Potchefstroom, South Africa

Contributions of the various co-authors were as follows. The bulk of the work was done by the candidate A. D. Venter (including sample analysis, data processing research and writing of the scientific paper), with conceptual ideas and recommendations by the promoters P.G. van Zyl and J.P. Beukes. The candidate (A.D. Venter), K. Jaars, W. Booyens, and M. Josipovic helped gather data at the Welgegund measurement station; J. Hendriks assisted during ICP analysis.

Formatting and current status of article

The article was formatted in accordance with the journal specifications to which it will be submitted, i.e. *Atmospheric Chemistry and Physics*, a European Geosciences Union journal. The figures and tables of this article are also added at the end of the text, as prescribed by the journal. The author's guide that was followed in preparation of the article was available at http://www.atmospheric-chemistry-and-physics.net/for_authors/submit_your_manuscript.html (Date of access: 26 November 2015). At the time when this PhD was submitted for examination, this article had not yet been submitted for review, but the intention was to submit it soon thereafter.

Consent by co-authors

All the co-authors on the article have been informed that the PhD will be submitted in article format and have given their consent.

Measurement of atmospheric trace metals at a regional background site (Welgegund) in South Africa

A. D. Venter[1], P.G. van Zyl[1], J. P. Beukes[1], M. Josipovic[1], K. Jaars[1], J. Hendriks[1], W. Booyens[1]

[1]{Unit of Environmental Sciences and Management, North-West University, Potchefstroom, South Africa}

Correspondence to: P.G. van Zyl (pieter.vanzyl@nwu.ac.za)

Abstract

Trace metals represent a relatively small fraction of atmospheric aerosols. However, these species can cause a variety of health-related and environmental problems. Only a few studies on atmospheric trace metal concentrations have been conducted in South Africa. The aim of this study was to determine trace metals concentrations in aerosols collected at Welgegund, South Africa. PM_1, $PM_{1\text{-}2.5}$ and $PM_{2.5\text{-}10}$ samples were collected for 13 months and 32 atmospheric trace metal species were detected. Atmospheric Fe had the highest concentrations in all three size fractions, while Ca was the second most abundant species. Cr and Na concentrations were the third and fourth most abundant species, respectively. The concentrations of the trace metal species in all three size ranges were similar, with the exception of Fe that had higher concentrations in the PM_1 size fraction. Welgegund trace metal species were compared to those in the western Bushveld Igneous Complex, and it was found that at both locations similar species were observed with Fe being the most abundant. However, concentrations of these trace metal species were

significantly higher in the western Bushveld Igneous Complex. Fe concentrations at the Vaal Triangle were similar to levels thereof at Welgegund, while concentrations of species associated pyrometallurgical smelting were lower. With the exception of Ni, none of the trace metals measured at Welgegund exceeded local and international standard limit values. No distinct seasonal pattern was observed in the $PM_{2.5-10}$ size fraction, while the PM_1 and $PM_{1-2.5}$ size fractions indicated elevated trace metal concentrations coinciding with the end of the dry season, which could partially be attributed to decreased wet removal and increases in wind generation of particulates. With the exception of Ti, Al and Mg, 65% or more of the trace metal species detected were in the two smaller size fractions, with approximately 40 to 45% occurring in the PM_1 size fraction, which indicated the influence of industrial activities on trace metals measured at Welgegund. However, the large influence of wind-blown dust on trace metal concentrations determined at Welgegund is reflected by 35% and more of trace metals being present in the $PM_{2.5-10}$ size fraction, while Ti, Al and Mg were predominantly in the $PM_{2.5-10}$ size fraction.. Principal component factor analysis (PCFA) revealed three meaningful factors in the PM_1 size fraction, i.e. fly ash, pyrometallurgical-related and crustal. No meaningful factors were determined for the $PM_{1-2.5}$ and $PM_{2.5-10}$ size fractions, which was attributed to the large influence of wind-blown dust on atmospheric trace metals determined at Welgegund. Pollution roses confirmed the impact of wind-blown dust on trace metal concentrations, while the influence of industrial activities was also substantiated.

Introduction

Atmospheric aerosols are either directly emitted into the atmosphere (primary aerosols) from natural and/or anthropogenic sources, or are formed through gaseous reactions and gas-to-particle conversions (secondary aerosols). Aerosols have high temporal and spatial variability, which increases the need and importance for detailed physical and chemical characterisation on a regional scale in order to assess the impacts of aerosols (Koulouri et al., 2008). Particulate

matter (PM) is classified according to its aerodynamic diameter, as PM_{10}, $PM_{2.5}$, PM_1 and $PM_{0.1}$, which relates to aerodynamic diameters being smaller than 10, 2.5, 1 and 0.1 μm, respectively. Larger particulates have shorter lifetimes in the atmosphere compared to smaller particles, while the impacts of these species are also determined by their size. Aerosols consist of a large number of organic and inorganic compounds. The highest uncertainty related to atmospheric aerosols is related to the exact chemical composition of atmospheric aerosols. A large number of inorganic species are present in aerosols, which include ionic species and trace metals.

Natural sources of atmospheric trace metals include mineral dust, crustal species, oceans and biomass burning (wild fires), while major anthropogenic sources are pyrometallurgical processes, fossil fuel combustion and incineration. Larger aerosols are usually associated with natural emissions through processes such as rock weathering and soil erosion. Trace metal species usually associated with natural emissions include sodium (Na), silicon (Si), magnesium (Mg), aluminium (Al), potassium (K), calcium (Ca), titanium (Ti), chromium (Cr), manganese (Mn) and iron (Fe) (Adgate et al., 2007). Arsenic (As), barium (Ba), cadmium (Cd), copper (Cu), nickel (Ni), zinc (Zn), vanadium (V), molybdenum (Mo), mercury (Hg) and lead (Pb) are mostly related to anthropogenic activities (Pacyna (1998); Polidori et al., 2009). One of the most significant sources of anthropogenic trace metal emissions is the industrial smelting of metals. Industrial pyrometallurgical processes produce the largest emissions of As, Cd, Cu, Ni and Zn (Zahn et al., 2014). Cr, Ba, Mo, Zn, Pb and Cu are typically associated with motor-vehicle emissions and oil combustion, while Fe, Pb and Zn are emitted from municipal waste incinerators (Adgate et al., 2007). However, most of these atmospheric trace metals are emitted through a combination of different anthropogenic sources (Polidori et al., 2009).

Although heavy metals (>Ca) represent a relatively small fraction of atmospheric aerosols, these species can cause a variety of health-related and environmental problems, which depends on the aerosol composition, extent and time of exposure (Pöschl, 2005). The potential hazard of several toxic species is well documented

as discussed, for instance, by Polidori et al. (2009), indicating that trace metals such as As, Cd, Co, Cr, Ni, Pb and Se are considered human and animal carcinogens even in trace amounts (CDC, 2015). It has also been shown that Cu, Cr and V can generate reactive oxygen species that can contribute to oxidative DNA damage (Nel, 2005). Furthermore, trace metals such as Cr, Fe and V have several oxidation states that can participate in many atmospheric redox reactions (Seigneur & Constantinou, 1995), which can catalyse the generation of reactive oxygen species (ROS) that have been associated with direct molecular damage and with the induction of biochemical synthesis pathways (Rubasinghege et al., 2010). Guidelines for atmospheric levels of many trace metals are provided by the World Health Organization (WHO) (WHO 2005).

South Africa has the largest industrialised economy in Africa, with significant mining and metallurgical activities. South Africa is a well-known source region of atmospheric pollutants, which is signified by three regions being classified through legislation as air pollution priority areas due to high levels of atmospheric pollutants emitted from industrial activities located in these areas, i.e. Vaal Triangle Airshed Priority Area (SA, 2006), Highveld Priority Area (SA, 2007) and Waterberg Priority Area (SA, 2012a). Air quality outside these priority areas is often adversely affected due to regional transport and the general climatic conditions, such as low precipitation and poor atmospheric mixing in winter. Only a few studies on the concentrations of atmospheric trace metals in South Africa have been conducted (Van Zyl *et al.*, 2014; Kgabi, 2006; Kleynhans, 2008). In a recent study conducted by Van Zyl et al. (2014), the atmospheric trace metal concentrations at an atmospheric measurement site situated within the highly industrialised western Bushveld Igneous Complex were assessed. This region forms part of the Waterberg Priority Area. Diurnal and seasonal trends were discussed, while source apportionment was performed by applying a statistical method. However, this atmospheric monitoring site was situated within a source region with a significant number of large point sources, and regional impacts of atmospheric trace metals could therefore not be assessed.

In this study, trace metals were determined in three size ranges in aerosol samples collected for one year at the Welgegund atmospheric measurement station in South Africa. Welgegund is a comprehensively equipped regional background atmospheric measurement station that is ~100 km downwind and influenced by the most important source regions in the interior of South Africa. In an effort to determine major sources of trace metals on a regional scale, source apportionment was performed by applying statistical methods.

Experimental

Site description

Aerosol sampling was performed at Welgegund (www.welgegund.org, 26°34'11.23"S, 26°56'21.44"E, 1480 m.asl) in South Africa. As indicated in Figure 1, Welgegund is situated in the interior of South Africa. It is frequently affected by air masses moving over the most important source regions in the interior of South Africa (Beukes et al., 2013). Also indicated in Figure 1 are the major industrial point sources, i.e. coal-fired power plants, petrochemical industries and pyrometallurgical smelters. In Beukes et al. (2013), reasons for the site selection, prevailing biomes and pollution sectors are discussed in detail. In summary, air masses affecting the site from the west, between north- and south-west, are considered to be representative of the regional background, since they move over a sparsely populated region without any large point sources. In the sector between north and north-east from Welgegund lays the western limb of the Bushveld Igneous Complex, which holds eleven pyrometallurgical smelters within a ~ 55 km radius, in addition to other industrial, mining and residential sources. In the north-east to eastern sector, the Johannesburg-Pretoria (Jhb-Pta) conurbation is situated, which is inhabited by more than 10 million people, making it one of the fourty largest metropolitan areas in the world. In the sector between east and south-east from Welgegund is the Vaal Triangle region, where most of the South African petrochemical and petrochemical-related industries are located, together with other large point sources, such as two coal-fired power

stations (without de-SOx and de-NOx) and several large pyrometallurgical smelters. Welgegund is also affected by the Mpumalanga Highveld in the eastern sector (indicated by MP in Figure 1). In this region, there are 11 coal-fired power stations (without de-SOx and de-NOx technologies) with a combined installed generation capacity of ca. 46 GW, as well as a very large petrochemical plant, several pyrometallurgical smelters and numerous coal mines, all within a ca. 60 km radius. Furthermore, Welgegund is also affected by air masses passing over the pyrometallurgical smelters in the eastern limb of the Bushveld Igneous Complex situated north-east from Welgegund in the Limpopo Provence (indicated by LP in Figure 1).

Insert Figure 1

Sampling and analysis

Aerosol samples were collected for one year from 24 November 2010 until 28 December 2011. A Dekati (Dekati Ltd., Finland) PM_{10} cascade impactor (ISO23210) equipped with PTFE filters was used to collect different particulate size ranges, i.e. $PM_{2.5\text{-}10}$ (aerodynamic diameter ranging between 2.5 and 10 μm), $PM_{1\text{-}2.5}$ (aerodynamic diameter ranging between 1 and 2.5 μm) and PM_1 (aerodynamic diameter <1 μm). The pump flow rate was set at 30 $L.min^{-1}$. Samples were collected continuously for one week, after which filters were changed. A total of 54 samples were collected for the 54-week sampling period for each of the three size ranges. The trace metals in the PM collected on the 216 PTFE filters were extracted by hot acid leaching (20 ml HNO_3 and 5 ml HCl) and diluted in deionised water (18.2 MΩ) up to 100 mL for subsequent analysis with an inductively coupled plasma mass spectrometer (ICP-MS). In total, 32 trace metals could be detected with ICP-MS analysis, which included Na, Si, Mg, Al, K, Ca, Ti, Cr, Mg, Fe, As, Ba, Cd, Cu, Ni, Zn, V, Mo, Hg, Pb, manganese (Mn), cobalt (Co), platinum (Pt), beryllium (Be), boron (B), selenium (Se), palladium (Pd), barium (Ba), gold (Au), thallium (Tl), antimony (Sb) and uranium (U). It

must be noted that nitric acid digestion does not dissolve silicate minerals, and hence Si and, to a lesser extent, Al and K were not completely quantified. It is estimated that only 7 % Si and 30 % Al is extracted by nitric acid leaching (Ahn *et al.*, 2011). Trace metal concentrations below the detection limit of the ICP-MS were considered to have concentrations half the detection limit of the species considered. This is a precautionary assumption that is frequently used in health-related environmental studies. (Al-Momani et al., 2005; Kulkarni et al., 2007, Van Zyl et al., 2012).

Statistical analysis

In an attempt to identify possible sources of trace metals detected, principal component factor analysis (PCFA) with Varimax rotation (v. 13.0 SPSS Inc., Chicago, IL, USA) was performed on the dataset. PCFA has been used widely in receptor modelling to identify major source sectors. The technique operates on sample-to-sample fluctuations of the normalised concentrations. It does not directly yield concentrations of species from various sources, but identifies a minimum number of common factors for which the variance often accounts for most of the variance of species (Van Zyl et al., 2014 and references therein). The trace metal concentrations determined for the 32 species in all three size fractions were subjected to multivariate analysis of Box-Cox transformation and Varimax rotation, followed by subsequent PCFA. In addition, Spearman correlations were also performed in order to establish correlations between trace metals in order to substantiate results obtained with PCFA. In this article, species reported on were above the detection limits at least 60 % of the time during the sampling campaign.

Back trajectory analysis

Individual 96h-hourly back trajectories with an arrival height of 100 m were calculated with HYSPLIT 4.820.19 (Lourens et al., 2011, Venter et al., 2012). An arrival height of 100 m was chosen since the orography in HYSPLIT is not very well defined. Therefore, lower arrival heights could result in increased error margins on individual trajectory calculations. Considering the above, 24 hourly

back trajectories for each day were obtained for the entire sampling period. Individual back trajectories generated in HYSPLIT (24 x 365 days) were superimposed and further analysed in MATLAB. In the overlay back trajectory presentation compiled with MATLAB, a colour code indicates the percentage of trajectories passing over 0.2° x 0.2° grid cells, with red being the highest percentage and blue the lowest.

Results

Size distribution of trace metals

In Figure 2, the size distributions of each of the trace metal species identified above the detection limit in the three size fractions are presented. Si, although an abundant element in crustal matter, is not reported on due to analytical constraints and therefore omitted from this discussion. Although some species were not detected at least 60% of the time, the results were still included to indicate their distribution pattern. In all three size fractions, Ag and Hg were rarely detected in addition to K and Se seldom being detected in the $PM_{1\text{-}2.5}$ and $PM_{2.5\text{-}10}$ size fractions. Pt was also detected less than 60 % of the time in the $PM_{1\text{-}2.5}$ size fraction. In Figure 2, the majority of Cd and Pb in the smaller size fractions indicate that industrial (high temperature) activities can most likely be considered the sources of these species. Ti, Al, Mg and Zn, had relatively higher contributions (25-80%) in the $PM_{2.5\text{-}10}$ size fraction, which indicates that wind-blown dust is the major source of these species. The $PM_{2.5\text{-}10}$ size fraction is usually associated with wind-blown dust typically comprising Al, Fe, Na, Mg and Ti (Polidori et al., 2009). 65% or more of all the other trace metal species detected were in the two smaller size fractions, with approximately 40 to 60% occurring in the PM_1 size fraction. More than 50% of Co, K and Pb were present in the PM_1 size fraction. The presence of these trace metal species predominantly in the smaller size fractions, especially considering the relatively large contribution in the PM_1 size fractions, indicates the influence of industrial activities on air masses measured at Welgegund. However, the large influence of wind-blown

dust on trace metal concentrations determined at Welgegund is also reflected with approximately 35% of most of these trace metals being present in the $PM_{2.5-10}$ size fraction. Trace metal concentrations measured at Marikana indicated that Cr, Mn, V, Zn and Ni only occurred almost exclusively in the $PM_{2.5}$ size fraction, with no contribution of wind-blown dust levels of these species measured.

Insert Figure 2

Size-resolved trace metal concentrations

In Figure 3, the combined trace metal concentrations in all three size fractions (Figure 3(a)), as well as concentrations of the trace metals determined in each of the size fractions (Figure 3 (b), (c) and (d)) are presented on a log-axis. The detection limits of each species are indicated with green stars.

Insert Figure 3

The highest median concentration was determined for atmospheric Fe, i.e. 1.1 μgm^{-3}, while Ca was the second most abundant species with a median concentration of 0.9 μgm^{-3}. Fe concentrations were significantly higher compared to the other trace metal species determined at Welgegund. Cr and Na concentrations were the third and fourth most abundant species, respectively. The median Cr concentration was 0.5 μgm^{-3}, while the median Na level was 0.3 $\mu g.m\text{-}^{3}$. Relatively higher concentrations were also determined for Al, B, Mg, Ni, K and P with median concentrations of 0.2 μgm^{-3}, 0.3 μgm^{-3}, 0.2 μgm^{-3}, 0.1 μgm^{-3}, 0.2 μgm^{-3} and 0.2 μgm^{-3}, respectively. The combined atmospheric concentrations of the other trace metals in all the size fractions were relatively low. It must be noted that Si is an abundant element but due to analytical constraints, omitted from this discussion.

A comparison of the trace metal concentrations in the three size fractions indicates that Fe and Ca were the most abundant species in all three size fractions. Fe had the highest median concentration in the PM_1 size fraction, i.e. 0.5 μgm^{-3}, while Ca had the highest median concentrations in the $PM_{1-2.5}$ and $PM_{2.5-10}$ size fractions, i.e. 0.3 μgm^{-3} and 0.2 μgm^{-3}, respectively. However, it is evident that Fe concentrations had the largest statistical spread in all three size fractions. The median concentration of Fe in the PM_1 was significantly higher compared to the median concentrations thereof in the $PM_{1-2.5}$ and $PM_{2.5-10}$ size fractions. The third and fourth most abundant species in all three size fractions were Cr and Na, respectively. Relatively higher concentrations were also determined for Al, B, Mg, Ni, K and P in all three size fractions. As mentioned previously, Ag and Hg were 60% or less of the time detected in all size fractions. However, in the PM_1 fraction, K, Se and Pt were detected more than the required 60% threshold unlike these species in the larger size fractions. The concentration of K in the PM_1 size fraction is comparable to concentrations of Al, B, Mg, Ni, K and P, while Se and Pt concentrations are comparable with those of other heavy and precious metals (e.g. Pd, Cd and Au). With the exception of Fe concentrations in the PM_1 size fraction, as well as the concentrations of species only detected in certain size fractions, the concentrations of each of the trace metal species were similar in all size fractions.

The major source of the trace metal species with elevated levels in all three size fractions can be considered to be wind-blown dust. Elements typically associated with wind-blown dust include Fe, Ca, Mg, Al and K. As mentioned, Welgegund is a regional background station affected by air masses passing over large pollutant source regions and a relatively clean background area (Figure 1). It is therefore expected that wind-blown dust could have a major impact on atmospheric trace metal concentrations. Furthermore, the western Bushveld Igneous Complex is a major source region affecting Welgegund, with a large number of pyrometallurgical smelters and mining activities (Tiitta et al., 2014; Jaars et al., 2014). This source region could attribute to regional elevated levels of Fe, Cr, Ni, Zn, Mn and V measured at Welgegund. The possible sources of trace metal species measured at Welgegund will be further explored later in this paper.

Contextualisation of trace metal concentrations and comparison to ambient air quality standards

The annual average elemental concentrations were also calculated in order to regionally and globally compare trace metal concentrations reported in a selection of previous studies in similar environments. In Table 1, the annual average trace metal concentrations determined in this study are listed in conjunction with elemental concentrations determined in other studies. Although the aerosol sampling periods and frequencies for most of these previous elemental studies were not similar to the aerosol sampling period and frequency in this investigation, these results could be utilised to contextualise the trace metal concentrations. Three of these studies were conducted in South Africa, i.e. Marikana (Van Zyl et al., 2014), Rustenburg (Kgabi, 2006) and the Vaal Triangle (Kleynhans, 2008), while the other investigations were performed in at regional background sites in China (Duan et al., 2012), the Mediterranean (Pio et al., 1996) and Spain (Querola et al. 2007). As mentioned previously, Ag, Hg, K, Se and Pt concentrations were frequently below the detection limit of the analytical technique. Therefore, concentrations presented for these species are most likely to be an over estimate due to the precautionary assumption of substituting half the detection limit for periods below the detection threshold.

Marikana and Rustenburg are situated within the industrialised western Bushveld Igneous Complex with a large number of pyrometallurgical smelters, as indicated in Figure 1, which is one of the major source regions affecting air masses arriving at Welgegund. Pyrometallurgical smelters directly related to the production of Cr, Fe, V and Ni are typical in the western Bushveld Igneous Complex. Fe was also the most abundant species at these two sites. However, Fe concentrations were two times higher at Marikana, while Fe levels were nine times higher at Rustenburg compared to levels thereof at Welgegund. Mg was the second most abundant species at Marikana, with Mg concentrations being an order of magnitude higher compared to levels thereof at Welgegund. Na, B and Al were also relatively abundant at Marikana, similar to Welgegund. However,

the concentrations of these species were much higher at Marikana. The Ca concentrations determined at Welgegund were similar to the levels thereof determined at Marikana, while K levels were three times higher at Marikana. Mn and Cr concentrations were the second and third highest at Rustenburg, respectively. As mentioned previously, Cr was also the third most abundant species measured at Welgegund. However, Cr levels at Rustenburg were approximately 2.5 times higher. Cr concentrations measured at Welgegund were approximately two times higher compared to Cr levels determined at Marikana. Significantly lower Mn concentrations were determined at Welgegund compared to levels thereof measured at Rustenburg, with Mn concentrations measured at Welgegund being similar to Mn levels at Marikana. Ni concentrations at Welgegund were approximately three times lower compared to levels thereof at Marikana, while Ni levels in Rustenburg were approximately seven times higher. Zn levels measured were also lower at Welgegund. V concentrations measured at Welgegund were similar to V levels determined at Marikana, but significantly lower to levels thereof at Rustenburg. It is expected that lower concentrations of trace metal species will be determined at Welgegund compared to levels thereof within the source region. The higher Cr concentration measured at Welgegund could be attributed to the contribution of Cr units from wind-blown mineral dust.

The Vaal Triangle is also one of the source regions that has an impact on air masses measured at Welgegund. This area has been described by Beukes et al. (2013 and references therein). Atmospheric Na had the highest concentrations in the Vaal Triangle, while Fe and K were the second and third most abundant species, respectively. Na concentrations were seven times higher, while K levels were six times higher at the Vaal Triangle compared to levels of these species measured at Welgegund. Similar Fe concentrations were determined at Welgegund and the Vaal Triangle. In addition, Mg concentrations were five times higher in the Vaal Triangle. Cr, Ni and Zn that are typically associated with pyrometallurgical industries were significantly lower in the Vaal Triangle compared to levels thereof at Welgegund, as well as within the western Bushveld Igneous Complex. However, Mn concentrations at the Vaal Triangle were an

order of magnitude higher compared to levels thereof at Welgegund and Marikana. This can be attributed to the presence of a ferromanganese (FeMn) smelter in the Vaal Triangle region, as indicated in Figure 1.

The atmospheric trace metal concentrations determined at Welgegund were also compared to measurements of these species near Beijing, China, since China is also considered to be a developing country. The trace metal concentrations determined at a regional background site near Beijing in China indicated that Al concentrations were significantly higher compared to other trace metal species, while Na was the second most abundant species. Elevated levels of K, Fe and Ca were also determined in Beijing, with concentrations being similar for these species. The Mg concentration was approximately two times lower compared to levels of K, Fe and Ca. Al, Na and K concentrations determined near Beijing were an order of magnitude higher compared to Al, Na and K levels determined at Welgegund. Fe levels were twice as low near Beijing, while Ca concentrations were similar at both sites. Mg concentrations were three time higher near Beijing. Pb and Mn concentrations at Welgegund were similar to levels thereof near Beijing. All the other trace metal species measured near Beijing were an order or two orders of magnitude lower compared to concentrations of these species at Welgegund.

Trace metal concentrations determined at the two European regional background sites indicate that annual average trace metal concentrations were an order or two orders of magnitude lower compared to trace metal levels determined at Welgegund, with the exception of the annual average Al concentration determined at the Mediterranean site.

Also indicated in Table 1 are the existing ambient air quality guidelines and standard limit values for trace metal species prescribed by the WHO air quality guidelines for Europe (WHO, 2005), the European Commission Air Quality Standards (ECAQ, 2008) and the National Air Quality Act of the South African Department of Environmental Affairs (DEA) (SA, 2009). There are currently only guidelines and standards for seven trace metal species, of which the above-mentioned institutions only prescribe limit values for some of these trace metal

species. A comparison of the annual average trace metal concentrations determined at Welgegund with the annual average standard limit values indicates that Ni and As exceeded the limits set by the European Commission of Air Quality Standards. The annual average Ni level of 0.079 μgm^{-3} and the annual average As concentration of 0.008 $\mu g\ m^{-3}$ exceeded their annual standard limits of 0.020 μgm^{-3} and 0.006 μgm^{-3}, respectively. This can most probably be ascribed to the impacts of pyrometallurgical activities in the Bushveld Igneous Complex, especially industries associated with base metal refining. Van Zyl et al. (2014) indicated that the exceedance of Ni at Marikana situated within the western Bushveld Igneous Complex could be attributed to base metal refining. This will also be further explored later in this paper when possible sources of trace metals are evaluated.

The WHO guideline of $2.5x10^{4}$ μgm^{-3} listed for Cr is only for atmospheric concentrations of Cr(VI) with a lifetime risk of 1:1 000 000. The 0.497 μgm^{-3} annual average Cr concentration determined can therefore not be compared to the guideline, since this value represents the total atmospheric Cr concentrations in all the oxidation states. V only has a 24-hour standard limit value. Therefore, V concentrations determined in this study cannot directly be compared to this standard limit. However, the highest weekly V concentration was 0.085 μgm^{-3}, which was lower than the 24-hour V standard limit.

Since Pb is the only trace metal for which a South African ambient air quality standard limit exists, it must also be noted that Pb concentrations did not exceed any standard limit. The Pb concentrations determined at Welgegund were also similar to levels determined at the Vaal Triangle, while the annual average Pb concentration was approximately 2.5 times higher at Marikana and an order of magnitude higher at Rustenburg. However, the annual average Pb concentrations at Marikana and Rustenburg were below the standard limit (Van Zyl et al., 2014). These low Pb concentrations can be partially ascribed to de-leading of petrol in South Africa. Furthermore, Pb concentrations determined at Beijing were similar to levels thereof determined at Welgegund.

It is also important to refer to the Hg concentrations, which were below the detection limit of the analytical instrument for a majority of the sampling period. Van Zyl et al. (2014) also indicated that Hg was below the detection limit of the analytical technique for aerosol samples collected at Marikana. This can be expected, since particulate Hg only forms a small fraction of the total atmospheric Hg, with Hg being predominantly present in the atmosphere as gaseous elemental Hg (GEM) (Venter et al., 2015, Slemr et al., 2011). The measurement of the ambient Hg concentrations is receiving increasing attention in South Africa and it is foreseen that a standard limit value for Hg levels will be prescribed in the near future.

Insert Table 1

Seasonal trends

South Africa is well known for distinct metrological seasonal trends, which have an influence on concentrations of atmospheric species. Therefore, in Figure 4, the total concentrations of the trace metal species in the PM_1 (a), $PM_{1\text{-}2.5}$ (b) and $PM_{2.5\text{-}10}$ (c) size fractions measured at Welgegund for each month are presented, with the contributing concentrations of each of the trace metals indicated. No distinct seasonal pattern is observed for trace metal concentrations in the $PM_{2.5\text{-}10}$ size fraction, with the exception of November that had significantly higher trace metal levels, especially Ca. However, the PM_1 and $PM_{1\text{-}2.5}$ size fractions do indicate relatively higher total trace metal concentrations from September to November and August to November, respectively. These periods coincided with the end of the dry season, which occurs in this part of South Africa from mid-May to mid-October. Furthermore, the end of the dry season is also characterised by increases in wind speed in August. Therefore, these elevated trace metal concentrations determined in the PM_1 and $PM_{1\text{-}2.5}$ size fractions can partially be attributed to decreased wet removal in conjunction with increases in wind generation thereof. In addition, slightly higher trace metal concentrations are

observed in the PM_1 size fraction in the winter months from June to August, which can be ascribed to the presence of more pronounced inversion layers during this time of the year that trap pollutants near the surface.

Insert Figure 4

The monthly concentrations of each of the trace metal species determined in the PM_1 and $PM_{1\text{-}2.5}$ size fractions reveal the highest contributions from Fe and Ca in both these size fractions for each of the months. The concentrations of Na and Cr that were the third and fourth most abundant species, respectively, as well as the elevated levels of Al, B, Mg, Ni, K and P are also reflected in the monthly distributions in the PM_1 and $PM_{1\text{-}2.5}$ size fractions. However, although Fe and Ca were slightly higher in the $PM_{2.5\text{-}10}$ size fraction, a more even contribution from the concentrations of Fe, Ca, Na, Cr, Al, B, Mg, Ni, K and P is observed, with the exception of November. This can be attributed to this larger size fraction consisting predominantly of wind-blown dust. A significantly higher monthly Ca concentration was determined in November that contributed to a considerable increase in the measured total trace metal level. The Ca concentration in the $PM_{2.5\text{-}10}$ size fraction also had a higher contribution in October and similarly higher levels during October in the PM_1 size fraction.

Source apportionment

As a first approach in the source apportionment investigation, Spearman correlation diagrams were prepared for each size fraction. In Figure 5, the PM_1, $PM_{1\text{-}2.5}$ and $PM_{2.5\text{-}10}$ size fractions are presented, i.e. Figures 5a, 5b and 5c, respectively. In Figure 5a, Na, Mg, Ca as well as Fe and Cr correlate with each other, suggesting a crustal influence. Strong correlations to the above are indicated by Sr. A correlation between Sr and B can also be seen. V indicated no correlation to Ni or Mn; instead, Ni is associated to Mn as Cr is to Fe. In the fine fraction, the trace metals originating from metallurgical industries are expected.

In Figure 5b, Sr remains correlated to Na, Mg, Ca and Al. P indicated little to no correlations. In Figure 5c, P and K showed little to no associations while Sr remained correlated to the crustal species. In addition, Cr and Fe have more prominent associations suggesting their crustal origins.

Insert Figure 5

In an effort to determine sources of trace metals, PCFA was applied as an exploratory tool, since much larger datasets are required for definitive source apportionment with PCFA. Therefore, only the most apparent groupings of metal species relating to expected sources in the region were identified. In Figure 6, the factor loadings obtained for the PM_1 size fraction are presented indicating three meaningful factors with eigenvalues equal to or greater than one (Pollisar et al., 1998). These three factors obtained explained 78% of the variance. PCFA of the $PM_{1\text{-}2.5}$ and $PM_{2.5\text{-}10}$ size fractions did not reveal any meaningful factors. This was attributed to the large influence of wind-blown dust on trace metals measured at Welgegund with all the factors obtained for the $PM_{1\text{-}2.5}$ and $PM_{2.5\text{-}10}$ size fractions containing mostly crustal species loadings. In this analysis, species that were not detected at least 60% of the time, were excluded.

Insert Figure 6

Factor 1 was mainly loaded with trace metal species that are typically associated with wind-blown dust, i.e. Ca, Fe, Na, Mg and Al. Therefore, this factor was identified as the crustal factor. The contribution of small Cr units from wind-blown dust is also reflected in this factor with a relatively high loading. This factor explained 53.7% of the total system variance. However, this factor also exhibits a strong loading of V. The use of $NaNO_3$ in V extraction is well

documented (Liu *et al.*, 2012), as is the use of limestone (CaO) as a de-slagging agent in steel production (Rodriguez-Navarro *et al.*, 2009).

Factor 2 explained 13.8% of the variance in the data and was identified as the pyrometallurgical-related factor. This factor revealed higher loadings of Be, Cr, Fe Ni, Mn and Mo. Fe and Cr are associated with the large number of ferrochromium smelters in the Bushveld Igneous Complex, while Ni related to base metal smelters that refine base metals extracted from the PGM production processes. Mn is present in most of the ores from which metals are produced in the western Bushveld Igneous Complex. Mn has a substantially lower vapour pressure than most of the heavy metals produced in this region and is therefore more volatile.

Factor 3 was predominantly loaded with Be, P, Mn, Co, Mo, Cd, Sb, Tl, Pb and U. This factor explained 7.1% of the variance and was identified as the fly ash factor, originating from a variety of combustion processes. Si, Ca and Al are typically associated with fly ash. elements such as Be, B, Cd, Cr, Co, Pb, Mn, Mo, Sr, and Tl have been reported on and may be produced during high temperature processes, which include coal combustion (Goodarzi, 2006). The high variability of the coal composition in combustion and metallurgical processes, contributes to the variability in fly-ash composition.

Pollution roses of each of the trace metal species detected were also compiled in an effort to substantiate the sources identified with PCFA for the PM_1 size fraction, as well as to verify the influence of wind-blown dust that contributed to obtaining no meaningful factors for $PM_{1\text{-}2.5}$ and $PM_{10\text{-}2.5}$. In Figure 7, these pollution roses are presented, which indicate higher trace metal concentrations associated with wind directions from the north to western sector from Welgegund for all the species. As mentioned previously, the north to south-western sector from Welgegund is considered to be a relatively clean region without any large pollutant sources. Therefore, the most significant source of atmospheric trace metal species originating from this sector can be considered to be wind-blown dust (e.g. from the Karoo and Kalahari). This is also indicated by the higher atmospheric concentrations of specifically Ca, Fe, Na, Mg and Al associated with

the north-western sector. Furthermore, the concentrations of trace metal species originating from the north can also be associated with the western Bushveld Igneous Complex source region, as well as the anticyclonic recirculation of pollutant species over the interior of South Africa. This is also reflected by slightly higher concentrations of Ni, Cr, Mn and Sb associated with winds originating in the north. It is also evident that Fe has a contribution from wind-blown dust from the north-western sector, as well as from pyrometallurgical activities in the north.

Insert Figure 7

Conclusions

Of the elements analysed in the aerosol samples, atmospheric Fe had the highest concentrations in all three size fractions, while Ca was the second most abundant species. Cr and Na concentrations were the third and fourth most abundant species, respectively, while relatively higher concentrations were also determined for Al, B, Mg, Ni, K and P. With the exception of Fe that had higher concentrations in the PM_1 size fraction, the concentrations of the trace metal species in all three size ranges were similar.

A comparison of trace metal concentrations determined at Welgegund with trace metal measurements conducted in the western Bushveld Igneous Complex indicated that Fe was also the most abundant species, while other trace metals determined at Welgegund were also measured in the western Bushveld Igneous Complex. However, concentrations of these trace metal species were significantly higher in the western Bushveld Igneous Complex. Trace metal concentrations were also compared to levels thereof in the Vaal Triangle, where Na, Fe and K were the most abundant species. Fe concentrations at the Vaal Triangle were similar to levels thereof at Welgegund, while concentrations of species associated with pyrometallurgical smelting were lower. Comparison to atmospheric trace

metal species measured at a background site in China revealed similar concentrations for Fe and Ca, while Al, Na and K were an order of magnitude higher. Atmospheric trace metal concentrations were much lower at two European background sites. With the exception of Ni and As, none of the trace metals measured at Welgegund exceeded local and international standard limit values. The relatively high Ni and As concentration could possibly be attributed to the influence of base metal refining in the western Bushveld Igneous Complex.

No distinct seasonal pattern is observed for total trace metal concentrations in the $PM_{2.5-10}$ size fraction, while the PM_1 and $PM_{1-2.5}$ size fractions indicated elevated trace metal concentrations coinciding with the end of the dry season. This could partially be attributed to decreased wet removal and increases in wind generation of particulates.

With the exception of Ti, Al and Mg, 65% or more of the trace metal species detected were in the two smaller size fractions, with approximately 40 to 45% occurring in the PM_1 size fraction, which indicated the influence of industrial activities on trace metals measured at Welgegund. However, the large influence of wind-blown dust on trace metal concentrations determined at Welgegund is reflected by 35% and more of trace metals being present in the $PM_{2.5-10}$ size fraction, while Ti, Al and Mg were predominantly in the $PM_{2.5-10}$ size fraction.

PCFA analysis revealed three meaningful factors in the PM_1 size fraction, i.e. fly ash, pyrometallurgical-related and crustal. No meaningful factors were determined for the $PM_{1-2.5}$ and $PM_{2.5-10}$ size fractions, which were attributed to the large influence of wind-blown dust on atmospheric trace metals determined at Welgegund. Pollution roses confirmed this impact of wind-blown dust on trace metal concentrations, while the influence of industrial activities was also substantiated.

Acknowledgements

The financial assistance of the National Research Foundation (NRF) towards this research is hereby acknowledged. Opinions expressed and conclusions

arrived at are those of the author and are not necessarily to be attributed to the NRF.

References

ADGATE, J. L., MONGIN, S. J., PRATT, G. C., ZHANG, J., FIELD, M. P., RAMACHANDRAN, G. & SEXTON, K. 2007. Relationships between personal, indoor, and outdoor exposures to trace elements in PM2.5. Science of the Total Environment: 386:21-32.

AL-MOMANI, I.F., DARADHEH, A.S. & HAJ-HUSSEIN, A.T. 2005. Trace elements in daily collected aerosols in Al-Hashimya, central Jordan. Atmospheric Research: 73:87-100.

BEUKES, J.P., VAKKARI, V., VAN ZYL, P.G., VENTER, A.D., JOSIPOVIC, M., JAARS, K., TIITTA, P., KULMALA, M., WORSNOP, D., PIENAAR, J.J., JÄRVINEN, E., CHELLAPERMAL, R., IGNATIUS, K., MAALICK, Z., CESNULYTE, V., RIPAMONTI, G., LABAN, T.L., SKRABALOVA, L., DU TOIT, M., VIRKKULA, A. & LAAKSO, L. 2013. Source region plume characterisation of the interior of South Africa, as measured at Welgegund. Clean Air Journal: 1-10.

CDC, Centers for Disease Control. 2015. Agency for Toxic Substances and Disease Registry. http://www.atsdr.cdc.gov/toxprofiles/index.asp Date of access: 14 July 2015.

DUAN J., TAN J., WANG S., HAO J., CHAI F. 2012. Size distributions and sources of elements in particulate matter at curbside, urban and rural sites in Beijing. Journal of Environmental Sciences, 24:87-94.

ECAQ, European Commission on Air Quality. http://ec.europa.eu/environment/air/quality/standards.htm, Last updated: 19/11/2015, Date of access: 01/12/2015, Directive 2008/50/EC adopted on 21 May 2008.

FOMBA, K. W., MULLER, K., VAN PINXTEREN, D. & HERRMANN, H. 2012. Aerosol size-resolved trace metal composition in remote northern tropical Atlantic marine environment: case study Cape Verde Islands. Atmospheric Chemistry and Physics Discussions, 12:29535-29569.

GOODARZI, F. 2006. Characteristics and composition of fly ash from Canadian coal-fired power plants. Fuel. 85(10-11):1418-1427.

IPCC. 2014. Climate Change 2014: Mitigation of climate change. Contribution of Working Group III to the Fifth Assessment Report of the Intergovernmental Panel on Climate Change.

KGABI, N.A. 2006. Monitoring the levels of toxic metals of atmospheric particulate matter in the Rustenburg district. MSc Thesis. Potchefstroom: North-West University

KLEPPER, M. R. & WYANT, D.G. 1957. Notes on the Geology of Uranium. Washington D.C..

KLEYNHANS, E .L. J. BEUKES, J. P. , VAN ZYL, P. G. , KESTENS, P. H. I. & LANGA, J. M. 2012. Unique challenges of clay binders in a pelletised chromite pre-reduction process. Minerals Engineering: 34:55–62.

KLEYNHANS, E.H. 2008. Spatial and temporal distribution of trace elements in aerosols in the Vaal triangle. MSc thesis. Potchefstroom: North-West University.

KOULOURI, E., SAARIKOSKI, S., THEODOSI, C., MARKAKI, Z., GERASOPOULOS, E., KOUVARAKIS, G., MAKELA, T., HILLAMO, R. & MIHALOPOULOS, N. 2008. Chemical composition and sources of fine and coarse aerosol particles in the Eastern Mediterranean. Atmospheric Environment: 42:6542-6550.

KULKARNI, P., CHELLAM, S., FLANAGAN, J.B. & JAYANTY, R.K.M. 2007. Microwave digestion—ICP-MS for elemental analysis in ambient airborne fine particulate matter: Rare earth elements and validation. Analytica Chimica Acta: 599:170-176.

LAAKSO L., VAKKARI V., VIRKKULA A., LAAKSO H., BACKMAN, J., KULMALA M., BEUKES J. P., VAN ZYL P. G., TIITTA P., JOSIPOVIC M., PIENAAR J. J., CHILOANE K., GILARDONI S., VIGNATI E.,

WIEDENSOHLER A., TUCH T., BIRMILI W., PIKETH S., COLLETT K., FOURIE G. D., KOMPPULA M., LIHAVAINEN H., DE LEEUW G., KERMINEN V.-M., 2012 South African EUCAARI measurements: seasonal variation of trace gases and aerosol optical properties Atmospheric Chemistry and Physics, 12: 1847-1864.

LIU, B., DU, H., WANG, S., ZHANG, Y., ZHENG, S., LI, L., CHEN, D. 2012. A novel method to extract vanadium and chromium from vanadium slag using molten NaOH-$NaNO_3$ binary system. Reaction Engineering, Kinetics, and Catalysis. 59(2): 541-552.

LOURENS, A.S.M., BEUKES, J.P., VAN ZYL, P.G., FOURIE, G.D., BURGER, J.W., PIENAAR, J.J., READ, C.E. & JORDAAN, J.H. 2011. Spatial and temporal assessment of gaseous pollutants in the Mpumalanga Highveld of South Africa. South African Journal of Science, 107(1/2):8.

NEL, A. 2005. Air pollution-related illness: effects of particles. Science, 309:1326.

PACYNA J. M.: Source inventories for atmospheric trace metals. R.M HARRISON, R.E VAN GRIEKEN (Eds.), Atmospheric Particles, IUPAC Series on Analytical and Physical Chemistry of Environmental Systems, Vol. 5 Wiley, Chichester, UK (1998), pp. 385-423.

PIO C. A., CASTRO L. M., CERQUEIRA M. A., SANTOS I. M., BELCHIOR F., SALGUEIRO M. L., 1996 Source assessment of particulate air pollutants measured at the southwest European coast. Atmospheric Environment, 30:3309-3320.

POLIDORI, A., CHEUNG, K. L., ARHAMI, M., DELFINO, R. J., SCHAUER, J. J. & SIOUTAS, C. 2009. Relationships between size-fractionated indoor and outdoor trace elements at four retirement communities in Southern California. Atmospheric Chemistry and Physics, 9: 4521-4536.

1 POLISSAR, A. V., HOPKE, P. K., PAATERO, P., MALM, W. C., SISLER, J. F.
2 1998. Atmospheric aerosol over Alaska 2: Elemental composition and sources.
3 Journal of Geophysical Research and Discussions, 103:19045-19057.

4 POPE, C. A. & DOCKERY, D. W. 2006. Health effects of fine particulate air
5 pollution: lines that connect. Air & Waste Management Association, 56:709-742.

6 PÖSCHL, U. 2005 Atmospheric aerosols: Composition, transformation, climate
7 and health effects Angewandte Chemie International Edition, 44:7520-7540 DOI:
8 10.1002/anie.200501122.

9 QUEROLA X., VIANAA M., ALASTUEYA A., AMATOA F., MORENOA T.,
10 CASTILLOA S., PEYA J., DE LA ROSAB J., SANCHEZ DE LA CAMPAB A.,
11 ARTINANOC B., SALVADORC P., GARCIA DOS SANTOS S., FERNANDEZ-
12 PATIERD R., MORENO-GRAUE S., NEGRALE L., MINGUILLONA M.C.,
13 MONFORTF E., GILG J.I., INZAG A., ORTEGAG L.A., SANTAMARIAH J.M.,
14 ZABALZAH J. 2007. Source origin of trace elements in PM from regional
15 background, urban and industrial sites of Spain. Atmospheric Environment,
16 41:7219-7231.

17 RODRIGUEZ-NAVARRO, C., RUIZ-AGUDO, E., LUQUE, A., RODRIGUEZ-
18 NAVARRO, A.B., ORTEGA-HUERTAS, M. 2009. Thermal decomposition of
19 calcite: Mechanisms of formation and textural evolution of CaO nanocrystals.
20 American Mineralogist. 94(4): 578-593.

21 RUBASINGHEGE G., ELZEY S., BALTRUSAITIS J., JAYAWEERA P.M.;
22 GRASSIAN, V.H. 2010. Reactions on Atmospheric Dust Particles: Surface
23 photochemistry and size-dependent nanoscale redox chemistry. Journal of
24 Physical Chemistry Letters, 1:1729-1737 DOI: 0.1021/jz100371d.

25 SLEMR, F., BRUNKE, E.-G., EBINGHAUS, R. & KUSS, J. 2011, Worldwide
26 trend of atmospheric mercury since 1995, Atmospheric Chemistry and Physics,
27 11:4779–4787.

SOUTH AFRICA. 2009. National Environmental Management: Air Quality Act, 2004 (ACT NO. 39 OF 2004) National ambient air quality standards, *Government Gazette*, 24 December 2009, pp. 6-9.

SOUTH AFRICA. 2006. Department of Environmental Affairs and Tourism. Declaration of the Vaal Triangle Airshed Priority Area in terms of section 18(1) of the National Environmental Management: Air Quality Act 2004 (Act no. 39 of 2004).

SOUTH AFRICA, M. 2007. Department of Environmental Affairs and Tourism. Declaration of the Highveld as priority area in terms of section 18(1) of the National Environmental Management: Air Quality Act 2004 (Act no. 39 of 2004).

SOUTH AFRICA. 2012. National Environmental Management: Air Quality Act, 2004 (ACT NO. 39 OF 2004) Declaration of the Waterberg National Priority Area. *Government gazette*, 35435: 15 Jun. Date of access: 15 Oct. 2015.

THURSTON, G. D., ITO, K., MAR, T., CHRISTENSEN, W. F., EATOUGH, D. J. & HENRY, R. C. 2005. Workgroup report: workshop on source apportionment of particulate matter health effects: intercomparison of results and implications. Environmental Health Perspectives, 113:1768-1774.

VAN ZYL, P. G., Beukes, J. P., DU TOIT, G., MABASO, D., HENDRIKS, J., VAKKARI, V., TIITTA, P., PIENAAR, J.J., KULMALA, M. & LAAKSO, L. 2014. Assessment of atmospheric trace metals in the western Bushveld Igneous Complex, South Africa. South African Journal of Science, 3/4(110).

VENTER, A. D., BEUKES, J. P., VAN ZYL, P. G., BRUNKE, E.-G., LABUSCHAGNE, C., SLEMR, F., EBINGHAUS, R. & KOCK, H. 2015. Statistical exploration of gaseous elemental mercury (GEM) measured at Cape Point from 2007 to 2011. Atmospheric Chemistry and Physics, 15:10271–10280, doi:10.5194/acp-15-10271-2015.

VENTER, A.D., VAKKARI, V., BEUKES, J.P., VAN ZYL, P.G., LAAKSO, H., MABASO, D., TIITTA, P., JOSIPOVIC, M., KULMALA, M., PIENAAR, J.J. & LAAKSO, L. 2012. An air quality assessment in the industrialized western

1 Bushveld Igneous Complex, South Africa, South African Journal of Science,
2 2012, 9/10(108):1059. doi: 10.4102/sajs.v108i9/10.1059

3 World Health Organization: Air quality guidelines - global update 2005
4 http://www.who.int/phe/health_topics/outdoorair/outdoorair_aqg/en/ (Date of
5 access 22 November 2015)

6 ZHAN, H., JIANG, Y., YUAN, J., HU, X., NARTEY, O., WANG, B., 2014. Trace
7 metal pollution in soil and wild plants from lead–zinc smelting areas in Huixian
8 County, Northwest China. Journal of Geochemical Exploration. 147:182-188.

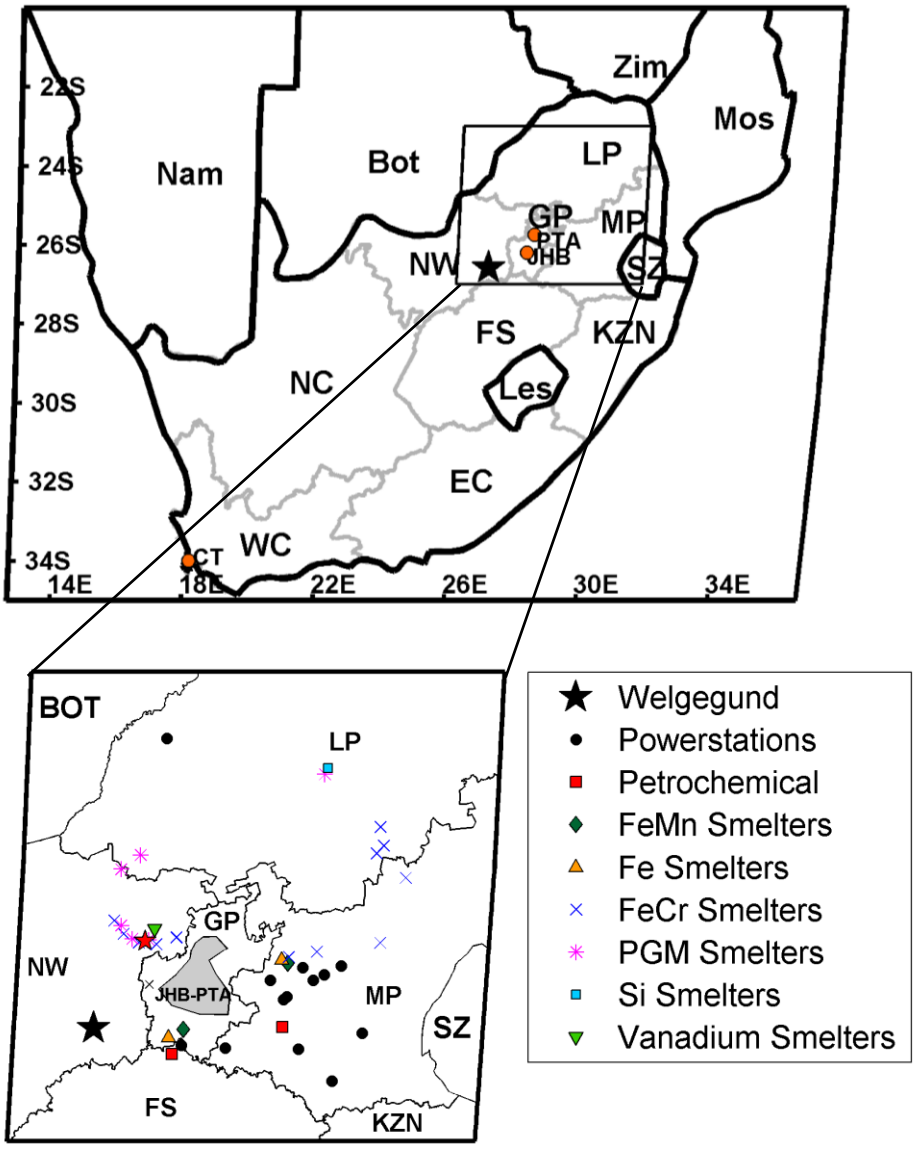

Figure 1: Geographical map indicating Welgegund (black star), as well as the major point sources and the JHB-PTA conurbation that have an impact on air masses measured at Welgegund.

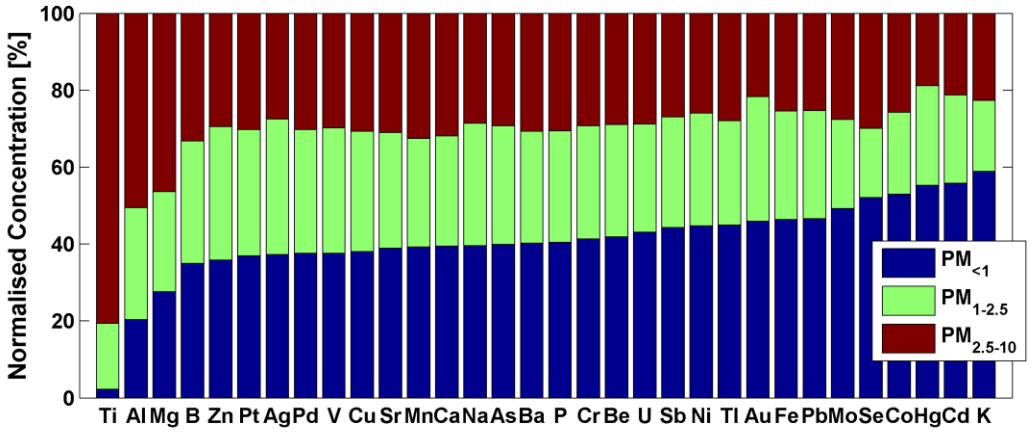

Figure 2: Size distributions of individual trace metal species detected

1

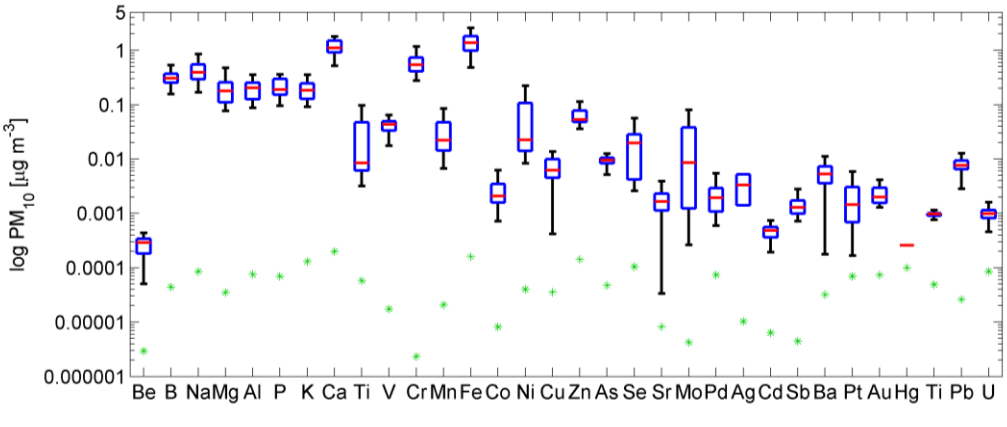
log PM10 [µg m-3]
5
1
0.1
0.01
0.001
0.0001
0.00001
0.000001
Be B NaMg Al P K Ca Ti V Cr Mn Fe Co Ni Cu Zn As Se Sr Mo Pd Ag Cd Sb Ba Pt Au Hg Ti Pb U

2 (a)

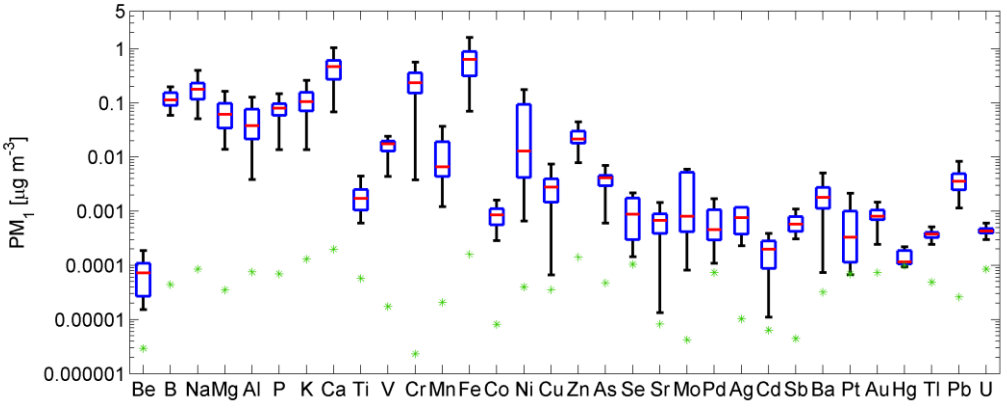
PM1 [µg m-3]
5
1
0.1
0.01
0.001
0.0001
0.00001
0.000001
Be B NaMg Al P K Ca Ti V Cr Mn Fe Co Ni Cu Zn As Se Sr Mo Pd Ag Cd Sb Ba Pt Au Hg Tl Pb U

3 (b)

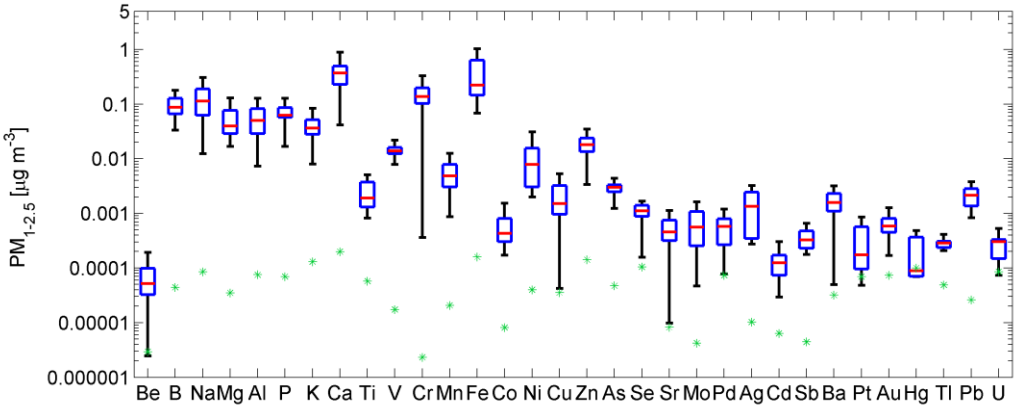
PM1-2.5 [µg m-3]
5
1
0.1
0.01
0.001
0.0001
0.00001
0.000001
Be B NaMg Al P K Ca Ti V Cr Mn Fe Co Ni Cu Zn As Se Sr Mo Pd Ag Cd Sb Ba Pt Au Hg Tl Pb U

4 (c)

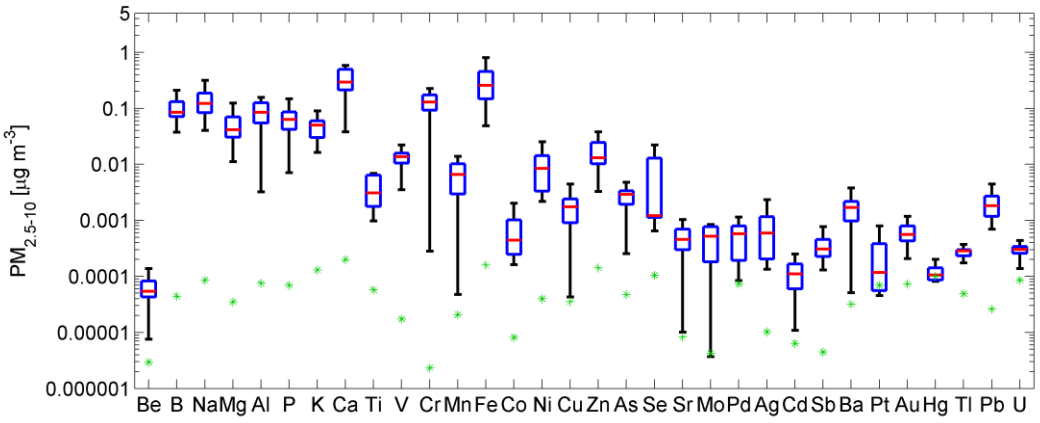

(d)

Figure 3: Box and whisker plots of trace metal concentrations in the (a) PM_{10} (sum of trace metal concentrations in the three size fractions), (b) PM_{1}, (c) $PM_{1-2.5}$, and (d) $PM_{2.5-10}$ size fractions. The red line indicates the median concentrations, the blue rectangle of the boxplot represents the 25th and 75th percentiles, while the whiskers indicate ± 2.7 times the standard deviation. The green stars are the detection limits of each species.

Table 1: Annual average trace metal concentrations measured at Welgegund, annual average standard limits, as well as annual average trace metal levels determined in other studies in South Africa, China and Europe. Concentration values are presented in μgm^{-3}

PM_{10} Annual Average	This study Welgegund	Annual standard limit	South Africa			Duan et al. Beijing	Pio et al. Mediterranean	Querol et al. Spain
			Van Zyl et al.	Kgabi	Kleynhans			
Be	**0.158**		0.020			0.100		<0.001
B	**0.283**		1.300					
Na	**0.377**		1.410		2.800	1.450		
Mg	**0.227**		2.040		1.000	0.637		
Al	**0.170**		1.280			2.180	0.200	
P	**0.172**							
K	**0.138**		0.680		1.300	1.170		
Ca	**1.089**		1.080			0.996		
Ti	**0.072**		0.120	0.180	0.020	0.069		0.019
V	**0.037**	1.000[(b)#]	0.040	0.160			<0.001	0.005
Cr	**0.497**	2.50x10^{4}[(a)*]	0.240	1.370	0.050	0.022	<0.001	0.001
Mn	**0.026**	0.150[(a)]	0.060	4.390	0.120	0.036	0.002	0.005
Fe	**1.195**		2.540	9.760	1.280	1.090	0.028	
Co	**0.004**		0.140			<0.001		<0.001
Ni	**0.079**	0.020[(b)]	0.330	0.770	0.040	0.020	<0.001	0.003
Cu	**0.007**		0.180	0.210	0.050	0.010	0.003	0.008
Zn	**0.053**		0.490	0.340	0.090	0.027	0.003	0.026
As	**0.008**	0.006 [(b)]	0.260			0.003	0.002	<0.001
Se	**7.400**		0.580			0.001	<0.001	0.001<
Sr	**0.002**					0.010		0.005
Mo	**0.002**					0.007		0.004
Pd	**0.015**		0.410					

Table 1: continued...

Ag	**0.536**					<0.001		
Cd	**0.385**	0.005 (a)(b)	0.030			<0.001	<0.001	<0.001
Sb	**0.001**					<0.001		<0.001
Ba	**0.004**		0.140			0.018		<0.008
Pt	**0.002**		0.350					
Au	**0.003**		0.380					
Hg	**0.184**	1.000(a)	0.550					
Tl	**0.713**		0.270					<0.001
Pb	**0.008**	0.5 (a)(b)(c)	0.080	0.420	0.040	0.053	0.003	0.009
U	**0.891**							

** WHO guideline for Cr(VI) concentrations associated with an excess lifetime risk of 1:1 000 000*

 # 24-h limit value

a) *WHO air quality guidelines for Europe,* b) *European Commission Air Quality Standards, c) National Air Quality Act of the South African Department of Environmental Affairs*

Yellow shading is indicative of species with concentration values in ng.m-3. A value half of the detection limits is used here in accordance with health related studies

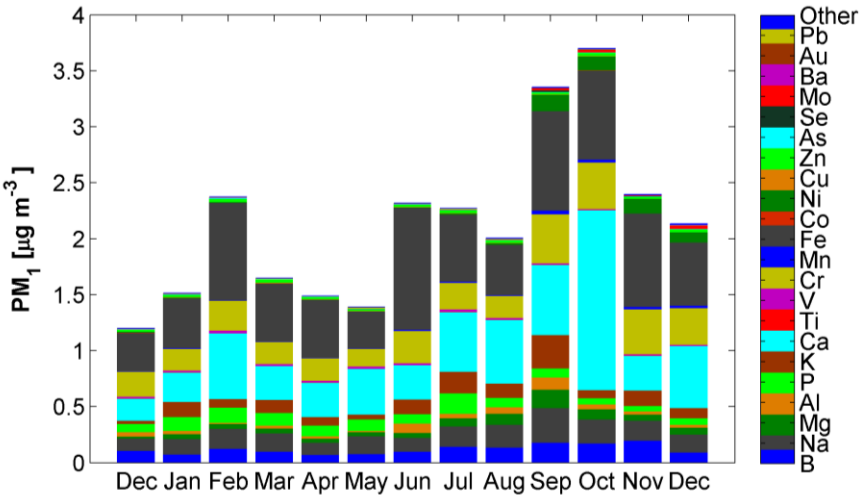

(a)

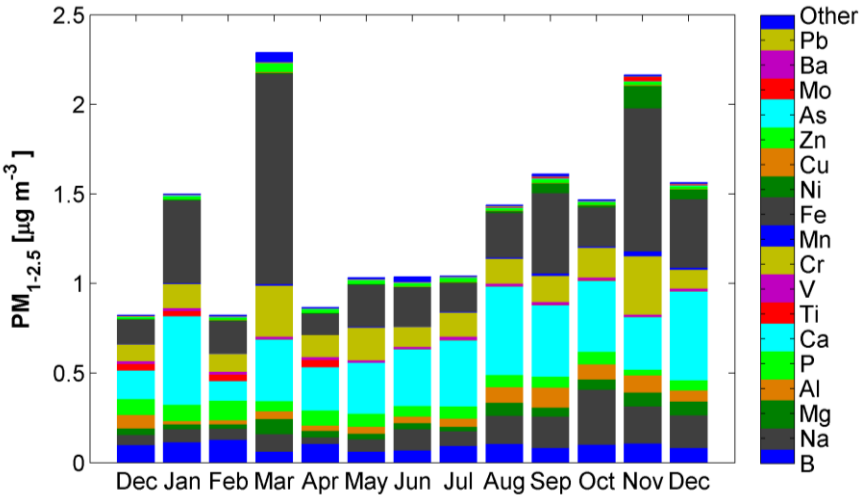

(b)

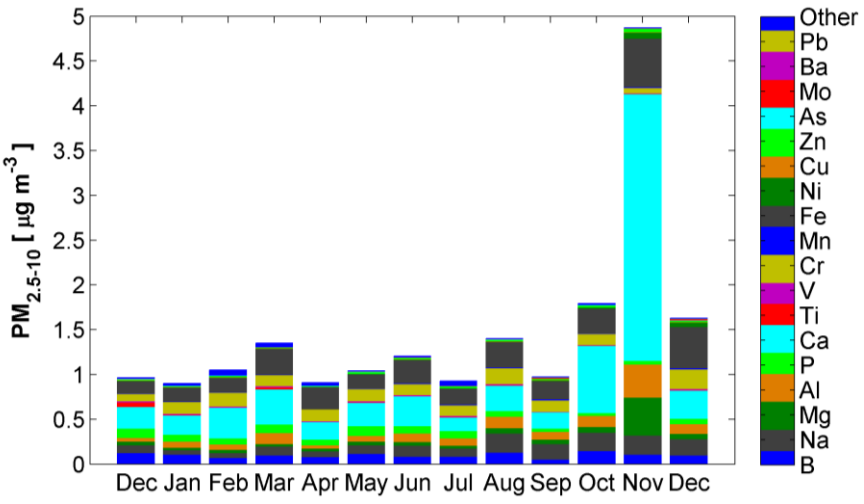

(c)

Figure 4: The monthly median trace metal concentrations in the PM_1 (a), $PM_{1–2.5}$ (b) and $PM_{2.5–10}$ (c) size fractions

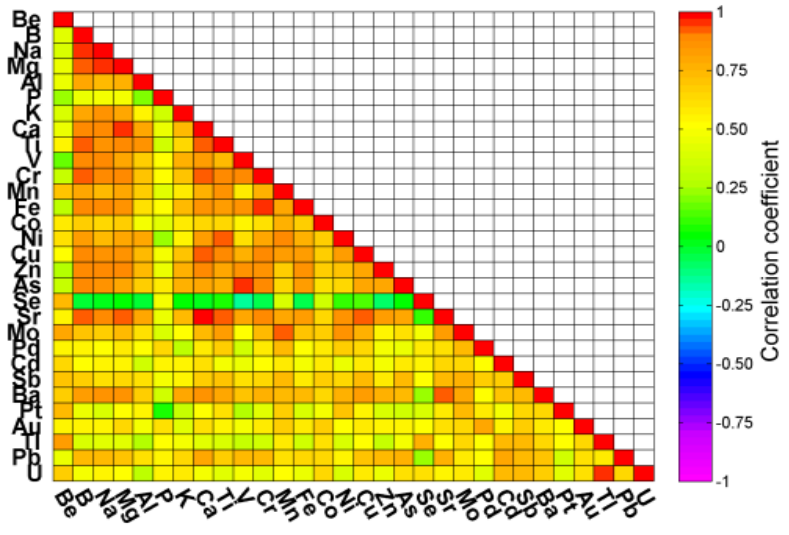

(a)

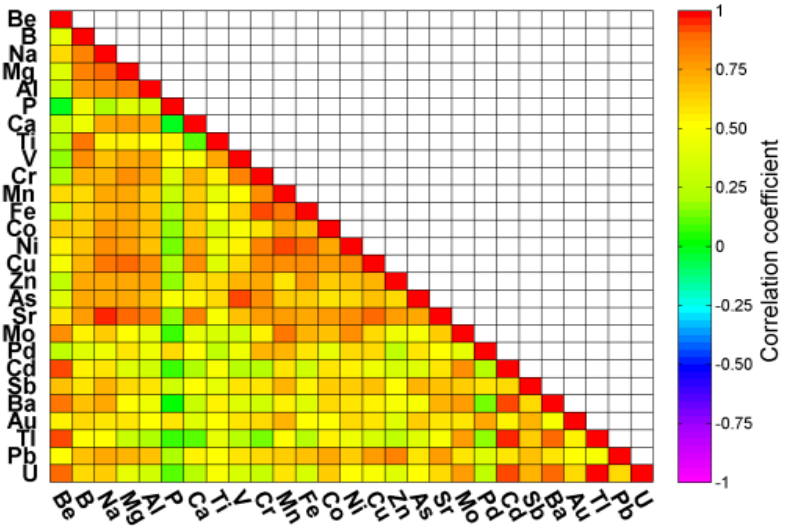

(b)

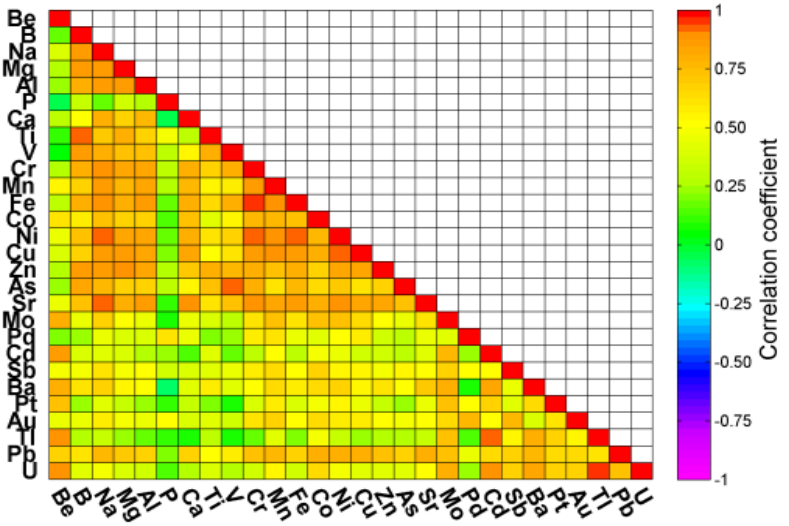

(c)

4 Figure 5: Spearman correlations of trace metal species in the PM_1 (a), $PM_{1\text{-}2.5}$ (b)
5 and $PM_{2.5\text{-}10}$ (c) size fractions

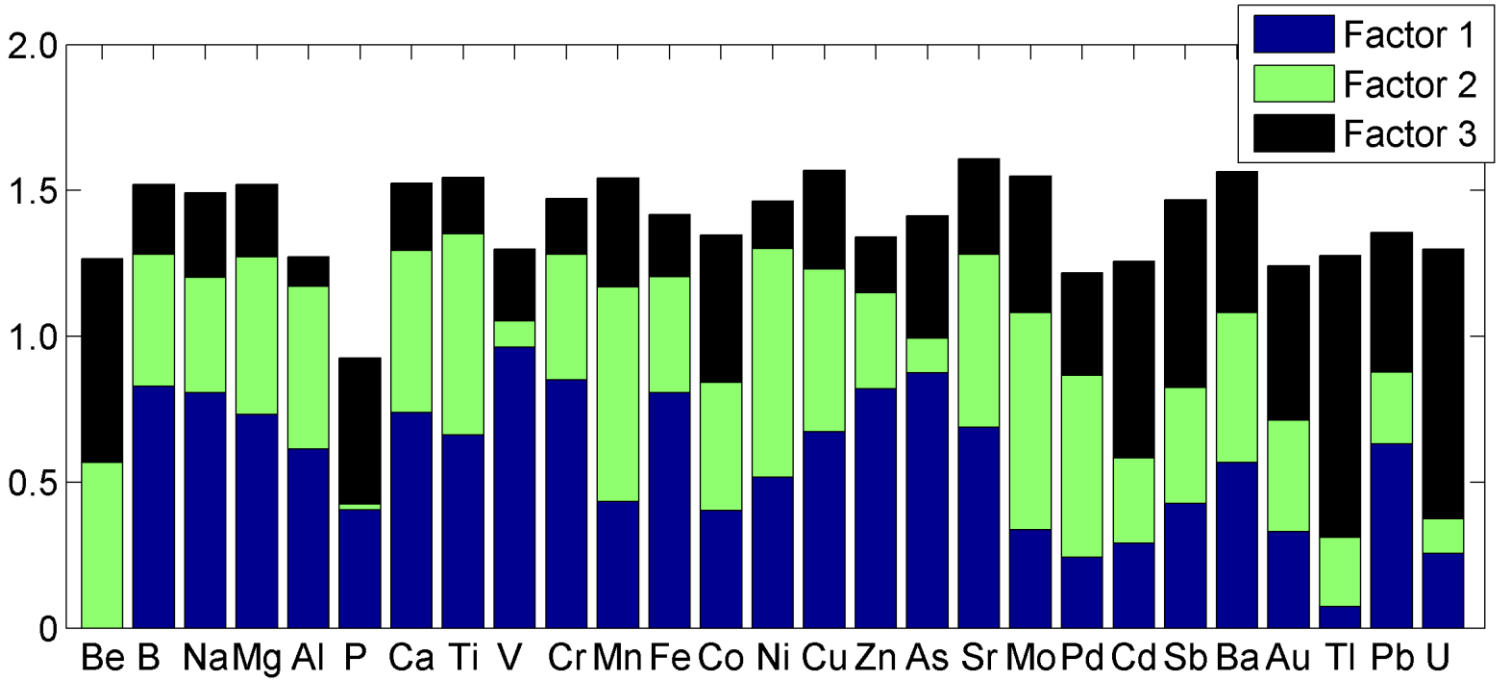

1

2 Figure 6: PCA/FA of the trace metal concentration in the PM_1 size fraction. Three dominant factors are identified.

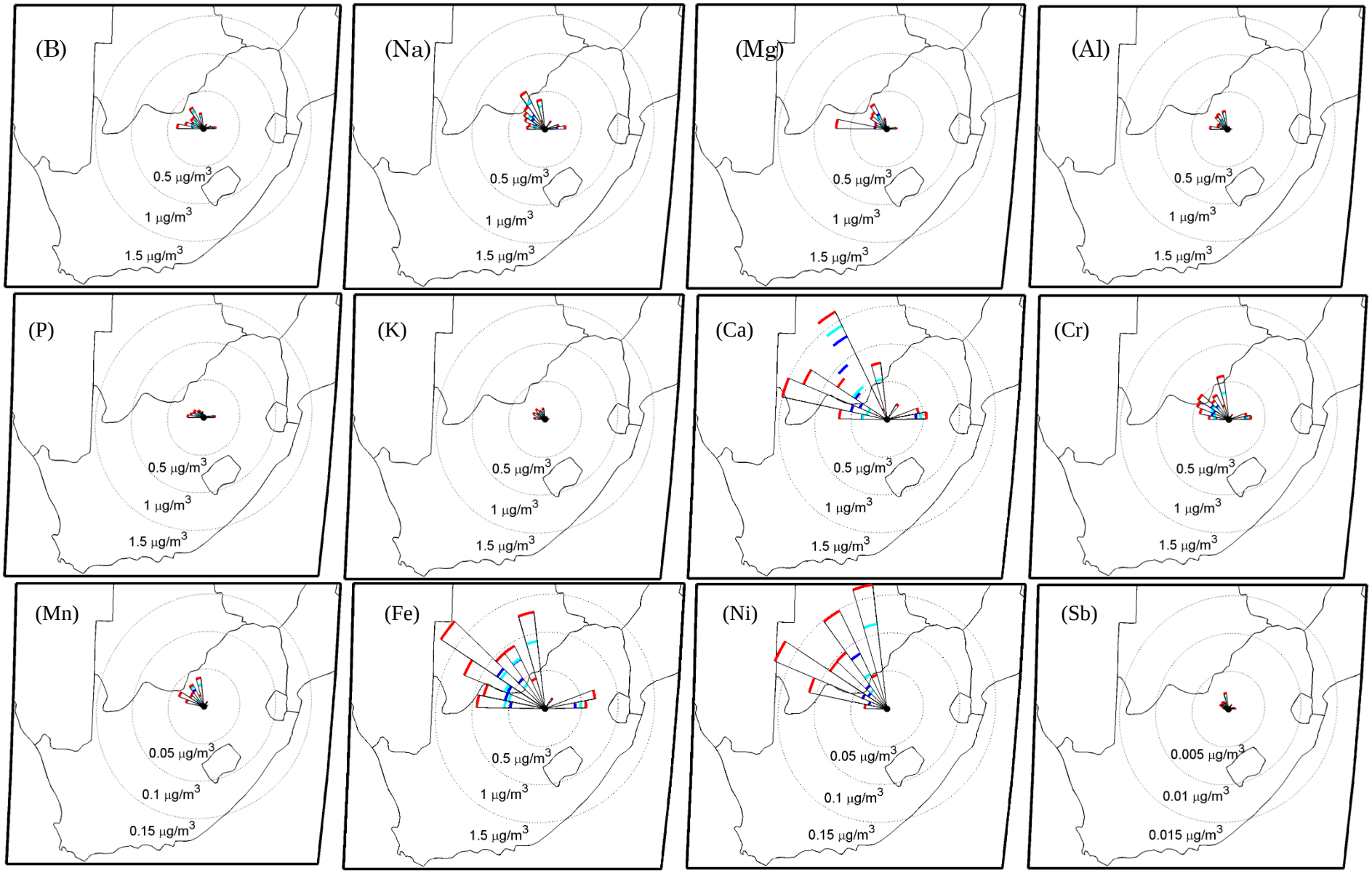
(B)
0.5 µg/m3
1 µg/m3
1.5 µg/m3
(Na)
0.5 µg/m3
1 µg/m3
1.5 µg/m3
(Mg)
0.5 µg/m3
1 µg/m3
1.5 µg/m3
(Al)
0.5 µg/m3
1 µg/m3
1.5 µg/m3
(P)
0.5 µg/m3
1 µg/m3
1.5 µg/m3
(K)
0.5 µg/m3
1 µg/m3
1.5 µg/m3
(Ca)
0.5 µg/m3
1 µg/m3
1.5 µg/m3
(Cr)
0.5 µg/m3
1 µg/m3
1.5 µg/m3
(Mn)
0.05 µg/m3
0.1 µg/m3
0.15 µg/m3
(Fe)
0.5 µg/m3
1 µg/m3
1.5 µg/m3
(Ni)
0.05 µg/m3
0.1 µg/m3
0.15 µg/m3
(Sb)
0.005 µg/m3
0.01 µg/m3
0.015 µg/m3

1

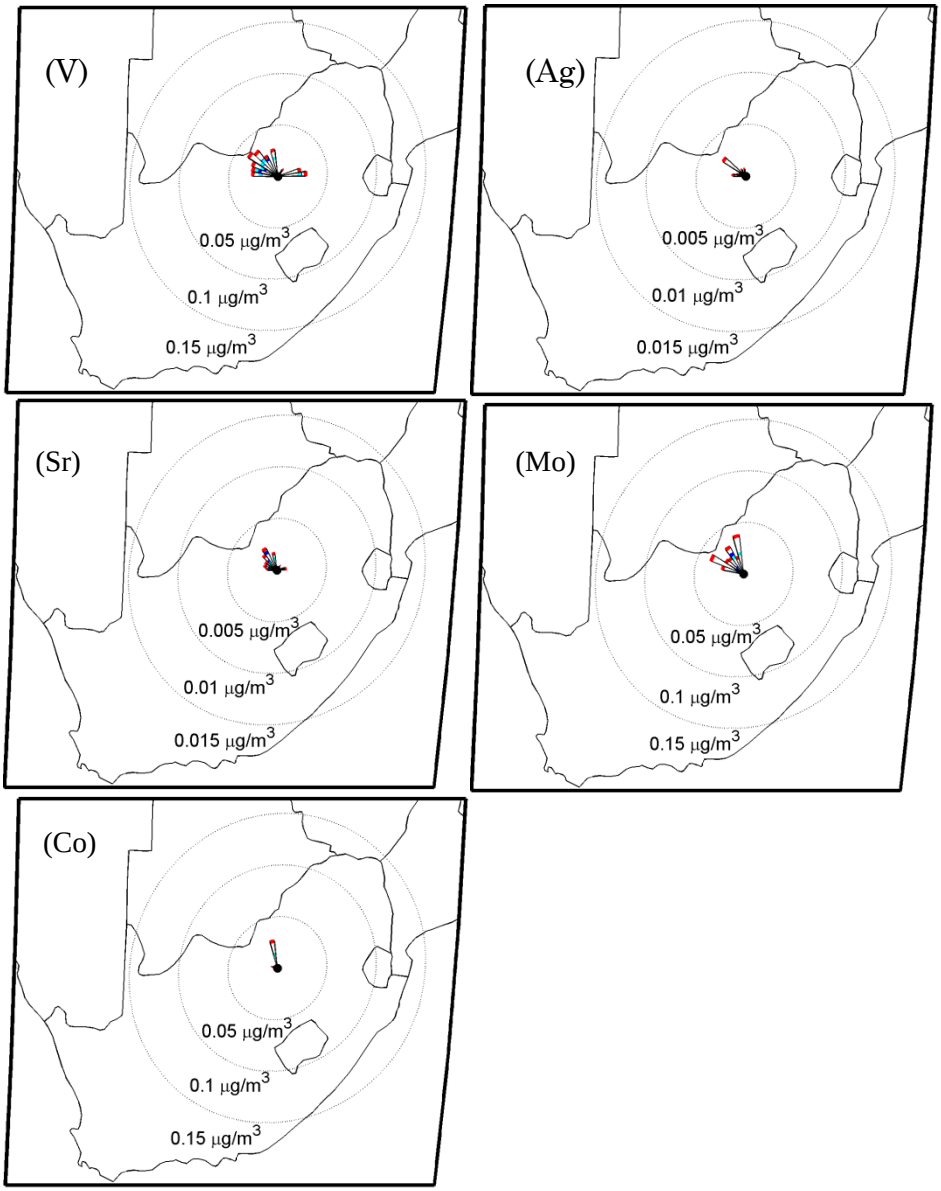

Figure 7: Pollution roses of trace metal species that were 25% or more of the time detected with the analytical technique

Chapter 7

Measurement of atmospheric inorganic ionic species at Welgegund, South Africa

Author list and contributions

A. D. Venter[1], P.G. van Zyl[1], J. P. Beukes[1], J. Swartz[1], K. Jaars[1], M. Josipovic[1], W. Booyens[1]

1 Unit for Environmental Sciences and Management, North-West University, Potchefstroom, South Africa

Contributions of the various co-authors were as follows. The bulk of the work was done by the candidate A. D. Venter (including sample analysis, data processing research and writing of the scientific article), with conceptual ideas and recommendations by the promoters P.G. van Zyl and J.P. Beukes. The candidate (A.D. Venter), K. Jaars, W. Booyens and M. Josipovic helped gather data at the Welgegund measurement station, J. Swartz assisted with ion chromatography (IC) analysis.

Formatting and current status of article

The article was formatted in accordance with the journal specifications to which it will be submitted, i.e. *Atmospheric Chemistry and Physics,* a European Geosciences Union journal. The figures and tables of this article are also added at the end of the text, as prescribed by the journal. The authors' guide that was followed in preparation of the article was available at http://www.atmospheric-chemistry-and-physics.net/for_authors/submit_your_manuscript.html (Date of access: 26 November 2015). At the time when this PhD was submitted for examination, this article had not yet been submitted for review, but the intention was to submit it soon thereafter.

Consent by co-authors

All the co-authors on the article have been informed that the PhD will be submitted in article format and have given their consent.

Measurement of atmospheric inorganic ionic species at Welgegund, South Africa

A. D. Venter[1], P.G. van Zyl[1], J. P. Beukes[1], J. Swartz[1], K. Jaars[1], M. Josipovic[1], W. Booyens[1]

[1]{Unit for Environmental Sciences and Management, North-West University, Potchefstroom, South Africa}

Correspondence to: P.G. van Zyl (pieter.vanzyl@nwu.ac.za)

Abstract

The physical and chemical characterisation of atmospheric aerosols is essential in establishing their impacts on climate change and human health. Aerosols consist of a large number of organic and inorganic species, which depend on the sources of these species. Inorganic ionic species in atmospheric aerosols have a significant influence on the acidity potential of the atmosphere, which will also have an impact on ecological systems through wet and dry deposition thereof. The aim of this study was to conduct an assessment of major inorganic ions determined in three aerosol size ranges, i.e. PM_1, $PM_{1-2.5}$ and $PM_{2.5-10}$ collected for one year at Welgegund in South Africa. Results indicated that SO_4^{2-} concentrations in the PM_1 size fraction were significantly higher compared to the other species in all three size fractions. SO_4^{2-} and NH_4^+ dominated the PM_1 size fraction, while SO_4^{2-} and NO_3^- were the predominant species in the $PM_{1-2.5}$ and $PM_{2.5-10}$ size fractions. SO_4^{2-} had the highest contribution in the two smaller size fractions, while NO_3^- had the highest contribution in the $PM_{2.5-10}$ size fraction. SO_4^{2-} levels were attributed to the impacts of aged air masses passing over source regions, while marine air masses were considered to be the major source of NO_3^-. The reaction of SO_4^{2-} with gas-phase NH_3 was considered to be the major source of NH_4^+ in the PM_1 size fraction. The PM at Welgegund was determined to be

acidic, mainly due to the excess concentrations of SO_4^{2-}. Comparison of the inorganic ion concentrations determined at Welgegund to measurements thereof at Marikana situated in one of the major source regions impacting on Welgegund indicated that the concentrations of almost all the inorganic ion species were higher at Marikana. At Welgegund, PM_1 and $PM_{1-2.5}$ fractions revealed a seasonal pattern, with higher inorganic ion concentrations measured from May to September. Higher concentrations were attributed to decreased wet removal of these species, since these months coincide with the dry season in this part of South Africa. Increases in pollutant concentrations due to more pronounced inversion layers trapping pollutants near the surface, as well as increases in household combustion and wild fires during these months were also considered contributing to elevated levels of inorganic ions. Back trajectory analysis of each of the sampling months also revealed higher concentrations of inorganic ionic species corresponding to air mass movements over source regions.

Keywords: inorganic ions, seasonal trends, precipitation, back trajectories, South Africa

Introduction

Atmospheric aerosols or particulate matter (PM) are important components of the atmosphere, which can have significant impacts on general air quality and play a significant role in the climate forcing (IPCC, 2014). Aerosols show high temporal and spatial variability, increasing the necessity for detailed physical and chemical characterisation (Koulouri et al., 2008). A significant number of studies have been performed on aerosols to determine the sources, characteristics, as well as the potential impacts on human health and climate in recent times. Although the impacts of greenhouse gases (especially CO_2) on climate change are well understood, large uncertainties are associated with regard to the impacts of aerosols on climate change (IPCC, 2014). The impacts of PM on climate change and human health can only be established by physically and chemically characterising these species.

PM is usually classified according to their size as course (PM_{10} – aerodynamic diameter < 10 μm), fine ($PM_{2.5}$ – aerodynamic diameter < 2.5 μm) or ultrafine (PM_1 and $PM_{0.1}$ – aerodynamic diameter < 1 and < 0.1 μm, respectively) particulates. Larger particles have shorter lifetimes in the atmosphere compared to smaller aerosols. Some of the impacts of these species are also determined by their size. Fine and ultrafine particles, for instance, can more readily penetrate into the lungs and are therefore more likely to increase respiratory and mutagenic diseases (Schwartz et al., 1996). In addition to size, the chemical composition of aerosols is important. Aerosols consist of a large number of organic (which include black carbon, i.e. BC and organic compounds, i.e. OC) and inorganic species, which depends on the sources of PM. The highest uncertainty related to atmospheric aerosols is associated with the exact chemical composition of atmospheric aerosols, especially relating to organic compounds (Booyens et al, 2014, Tiitta, et al, 2014). A large number of inorganic species are present in aerosols, which include trace metals and ionic species. The major inorganic ionic species usually considered in atmospheric aerosols include sulphate (SO_4^{2-}), nitrate (NO_3^-) and ammonium (NH_4^+), sodium (Na^+), potassium (K^+), chloride (Cl^-), calcium (Ca^{2+}), magnesium (Mg^{2+}) and fluoride (F^-). These inorganic ions in atmospheric aerosols have a significant influence on the acidity potential of the atmosphere, which will also have an impact on ecological systems through the wet and dry deposition of these species. Furthermore, chemical properties of aerosols also have an influence on the physical properties of PM. Inorganic SO_4^{2-} species, for instance, are lightly coloured particulates that reflect incoming solar radiation that causes a net cooling effect in the atmosphere, while dark particles such as BC absorb radiative energy, leading to the warming of the atmosphere.

Aerosols can be directly emitted into the atmosphere as primary aerosols from natural and/or anthropogenic sources, or are formed as secondary aerosols through chemical reactions and gas-to-particle conversions. Typical natural sources include volcanic eruptions, wind-blown dust, pollen, maritime, biogenic emissions and natural wild fires. Biomass burning (human-induced wild fires, and household combustion for cooking and space heating), fossil fuel combustion

(industrial activities and vehicular emissions), as well as mining and agricultural activities are considered to be the most important anthropogenic sources. Atmospheric inorganic and organic gaseous species emitted from natural and anthropogenic sources are considered important precursor species for secondary aerosols, e.g. SO_2, NO_2 and NH_3 that form SO_4^{2-}, NO_3^- and NH_4^+, respectively.

South Africa is a well-known source region of atmospheric pollutants as indicated by ground measurements and satellite retrievals over this region (Lourens et al., 2012; Ghudea et al., 2009). South Africa has the largest industrialised economy in Africa, with significant industrial, mining and agricultural activities. Electricity is predominantly generated with coal-fired power plants that are centralised in the interior of South Africa. In addition, seasonal biomass burning (wild fires) also has a large impact on this region (Wai et al., 2014). In an effort to determine the regional impacts of the major pollutant source regions in the interior of South Africa, the long-term Welgegund atmospheric measurement station was established, which is comprehensively equipped to measure a large number of atmospheric parameters, which include atmospheric aerosol properties (Beukes et al., 2015).

In this study, an assessment of major inorganic ions determined in three aerosol size ranges collected for one year at Welgegund is presented. The measurement of inorganic ions is especially important in South Africa, since the coal-fired power stations and most of the industries do not apply de-SOx and de-NOx technologies, which leads to elevated emissions of SO_2 and NO_2, and the consequent formation of SO_4^{2-} and NO_3^-. Statistical methods were applied in an effort to determine major sources of inorganic ions. This paper is an extension of the previous papers wherein trace metals (Venter et al, 2015) and organic compounds (Booyens et al., 2014) determined in different size ranges for atmospheric aerosols collected at Welgegund were presented. In addition, this work also supplements the work conducted by Tiitta et al. (2014), where PM_1 aerosols were chemically characterised with aerosol chemical specification monitor (ACMS) measurements during which organic aerosol (OA), SO_4^{2-}, NH_4^+, NO_3^- and Cl^- concentrations were determined. Furthermore, in order to compare

inorganic ion concentrations determined at Welgegund (a regional background site) with levels of these species within a declared air quality priority area (indicating a source region with significantly high pollutant concentrations), inorganic ion concentrations determined at Marikina are also presented. Marikana is situated within the Bushveld Igneous Complex that forms part of the Waterberg Priority Area (SA, 2012a), which is one of the major source regions impacting on Welgegund.

Experimental

Site description

Welgegund

Aerosol sampling was performed at the Welgegund atmospheric measurement station (www.welgegund.org, 26.569786 S and 26.939289 E, 1 480 m a.s.l.). Welgegund is situated on a commercially owned farm with no large pollution sources within close proximity. The site is strategically situated in the interior of South Africa, since it is frequently impacted by air masses moving over the most important source regions in the interior of South Africa (e.g. the western Bushveld Igneous Complex, Vaal Triangle, Mpumalanga Highveld and the Johannesburg-Pretoria conurbation), as well as a relatively clean background region with no large point sources. In Beukes et al. (2013), Jaars et al. (2014) and Tiitta et al. (2014), maps indicating the location of Welgegund and a detailed description of site, which include site selection, prevailing biomes and major source regions are presented.

Marikana

Marikana (25.69845 S, 27.48056 E, 1170m a.s.l.) is a small village situated approximately 35 km east of Rustenburg, in the North West Province of South Africa – maps indicating the location of Marikana were presented by Venter et al. (2012), Hirsikko et al. (2012) and Van Zyl et al. (2014). Marikana is located

within the western Bushveld Igneous Complex, which is well known for comprehensive mining and metallurgical activities (Van Zyl et al., 2014; Beukes et al., 2013; Venter et al., 2012). The site was situated in a residential area on the property of the Marikana municipal clinic. A detailed description of the measurement site and possible sources of pollutants is presented in Venter et al. (2012).

Sampling and analysis

PM samples were collected at Welgegund from 24 November 2010 until 28 December 2011. A Dekati (Dekati Ltd., Finland) PM_{10} cascade impactor (ISO23210) equipped with Teflon filters was used to collect different particulate size ranges, i.e. $PM_{2.5\text{-}10}$ (aerodynamic diameter ranging between 2.5 and 10 μm), $PM_{1\text{-}2.5}$ (aerodynamic diameter ranging between 1 and 2.5 μm) and PM_1 (aerodynamic diameter <1). The pump flow rate was set at 30 L/min. Samples were collected continuously for one week, after which filters were changed. A total of 54 samples were collected for each of the three size ranges.

An Airmetrics MiniVol™ portable air sampler was used for aerosol sample collection at Marikana. Two MiniVol samplers were used simultaneously to collect PM <10μm (PM_{10}) and PM <2.5μm ($PM_{2.5}$) samples (Airmetrics, 2011). A programmable timer controlled the pump in order to achieve sample collection of 12 hours per day for six days, beginning either at 06:00 for daytime data, or at 18:00 for night time data. Each sample contained PM collected for 72 hours. The actual sampling time and flow rate (5 L/min) were taken into consideration to determine the atmospheric concentrations of the species. All filter samples collected at Welgegund and Marikana were sealed-off in containers, which were stored in a freezer prior to analyses.

The filters were divided into two equal parts by a specially designed punching system, to be able to analyse both trace metals (Venter et al., 2015) and inorganic ions using a single set of samples. The inorganic ions in the aerosols collected on

the Teflon filters were extracted with 5 mL deionised water (18.2 MΩ) in an ultrasonic bath for 30 minutes. Extracted aqueous samples were subsequently analysed with a Dionex ICS 3000 ion chromatograph (IC), with an IonPac AG18 (2 mm x 50 mm) guard and IonPac AS18 (2 mm x 50 mm) analytical column. The inorganic ionic species determined included SO_4^{2-}, NH_4^+, NO_3^-, Na^+, K^+, Cl^-, Ca^{2+} and Mg^{2+}. Concentrations below the detection limit of the IC were considered to have concentrations half the detection limit of the species considered. This is a precautionary assumption that is frequently used in health-related environmental studies (Al-Momani et al., 2005; Kulkarni et al., 2007, Van Zyl et al., 2014).

Back trajectory analysis

Individual 96 hour, hourly back trajectories with an arrival height of 100 m were calculated with HYSPLIT 4.820.19 (Draxler & Hess, 2004; Lourens et al., 2011; Venter et al., 2012). An arrival height of 100 m was chosen since the orography in HYSPLIT is not very well defined with lower arrival heights resulting in increased error margins on individual trajectory calculations. 24-hourly arriving back trajectories for each day were obtained for the entire sampling period. Individual back trajectories produced in HYSPLIT (24 x 365 days) were superimposed and further analysed in MATLAB. In the overlay back trajectory presentation compiled with MATLAB, a colour code indicates the percentage of trajectories passing over 0.2° x 0.2° grid cells, with red being the highest percentage and blue the lowest.

Results

Size resolved inorganic ion concentrations

In Figure 1, the concentrations of each of the inorganic ionic species determined in the three size ranges for Welgegund samples are presented. SO_4^{2-}, NH_4^+, K^+

and F^- concentrations were significantly higher in the PM_1 size fraction, with concentrations of these species in the PM_1 size fraction approximately an order of magnitude higher compared to the levels of these species in the $PM_{1\text{-}2.5}$ and $PM_{2.5\text{-}10}$ size fractions. Slightly higher levels of NO_3^-, Cl^- and Mg^{2+} were measured in the $PM_{2.5\text{-}10}$ size fraction in relation to the other two size fractions, while Na^+ and Ca^{2+} concentrations were evenly distributed in all three size ranges. SO_4^{2-} levels in PM_1 were approximately three times higher than NH_4^+ in the PM_1 size fraction, while being an order magnitude higher compared to the concentrations of NO_3^-, Na^+, K^+ and Ca^{2+} in all three size ranges, as well as to the concentrations of $SO_4^{2-}$and NH_4^+ in the $PM_{1\text{-}2.5}$ and $PM_{2.5\text{-}10}$ size fractions. SO_4^{2-} concentrations in the PM_1 size fraction were two orders of magnitude higher compared to Cl^-, Mg^{2+} and F^- levels in all three size ranges. The median SO_4^{2-}, NH_4^+, K^+ and F^- concentrations in the PM_1 fraction were 1.35 $\mu g/m^3$, 0.440 $\mu g/m^3$, 0.032 $\mu g/m^3$ and 0.015 $\mu g/m^{-3}$, respectively. The median levels of NO_3^-, Cl^- and Mg^{2+} in the $PM_{2.5\text{-}10}$ size fraction were 0.057 $\mu g/m^3$, 0.007 $\mu g/m^3$ and 0.006 $\mu g/m^3$, respectively. The highest median concentrations for Na^+ were 0.021 $\mu g/m^3$ in the $PM_{1\text{-}2.5}$ size fraction, while Ca^{2+} had the highest median of 0.014 $\mu g/m^3$ in the $PM_{2.5\text{-}10}$ size fraction.

Insert Figure 1

The normalised contribution percentages of each of the inorganic ionic species in terms of their ionic concentrations observed at Welgegund are presented in Figure 2 for the three size fractions. It is evident that the PM_1 size fraction is dominated by SO_4^{2-} and NH_4^+, while the $PM_{1\text{-}2.5}$ and $PM_{2.5\text{-}10}$ size fractions are dominated by SO_4^{2-} and NO_3^-. However, SO_4^{2-} was the most dominant species in both the smaller size fractions, while NO_3^- had the highest concentration in $PM_{2.5\text{-}10}$. Tiitta et al. (2014) also indicated, with ACMS measurements, higher contributions of SO_4^{2-} and NH_4^+ in PM_1 aerosols. SO_4^{2-} in the smaller size fractions (especially PM_1) is generally considered to be a secondary pollutant

resulting from the oxidation of SO_2 in aged air masses in South Africa. Most industries in South Africa utilise particulate filters to filter out particulates in off-gas. Therefore, primary emissions of SO_4^{2-} are unlikely. However, as mentioned previously, most industries in South Africa do not employ de-SOx and de-NOx technologies, which leads to higher SO_2 and NO_2 emissions. Furthermore, the highly industrialised interior of South Africa is characterised by anti-cyclonic recirculation of air masses wherein the aging of pollutant species occurs. As the primary sources of SO_2 and NO_2 are the coal fired power stations. SO_2 is directly proportional to the amount of coal combusted whereas NO varies depending on the burner technology implemented by the power station. In the 2015 annual report of ESKOM, South Africa's main power supplier, it is reported that 119.2 Mt of coal was combusted with an average ash and sulphur content of 27.63% and 0.80% respectively. The report quantifies SO_2, NO_2 and N_2O emissions as 1 834 kt, 937 kt and 2 919 kt respectively (ESKOM, 2015). Vakkari et al. (2014) also indicated the importance of SO_4^{2-} as a precursor for new particle formation in South Africa. In general, most of the inorganic ions in the PM_1 fraction can be considered to be secondary aerosols.

Insert Figure 2

Atmospheric NO_3^- can mainly be attributed to the oxidation of NO_2 gaseous emissions to form HNO_3. The higher NO_3^- contribution in the $PM_{2.5-10}$ size fraction is most likely related to aged marine air masses, where hydrogen chloride has been displaced from NaCl by HNO_3 vapour to form $NaNO_3$ (Turner & Colbeck, 2008). On the other hand, NO_3^- observed in the smaller size fractions may be the product of the formation of NH_4NO_3 from the neutralisation reaction between HNO_3 vapour by NH_3 (Turner & Colbeck, 2008). The much lower NO_3^- concentrations in the PM_1 fraction can most likely be attributed to the high SO_4^{2-} levels that will substitute the NO_3^- in NH_4NO_3 to form $(NH_4)_2SO_4$ if SO_4^{2-} that is not completely neutralised (Sienfeld & Pandis, 2006). The high NH_4^+ observed in

the PM_1 size fraction can most probably be ascribed to particulate SO_4^{2-} reacting with NH_3 in the gas phase due to the high acidity of SO_4^{2-} particles (Squizzato et al., 2013). Furthermore, the $PM_{2.5-10}$ size fraction has higher percentage contributions from Cl^-, Mg^{2+}, Ca^{2+} and Na^+ compared to the other two size fractions, which can be attributed to larger particle originating from marine (e.g. Na^+ and Cl^-) and terrigenous sources (e.g. Ca^{2+} from wind-blown dust). Although Figure 1 indicated that the concentrations of Na^+ and Ca^+ species were evenly distributed in all three size fractions, much lower contributions from SO_4^{2-} and NH_4^+ in the $PM_{2.5-10}$ size fraction lead to an increase in the relative contribution of these species to the total inorganic ionic content. In addition, the NO_3^-, Cl^- and Mg^{2+} concentrations are higher in the $PM_{2.5-10}$ size fraction (Figure 1).

The acidity of atmospheric aerosols has an influence on their hygroscopicity and their ability to produce secondary aerosols. Several studies employed the Extended Aerosol Inorganics Model (E-AIM) to estimate pH, which is considered to produce the best estimates (Squizzato et al., 2013; Hennigan et al., 2015; Zhang et al., 2007). However, this model was not utilised for the Welgegund inorganic ionic data, instead, as discussed by Tiitta et al. (2014) for Welgegund, it is possible to estimate the acidity of PM by comparing the measured NH_4^+ mass concentration to the amount of NH_4^+ needed to completely neutralise the anions that were calculated using Eq. (1):

$$NH_{4\,cal}^{+} = 18 \times \left(2 \times \frac{SO_4^{2-}}{96} + \frac{NO_3^-}{62} + \frac{Cl^-}{35.5}\right) \quad (1)$$

Here, SO_4^{2-}, NO_3^- and Cl^- are the mass concentrations of the ions ($\mu g/m^{-3}$) and the denominators correspond to their molecular weights, with 18 being the molecular weight of NH_4^+. If the calculated NH_4^+ concentration is lower than the measured values, particles are considered to be 'more acidic' or, on the contrary, if the two values are equal, they are considered 'bulk neutralised'. This approach assumes a minimal influence of metal ions, organic acids and bases on NH_4

concentration (Zhang et al., 2007). The calculated NH_4^+ concentrations plotted against the measured values are presented in Figure 3. In this figure, the 1:1 line corresponds to the bulk neutralised state. It is evident from the results that the aerosols are closer to the neutralised state in the dry season (Jul'11 and Sep'11) than in the wet season (Dec'10-Feb'11 and Nov'11-Dec'11). SO_2 oxidation to SO_4^{2-} is moisture limited, with little such oxidation occurring at relatively humidity (RH) below 70% (Connel, 2005). Therefore, even with elevated SO_2 concentrations in the dry season, less SO_4^{2-} will form, resulting in more neutralised aerosols. In contrast, more acidic aerosols form in the wet season. However, in both seasons, the aerosols are essentially acidic in nature, implying that the atmospheric NH_4^+ concentration was insufficient to neutralise all SO_4^{2-}, NO_3^- and Cl^- anions. From the results presented in Figures 1 and 2, it could be deduced that SO_4^{2-} was the dominating acidic ion, which indicates that a fraction of NO_3^- and Cl^- anions must be associated with cations other than NH_4^+. In Figure 3, numerous points (circled) did not lay close to the linear fitted lines of the dry and wet season data. These data points were considered in the afore-mentioned linear fits, but clearly indicate somewhat different behaviour. Obviously, these 'outliers' could be as a result of the assumptions made in this approach, i.e. minimal influence of metal ions, organic acids and bases on NH_4^+ concentrations (Zhang et al., 2007). However, these data points could also indicate that the aerosol acidities might be extremely acidic or basic on certain occasions. Especially aerosols in the wet season indicate such behaviour. This could be linked to the RH dependency of SO_4^{2-} formation, since six of the eight 'outliers' close to the x-axis are wet season data points. This result indicates extreme acidity in some aerosol samples gathered in the wet season.

Insert Figure 3

Comparison with inorganic ion concentrations measured within a source region

In order to contextualise the inorganic ion concentrations measured at Welgegund, the results were compared to levels determined for inorganic ionic species at Marikana. As mentioned previously, Marikana is situated within the industrialised Bushveld Igneous Complex, which is one of the major source regions influencing air masses measured at Welgegund (Beukes et al., 2013, Tiitta et al., 2014, Jaars et al., 2014). Venter et al. (2012) reported high PM_{10} concentrations measured at Marikana, with PM_{10} levels exceeding South African legislative standard limits.

In Figure 4, the concentrations of each of the inorganic ionic species determined in two size ranges, i.e. $PM_{2.5}$ and PM_{10} at Marikana are presented. As mentioned, MiniVol samplers were used to collect total PM_{10} and $PM_{2.5}$ at Marikana. SO_4^{2-}, NH_4^+ and K^+ concentrations were similar in the two size ranges, with marginally higher median concentrations in the PM_{10} size fraction, i.e. 2.20 μg/m^3, 0.64 μg/m^3 and 12.9 μg/m^3, respectively. Since the PM_{10} size fraction also contains the $PM_{2.5}$ size fraction, the afore-mentioned results prove that these species (SO_4^{2-}, NH_4^+ and K^+) mainly occurred in the $PM_{2.5}$ size fraction. NO_3^-, Cl^-, Mg^{2+} Na^+ and Ca^{2+} concentrations were higher in the PM_{10} size fractions with median concentrations of 0.67 μg/m^3, 0.14 μg/m^3, 0.06 μg/m^3, 0.16 μg/m^3 and 0.25 μg/m^3, respectively. SO_4^{2-} levels were approximately between three and four times higher than NH_4^+ and NO_3^- levels, while being an order magnitude higher compared to the concentrations of Na^+, K^+, Ca^{2+}, Cl^- and Mg^{2+} in both size ranges. The concentrations of all the inorganic species were higher at Marikana compared to Welgegund, with the exception of NH_4^+ and K^+. Concentrations measured for NH_4^+ and K^+ in the PM_1 size fraction at Welgegund were similar compared to levels thereof in $PM_{2.5}$ at Marikana. However, significantly higher concentrations of NH_4^+ and K^+ were determined in the PM_{10} size fraction at Marikana. SO_4^{2-} levels were approximately 2.5 times higher at Marikana, while concentrations of NO_3^-, Cl^-, Mg^{2+} Na^+ and Ca^{2+} were an order of magnitude higher compared to levels thereof at Welgegund. Higher levels of these species are

expected, since Marikana is situated within a source region with a large number of industrial and mining activities, as well as a dense population that contributes to emissions from household combustion for space heating and cooking.

Insert Figure 4

In Figure 5, the normalised distribution percentages of each inorganic ionic species in the $PM_{2.5}$ and PM_{10} size-fractions measured at Marikana are presented. It is evident that both size fractions are dominated by SO_4^{2-}. NH_4^+ was the second most abundant species in the $PM_{2.5}$ size fraction, while NO_3^- and NH_4^+ had similar contributions in PM_{10} being the second most dominant species in this size fraction. The contribution of SO_4^{2-} in the $PM_{2.5}$ size fractions at Marikana is similar to the SO_4^{2-} contributions in PM_1 and $PM_{1-2.5}$ determined at Welgegund. Therefore, secondary aerosol formation from SO_2 emitted from local sources in this region can be considered the main source of these species. However, a considerably higher SO_4^{2-} contribution is observed in the PM_{10} size fraction at Marikana compared to the SO_4^{2-} contribution determined at Welgegund, which leads to much lower contributions of NO_3^-, Cl^-, Mg^{2+}, Ca^{2+} and Na^+. This can be attributed to the strong influence of pyrometallurgical activities on the aerosols sampled in this region. It is well known that the platinum group metals (PGM) industries in the western Bushveld Igneous Complex are associated with high SO_2 emissions resulting from sulphidic ores, without the formation of NO associated with coal fired power plant emissions. Van Zyl et al. (2014) also indicated the high sulphur (S) content in PM sampled in this region.

Insert Figure 5

As mentioned previously, day- and night-time samples were collected at Marikana. Comparisons between the concentrations of the inorganic ions measured during day- and night-time in the PM_{10} size fraction did not statistically reveal differences in concentrations of any of the ionic species. However, comparisons between day- and night-time measurements in the $PM_{2.5}$ size fraction did indicate differences in SO_4^{2-} and NO_3^- concentrations with levels of these species being higher in the night time, as indicated in Figure 6. All the other ionic species in the $PM_{2.5}$ had similar concentrations in day- and night-time samples. The higher SO_4^{2-} nigh-time median can be attributed to the influx of aged regional air masses at Marikana. Venter et al. (2012) indicated the influence of regional air masses on concentrations of the secondary pollutant O_3 at Marikana. Furthermore, although Venter et al. (2012) indicated that SO_2 levels were much lower during night time, the stable meteorological conditions usually occurring during nigh time could also lead to an increase of local conversion of local SO_2 to SO_4^{2-}. The higher night-time median of NO_3^- can most likely be attributed to elevated levels of NO_2, which are associated with household combustion for space heating and cooking, as indicated by Venter et al. (2012). During night time, $NO_3^{\bullet}$ is considered the most reactive oxidative intermediate in the atmosphere, which formed through the reaction of O_3 with NO_2. The higher NO_2 night-time concentrations therefore result in higher $NO_3^{\bullet}$, which increases the night-time oxidative capacity of the atmosphere.

Insert Figure 6

Temporal and spatial variability

In Figure 7, the total monthly concentrations of the inorganic ionic species in $PM_{2.5-10}$ (a), $PM_{1-2.5}$ (b) and $PM_{<1}$ (c) measured at Welgegund are presented, with the contributing concentrations of each of the inorganic ions indicated. No distinct seasonal pattern is observed for the $PM_{2.5-10}$ size fraction. However, the

$PM_{1\text{-}2.5}$ and PM_1 size fractions indicated higher inorganic ion concentrations from May to September and May to August, respectively. These periods with elevated inorganic ion levels can at least partially be ascribed to seasonal variations in meteorological parameters. The months with higher inorganic ion concentrations in the $PM_{1\text{-}2.5}$ and PM_1 size fractions coincide with the cold and dry winter months experienced in this part of South Africa. Winter in South Africa occurs between June and August, which is associated with more pronounced lower inversion layers that inhibit vertical mixing in the atmosphere and trap pollutant species near the surface. Winter is also related to additional combustion of coal and wood for domestic heating. Furthermore, this part of South Africa is characterised by distinct wet and dry seasons, with the wet season occurring between mid-May and mid-October. In Figure 8, the monthly precipitation measured during the entire sampling period at Welgegund is presented, which clearly indicates a period with low rainfall, i.e. May to September. Therefore, wet removal of inorganic ions is suppressed during these dry months, which leads to increased concentrations of these species. The influence of wet deposition on atmospheric inorganic ion concentrations is also illustrated by the difference in the concentrations measured for December 2010 and December 2011. Precipitation was higher in December 2010 compared to December 2011, which resulted in increased wet deposition of inorganic ionic species in December 2010. In addition, the periods with elevated levels of inorganic ions in the $PM_{1\text{-}2.5}$ and PM_1 size fractions also coincide with increased occurrences of biomass burning (wild fires) from July to September.

Insert Figure 7

Insert Figure 8

Although no clear seasonal pattern is observed for $PM_{2.5\text{-}10}$, the influence of meteorology (winter and precipitation) and regional biomass burning is to a

certain extent reflected in higher inorganic ion concentrations measured in July and September in this size fraction. This is also indicated by the much lower inorganic ion concentrations measured in December 2010 and January 2011 in the $PM_{2.5-10}$ size fractions that are associated with significantly higher rainfall occurring during these two months (Figure 8). Furthermore, the influence of precipitation on inorganic ions in the larger size fraction is also indicated by the lower inorganic ion concentrations measured in December 2010 compared to December 2011, as observed in the smaller size fractions. Inorganic ion levels in the $PM_{2.5-10}$ were also related to air mass history by performing back trajectory analysis in an effort to explain the inorganic ion concentration measured during different months, which will be presented later in this paper.

The monthly concentrations of each of the inorganic ions in the three size fractions reflect the normalised contributing concentrations for the entire sampling period at Welgegund presented in Figure 2, i.e. the smaller size fractions are dominated by SO_4^{2-}, while NO_3^- concentrations were the highest in the $PM_{2.5-10}$ size fractions. The relatively large contribution from NH_4^+ in the PM_1 size fraction is also evident for each of the months, while the influence of the marine and crustal species on the $PM_{2.5-10}$ size fraction is also reflected in the monthly concentrations. A distinct seasonal pattern is observed for NO_3^- in the $PM_{<1}$ size fraction, with NO_3^- concentrations only evident from June to October with elevated concentrations thereof from July to September. These higher NO_3^- levels coincide with the peak biomass burning season from July to September. Vakkari et al. (2014) indicated that aerosols in fresh biomass burning (wild fires) plumes measured at Welgegund consisted of 7 to 10% NO_3^-. In aged biomass burning plumes, lower NO_3^- concentrations are expected, since SO_4^{2-} would have reacted with NH_4NO_3, which effectively removes NO_3^- from that particulate phase. Therefore, fresh biomass burning plumes can be considered a source of NO_3^- in the PM_1 size fraction. Higher NO_3^- concentrations are also evident in August and September in the $PM_{1-2.5}$ size fractions, which can also be attributed to biomass burning emissions. A similar seasonal pattern is observed for Cl^- in the $PM_{1-2.5}$ size fraction with relatively higher Cl^- levels from July to September,

which can be attributed to primary biomass burning emissions (Vakkari et al., 2014). Tiitta et al. (2014) indicated a strong influence of biomass burning on organic aerosol and total PM_1 concentrations. However, a less significant impact of biomass burning is observed on the inorganic ionic species concentrations.

ACMS measurements conducted by Tiitta et al. (2014) indicated that SO_4^{2-}, NH_4^+, NO_3^- and Cl^- concentrations in PM_1 depended strongly on air mass history. Therefore, back trajectory analysis was performed for each of the sampling months, which is presented in Figure 9 in order to establish the influence of air mass history on monthly inorganic ion concentrations. In Figure 9, the typical source areas are represented by polygons. The blue polygon indicates the combined Vaal Triangle Airshed Priority Area, Highveld Priority Area and Gauteng (i.e. Johannesburg-Pretoria megacity conurbation). The red polygon incorporates the Waterberg Priority Area and the typical anti-cyclonic recirculation pathway of air masses sampled at Welgegund. From Figure 9, it is evident that the frequency of air masses arriving at Welgegund passing over the two source regions and the background regions is different for certain months.

Insert Figure 9

Similar air mass movements are observed for December 2010, April 2011, May 2011, August 2011, October 2011, November 2011 and December 2011 indicating frequent influences from the anti-cyclonic recirculation pathway passing over the Bushveld Igneous Complex (part of the Waterberg Priority Area) (SA, 2012a). The difference in inorganic ion concentrations measured in December 2010 and December 2011 can be ascribed to the impact of wet deposition on atmospheric PM, as discussed previously (Figure 8). The inorganic ion levels determined in April 2011, October 2011, November 2011 and December 2011 were similar in all three size fractions, with the exception of inorganic ion concentrations in $PM_{1\text{-}2.5}$ in October. These months also had similar levels of rainfall, as indicted in Figure

8. Higher inorganic ion concentrations were determined in May 2011 and August 2011 (especially in May 2011) in the PM_1 and $PM_{1-2.5}$, which can be attributed to these months being dry leading to a decrease in wet removal thereof. During June 2011, much lower inorganic ion concentrations were determined in the PM_1 and $PM_{1-2.5}$ size fractions compared to the higher inorganic ion concentrations measured in these two size fraction during the other colder and dryer months (May to September). Back trajectory analysis (Figure 9) reveals that during June 2011, Welgegund was much more frequently influenced by air masses passing over the background region, leading to lower concentrations of inorganic ions. It is also evident from Figure 9 that Welgegund was more frequently influenced by air masses passing over the Johannesburg-Pretoria conurbation in July 2011, with associated higher inorganic ion concentrations in all three size fractions, especially in the $PM_{2.5-10}$ size fractions. January 2011 and February 2011 back trajectories indicated more frequent impacts from marine air masses at Welgegund, which are reflected in the higher NO_3^- and Na^+ concentrations measured in the $PM_{2.5-10}$ size fraction in February 2011. As mentioned previously, the lower inorganic ion concentrations in January 2011 can be attributed to high precipitation and the associated wet deposition (Figure 8).

Conclusions

This paper presents the concentrations of inorganic ion species determined in aerosol samples collected in three size ranges, i.e. PM_1, $PM_{1-2.5}$ and $PM_{2.5-10}$ collected at Welgegund. SO_4^{2-} concentrations in the PM_1 size fraction were significantly higher compared to the other species in all three size fractions, as well as levels thereof in the $PM_{1-2.5}$ and $PM_{2.5-10}$ size ranges. NH_4^+ in the PM_1 size fraction and NO_3^- in the $PM_{2.5-10}$ size fraction were the second and third most abundant species, respectively. Normalised contribution percentages indicated that SO_4^{2-} and NH_4^+ dominated the PM_1 size fraction, while SO_4^{2-} and NO_3^- were the predominant species in the $PM_{1-2.5}$ and $PM_{2.5-10}$ size fractions. SO_4^{2-} had the highest contribution in the two smaller size fractions, while NO_3^- had the highest

contribution in the $PM_{2.5-10}$ size fraction. SO_4^{2-} levels were attributed to the impacts of aged air masses passing over source regions with high SO_2 emissions, while marine air masses were considered to be the major source of NO_3^-. The major source of NH_4^+ in the PM_1 size fraction was attributed to the reaction of SO_4^{2-} with gas-phase NH_3.

Recent publications indicate that conventional molar ratios or net balance between ionic species are not ideal to determine the pH of PM and that the use of models are more accurate. However, conditions experienced at Welgegund (low humidity and high temperatures) made the utilisation of these models problematic. Instead, a simple calculation was used to indicate whether aerosol samples were acidic or not. The PM at Welgegund was determined to be acidic, which was related to the high SO_4^{2-} concentrations. It is proposed that the future implementation of these models are investigated in more detail.

Comparison of the inorganic ion concentrations measured at Welgegund to measurements of these species at Marikana, which is situated within one of the major source regions influencing Welgegund, indicated that the concentrations of almost all the inorganic ion species were higher at Marikana. SO_4^{2-} concentrations at Marikana were 2.5 times higher, while the concentrations of the other species were an order of magnitude higher. The smaller size fraction at Marikana was also dominated by SO_4^{2-} and NH_4.

No distinct seasonal pattern was observed at Welgegund for $PM_{2.5-10}$, while the PM_1 and $PM_{1-2.5}$ fractions had higher inorganic ion concentrations from May to September. These months coincide with the dry season in this part of South Africa with low precipitation. Therefore, higher concentrations were mainly attributed to a decrease in the wet removal of these species. In addition, increases in pollutant concentrations due to more pronounced inversion layers trapping pollutants near the surface, as well as increases in household combustion and wild fires during these months, were also considered contributing to elevated levels of inorganic ions. NO_3^- in the PM_1 size fraction and

Cl^- in the $PM_{1\text{-}2.5}$ size fraction showed a distinct seasonal pattern with elevated levels coinciding with the burning season in southern Africa.

Back trajectory analysis of each of the sampling months also revealed higher concentrations of inorganic ionic species corresponding to air mass movements over source regions.

Acknowledgements

The financial assistance of the National Research Foundation (NRF) towards this research is hereby acknowledged. Opinions expressed and conclusions arrived at are those of the authors and are not necessarily to be attributed to the NRF. The authors would also like to acknowledge financial support by the Academy of Finland Centre of Excellence (grant no. 272041).

References

AIRMETRICS. 2011. MiniVol portable air sampler: operation manual version 4.2c. USA.

AHN, J.W., CHUNG, D.W., LEE, K.W., AHN, J.-G., SOHN, H.Y. 2011. Nitric Acid Leaching of Base Metals from Waste PDP Electrode Scrap and Recovery of Ruthenium Content from Leached Residues. Materials Transactions, 52(5):1063-1069

AL-MOMANI, I.F., DARADHEH, A.S. & HAJ-HUSSEIN, A.T. 2005. Trace elements in daily collected aerosols in Al-Hashimya, central Jordan. Atmospheric Research, 73:87-100.

BEUKES, J.P., VAKKARI, V., VAN ZYL, P.G., VENTER, A.D., JOSIPOVIC, M., JAARS, K., TIITTA, P., KULMALA, M., WORSNOP, D., PIENAAR, J.J., JÄRVINEN, E., CHELLAPERMAL, R., IGNATIUS, K., MAALICK, Z., CESNULYTE, V., RIPAMONTI, G., LABAN, T.L., SKRABALOVA, L., DU TOIT, M., VIRKKULA, A. & LAAKSO, L. 2013. Source region plume characterisation of the interior of South Africa, as observed at Welgegund. Clean Air Journal. 23(1):1-10.

BEUKES, J.P., VENTER, A.D., JOSIPOVIC, M., VAN ZYL, P.G., VAKKARI, V., JAARS, K., DUNN, M., LAAKSO, L. 2015 Automated Continuous Air Monitoring. Monitoring of Air Pollutants, 1st Edition, Sampling, Sample Preparation and Analytical Techniques. Eds. P. Forbes. 408p.

BOOYENS, W., VAN ZYL, P.G., BEUKES, J.P., RUIZ-JIMENEZ, J., KOOPERI, M., RIEKKOLA, M.-L., JOSIPOVIC, M., VENTER, A.D., JAARS, K., LAAKSO, L., VAKKARI, V., KULMALA, M. & PIENAAR, J.J. 2015. Size-resolved characterisation of organic compounds in atmospheric aerosols collected at Welgegund, South Africa. Journal of Atmospheric Chemistry. 72:43-64.

CONNELL, D.W. 2005. Basic concepts of environmental chemistry. London: CRC-press.

DRAXLER, R. R. and HESS, G. D.: 2004 Description of the HYSPLIT 4 Modelling System, NOAA Technical Memorandum ERL ARL-224.

ESKOM. 2015. Integrated results for 2015. Fact sheets with additional information. Date of access: 6 May 2016. http://www.eskom.co.za/IR2015/Documents/Eskom_fact_sheets_2015.pdf

GHUDEA, S.D., VAN DER A, R.J., BEIGA, G., FADNAVISA, S. & POLADEA, S.D. 2009. Satellite derived trends in NO2 over the major global hotspot regions during the past decade and their inter-comparison. Environmental Pollution, 157(6):1873-1878.

HIRSIKKO, A., VAKKARI, V., TIITTA, P., MANNINEN, H. E., GAGNÉ, S., LAAKSO, H., KULMALA, M., MIRME, A., MIRME, S., MABASO, D., BEUKES, J. P., AND LAAKSO, L.: 2012. Characterisation of sub-micron particle number concentrations and formation events in the western Bushveld Igneous Complex, South Africa, Atmospheric Chemistry and Physics, 12:3951–3967, doi:10.5194/acp-12-3951-2012.

HENNIGAN, C. J., IZUMI, J., SULLIVAN, A.P., WEBER, R.J. & NENES, A. 2015. A critical evaluation of proxy methods used to estimate the acidity of atmospheric particles. Atmospheric Chemistry and Physics, 15:2775-2790.

IPCC. 2014. Climate Change 2014: Mitigation of Climate Change. Contribution of Working Group III to the Fifth Assessment Report of the Intergovernmental Panel on Climate Change [Edenhofer, O., R. Pichs-Madruga, Y. Sokona, E. Farahani, S. Kadner, K. Seyboth, A. Adler, I. Baum, S. Brunner, P. Eickemeier, B. Kriemann, J. Savolainen, S. Schlömer, C. von Stechow, T. Zwickel and J.C. Minx (eds.)]. Cambridge University Press, Cambridge, United Kingdom and New York, NY, USA.

KOULOURI, E., SAARIKOSKI, S., THEODOSI, C., MARKAKI, Z., GERASOPOULOS, E., KOUVARAKIS, G., MAKELA, T., HILLAMO, R. & MIHALOPOULOS, N. 2008. Chemical composition and sources of fine and

coarse aerosol particles in the Eastern Mediterranean. Atmospheric Environment: 42(26):6542-6550.

KULKARNI, P., CHELLAM, S., FLANAGAN, J.B. & JAYANTY, R.K.M. 2007. Microwave digestion—ICP-MS for elemental analysis in ambient airborne fine particulate matter: Rare earth elements and validation. Analytica Chimica Acta., 599(2):170-176.

KULMALA, M., PIRJOLA, L. & MÄKELÄ, J.M. 2000. Stable sulphate clusters as a source of new atmospheric particles. Nature 404:66-69.

LOURENS, A.S.M., BEUKES, J.P., VAN ZYL, P.G., FOURIE, G.D., BURGER, J.W., PIENAAR, J.J., READ, C.E. & JORDAAN, J.H. 2011. Spatial and Temporal assessment of Gaseous Pollutants in the Mpumalanga Highveld of South Africa. South African Journal of Science, 107(1/2):8.

LOURENS, A.S.M., BUTLER, T.M., BEUKES, J.P., VAN ZYL, P.G., BEIRLE, S. & WAGNER, T. 2012. Re-evaluating the NO2 hotspot over the South African Highveld. South African Journal of Science, 108(9/10)

SCHWARTZ, J., DOCKERY, D.W. & NEAS, L.M. 1996. Is Daily Mortality Associated Specifically with Fine Particles? Journal of the Air & Waste Management Association, 46(10):927-939.

SIENFELD, J H & PANDIS, S N. 2006. Atmospheric Chemistry and Physics. New Jersey: John Wiley & Sons.

SQUIZZATO, S., MASIOL, M.., BRUNELLI, A., PISTOLLATO, S., TARABOTTI, E., RAMPAZZO, G. & PAVONI, B. 2013. Factors determining the formation of secondary inorganic aerosol: a case study in the Po Valley (Italy). Atmospheric Chemistry and Physics, 13:1927-1939.

SOUTH AFRICA. 2012. National Environmental Management: Air Quality Act, 2004 (ACT NO. 39 OF 2004) Declaration of the Waterberg National Priority Area. *Government gazette*, 35435: 15 Jun. Date of access: 15 Oct. 2015.

TIITTA, P., VAKKARI, V., JOSIPOVIC, M., CROTEAU, P., BEUKES, J.P., VAN ZYL, P.G., VENTER, A.D., JAARS, K., PIENAAR, J.J., NG, N.L., CANAGARATNA, M.R., JAYNE, J.T., KERMINEN, V.-M., KULMALA, M., LAAKSONEN, A., WORSNOP, D.R. & LAAKSO, L. 2014. Chemical composition, main sources and temporal variability of PM1 aerosols in southern African grassland. Atmospheric Chemistry and Physics. 14(4):1909-1927.

TURNER, J. & COLBECK, I. 2008. Environmental Chemistry of Aerosols. University of Essex: Blackwell Publishing.

VAKKARI, V., KERMINEN, V.-M., BEUKES, J.P., TIITTA, P., VAN ZYL, P.G., JOSIPOVIC, M., VENTER, A.D., JAARS, K., WORSNOP, D.R., KULMALA, M. & LAAKSO, L. 2014. Rapid changes in biomass burning aerosols by atmospheric oxidation. Geophysical Research Letters. 41(7):1-8.

VAN ZYL, P.G., BEUKES, J.P., DU TOIT, G., MABASO, D., HENDRIKS, J., VAKKARI, V., TIITTA, P., PIENAAR, J.J., KULMALA, M. & LAAKSO, L. 2014. Assessment of atmospheric trace metals in the western Bushveld Igneous Complex, South Africa. South African Journal of Science, 110(3/4)(Art. #2013-0280):11.

VENTER, A. D., VAKKARI, V., BEUKES, J. P., VAN ZYL, P. G., LAAKSO, H., MABASO, D., TIITTA, P., JOSIPOVIC, M., KULMALA, M., PIENAAR, J. J. & LAAKSO, L. 2012. An air quality assessment in the industrialised western Bushveld Igneous Complex, South Africa. South African Journal of Sciences, 108(9/10).

VENTER, A.D., VAN ZYL, P.G., BEUKES, J.P., JAARS, K., JOSIPOVIC, M., BOOYENS, W., HENDRIKS, J., VAKKARI, V. & LAAKSO, L. 2015. Measurement of atmospheric trace metals at a regional background site (Welgegund) in South Africa. In preparation for Atmospheric Chemistry and Physics Discussions

WAI, K.M., WU, S., KUMAR, A. & LIAO, H. 2014. Seasonal variability and long-term evolution of tropospheric composition in the tropics and Southern Hemisphere. Atmospheric Chemistry and Physics, 14(10):4859-4874.

ZHANG, Q.I., JIMENEZ, J.L., WORSNOP, D.R. & CANAGARATNA, M. 2007. A case study of urban particle acidity and its influence on secondary organic aerosol. Environmental Science and Technology, 41(9):3213-3219.

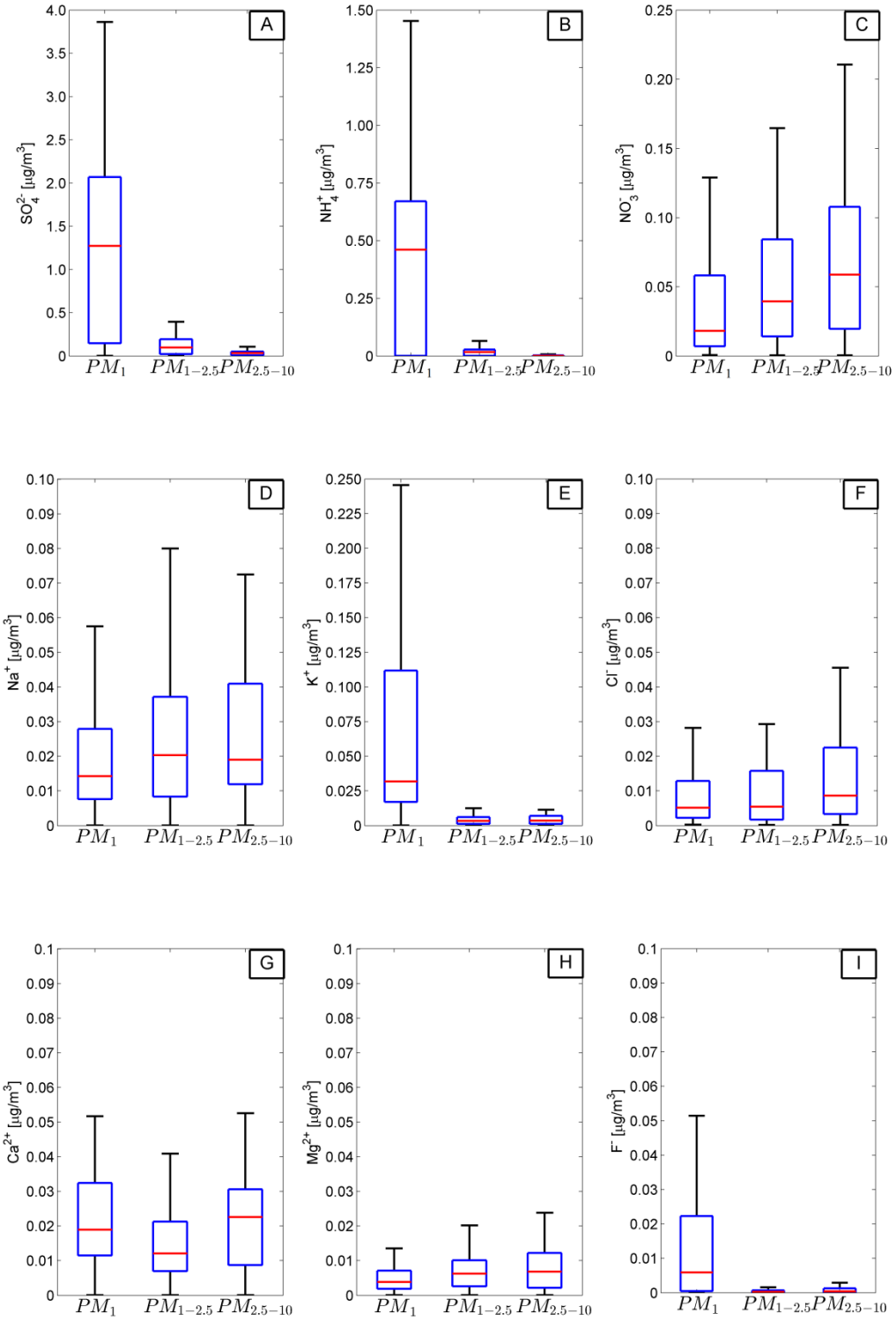

Figure 1: Speciated size distribution boxplots indicate the concentration distribution of inorganic ionic species at Welgegund. The median (red line), 25th and 75th percentiles (blue box) and ± 2.7 times the standard deviation (whiskers) are indicated.

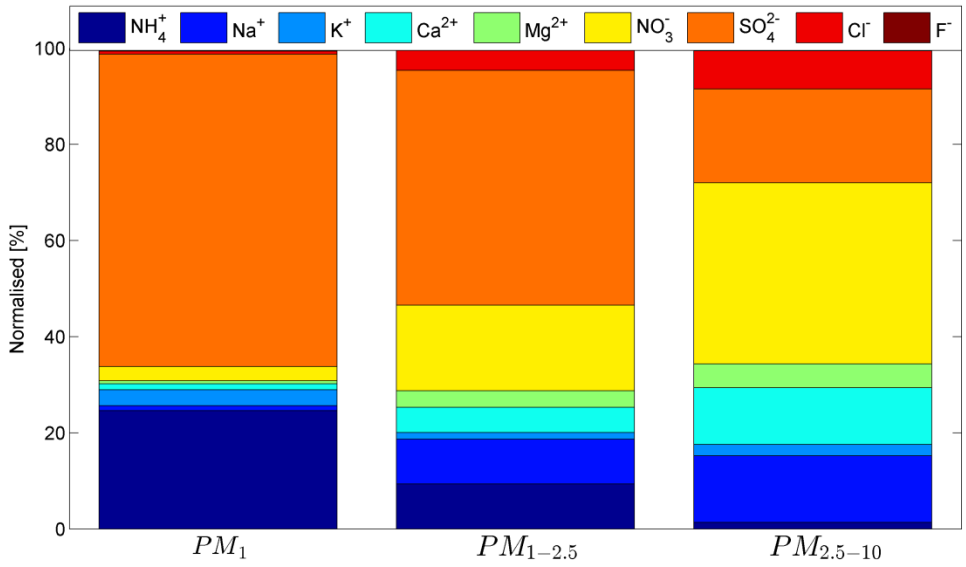

Figure 2: The normalised concentration distribution of the inorganic ionic species investigated. An increase in SO_4^{2-} and NH_4^+ is observed in the PM_1 fraction and an increase in NO_3^-, Na^+, Ca^{2+} and Cl^- is seen in the $PM_{2.5-10}$ size range.

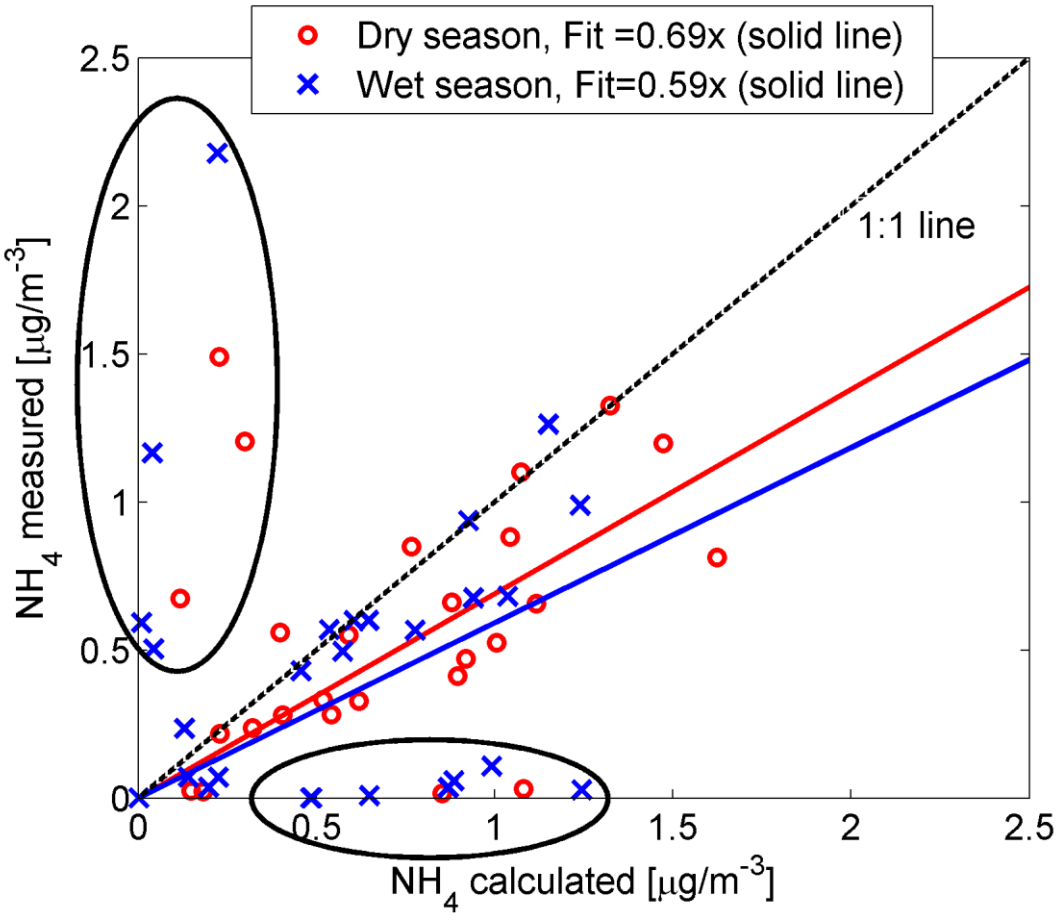

Figure 3: The measured NH_4 concentrations are plotted in relation to the calculated NH_4 values. The red circle and red trend line represent the dry season, while the blue crosses and blue trend line are for the wet season. The circled NH_4 values were excluded to yield a better fit

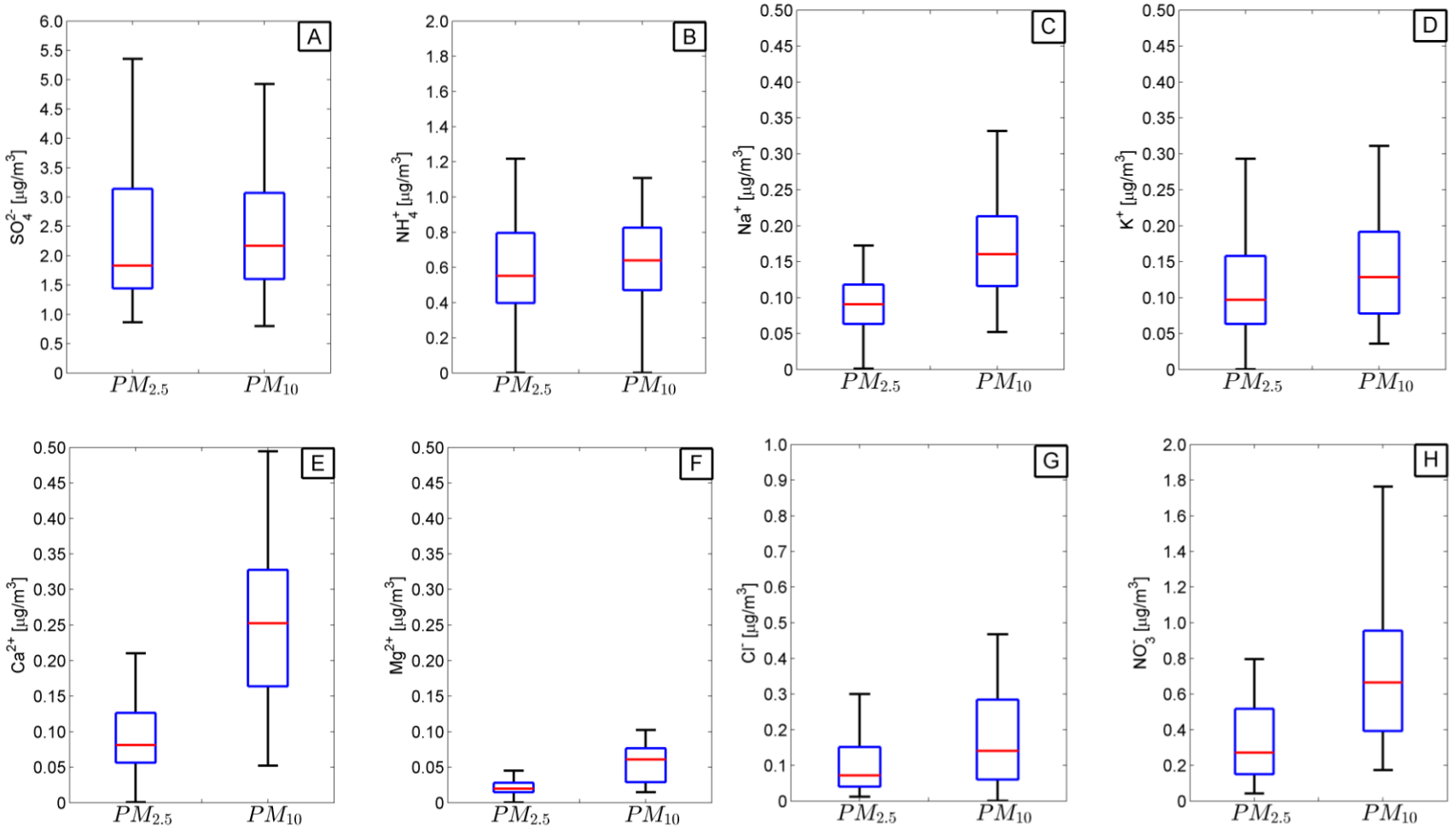

Figure 4: Marikana inorganic ionic species for (a) $PM_{2.5}$, and (b), PM_{10}. The red line represents the median values, while the outer limits of the blue box are the 25th and 75th percentiles and the whiskers are ± 2.7 times the standard deviation

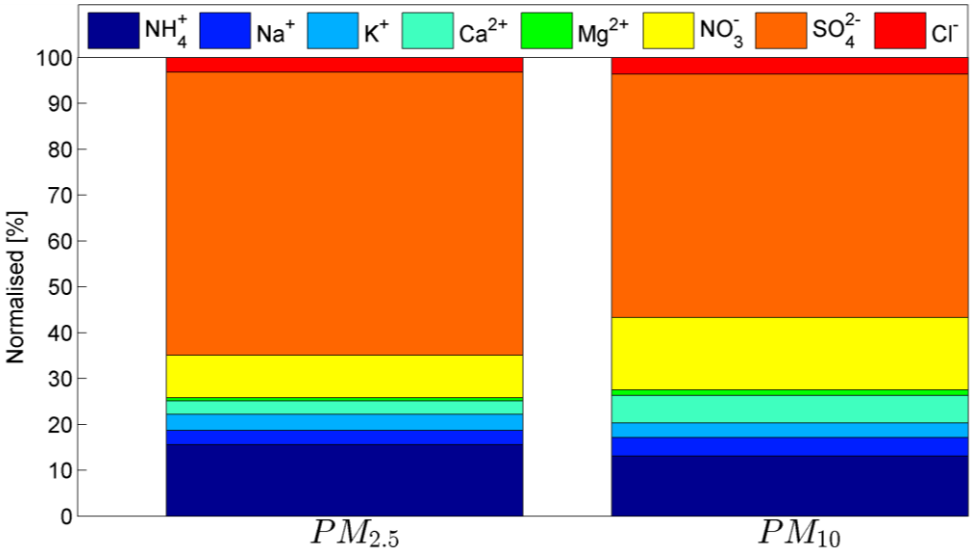

Figure 5: The normalised concentration distribution of inorganic ionic species measured at Marikana

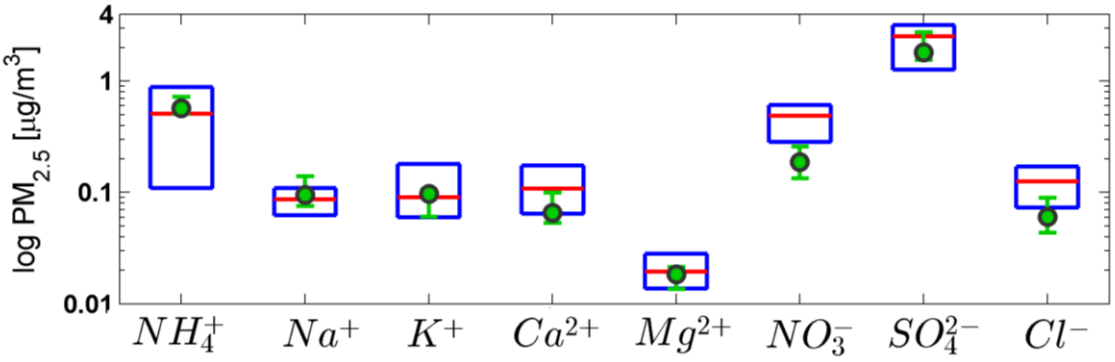

Figure 6: The concentration distribution of inorganic ionic species measured at Marikana during the day time (green circle) and night time (blue box). The green circle and red line represent the median values, while the outer limits of the green whiskers and blue box are the 25th and 75th percentiles

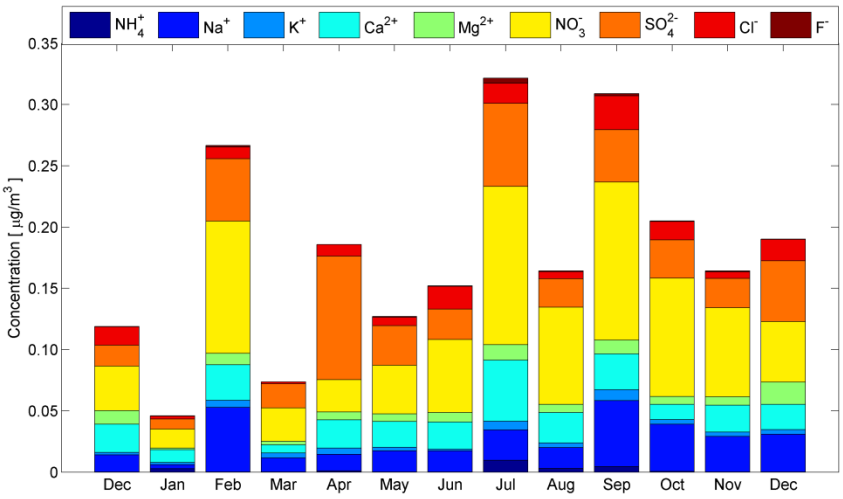

(a)

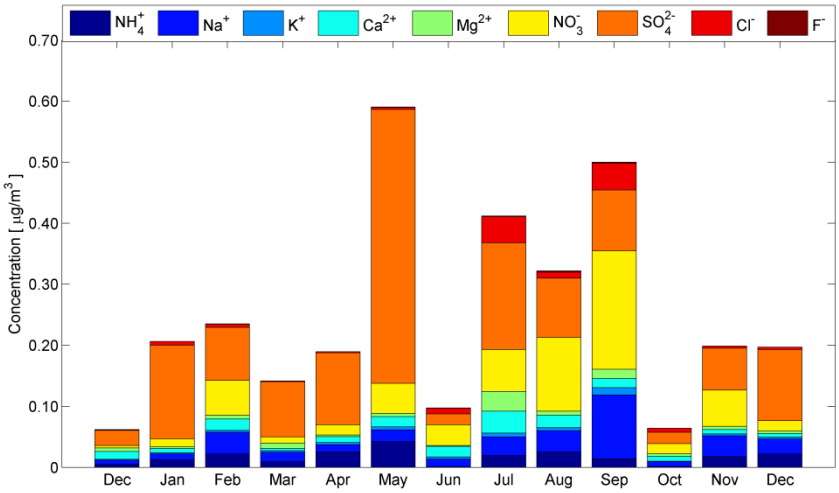

(b)

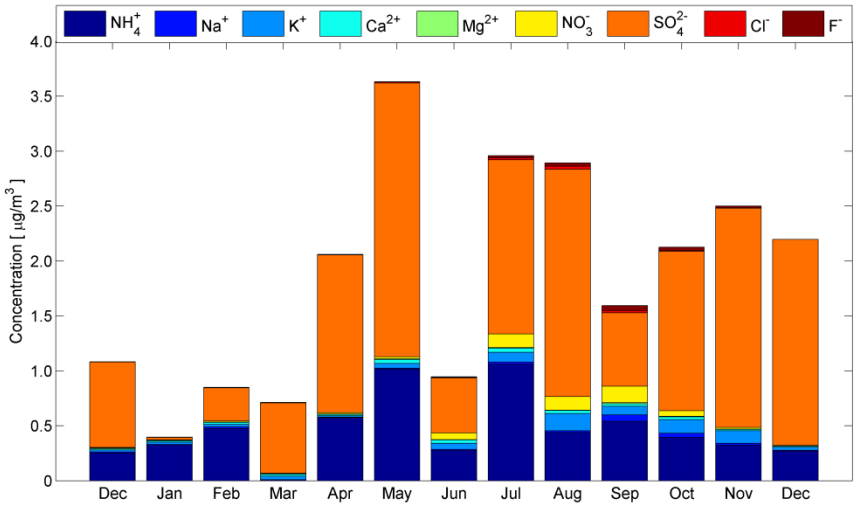

(c)

Figure 7: Welgegund monthly concentration distributions for (a) $PM_{2.5-10}$, (b), $PM_{1-2.5}$ (c), $PM_{<1}$ are shown and possible seasonality is investigated

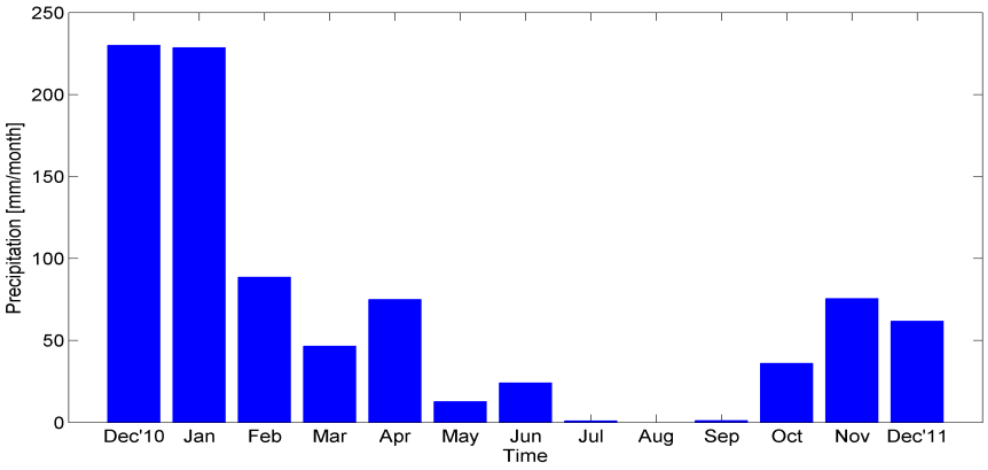

Figure 8: Monthly accumulated rainfall measured at Welgegund for the sampling duration. Dry winter months (Jun-Aug) are differentiated from the wet summer months (Dec-Feb)

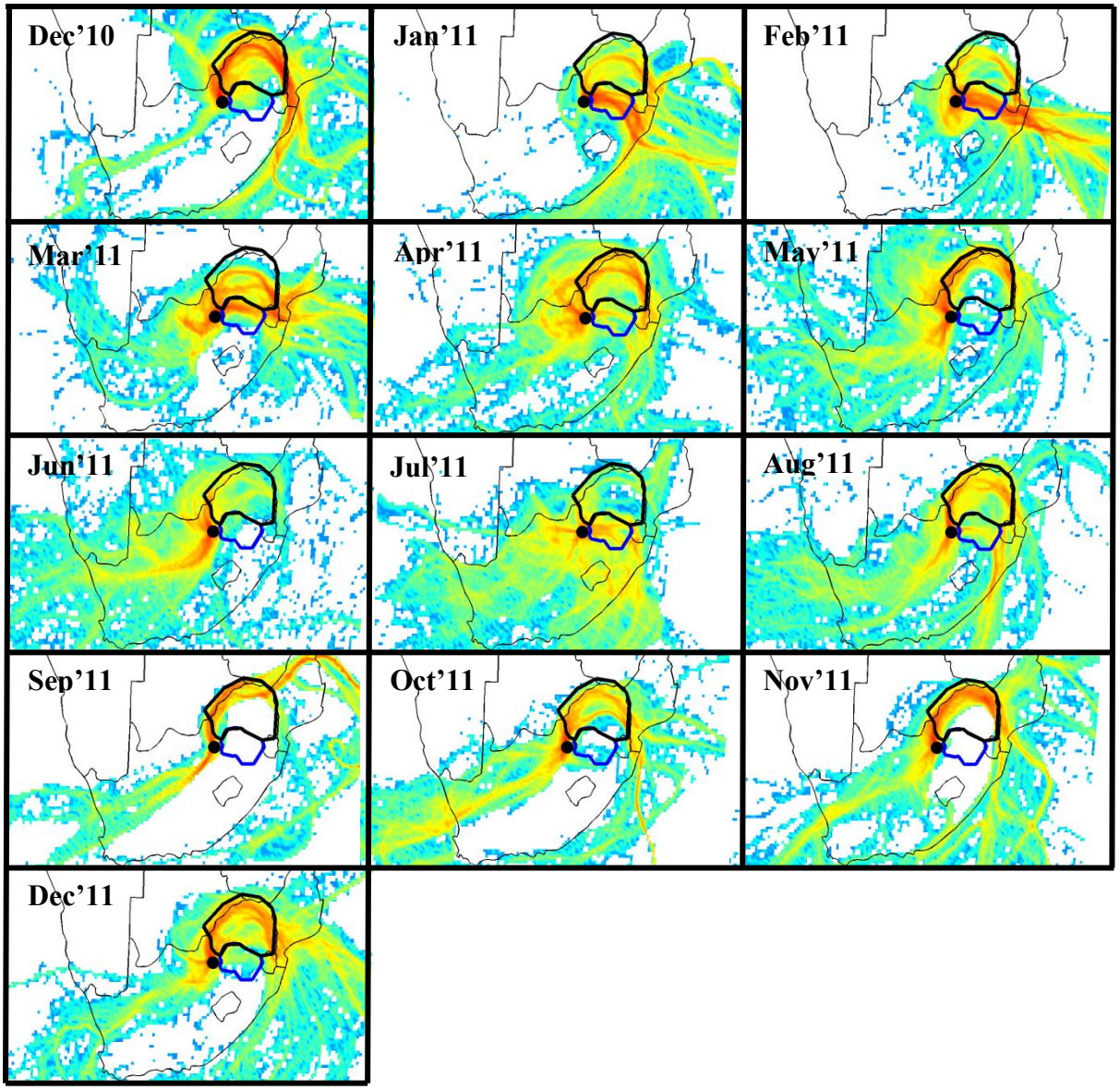

Figure 9: Monthly air-mass back trajectories as measured at Welgegund during the sampling period

Chapter 8

Case study – inorganic constituents emitted from a typical South African braai

Author list and contributions

A.D. Venter[1], K. Jaars[1], W. Booyens[1], J.P. Beukes[1], P.G. van Zyl[1], M. Josipovic[1], J. Hendriks[1], V. Vakkari[2,3], H. Hellén[3], H. Hakola[3], H. Aaltonen[3], J. Ruiz-Jimenez[4], M-L. Riekkola[4] and L. Laakso[1,3]

1 Unit for Environmental Sciences and Management, North-West University, Potchefstroom, South Africa

2 Department of Physics, P.O. Box 64, FIN-00014, University of Helsinki, Finland.

3 Finnish Meteorological Institute, Research and Development, FI-00101 Helsinki, Finland

4 Department of Chemistry, P.O. Box 55, FIN-00014, University of Helsinki, Finland.

Contributions of the various co-authors were as follows. The bulk of the work was done by the candidate A. D. Venter (including sample analysis, data processing research and writing), with conceptual ideas and recommendations by the promoters P.G. van Zyl and J.P. Beukes. K. Jaars, W. Booyens and M. Josipovic helped with data gathering and sample preparation, J. Hendriks helped with specialised ICP analysis, while H. Hellén, H. Hakola, H. Aaltonen, J. Ruiz-Jimenes, M.-L. Riekkola helped with specialised sample analysis and expert opinions and V. Vakkari, and L. Laakso helped with establishing and maintaining infrastructure.

Formatting and current status of article

The article was formatted in accordance with the journal specifications to which it was submitted, i.e. *South African Journal of Chemistry*. The authors' guide that was followed in preparation of the article was available at http://www.journals.co.za/sajchem/chem_aut.html (Date of access: 27 November 2014). The article was submitted for review on 30 March 2015 and accepted on 1 July 2015.

Consent by co-authors

All the co-authors in the article have been informed that the PhD will be submitted in article format and have given their consent.

Plume Characterization of a Typical South African Braai

A.D. Venter[a], K. Jaars[a], W. Booyens[a], J.P. Beukes[a], P.G. van Zyl[a,*], M. Josipovic[a], J. Hendriks[a], V. Vakkari[b,c], H. Hellén[c], H. Hakola[c], H. Aaltonen[c], J. Ruiz-Jimenez[d], M-L. Riekkola[d] and L. Laakso[a,c]

[a]*Unit for Environmental Sciences and Management, North-West University, Potchefstroom, South Africa.*

[b]*Department of Physics, P.O. Box 64, FIN-00014, University of Helsinki, Finland.*

[c]*Finnish Meteorological Institute, Helsinki, Finland.*

[d]*Department of Chemistry, P.O. Box 55, FIN-00014, University of Helsinki, Finland.*

Received 30 March 2015, revised 26 June 2015, accepted 1 July 2015.

ABSTRACT

To braai is part of the South African heritage that transcends ethnic barriers and socio-economic groups. In this paper, a comprehensive analysis of atmospheric gaseous and aerosol species within a plume originating from a typical South African braai is presented. Braai experiments were conducted at Welgegund – a comprehensively equipped regional background atmospheric air quality and climate change monitoring station. Five distinct phases were identified during the braai. Sulphur dioxide (SO_2), nitrogen oxides (NO_x) and carbon monoxide (CO) increased significantly, while ozone (O_3) did not increase notably. Aromatic and alkane volatile organic compounds were determined, with benzene exceeding the 2015 South African one-year ambient air quality limit. A comparison of atmospheric PM_{10} (particulate matter of an aerodynamic diameter ≤10 μm) concentrations with the 24-hour ambient limit indicated that PM_{10} is problematic during the meat grilling phase. From a climatic point of view, relatively high single scattering albedo (ω_o) indicated a cooling aerosol direct effect, while periods with lower ω_o coincided with peak black carbon (BC) emissions. The highest trace metal concentrations were associated with species typically present in ash. The lead (Pb) concentration was higher than the annual ambient air quality limit. Sulphate (SO_4^{2-}), calcium (Ca^{2+}) and magnesium (Mg^{2+}) were the dominant water-soluble species present in the aerosols. The largest number of organic aerosol compounds was in the $PM_{2.5-1}$ fraction, which also had the highest semi-quantified concentration. The results indicated that a recreational braai does not pose significant health risks. However, the longer exposure periods that are experienced by occupational vendors, will significantly increase health risks.

KEYWORDS

Braai (barbeque), atmospheric gaseous species, aerosols, atmospheric organic compounds, optical properties, chemical properties.

1. Introduction

A braai (plural braais) is the practice by which wood or charcoal is burned in an open fire to grill meat. The word braai is an Afrikaans word for barbecue or grill. Although the term originated from Afrikaans-speaking people, it was adopted by South Africans of many ethnic backgrounds. The application of braai transcends ethnic barriers and is practised by people of all socio-economic groups in South Africa. This form of cooking is not just a means to an end, but is an important social activity that strengthens the inter- and intra-relations of communities. It is common practice to include this type of cooking in casual family time, formal team-building events, meetings and business entertainment.[1] In describing the essentials needed at the ideal campsite (stand), a portable braai is listed among other fundamentals such as electrical outlets and water points.[2] It has been stated that a braai started at lunchtime could last the entire afternoon and well into the evening.[3]

Braai meat is also sold by many vendors on street markets in formal, semi-formal and informal settlements in South Africa. In addition, wood and charcoal are commonly burned in many households for cooking and space heating, especially in semi-formal and informal settlements, which significantly contributes to poor air quality.[4,5] Alternative, cleaner burning fuels have been suggested to replace wood-fired braais used by meat traders and households.[6]

Historically, wood was the most widely used braai fuel. However, in modern times, the use of charcoal or charcoal-related products, such as briquettes, has increased due to the availability and competitive price thereof. A charcoal fire also emits less smoke and particulate matter compared to a wood fire.[7] Although wood and charcoal are not the primary energy source in most developed countries, it is currently one of the most commonly used fuels for cooking.[8] The population growth in the developing world, with its associated increasing demand in oil- and gas-based energy, may in future promote the increased use of wood and charcoal for cooking.

Although wood- and charcoal-based cooking is currently not treated as a significant source of airborne pollution compared to other well-known sources, e.g. motor vehicles, industries, coal-fired power plants and biomass burning, cooking emissions and its associated adverse impacts on human health and the environment should not be neglected.[9] Typical emissions usually associated with biomass burning (veld fires and household combustion) that could be similar to emissions from a typical braai include nitrogen oxides (NO_x), carbon monoxide (CO), volatile organic compounds (VOCs), black carbon (BC), as well as particulate inorganic and organic compounds. Gases and particulate species also have a significant impact on climate change. Particulate species, for instance, have a cooling or warming effect (direct and indirect) on the atmosphere, depending on their chemical and physical properties. Gaseous species could

* To whom correspondence should be addressed. E-mail: pieter.vanzyl@nwu.ac.za

ISSN 0379-4350 Online / ©2015 South African Chemical Institute / http://saci.co.za/journal
DOI: http://dx.doi.org/10.17159/0379-4350/2015/v68a25

also react to form particulates through gas-to-particle transformations.[10]

Few studies have been published that characterize airborne species emitted from braais to determine the associated pollution[11] and impacts on climate change. Therefore, in this paper, a comprehensive analysis of atmospheric species within a plume originating from a typical South African braai is presented.

2. Site Description

Measurements were conducted at Welgegund (www.welgegund.org) located on a grazed grassland savanna approximately 100 km west of Johannesburg in the North West Province of South Africa. There are no major mining and/or industrial activities within the vicinity of the site. The nearest surroundings included grazed fields and farmland used in maize cultivation. Additionally, the entire western sector (from north to southeast) contains no major point sources. This sector is therefore representative of the regional background of the interior of South Africa and to some extent of southern Africa. However, the site is also frequently impacted by air masses that have passed over various source regions, which include petrochemical industries, coal-fired power stations, the Johannesburg–Pretoria megacity conurbation and the Bushveld Igneous Complex that contains various pyrometallurgic operations.[12] A detailed description of the location and instrumentation of the Welgegund monitoring stations was presented by Beukes *et al.*[12] Currently, this measurement station is one of the most comprehensively equipped in South Africa to measure air quality and climate change-relevant parameters.[12–16]

3. Materials and Methods

3.1. Materials

During each braai experiment, four bags of 4 kg Weber™ briquettes purchased from a local supermarket were used. Two briquettes were removed from each bag for subsequent material characterization. Blitz™ firelighters were used to light the braais.

Lamb chops and beef sausages were purchased from a local supermarket for each braai experiment. Eight lamb chops weighing 796 ± 2 g and eight beef sausages weighing 804 ± 5 g were placed on each braai used in the experiments. One lamb chop and one beef sausage were randomly selected and analyzed in order to characterize the raw meat utilized. Although other types of meat are also used for a braai, lamb chops and beef sausages are often used. It can be expected that different types of meat will result in different atmospheric emissions.[17] However, it was not the aim of this study to determine emissions associated with different meat types. The aim was to determine air quality impacts and aerosol direct effects associated with a typical braai. Therefore, the emission measurements obtained with meat used in this study can be considered to be representative.

3.2. Material Characterization

Similar to the procedures described by Kleynhans *et al.*, randomly selected charcoal briquettes were pulverized to obtain a homogeneous composition for subsequent material characterization (based on ISO 13909-4:2001).[18] Proximate analysis (air-dried basis) was performed to obtain moisture (SANS 5925:2007), ash (ISO 1171:2010) and volatile matter contents (ISO 562:2010), while ultimate analysis determined the total carbon (C), hydrogen (H), nitrogen (N), oxygen (O) (ISO 29541:2010) and sulphur (S) contents (ISO 19579:2006).

Representative samples of raw meat, i.e. one lamb chop and one beef sausage, were chemically analyzed according to the guidelines of the association of official analytical chemists (AOAC) to determine the moisture (AOAC 950.46), ash (AOAC 923.03), total fat (AOAC 996.06), protein (Dumas Combustion Method), N (Dumas Combustion Method) and sodium (Na) (AOAC Method 984.27) contents.

3.3. Braai Setup

The first braai experiment was conducted on 20 February 2012 and the second experiment on 29 January 2013. Participants in the experiments arrived at the Welgegund site at 09:55 for the first braai experiment and 09:45 for the second braai experiment. Vehicles were parked at least 100 m from the site to ensure that exhaust fumes did not bias the baseline measurements prior to the commencement of the braai experiments. For both experiments, 4.0 ± 0.1 kg charcoal briquettes were placed in each of the four identical braais and each braai was lit using 28 ± 0.6 g firelighters. During the first braai experiment, the firelighters were lit at approximately 10:13, while firelighters were lit at approximately 10:20 during the second experiment. In order to ensure that the plumes originating from the braais reached all the instrument inlets, the four identical braais were strategically placed upwind of the monitoring station at a distance of 5.4 m from the inlets during both experiments. Figure 1 indicates a schematic illustration and photographs of the braai experimental setup, as well as the general plume direction.

For each braai experiment, the concentrations of all atmospheric gaseous species and aerosols measured are presented in time series graphs from 09:00 to 13:00. Five different phases were defined during the braai experiment, i.e. prior to the braai (prior phase), the phase when the braai is ignited, followed by the presence of fire and smoke (fire and smoke phase), a stable period during which all the charcoal briquettes were glowing (stable phase), grilling the meat stage (grill phase) and a phase after the meat is cooked and removed from the braai (post-phase). The fire and smoke, stable and grill phases are also presented in Fig. 1. The charcoal was allowed to burn for one hour after it was lit (fire and smoke phase) in order to achieve peak combustion. At that stage, smoke emanating from the burning charcoal briquettes had totally subsided and all briquettes glowed red. This stable phase was allowed to continue for 18 minutes during the first experiment and 15 minutes during the second experiment in order to clearly differentiate between the stable phase and the grill phase. Grilling of the meat (grill phase) started at 11:40 during the first experiment and at 11:30 during the second experiment. The meat was grilled until it was well done. The grilled meat was removed at 12:10 and 12:00 during the first and second braai experiments, respectively. Thereafter, the braais from which the meat had been removed were left as is until 12:40 during the first experiment and 12:28 during the second experiment. This allowed the embers to cool down, while post-grilling atmospheric measurements were obtained.

3.4. Sampling Methods

Most of the measurement instruments were housed inside an Eurowagon 4500u trailer. Detailed descriptions of the measurement station, as well as procedures for quality assurance, maintenance and data analysis were presented in previous papers.[4,12–14,19]

Various continuous measurements of atmospheric gaseous species and aerosols are performed at the Welgegund station. Atmospheric gaseous species, i.e. sulphur dioxide (SO_2), nitrogen oxide and (NO) nitrogen dioxide (NO_2), ozone (O_3) and CO were measured with the following instruments: a Thermo-Electron 43S SO_2 analyzer (Thermo Fisher Scientific Inc., Yokohama-shi,

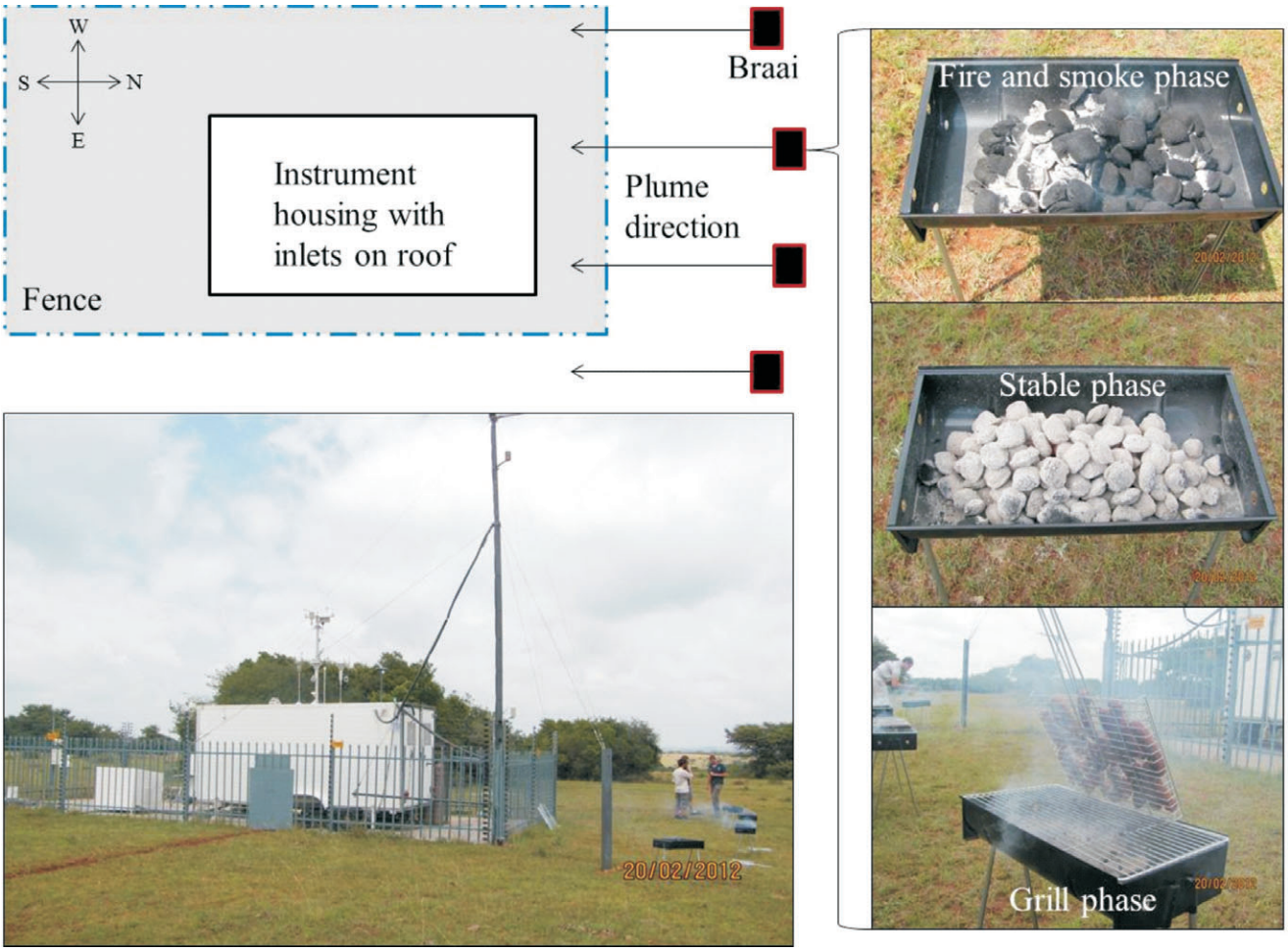

Figure 1 A schematic and photographic representation of the braai experiment location and setup at Welgegund Atmospheric Monitoring Station.

Japan), a Teledyne 200AU NO/NO_x analyzer (Advanced Pollution Instrumentation Inc., San Diego, Cam USA), an Environment SA 41M O_3 analyzer (Environment SA, Poissy, France) and a Horiba APMA-360 CO analyzer (Horiba, Kyoto, Japan). The atmospheric aerosol measurement instrumentation were equipped with PM_{10} (particulate matter with aerodynamic diameter ≤10 μm) inlets. A synchronized hybrid ambient real-time particulate (SHARP) monitor (model 5030, Thermo Fisher Scientific Inc.) was used to determine the total mass of atmospheric PM_{10} particles. A multi-angle absorption photometer (MAAP) (model 5012 Thermo Fisher Scientific Inc.) was used to determine the aerosol absorption at 637 nm and atmospheric black carbon (BC) concentrations. No filter change artefact[20] occurred in the MAAP measurements during the experiment. An Aurora 3000 three-wave length nephelometer (Ecotech Inc., Knoxfield, VIC, Australia) was used to determine light scattering of aerosols at three wavelengths, i.e. 450, 525 and 635 nm. A custom-built differential mobility particle sizer (DMPS) equipped with a TSI condensation particle counter (CPC) (model 3010, TSI Inc., Shoreview, MN, USA) was used to determine the total number concentration of aerosols between 12 and 840 nm. All measurements were logged at one minute intervals, with the exception of the aerosol size distribution that was recorded every nine minutes. All permanently operating instruments at the Welgegund atmospheric research station had been running upon arrival, providing a sufficient baseline before the braai experiments.

Absorption measurements are not presented separately in this paper, because BC concentrations are derived from absorption measured at 637 nm and would mimic BC results.[21] The single scattering albedo (ω_o) was calculated as

$$\omega_0 = \frac{\sigma_{AP}}{\sigma_{AP} + \sigma_{SP}}, \quad (1)$$

where σ_{AP} is the aerosol absorption determined with the MAAP (637 nm) and σ_{SP} is the aerosol scattering at 637 nm; σ_{SP} is extrapolated from aerosol scattering measurements using Ångström exponents, *cf.* Laakso *et al.*[22]

VOCs were collected on 20 stainless steel adsorbent tubes (6.3 mm ED × 90 mm, 5.5 mm ID, Tenax-TA packing material) during the different phases of the first braai experiment. Duplicate VOC samples were collected for 10 minutes during the different phases of the braai, i.e. four times during the fire and smoke phase, once during the stable phase, twice during the grill phase and three times after the meat was removed from the grill. The first 1.25 m of the adsorbent tube inlet (made from stainless steel) was heated to 120 °C to remove O_3 that leads to sample degradation.[23] A constant flow-type automated programmable pump sampler was used at a flow rate of 10 mL min^{-1} After sampling, the tubes were removed and closed with Swagelok® caps. Each tube was separately wrapped in aluminium foil and transported to the laboratory, where it was stored in a freezer. The analysis was performed with a thermal desorption (TD) system (Perkin-Elmer TurboMatrix™ 650, Waltham, USA) coupled to a gas chromatograph (GC) (Perkin-Elmer® Clarus® 600, Waltham, USA) with a mass spectrometer (MS) detector (Perkin-Elmer® Clarus® 600T, Waltham, USA). Quality assurance of the data was performed as previously described.[13,23]

A Dekati (Dekati Ltd., Finland) PM_{10} cascade impactor (ISO23210) was used to collect $PM_{10-2.5}$ (particulate matter with aerodynamic diameter 2.5 μm ≥10 μm), $PM_{2.5-1}$ (particulate matter with aerodynamic diameter 1 μm ≤2.5 μm) and PM_1 (particulate matter with aerodynamic diameter≤1 μm) at a flow rate of 30 L min^{-1}. Teflon® filters were used to collect the water-soluble anion and cation species, as well as trace metals. All collected filters were divided into two equal parts with a fit-for-purpose stainless steel punch. One part was used to determine water-soluble anion and cation content, while the second part was used for trace metal analysis. For water-soluble anion and cation analysis, each sample was leached in 5 mL deionized water (18.2 MΩ) and subsequently analyzed on an ion chromatograph (IC) with conductivity detector (Dionex ICS–3000). The particulates collected on the second half of the Teflon® filters were extracted by means of hot acid leaching (20 mL HNO_3 and 5 mL HCl) and diluted in deionized water to 100 mL for subsequent trace metal analysis with an inductively coupled plasma mass spectrometer (ICP–MS) Agilent 7500c).[24,25]

A second Dekati PM_{10} cascade impactor (ISO23210) equipped with quartz filters was used to collect particulates at the same flow rate and in the same size ranges ($PM_{10-2.5}$, $PM_{2.5-1}$ and PM_1) as mentioned above. After sampling, the filters were kept in a freezer until analysis. These filters were used to characterize and semi-quantify organic compounds. Each filter was extracted with a 1:1 mixture of methanol and acetone by utilizing dynamic ultrasonic assisted extraction for 40 min as described by Booyens *et al.*[15] The analysis was performed with comprehensive two-dimensional gas chromatography coupled with a time-of-flight mass spectrometer (GCxGC-TOFMS). A LECO Pegasus 4D GCxGC-TOFMS system equipped with an Agilent 7890 A GC and an Agilent 7683 B auto sampler was used. The organic compounds were identified with LECO ChromaTOF and Guineu software according to mass spectral matches (similarity fits 700/1000) and retention indices (*I*) (*I* confidence intervals fewer than 150 units). More restrictive characterization parameters could have been applied, which would have resulted in the more accurate characterization of organic compounds. Additionally, identified organic species could also be verified and supported by the analysis of standards. However, this was not applied in this study. Therefore, the compounds characterized in this paper are considered to be pre-identified organic species. Thereafter, the compounds were categorized according to their functional groups, i.e. hydrocarbons (alkanes, alkenes, alkynes, aromatics), oxygenated species (alcohols, ethers, aldehydes, ketones, carboxylic acids, esters), halogenated compounds (chloride (Cl), bromide (Br), iodine (I), fluorine (F)), as well as N- and S-containing organic compounds. The organic compounds were sem-quantified, which is an approximation of the concentration of the organic compounds. In this study, 1-1′binaphthyl was used as an internal standard and the relative concentrations of the organic compounds were expressed as the sum of the normalized response factors (ΣNRF), which is a measure of the detector response of an analyte compared to the internal standard. The calculation of these ΣNRF values is described in Booyens *et al.*[15]

In addition to the atmospheric measurements, a thermocouple was also used to determine the temperature in the centre of the briquettes during the different braai phases previously indicated, i.e. fire and smoke, stable, grill and post.

4. Results

All measurements were logged at one-minute intervals, with the exception of the aerosol size distribution that was recorded every nine minutes. Twenty VOC's samples were taken, each after 10 minutes of sampling. The filters used for trace metal, anion, cation and organic analysis sampled for the duration of the experiment. Since the experiment is dependent on ambient conditions (e.g. wind direction, speed, turbulence and natural chemistry) it was repeated one year later. All permanently operating instruments at the Welgegund atmospheric research station had been running upon arrival, providing a sufficient baseline before the two braai experiments. The resemblances between the two experiments, (a) and (b), can be seen in each figure, where (a) is first and (b) second braai experiment, respectively.

4.1. Material Characterization

The characterization of the raw materials, *viz.* charcoal briquettes, beef sausage and lamb chops, utilized in the braai experiments is presented in Table 1. Proximate analysis of the charcoal briquettes indicated that the briquettes had a fixed carbon content of 41.70 %, ash content of 20.47 % and 32.20 % volatile matter. The use of a binding agent when the charcoal pulp was compressed into briquettes possibly contributed to the relatively high volatile content measured. The ultimate analysis revealed very low percentages of N and S present in the briquettes, with expected higher percentages of N, C and O.

Analyses of the meat samples indicated that the beef sausages had higher ash content, moisture, protein, N and Na levels than the lamb chops did. The high Na concentration in the sausages can be expected, since it is a processed form of meat with table salt and other spices added according to a specific recipe. The lamb chops contained more fat than the beef sausages did, which was likely due to the fat layer attached to the chops. Beef sausages are usually prepared from specific recipes that require a certain amount of fat to be added.

Table 1 The chemical characterization of the briquettes and meat used during the braai experiments.

	Charcoal		
Proximate analysis	%	Ultimate analysis	%
Inherent moisture	5.40	Carbon	52.91
Ash	20.47	Hydrogen	2.53
Volatile matter	32.20	Nitrogen	0.89
Fixed carbon	41.70	Oxygen	17.48
		Sulphur	0.09

	Meat	
Chemical analysis	Beef sausage	Lamb chops
Moisture /g 100 g^{-1}	68.3	51.8
Ash /g 100 g^{-1}	3.3	0.8
Fat/g 100 g^{-1}	6.8	26.6
Nitrogen /g 100 g^{-1}	2.7	2.1
Sodium /mg 100 g^{-1}	1045	54.2
% Protein	17.2	13.1

4.2. Gaseous Species

In Fig. 2, the SO_2 concentrations for the two braai experiments are presented. It is evident that the SO_2 concentrations were relatively low prior to the onset of the braai experiments. However, after the braai was ignited, SO_2 concentrations started to increase and peaked during the fire and smoke phase. High temperature oxidation of S present in both the firelighters and charcoal (Table 1) is most likely the source of SO_2 during this stage. A

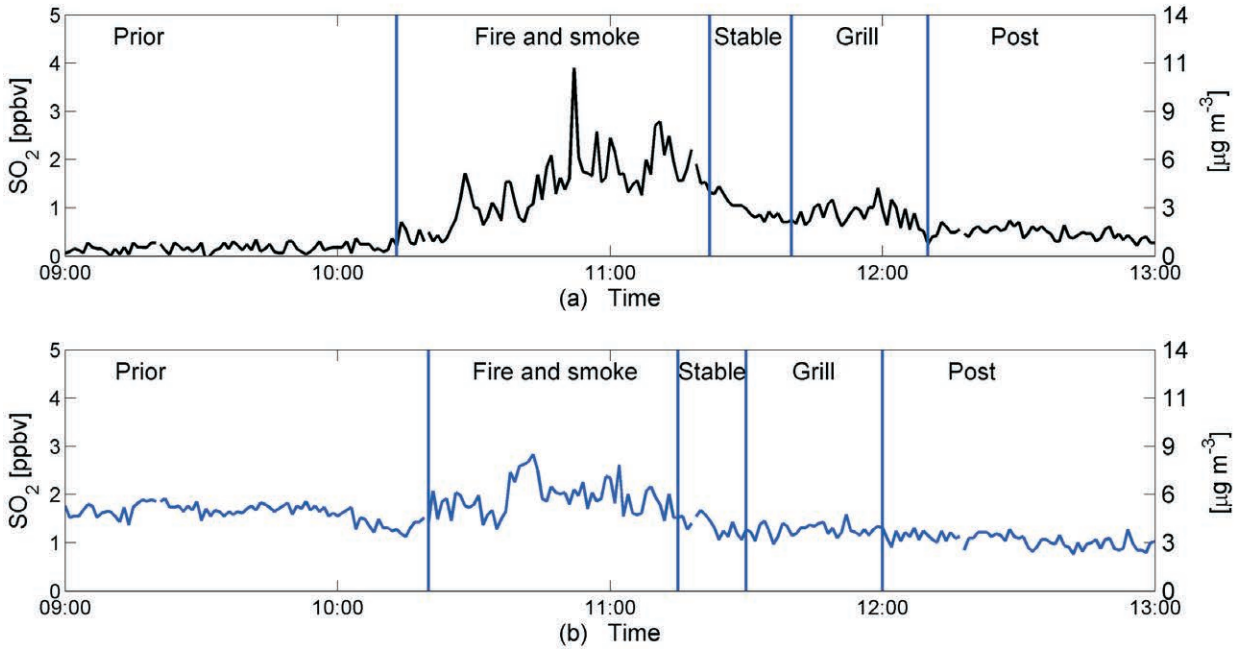

Figure 2 The SO_2 concentrations of the first (**a**) and second (**b**) braai experiment.

decrease in SO_2 concentrations was observed as the charcoal briquettes started burning optimally (stable phase). When the meat was added and grilling started, SO_2 concentrations increased slightly, returning to ambient levels as the grilled meat was removed from the braais. The minor increase in SO_2 concentrations during the grill phase could be ascribed to possible low S concentrations in the meat and dripping fat (Table 1), which is oxidized and volatilized.

In order to contextualize the above-measured SO_2 concentrations, the measurements were compared to relevant current and future air quality limits. In Table 2, the limits prescribed by the South African and European ambient air quality standards are listed. Throughout the braai experiments, SO_2 concentrations remained well below the prescribed South African 10-minute ambient standard limit of 500 $\mu g\ m^{-3}$.

In Fig. 3, atmospheric concentrations of NO and NO_2 are presented. Ambient NO and NO_2 levels were constant and relatively low before the fires were lit. NO_2 were also higher than NO, which is typical for ambient NO_x since NO emitted into the atmosphere is oxidized to NO_2. Concentrations of NO and NO_2 increased significantly and remained elevated for the duration of both braai experiments. Additionally, no distinct trends in relation to the various braai phases were observed. In contrast to typical ambient conditions, NO and NO_2 were also in the same concentration range, which is indicative of a fresh plume that has not been oxidized. NO and NO_2 levels returned to ambient concentrations once the braais were removed. The possible sources of the enhanced NO and NO_2 concentrations during the braai could be from the N present in the charcoal fuel and the meat (Table 1), as well as the thermal oxidation of N_2. However, since a maximum temperature of 750 °C was measured in the glowing charcoal briquettes, it is unlikely that the contribution from the latter source would be significant. Thermal NO_x formation usually occurs above 1600 °C when N_2 and O_2 in the combustion air disassociate into their atomic states.[28] Therefore, the most likely source of NO_x would be the oxidation of N present in the briquettes, with a possible smaller contribution from the meat. Notwithstanding the afore-mentioned relatively significant increases of NO and NO_2 observed during both braai experiments, NO_2 remained well below the prescribed one-hour standard limit of 200 $\mu g\ m^{-3}$ indicated in Table 2.

Atmospheric O_3 concentrations presented in Fig. 4 fluctuated more during the fire and smoke, and the grill phases compared to the typical diurnal O_3 concentrations represented by the mean diurnal O_3 levels calculated for the summer of 2012. However, no significant O_3 increases were observed. In the first braai experiment, the O_3 levels did not significantly exceed the summer mean values indicated in Fig. 4a. During the second braai experiment (Fig. 4b), the O_3 concentrations exceeded the summer mean values, due to the background O_3 concentrations (prior phase) being significantly higher than during the first experiment. Atmospheric O_3 concentrations usually increase during daytime, since atmospheric O_3 formation is dependent on solar radiation, which was still observed during the braai experiments. The lower than typical ambient O_3 concentration that occurred during the various braai phases can possibly be

Table 2 South African and European air quality standards.

Chemical species	Annual /$\mu g\ m^{-3}$	24-hour /$\mu g\ m^{-3}$	8-hour /$\mu g\ m^{-3}$	1-hour /$\mu g\ m^{-3}$	10-minute /$\mu g\ m^{-3}$
SO_2	50[(a)]	125[(a)(c)]		350[(a)(c)]	500[a]
NO_2	40[(a)(c)]			200[(a)(c)]	
O_3			120[(a)(c)]		
CO			10000[(a)(c)]	30000[(a)]	
Benzene	10[(a)] 5[(b)(c)]				
Pb	0.5[(a)(c)]				
V				1[(c)]	
Ni	0.02[(c)]				
As	0.006[(c)]				
Cd	0.005[(c)]				
PM_{10}	50[(a)] 40[(b)(c)]	120[(a)] 75[(b)] 50[(c)]			

[a] Current National Air Quality Act of the South African Department of Environmental Affairs.[26]
[b] 2015 National Air Quality Act of the South African Department of Environmental Affairs.[26]
[c] European Commission Air Quality Standards.[27]

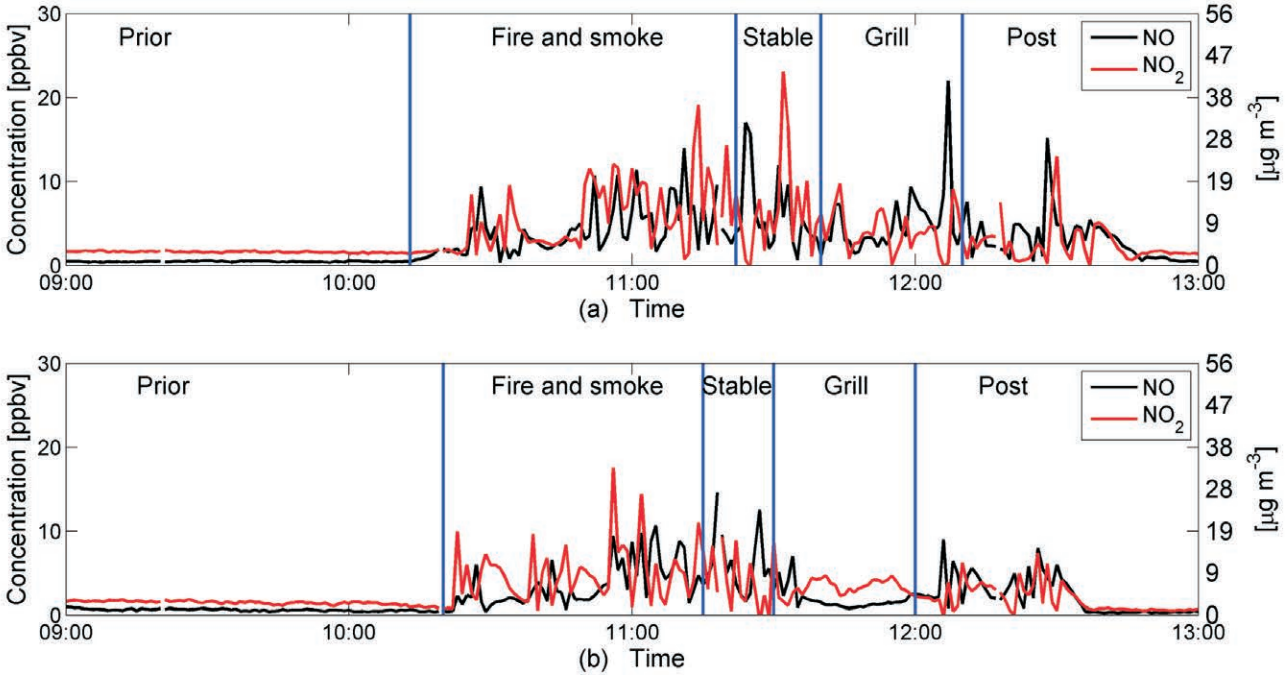

Figure 3 NO (black) and NO_2 (red) concentrations are closely related during the first (**a**) and second (**b**) braai experiment.

ascribed to periods when titration of O_3 occurred. However, the peaks that were observed during the braai experiments were unexpected and cannot be explained at this stage. The South African national ambient air quality standard limit and the European standard limit for O_3 is an eight-hour moving average of 120 μg m^{-3} (Table 2). The duration of the braai experiments was ~2.5 hours and the levels can therefore not be directly compared to the eight-hour limit. However, O_3 concentrations twice peaked above 120 μg m^{-3} during the second braai experiment. Although O_3 levels were not significantly elevated in the fresh braai plume, it is expected that O_3 levels could increase in the aging plume due to NO_x and VOC (discussed later in the paper) emissions from the braai.[13]

In Fig. 5, atmospheric CO concentrations are presented. CO levels sharply increased during the fire and smoke phase of the experiments shortly after the fires were lit. This was expected, since CO is a major product of incomplete combustion. CO concentrations remained elevated for the duration of both braai experiments. Similar to NO_x concentrations, CO levels did not exhibit a clear trend in relation to the various braai phases and ambient CO concentrations were restored after removal of the braais. Notwithstanding the afore-mentioned elevated levels, concentrations remained below the prescribed one-hour South African ambient standard limit of 30 000 μg m^{-3} (Table 2).

In Fig. 6, the concentrations of atmospheric VOCs measured during the first braai experiment are presented. These measurements were not conducted during the second experiment. The VOC species detected were primarily the aromatics (benzene,

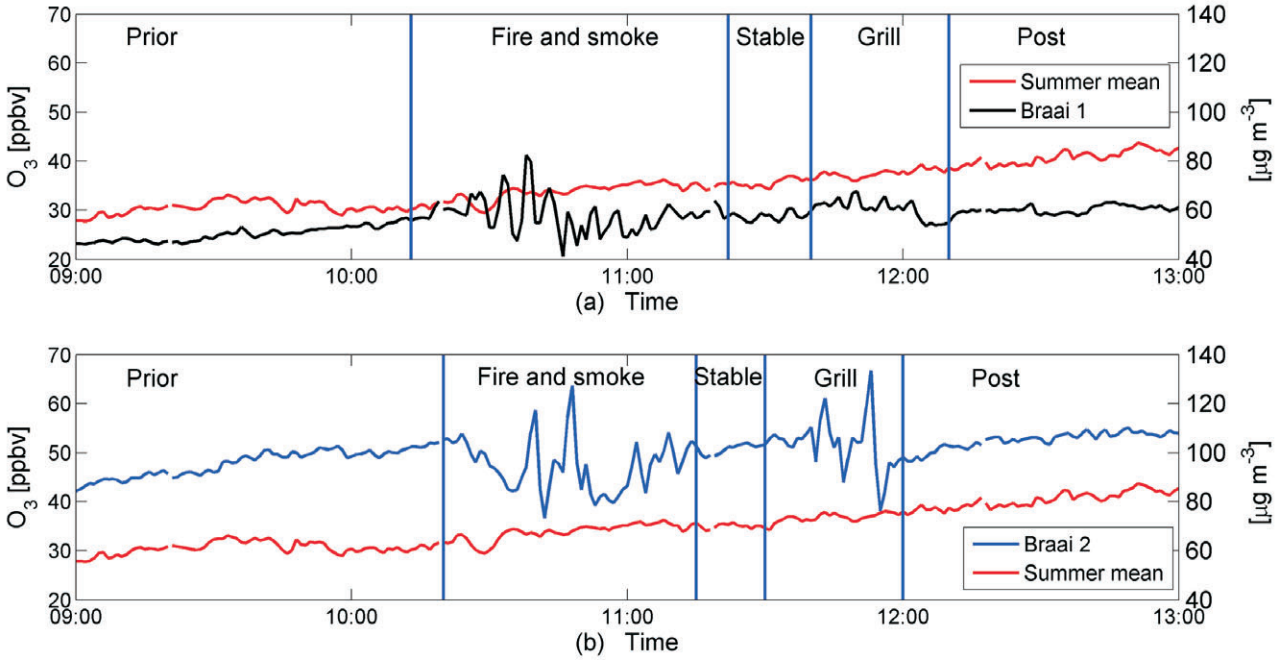

Figure 4 O_3 concentrations fluctuate during the first (**a**) and second (**b**) braai experiment (black) and deviate from the 2012 summer mean (red).

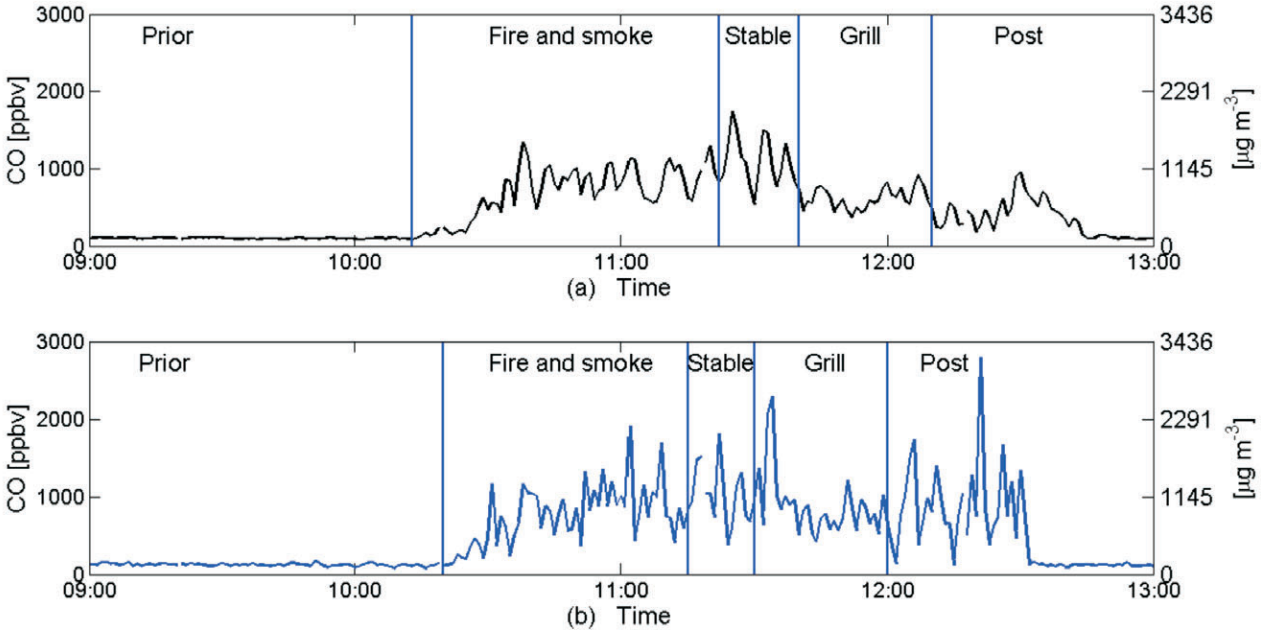

Figure 5 The CO concentrations of the first (**a**) and second (**b**) braai experiment show no difference between the separate braai phases.

toluene, ethyl benzene, xylene and styrene) and alkanes (heptane, hexane, octane, nonane and decane). All other VOCs were below the detection limit of the analytical instrument. Nonane and decane were also not detected in all the phases of the braai, as indicated by missing data points for these compounds in Fig. 6. Benzene was the main VOC emitted, while toluene had the second highest concentrations. The concentrations of all the aromatics, as well as the longer chain alkanes, nonane and decane, were higher during the fire and smoke phase. This can most likely be attributed to the paraffin-like compounds in the firelighters, as well as the volatile matter present in the charcoal briquettes (Table 1) being released during combustion. The concentrations of the aromatics, as well as the shorter chain alkanes, hexane, heptane and octane, were elevated during the grill phase. The shorter chain alkanes were significantly higher during the grill phase, compared to their levels in the fire and smoke phase. The emissions of VOCs during the grill phase can be mainly attributed to fat dripping on the coals. Fat lipids range from four- to 24-carbon chain lengths. Burning fats could reduce the carbon chain length and contributed to the higher concentrations of the shorter carbon chain alkanes. Cross-bridging between the carbon chains that occurs due to the high temperatures could account for the formation of aromatics. Furthermore, the cooking process breaks cell membranes, as well as alters protein structure and fat composition, which can release various VOCs that are perceived by the smell (aroma) of certain aromatics.

Benzene is currently the only VOC that has a South African ambient air quality standard limit, i.e. a one-year standard of 10 μg m^{-3}, which will change to 5 μg m^{-3} in 2015 (Table 2).

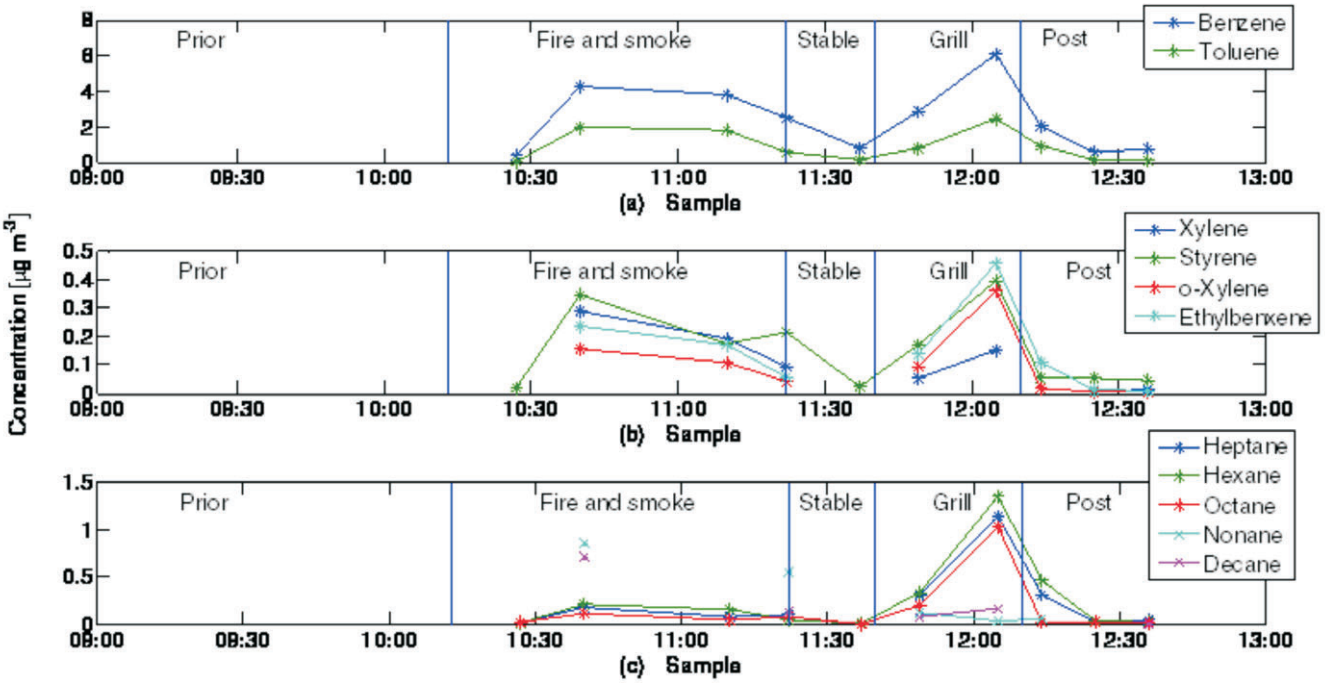

Figure 6 BTEX (**a**, **b**) and alkanes (**c**) display peaks during the fire and smoke, and grill phases.

Benzene concentrations were higher than the 2015 one-year limit during the fire and smoke, and grill phases. However, it must be noted that the entire braai experiment was conducted in approximately 2.5 hours and these short-term levels can therefore not be used to quantify possible impacts on human health associated with atmospheric benzene exposure during a typical braai. However, it is evident that benzene and toluene levels were substantially elevated above ambient concentrations during the braai, since the maximum benzene and toluene concentrations during the grill phase were 50 and four times higher than the ambient measured annual median benzene (0.13 ppb) and toluene (0.63 ppb) levels at Welgegund, respectively.[13]

4.3. Aerosol Species

The PM_{10} mass presented in Fig. 7 indicates that PM_{10} concentrations increased above the background concentrations during the fire and smoke phase, and even more significantly during the grill phase. During the fire and smoke phase, this increase was approximately an order of magnitude, while the increase during the grill phase was up to two orders of magnitude. In contrast to most of the measurements discussed, the PM_{10} levels during the stable phase were similar to background concentrations. The higher PM_{10} concentrations measured during the fire and smoke phase and the grill phase can be attributed to primary aerosols emitted from the incomplete combustion of different fuels, i.e. firelighters and charcoal during the fire and smoke phase, and fat dripping on the charcoal during the grill phase. It is unlikely that a significant amount of secondary aerosol formation occurred, since the braais were in close proximity to the inlets. The chemical composition of these aerosols will be explored later in the paper when the GCxGC-TOFMS analyses are considered. The current 24-hour South African ambient standard limit for PM_{10} is 120 μg m^{-3}, which will be revised in 2015 to 75 μg m^{-3} (Table 2). The duration of the braai experiments was ~2.5 hours and PM_{10} concentrations can therefore not be compared directly to the 24-hour limits. However, concentrations during the fire and smoke phase occasionally exceeded the current concentration limit, while the future limit was exceeded several times. During the entire grill phase, the current and future limits were significantly exceeded. The prevalence of high PM_{10} levels from charcoal combustion has previously been identified as a concern.[29]

The total number of sub-micron particles ranging between 12 and 840 nm measured during the braais, as presented in Fig. 8, increased after the firelighters were lit and reached a maximum at the end of the fire and smoke phase. During the first braai experiment, the sub-micron total number concentration reached 250 000 cm^{-3}, which is two orders of magnitude above the baseline measurements during the prior phase. However, the ~9 min scanning time of the DMPS negatively influence the resolution of the measurements and it can therefore not be stated with absolute certainty when peak number concentrations occurred. The total number of submicron particles decreased during the stable phase, remaining relatively stable during the grill phase and only returning to background concentrations after the braais were removed.

A comparison of the PM_{10} mass concentration (Fig. 7) and the submicron particle number concentration (Fig. 8) clearly indicates that smaller particles are emitted during the fire and smoke phase, while larger particles are mainly emitted during the grill phase. In addition, air ion spectrometer (AS) measurements of the 10–40 nm negative ion concentrations indicated that the negative ion levels during the fire and smoke phase were 10 to 20 times higher than during the prior phase. Furthermore, negative ion concentrations were twice as high during the fire and smoke phase compared to negative ion levels during the grill phase, which indicates higher ultrafine particle concentrations during the fire and smoke phase. The lower number of fine particulates observed during the grill phase could also be attributed to the high conversational sink of other species during this phase, e.g. by lower SO_2 emissions during the grill phase compared to the fire and smoke phase. The potential health risks associated with exposure to ultrafine particles released during charcoal-based cooking may be higher than acceptable[30], especially when this method of cooking is conducted in a confined space, e.g. household combustion. A typical South African braai, however, usually takes place outdoors or in a well-ventilated area.

In Fig. 9, the five-minute means for BC concentrations are presented. BC mass increased directly after igniting the

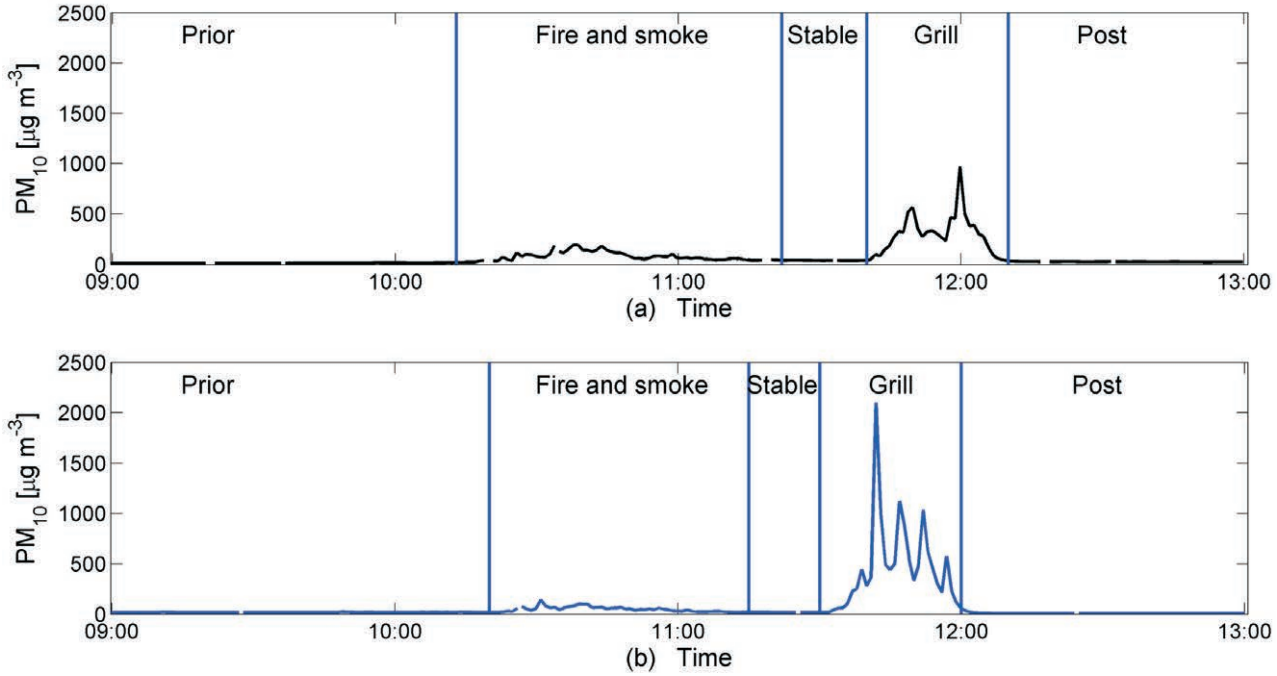

Figure 7 Concentrations of PM_{10} aerosols during the first (**a**) and second (**b**) braai experiment.

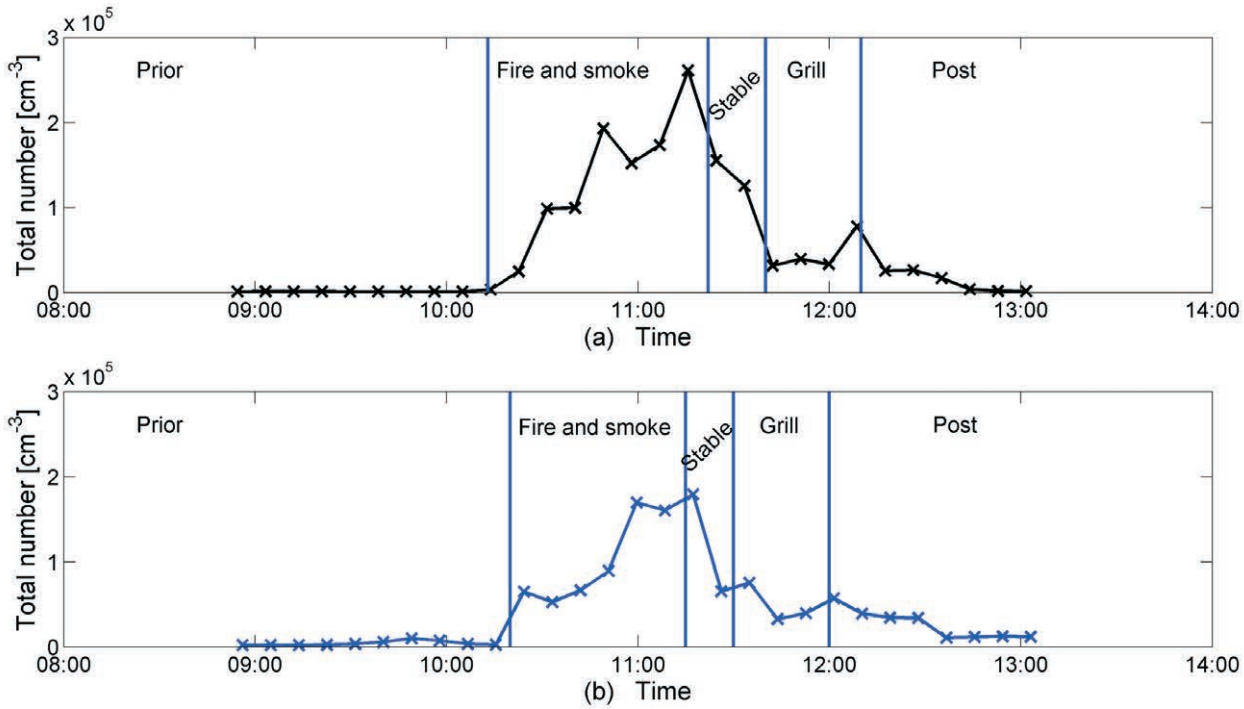

Figure 8 The total number ofparticles between 10 and 840 nm per cm^3 during the first (**a**) and second (**b**) braai experiment.

firelighters up to a maximum during the fire and smoke phase due the liberation of BC particles from the charcoal and possible incomplete combustion. As the braai reaches the stable phase, BC levels decreased and returned to background levels. BC concentrations again increased when the meat was placed on the grill. This could be attributed to two possible release mechanisms, i.e. BC particles can be liberated from the charcoal by the dripping action of the hot fat on the briquettes, as well as incomplete combustion of the dripping fat in the flames. After the meat was removed from the braai, background BC levels were again observed.

The intensity of light scattering measured by the three-wavelength nephelometer is presented in Fig. 10. From these data, it is evident that light scattering was elevated during the fire and smoke phase and reached its maximum during the grill phase, while it was similar to background levels during the other phases. A similar trend was observed for PM_{10} concentrations (Fig. 7). A comparison of these two measurements, i.e. scattering and PM_{10}, indicated that PM_{10} observed during the braai is more scattering than absorbing. This will be explored in the next paragraph where single scattering albedo (ω_o) is considered.

In Fig. 11, the five-minute averages of the calculated ω_o are presented. Depending on the surface albedo, ω_o can be used to estimate whether the aerosol direct effect is heating or cooling. Over grassland, for instance, the ω_o threshold between heating and cooling is approximately 0.75, i.e. $\omega_o > 0.75$ indicates a

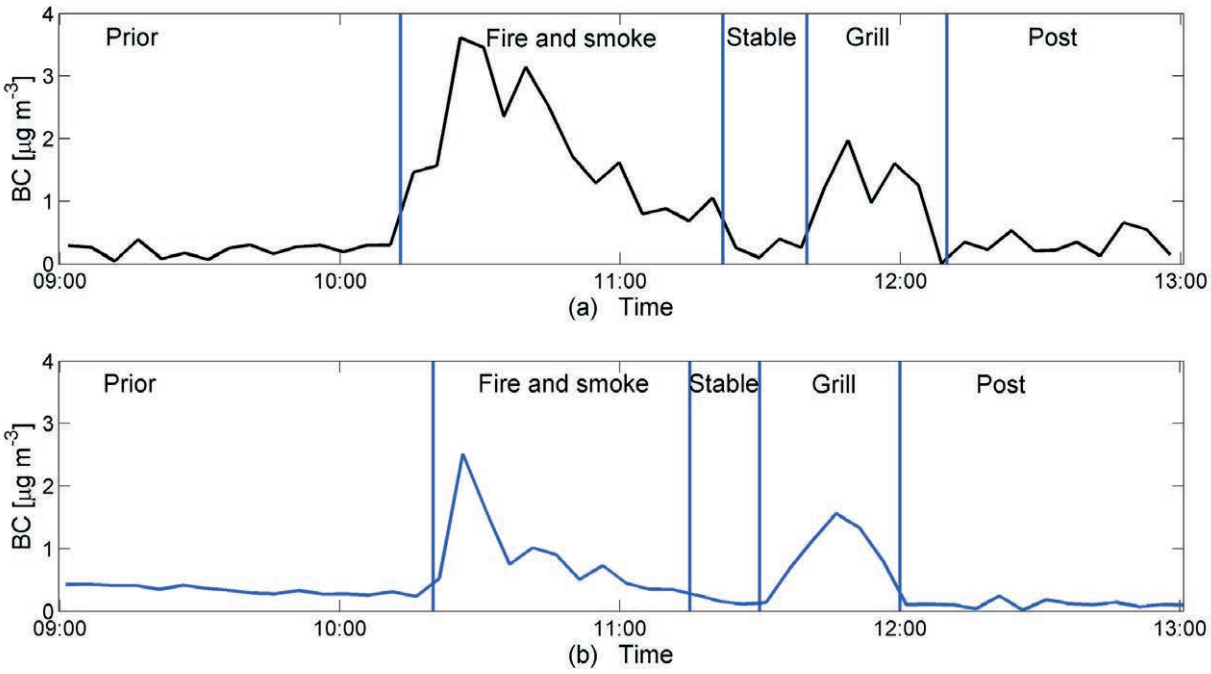

Figure 9 The absorption at 637 nm relating to BC concentrations during the first (**a**) and second (**b**) braai experiment.

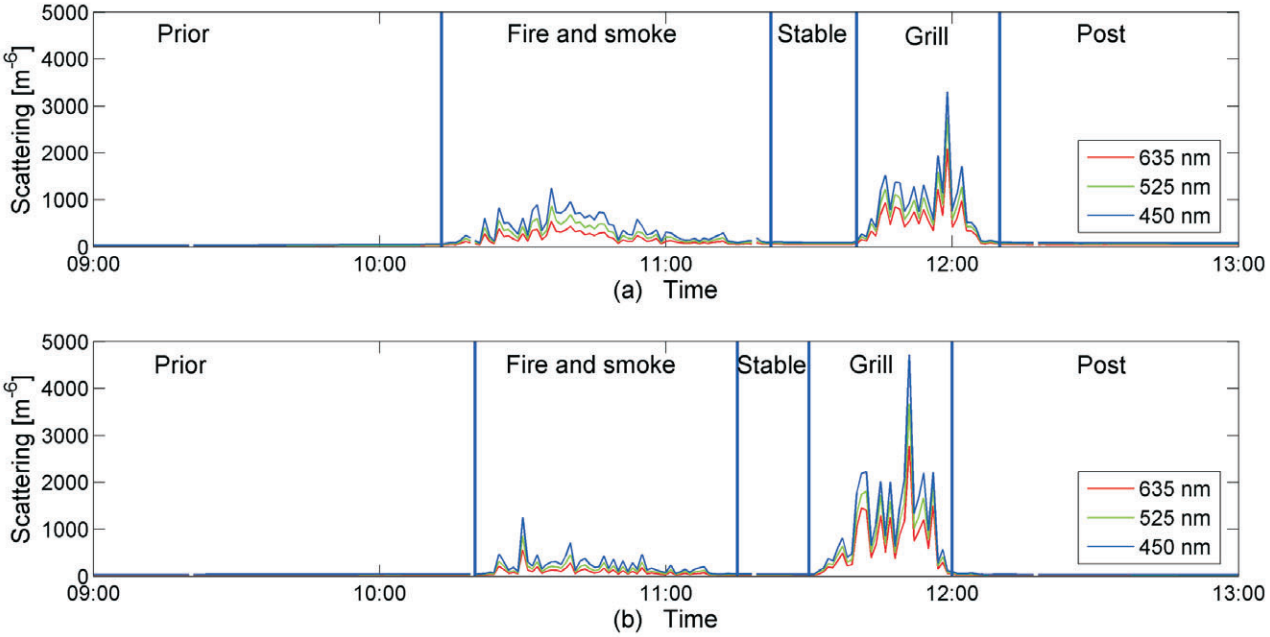

Figure 10 The backscattering from the three wavelengthnephelometer during the first (**a**) and second (**b**) braai experiment is given at each wavelength (450, 525 and 635 nm).

cooling aerosol direct effect. Laakso *et al.* presented a campaign average of 0.84 and summer-time average of 0.89 for measurements conducted at Elandsfontein in the Mpumalanga Highveld.[22] Beukes *et al.* reported a median ω_o of 0.89 for the relatively clean background sector at Welgegund.[12] From the comparison of the braai plume ω_o with the afore-mentioned literature data it is evident that aerosols for the entire measurement period were very reflective. Initially, during the fire and smoke phase, somewhat lower ω_o values were observed, which correlated with the peak release of BC (Fig. 9). Thereafter, the ω_o was similar to background levels, with the exception of the grill phase when very high ω_o was observed. This can most likely be attributed to fat dripping on the coals during the grill phase, increasing the emissions of organic aerosols, which is mostly reflective. This is supported by the increase in VOC emissions observed during this phase. During the fire and smoke phase, the mean ω_o was 0.94, while the grill phase had a mean of 0.98. The mean ω_o for the entire braai experiment was 0.96. These values are extremely high and indicate that aerosols emanating from a braai are very reflective resulting in a cooling aerosol direct effect on the atmosphere.

Barbecue charcoal combustion can be an important source of trace metal emissions to the atmosphere.[31] Therefore, the trace metal content of the aerosols from the braai was also quantified. In contrast to most of the other measurements, no prior and post-phase concentrations were determined. Therefore, trace metal concentrations cannot be contextualized in relation to background levels at Welgegund. In total, 32 trace elements

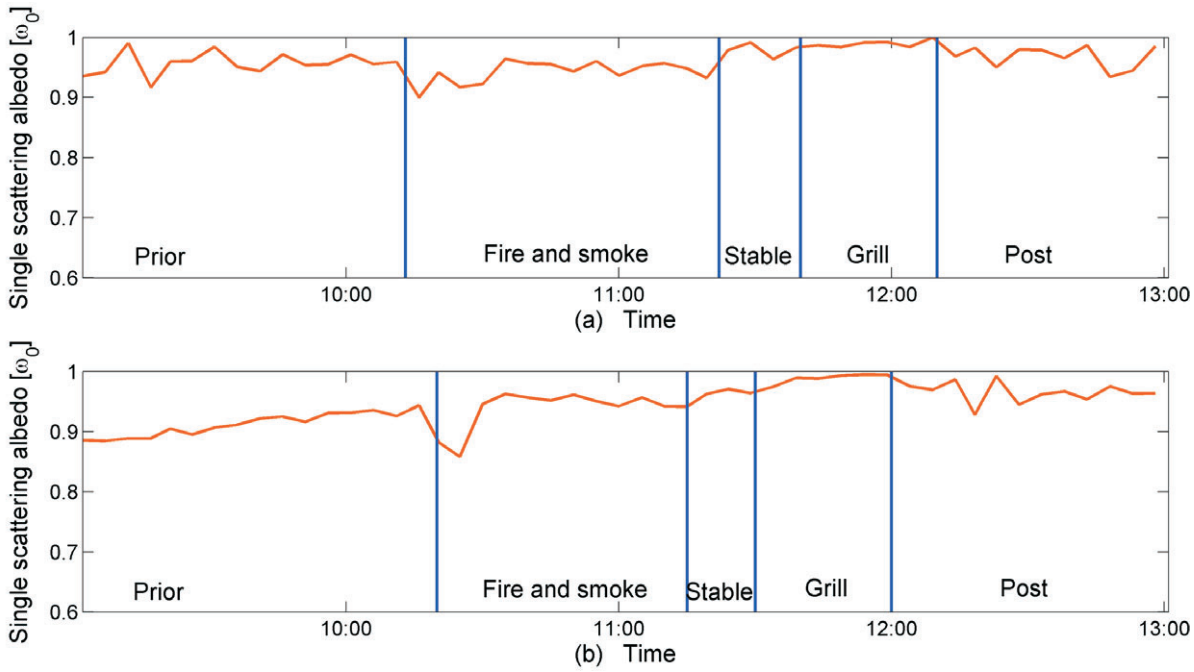

Figure 11 The single scattering albedo (637 nm) during the first (**a**) and second (**b**) braai experiment.

could be detected, which included beryllium (Be), boron (B), Na, magnesium (Mg), aluminium (Al), phosphorus (P), potassium (K), calcium (Ca), titanium (Ti), vanadium (V), chromium (Cr), manganese (Mn), iron (Fe), cobalt (Co), nickel (Ni), copper (Cu), zinc (Zn), arsenic (As), selenium (Se), strontium (Sr), molybdenum (Mo), palladium (Pa), silver (Ag), cadmium (Cd), antimony (Sb), barium (Ba), platinum (Pt), gold (Au), mercury (Hg) thallium (Tl), lead (Pb) and uranium (U). The concentrations of these trace elements measured in the different size fractions are presented in Fig. 12. Be, Se and Pt were below the detection limit of the analytical technique applied. Mo and Hg were below the detection limit in the $PM_{2.5-1}$ fraction, while Fe, Co, Ag and Hg were below the detection limit in the PM_1 fraction. The highest trace metal concentrations were measured for Ca, Na, Al, Fe, K, Mg, Cr, and B, which contributed 21.3, 19.3, 15.2, 9.9,8.3, 6.4, 3.3 and 2.7 %,respectively, to the total concentration. These species are typical ash components. The other trace metals contributed only 13.6 % of the total trace metal concentration. The size distribution results indicated that 46 % of the total trace metal mass was in the $PM_{2.5-1}$ size range. Trace metal concentrations determined by Van Zyl *et al.* in the highly industrialized western Bushveld Igneous Complex (BIC) in South Africa indicated that atmospheric Fe and Mg were the most abundant atmospheric metal species, while Na, B and Al also had relatively high atmospheric concentrations.[24]

Pb is the only metal species that has a limit prescribed by the South African ambient air quality standards, while limits also exist for V, Ni, As, Cd and Pb in Europe. The total Pb, V, Ni, As and Cd concentrations were 1.798, 0.301, 1.532, 0.068 and 0.007 $\mu g\ m^{-3}$, respectively. Pb exceeded the South African and European annual ambient air quality limit, while V, Ni, As and Cd exceeded European annual ambient air quality limits. These exceedences of the one-year standard limits of these metals cannot, however, be used to quantify the possible negative effects on human health exposure for the duration of a braai. The annual average concentrations of Pb, V and Ni in the western BIC determined by Van Zyl *et al.* were 0.08, 0.04 and 0.33 $\mu g\ m^{-3}$, while As and Cd were not detected.[24] The annual average concentration of 0.33 $\mu g\ m^{-3}$ measured for Ni exceeded the standard limit value by an order of magnitude, which was attributed to base metal refining in the western BIC. The Ni concentrations measured during the braai experiment were similar than the annual average Ni levels measured at the western BIC.

Water-soluble anion and cations were also quantified. As is evident from the results indicated in Fig. 13, sulphate (SO_4^{2-}) was the dominant anionic species, while calcium (Ca^{2+}) and magnesium (Mg^{2+}) were the dominant cationic species. It was also obvious that most of the water-soluble species occurred in the PM_1 fraction, while the concentrations of the cations and anions decreased with an increase in particle size. This can be attributed to the freshness of the plume emanating from the braais.

As previously mentioned, aerosols were also collected on quartz filters during the first braai experiment in order to identify organic compounds with GCxGC-TOFMS. Similar to trace metal measurements, aerosol samples were not collected prior to and after the braai experiment for organic compound characterization. The results can, however, be compared to a one-year sampling campaign conducted by Booyens *et al.* at Welgegund.[15] In Fig. 14a, the total number of compounds pre-identified in each of the size fractions and their corresponding ΣNRF are presented. A significant smaller number of compounds were pre-identified for the braai experiment, i.e. 50, compared to the 1056 organic compounds pre-identified by Booyens *et al.*[15] This can be attributed to the difference in sampling periods, i.e. Booyens *et al.*[15] collected 24-hour samples, while aerosol samples were only collected for ~2 hours. In addition, the number of organic compounds presented by Booyens *et al.*[15] was the combined number of organic compounds pre-identified for the entire one-year sampling campaign. It is also not possible to completely ascertain whether organic compounds pre-identified were exclusively from the braai experiment. The largest number of compounds pre-identified was in the $PM_{2.5-1}$ fraction, which also had the highest ΣNRF. Booyens *et al.* also indicated that the largest number of compounds and highest ΣNRF were in the $PM_{2.5-1}$ fraction.[15] However, blow-off of semi-VOCs is likely to occur for the PM_1 fraction that can contribute to an underestimation of the number of compounds and ΣNRF of species in this fraction.[32] The higher ΣNRF determined for

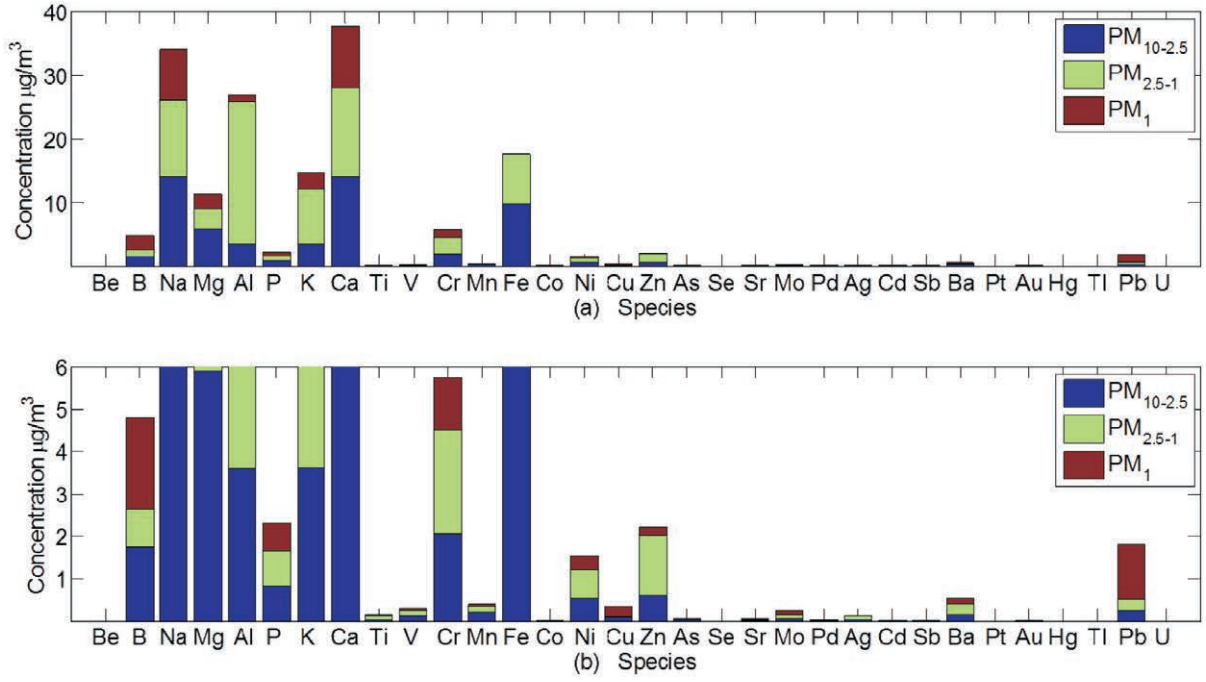

Figure 12 Trace metal analysis (**a**) ofaerosol species captured during the first braai experiment with enlargement (**b**).

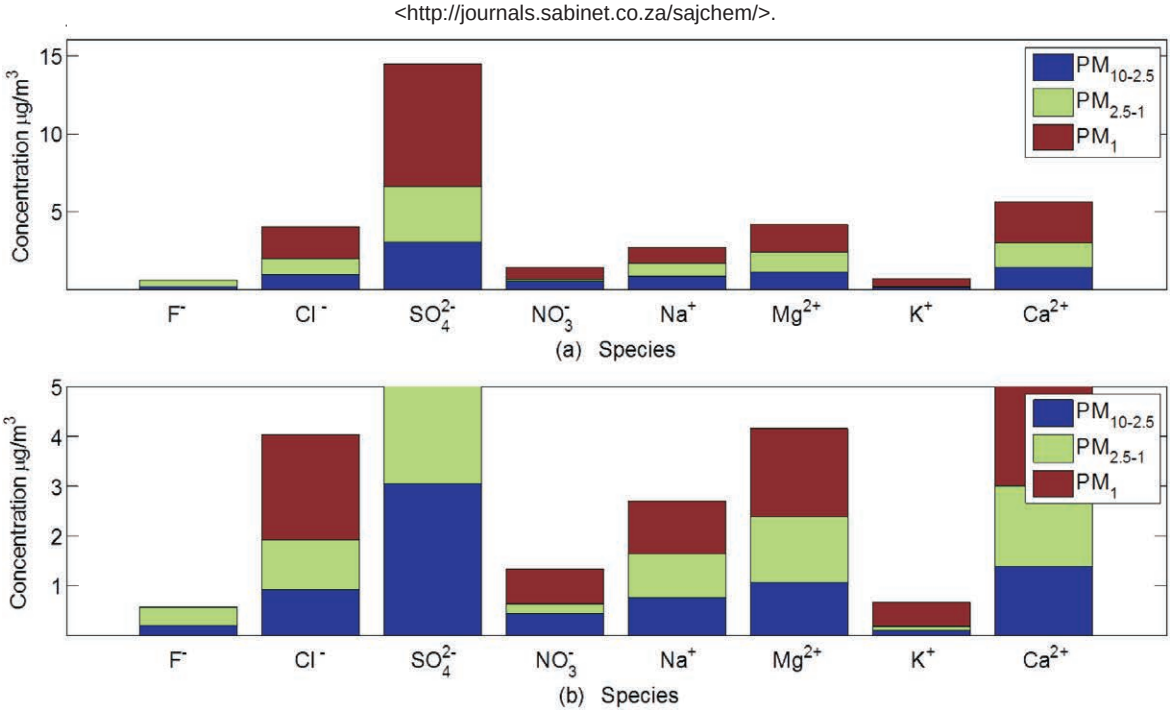

Figure 13 Anion and cation species identified (**a**) during the first braai experiment with enlargement (**b**).

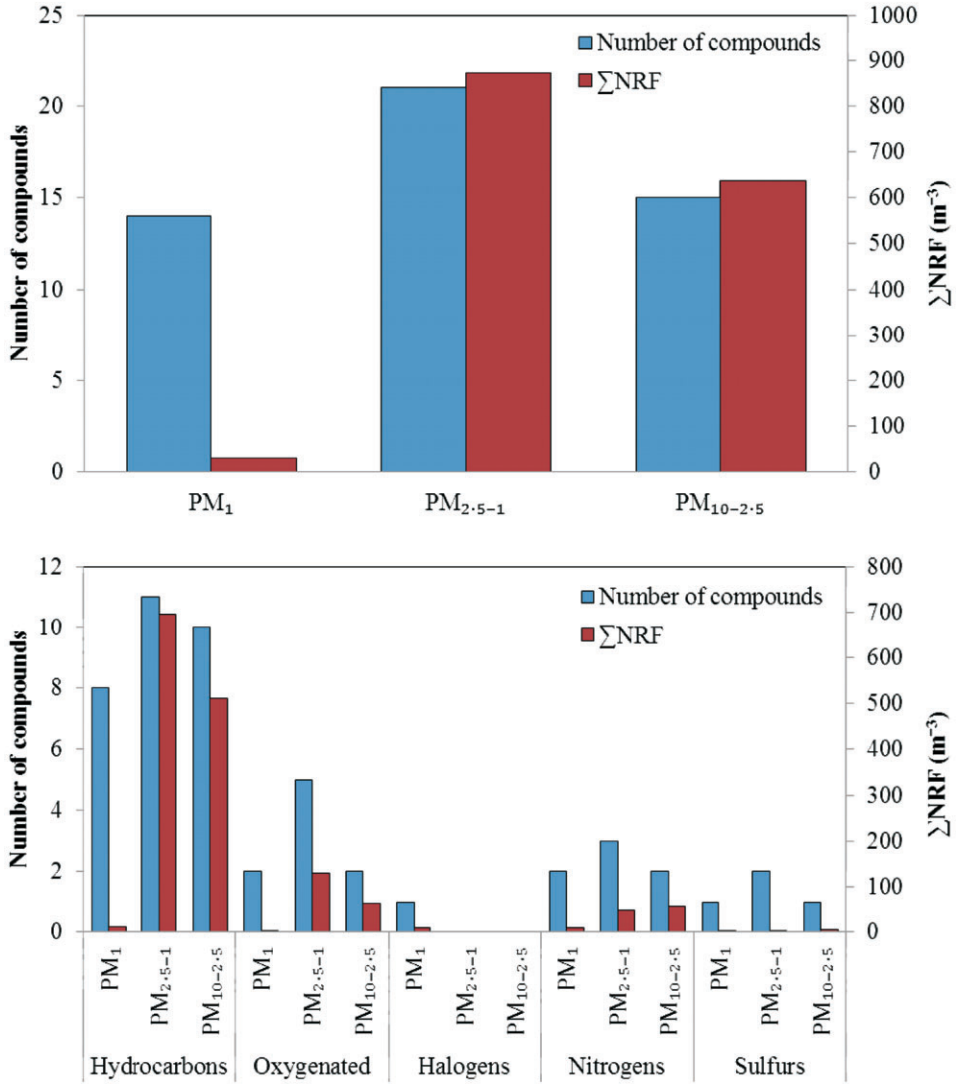

Figure 14 The total number and semi-quantification of size resolved (**a**) organic species and their functional groups (**b**).

particulates smaller than 2.5 μm indicate that these organic compounds can potentially be more harmful to human health compared to larger particles.

In Fig. 14b, the number of compounds and the ΣNRF of the different classes of organic functional groups are presented. The largest number of compounds detected was hydrocarbons in all the size fractions, while the second, third and fourth largest numbers of species were oxygenated, N- and S-containing compounds, respectively. Very few halogen-containing species were detected. The highest accumulated ΣNRF were determined for hydrocarbon species in the $PM_{2.5\text{-}1}$ and $PM_{10\text{-}2.5}$ fractions, while oxygenated and N-containing species were the second most abundant with similar ΣNRFs in the $PM_{2.5\text{-}1}$ and $PM_{10\text{-}2.5}$ fraction. In the study conducted by Booyens *et al.*, the largest number of organic compounds determined with the highest ΣNRF was oxygenated species that were indicative of aged air masses.[15] The higher occurrence of hydrocarbon species is expected for primary aerosols emitted from a fresh burning plume. The main organic compound contributing to the relatively high accumulated concentration of the hydrocarbon species in the $PM_{2.5\text{-}1}$ and $PM_{10\text{-}2.5}$ fraction was accession the predominant oxygenated and N-containing species contributing to the ΣNRFs were diisooctyl phthalate and 4H-1,2,4-triazol-4-amine, respectively. Oxidative decomposition of the fatty acids, especially unsaturated species, can be considered to be a source for many organic compound groups, including hydrocarbons, aldehydes, ketones, alcohols, esters, furans and lactones.[17]

5. Conclusions

According to the knowledge of the authors, this is the most comprehensive investigation of atmospheric species in a typical South African braai plume. Both air quality and climatically important aspects were considered.

Compared to background concentrations, SO_2, NO and NO_2, and CO increased significantly during the braai experiment, although they remained well below the ambient air quality limits. O_3 concentrations did not increase notably during the braai, although O_3 levels fluctuated more than usual. The predominant VOC species detected were aromatics and alkanes, with elevated levels observed during the fire and smoke, as well as grill phases. Benzene was higher than the proposed future South African one-year ambient air quality limit during the fire and smoke, and grill phases. These short-term elevated levels during a typical braai can therefore not be used to quantify possible negative impacts on human health.

The PM_{10} mass concentrations increased during the fire and smoke phase, and even more significantly during the grill phase. Elevated PM_{10} levels during the fire and smoke phase, and grill phase were attributed to emissions of primary aerosols associated with the incomplete combustion of charcoal and dripping fat, respectively. A comparison of PM_{10} with the 24-hour ambient standard limits indicated that PM_{10} is, especially, problematic during the grill phase. However, due to the relatively short duration of a typical braai, PM_{10} concentrations cannot be compared directly to standard limit values. The total number of sub-micron particles increased after the firelighters were lit and reached a maximum of 250 000 cm^{-3} at the end of the fire and smoke phase. A comparison ofPM_{10} and submicron particle number concentrations indicates that smaller particles are emitted during the fire and smoke phase, while larger particles are mainly emitted during the grill phase.

ω_o was calculated from scattering and absorption measurements. The ω_o was relatively close to one during all phases of the braai with the exception of the initial period of the fire and smoke phase that had somewhat lower ω_o values. These lower ω_o values coincided with the peak BC emissions. The results indicate that aerosols emanating from a braai are reflective and have a cooling aerosol direct effect. Particulates emitted from braai could also act as cloud condensation nuclei, which, through the indirect effect, can have a net cooling effect.

In total, 32 trace elements were analyzed for. The highest trace metal concentrations were associated with trace elements typically present in ash. 46 % of the total trace metal mass percentage could be attributed to the $PM_{2.5\text{-}1}$ size range. The Pb concentration was higher than the South African and European annual ambient air quality limit, while V, Ni, As and Cd exceeded European annual ambient air quality limits. However, the ~2.5-hour duration of the braai cannot be compared directly to these annual limits. SO_4^{2-} was the dominant anionic, while Ca^{2+} and Mg^{2+} were the dominant cationic water-soluble species present in the braai aerosols. The PM_1 size fraction also had the largest water-soluble cation and anion load.

The largest number of organic compounds pre-identified from GCxGC-TOFMS analysis was in the $PM_{2.5\text{-}1}$ fraction that also had the highest concentration, although blow-off of VOCS is likely to occur for the PM_1 fraction. The largest number of compounds detected was hydrocarbon species in all the size fractions. Few oxygenated, N- and S- containing species were detected. Hydrocarbon species in the $PM_{2.5\text{-}1}$ fraction had the highest accumulated ΣNRF. The main organic compounds that contributed to the relatively high accumulated concentration of the hydrocarbon species in $PM_{2.5\text{-}1}$ and $PM_{10\text{-}2.5}$ fraction were icosane. The dominant oxygenated and N-containing species were diisooctyl phthalate and 4H-1,2,4-triazol-4-amine, respectively.

In general, the results indicated that for a recreational braai no significant health-related risks occur due to the relatively short exposure period. However, if these short-term results are extrapolated to longer exposure periods that are experienced by occupational vendors on a daily basis, it is evident that health-related risks significantly increase. In addition, semi-formal and informal cooking practices also expose large numbers of people to both indoor and outdoor emissions that would be expected to be similar to the results presented here. Although some negative aspects might be associated with long-term exposure to braai plumes, the net climatic aerosol direct effect seems to be cooling. However, the climatic effects of long- and short-lived greenhouse gases (GHGs) were not evaluated in this study.

Our final conclusion and recommendation is: Braai our beloved country!

References

1 G. King, *The Hansie Cronjé Story: An Authorized Biography,* Global Creative Studios, Brackenfell, 2005.

2 C.H. Van Heerden, An exploratory analysis of leisure caravanning in the Kruger National Park in South Africa. *Innovative Marketing*, 2010, **6**(1), 66–72.

3 T. Morrison and W.A. Conaway, *Kiss, Bow, or Shake Hands: the Bestselling Guide to Doing Business in More than 60 Countries*, 2nd edn., Adams Media, Massachusetts, 2006.

4 A.D. Venter, V. Vakkari, J.P. Beukes, P.G. van Zyl, H. Laakso, D. Mabaso, *et al.*, An air quality assessment in the industrialized western Bushveld Igneous Complex, South Africa, *S. Afr. J. Sci.*, 2012, **108**(9/10), 1–10, Art. #1059, 10 pages, doi: 10.4102/sajs.v108i9/10.1059

5 P. Maritz, J.P. Beukes, P.G. van Zyl, E.H. Conradie, C. Liousse, C. Galy-Lacaux, *et al.*, Spatial and temporal assessment oforganic and black carbon at four sites in the interior of South Africa, *Clean Air J.*, 2015, **25**, 20–33.

6 E. Muchapondwa, A cost-effectiveness analysis of options for reduc-

ing pollution in Khayelitsha township, South Africa, *J. Transdisciplinary Res. Southern Afr.*, 2010, **6**(2), 333–358.

7 P. Harris, On charcoal, *Interdisciplinary Sci. Rev.,* 1999, **24**(4), 301–306, doi: http://dx.doi.org/10.1179/030801899678966

8 M. Rahman and K. Kim, Release of offensive odorants from the combustion of barbecue charcoals, *J. Hazard. Mat.*, 2012, **215-216**, 233– 242. http://dx.doi.org/10.1016/j.jhazmat.2012.02.055

9 E. Kabir, K.H. Kim and H.O. Yoon, Trace metal contents in barbeque (BBQ) charcoal products, *J. Hazard. Mat.,* 2011, **185**(2-3), 1418–1424, http://dx.doi.org/10.1016/j.jhazmat.2010.10.064

10 U. Pöscle, Atmospheric aerosols: composition, transformation, climate and health effects. *Angewandte Chemie*, 2005,**44**, 7520–7540, doi: 10.1002/anie.200501122

11 E. Kabira, K. Kima, J. Ahna, O. Honga and J.R. Sohnb, Barbecue charcoal combustion as a potential source of aromatic volatile organic compounds and carbonyls, *J. Hazard. Mat.,* 2009,**174**(2010), 492–499, http://dx.doi.org/10.1016/j.jhazmat.2009.09.079

12 J.P. Beukes, V. Vakkari, P.G. van Zyl, A.D. Venter, M. Josipovic, K. Jaars, *et al.,* Source region plume characterization of the interior of South Africa, as observed at Welgegund, *Clean Air J.*, 2013, **23**, 7–10.

13 K. Jaars, J.P. Beukes, P.G. Van Zyl, A.D. Venter, M. Josipovic, J.J. Pienaar, *et al.,* Ambient aromatic hydrocarbon measurements at Welgegund, South Africa, *Atmos. Chem. Phys*., 2014, **14**, 7075–7089, doi:10.5194/acp-14-7075-2014.

14 P. Tiitta, V. Vakkari, M. Josipovic, P. Croteau, J.P. Beukes, P.G. Van Zyl, *et al.,* Chemical composition, main sources and temporal variability of PM1 aerosols in southern African grassland, *Atmos. Chem. Phys*., 2014, **14**, 1909–1927, doi:10.5194/acp-14-1909-2014

15 W. Booyens, P.G. van Zyl, J.P. Beukes, J. Ruiz-Jimenez, M. Kopperi, M. Riekkola, *et al.,* Size-resolved characterization of organic compounds in atmospheric aerosols collected at Welgegund, South Africa, *J. Atmos. Chem.*, 2014, **72**, 43–64, doi: 10.1007/s10874-015-9304-6

16 V. Vakkari, V.M. Kerminen, J.P. Beukes, P. Tiitta, P.G. van Zyl, M. Josipovic, *et al.,* Rapid changes in biomass burning aerosols by atmospheric oxidation, *Geophys. Res. Lett*., 2014, **41**: 2644–2651. doi:10.1002/2014GL059396

17 W.F. Rogge, L.M. Hildemann, M.A. Mazurek, G.R. Cass and B.R.T. Simoneit, Sources of fine organic aerosol. 1. Charbroilers and meat cooking operations, *Environ. Sci. Technol.*, 1991, **25**, 1112–1125, doi: 10.1021/es00018a015

18 E. Kleynhans, J.P. Beukes, P.G. van Zyl, P. Kestens and J. Langa, Unique challenges of clay binders in a pelletized chromite prereduction process, *Miner. Eng*., 2012, **34**, 55–62, http://dx.doi.org/10.1016/j.mineng.2012.03.021

19 T. Petäjä, V. Vakkari, T. Pohja, T. Nieminen, H. Laakso, P.P. Aalto, *et al.,* Transportable aerosol characterization trailer with trace gas chemistry: design, instruments and verification. *Aerosol Air Quality Res*., 2013, **13**, 421–435, doi: 10.4209/aaqr.2012.08.0207

20 A.P. Hyvärinen, V. Vakkari, L. Laakso, R.K. Hooda, V.P. Sharma, T.S. Panwar, *et al.,* Correction for a measurement artifact of the Multi-Angle Absorption Photometer (MAAP) at high black carbon mass concentration levels, *Atmos. Meas. Tech*., 2013, **6**, 81–90, doi: 10.5194/amt-6-81-2013

21 A. Petzold and M. Schonlinner, Multi-angle absorption photometry a new method for the measurement of aerosol light absorption and atmospheric black carbon. *J. Aerosol Sci*., 2004, **23**, 421–441, http://dx.doi.org/10.1016/j.jaerosci.2003.09.005

22 L. Laakso, V. Vakkari, H. Laakso, A. Virkkula, M. Kulmala, J.P. Beukes, *et al.,* South African EUCAARI measurements: seasonal variation of trace gases and aerosol optical properties, *Atmos. Chem. Phys.,* 2012, **12**, 1847–1864, doi:10.5194/acp-12-1847-2012

23 H. Hellen, P. Kuronen and H. Hakola, Heated stainless steel tube for ozone removal in the ambient air measurements of mono- and sesquiterpenes. *Atmos. Environ.,* 2012, doi:10.1016/j.atmosenv.2012.04.019

24 P.G. van Zyl, J.P. Beukes, G. Du Toit, D. Mabaso, J. Hendriks, V. Vakkari, *et al.,* Assessment of atmospheric trace metals in the western Bushveld Igneous Complex, South Africa. *S. Afr. J. Sci*., 2014, **3/4**(110), Art. # 2013-0280, 11 pages, http://dx.doi.org/10.1590/sajs.2014/20130-280

25 P.C. Mouli, S.V. Mohan, V. Balaram, M.P. Kumar and S.J. Reddy, A study on trace elemental composition of atmospheric aerosols at a semi-arid urban site using ICP-MS technique. *Atmos. Environ.* 2006, **40**, 136–146, http://dx.doi.org/10.1016/j.atmosenv.2005.09.028

26 DEA, Department of Environmental Affairs, National Environmental Management: Air Quality Act (Act No. 39 of 2004), *Government Gazette*, 2009, 6–9.

27 EU, European Commission, Air Quality Standards, Updated April 22, 2015. http://ec.europa.eu/environment/air/quality/standards.htm (accessed July 22, 2015)

28 M.R. Beychok, NO_X emission from fuel combustion controlled, *Oil Gas J.*, 1973, 53–56.

29 C.A. Pope and D.W. Dockery, Health effects of particulate air pollution: lines that connect, *Air Waste Management Assoc*. 2006, **56**, 709–742, doi:10.1080/10473289.2006.10464485

30 S. Taner, B. Pekey and H. Pekey, Fine particulate matter in the indoor air of barbeque restaurants: elemental compositions, sources and health risks, *Sci. Total Environ*., 2013, **454-455**, 79–87. http://dx.doi.org/10.1016/j.scitotenv.2013.03.018

31 J. Susayaa, K. Kima, J. Ahna, M. Junga and C. Kangb, BBQ charcoal combustion as an important source of trace metal exposure to humans, *J. Hazard. Mat*., 2010, **176**(1-3), 932–937. http://dx.doi.org/10.1016/j.jhazmat.2009.11.129

32 P.B.C. Forbes, E.W. Karg, G.N.S.A. Geldenhuys, R. Zimmerman and E.R. Rohwer, Characterization of atmospheric semi-volitile organic compounds, in IUAPPA World Clean AIR Congress, Cape Town, 2013, p. 96.

Chapter 9

Project evaluation

9.1 Introduction

In this chapter, the project is evaluated by considering the successes achieved and shortcomings perceived by evaluating each specific objective of this investigation listed in Chapter 1. Future recommendations are also suggested.

9.2 Objectives

1. **Statistical assessment of gaseous elemental mercury (GEM) measured at Cape Point for at least a five year period**

The continuous high-resolution gaseous elemental mercury (GEM) data from the Cape Point Global Atmosphere Watch (CPT GAW) station between 2007 and 2011 were successfully evaluated with different statistical analysis techniques. GEM data were evaluated by cluster analysis and the results indicated that two clusters, separated at 0.904 ng m^{-3}, existed. The two-cluster solution was investigated by means of back-trajectory analysis to determine the air mass history. The net result indicated that not all low GEM concentrations of marine origin, and similarly, not all high GEM concentrations have a terrestrial origin. Equations were developed by means of multi-linear regression (MLR) analysis that allowed for the estimation and/or prediction of atmospheric GEM concentrations from other atmospheric parameters measured at the CPT GAW station. These equations also provided insight into the relation and interaction of GEM with other atmospheric parameters. Both measured and MLR calculated data confirm a decline in GEM concentrations at CPT GAW over the period evaluated.

From this statistical study of continuous GEM measurement at Cape Point, research questions were identified that is recommended for future studies. Data indicated by 5, 6 and 7 cluster solutions that were identified as extreme event should be investigated

as special case studies. Further research quantifying the contribution of shipping should also be undertaken, which should not only consider the southern African region, but also other busy shipping routes. In addition, source apportionment should be conducted in order quantify the contribution of specific sources.

2. **Evaluate the extent of regional atmospheric Cr(VI) pollution from the western Bushveld Complex, which is likely to be a source region with elevated atmospheric Cr(VI) levels**

Hexavalent chromium, Cr(VI), was successfully investigated and the regional atmospheric pollution of Cr(VI) from the ferrochromium and other related industries located in the western Bushveld Complex (wBC) of South Africa could be determined. Particulate matter was sampled for a full calendar year at a regional background site, which is situated downwind of the wBC on the dominant anti-cyclonic recirculation route of air mass over the South African interior. Results indicated that Cr(VI) concentrations in air masses that had passed over the regional background were below the detection limit of the analytical technique applied, but that Cr(VI) in air masses that had passed over the wBC were elevated and had a median concentration of 4.6 ng/m^3. The majority of Cr(VI) was found to be in the finer size fraction ($PM_{2.5}$), which could be explained by the properties of Cr(VI)-containing PM being emitted by the sources in the wBC and the atmospheric lifetimes of different PM size fractions. The results also indicated that it is possible that not only pyrometallurgical sources in the wBC, but also other combustion sources outside the wBC contributed to the observed atmospheric Cr(VI) concentrations.

It is recommended that the simultaneous measurements of atmospheric Cr(VI) concentrations in both the wBC and at Welgegund must be performed in future in order to quantify the range of atmospheric Cr(VI) half-life more precisely. Since a large number of meteorological parameters are measured at Welgegund, multivariate data analysis methods could also be applied to such a dataset to determine the effect of, for instance, relative humidity and temperature on the atmospheric half-life of Cr(VI). This would enable a better assessment and prediction of the regional dispersion of

Cr(VI) from priority areas, such as the wBC in South Africa and similar areas internationally.

3. Conduct characterisation of general trace metal concentrations at a regional background site and identify possible sources/source areas

Aerosol sampling was performed at Welgegund in South Africa, which is a regionally representative background site. PM_1, $PM_{1-2.5}$ and $PM_{2.5-10}$ samples were collected for thirteen months and 32 atmospheric trace metal species could be detected. Atmospheric Fe had the highest concentrations in all three size fractions, while Ca was the second most abundant species. Cr and Na concentrations were the third and fourth most abundant species, respectively. Trace metal concentrations determined at Welgegund could also be compared to levels thereof in the wBC that indicated that Fe was also the most abundant species, while similar trace metals determined at Welgegund were also measured in the wBC. However, concentrations of trace metal species in the wBC were significantly higher compared to levels thereof at Welgegund. With the exception of Ni, none of the trace metals measured at Welgegund exceeded local and international standard limit values. No distinct seasonal pattern was observed in the $PM_{2.5-10}$ size fraction, while the PM_1 and $PM_{1-2.5}$ size fractions indicated elevated trace metal concentrations coinciding with the end of the dry season, which could partially be attributed to decreased wet removal and increases in wind generation of particulates. Principle Component Factor Analysis (PCFA) analysis was successfully applied and revealed three meaningful factors in the PM_1 size fraction, i.e. fly ash, pyrometallurgical-related and crustal. No meaningful factors were determined for the $PM_{1-2.5}$ and $PM_{2.5-10}$ size fractions, Pollution roses confirmed this impact of wind-blown dust on trace metal concentrations, while the influence of industrial activities were also substantiated.

It is recommended that the collection of particulate matter for determining trace metal concentrations be continued at Welgegund. In this study PCFA analysis was applied as an explorative tool. A more comprehensive dataset would enable more definitive PCFA. Furthermore, other statistical methods such as Positive Matrix Factorisation (PMF) should also be applied to trace metal data.

4. **Evaluate the most prominent water soluble inorganic ionic species at the same regional background site that was considered in the general trace metal study**

PM_1, $PM_{1\text{-}2.5}$ and $PM_{2.5\text{-}10}$ samples were also collected for thirteen months at Welgegund and analysed in order to determine the concentrations of the major inorganic ionic species. Results indicated that SO_4^{2-} concentrations in the PM_1 size fraction were significantly higher compared to the other species in all three size fractions. SO_4^{2-} and NH_4^+ dominated the PM_1 size fraction, while SO_4^{2-} and NO_3^- was the predominant species in the $PM_{1\text{-}2.5}$ and $PM_{2.5\text{-}10}$ size fractions. SO_4^{2-} had the highest contribution in the two smaller size fractions, while NO_3^- had the highest contribution in the $PM_{2.5\text{-}10}$ size fraction. SO_4^{2-} levels could be attributed to the impacts of aged air masses passing over source regions, while marine air masses were considered to be the major source of NO_3^-. The reaction of SO_4^{2-} with gas-phase NH_3 was considered to be the major source of NH_4^+ in the PM_1 size fraction. The PM at Welgegund was determined to be acidic, mainly due to excess concentrations of SO_4^{2-}. Comparison of Welgegund inorganic ion measurements to measurements thereof at Marikana indicated that the concentrations of almost all the inorganic ion species were higher at Marikana. At Welgegund PM_1 and $PM_{1\text{-}2.5}$ fractions revealed a seasonal pattern with higher inorganic ion concentrations measured from May–September. Higher concentrations could be attributed to decreased wet removal of these species, since these months coincide with the dry season in this part of South Africa. Increases in pollutant concentrations due to more pronounced inversion layers trapping pollutants near the surface, as well as increases household combustion and wild fires during these months were also considered as contributing to elevated levels of inorganic ions. Back trajectory analysis of each of the sampling months was also successfully performed, which revealed higher concentrations of inorganic ionic species corresponding to air mass movements over source regions.

Continuous long-term measurements of atmospheric trace metal species with instruments such as aerosol mass spectrometer (AMS) must be considered for future investigations of inorganic ionic species at Welgegund. This will enable improved source region characterisation of inorganic ionic species. Furthermore, continuous

measurements will also allow for a better understanding of the acidity potential of the atmosphere that must be studied in conjunction with precipitation chemistry.

5. **Conduct an assessment of trace metal and water-soluble inorganic ionic species concentrations, as well as levels of other parameters/species in the plume of a typical South African braai as a special case study**

A comprehensive analysis of atmospheric gaseous and aerosol species within a plume originating from a typical South African braai at Welgegund was successfully conducted. Five distinct phases were identified during the braai. The highest trace metal concentrations were associated with species typically present in ash. The Pb concentration was higher than the annual ambient air quality limit. SO_4^{2-}, Ca^{2+} and Mg^{2+} were the dominant water-soluble species present in the aerosols. The largest number of organic aerosol compounds was in the$PM_{1\text{-}2.5}$ fraction, which also had the highest semi-quantified concentration. It was indicated that PM_{10} concentrations were problematic during the meat grilling phase. From a climatic point of view, a relatively high single scattering albedo (ω_o) indicated a cooling aerosol direct effect, while periods with lower ω_o coincided with peak black carbon (BC) emissions. SO_2, NO_x and CO increased significantly, while O_3 did not increase notably. Aromatic and alkane volatile organic compounds were determined, with benzene exceeding the 2015 South African one-year ambient air quality limit. The results indicated that a recreational braai does not pose significant health risks. However, the longer exposure periods that are experienced by occupational vendors, will significantly increase health risks.

Our final conclusion and recommendation from this study in the published paper was: Braai, our beloved country!

References

ADGATE, J. L., MONGIN, S. J., PRATT, G. C., ZHANG, J., FIELD, M. P., RAMACHANDRAN, G. & SEXTON, K. 2007. Relationships between personal, indoor, and outdoor exposures to trace elements in PM2.5. *Science of the Total Environment*, 386(1-):21-32.

AIRMETRICS. 2011. MiniVol portable air sampler: operation manual version 4.2c. USA.

AL-MOMANI, I.F., DARADHEH, A.S. & HAJ-HUSSEIN, A.T. 2005. Trace elements in daily collected aerosols in Al-Hashimya, central Jordan. *Atmospheric research*, 73(1-2):87-100.

ANDERSSON, S.M., MARTINSSON, B.G., FRIBERG, J., BRENNINKMEIJER, C.A.M., RAUTHE-SCHOCH, A., VAN VELTHOVEN, P.F.J. & ZAHN, A. 2013. Composition and evolution of volcanic aerosol from eruptions of Kasatochi, Sarychev and Eyjafjallajokull in 2008–2010 based on CARIBIC observations. *Atmospheric Chemistry and Physics*, 13:1781-1796.

ANDREAE, M.O. 1983. Soot carbon and excess fine potassium: long-range transport of combustion-derived aerosols. *Science*, 220(4602):1148–1151.

ANDREAE, M.O. & METLET, P. 2001. Emission of trace gases and aerosols from biomass burning. *Global biogeochemical cycles*, 15(4):955-966.

APOSTOLOVSKI-TRUJIC, T., GARDIC, V. & IVANOVIC, S. 2007. Pollution prevention and control techniques in the copper industry. *Metalurgija - journal of metallurgy*, 13(1):35-40.

APTE, A.D., VERMA, S., TARE, V. & BOSE, P. 2005. Oxidation of Cr (III) in tannery sludge to Cr (VI): Field observations and theoretical assessment. *Journal of Hazardous Materials*, 121(1-3):215-222.

ASHLEY, K., HOWE, A.M., DEMANGE, M. & NYGREN, O. 2003. Sampling and analysis considerations for the determination of hexavalent chromium in workplace air. *Journal of Environmental Monitoring*, 5:707-716.

BAKER, P.G.L., BRUNKE, E.-G., SLEMR, F. & CROUCH, A.M. 2002. Atmospheric mercury measurements at Cape Point, South Africa. *Atmospheric Environment*, 36(14):2459–2465.

BANERJEE, G.K., SRIVASTAVA, K.K. & CHAKRABORTY, M.K. 2001. SPM is the Major Pollution in Open Cast Mining - A Case Study. *Journal of Scientific & Industrial Research*, 60:416-420.

BARBANTE, C. & CESCON, P. 2000. Uses and environmental impact of automobile catalytic converters. (*In* BOUTRON, C., ed. From Weather Forecasting to Exploring the Solar System. Les Ulis, France: EDP Sciences. p. 125–145.)

BARBANTE, C., GABRIELI, J., GABRIELI, P., VALLELONGA, P., COZZI, G., TURETTA, C., HONG, S., ROSMAN, K., BOURTON, C.F. & CESCON, P. 2011. A Historical Record of Heavy Metal Pollution in Alpine Snow and Ice. (*In* QUANTE, M., EBINGHAUS, R. & FLOSER, G., *eds*. Persistent Pollution – Past, Present and Future. Geesthacht, Germany: Springer. p. 71-94.)

BARKAY, T., KROER, N. & POULAIN, A.J. 2011. Some like it cold: microbial transformations of mercury in polar regions. *Polar Research*, 30:15469.

BERNER, T.O., MURPHY, M.M. & SLESINSKI, R. 2004. Determining the safety of chromium tripicolinate for addition to foods as a nutrient supplement. *Food, Chemistry and Toxicology*, 42(6):1029-1042.

BEUKES, J.P., DAWSON, N.F. & VAN ZYL, P.G. 2010. Theoretical and practical aspects of Cr(VI) in the South African FeCr industry. *The journal of the South African Institute of Mining and Metallurgy*, 110:743-750.

BEUKES, J.P., VAKKARI, V., VAN ZYL, P.G., VENTER, A.D., JOSIPOVIC, M., JAARS, K., TIITTA, P., KULMALA, M., WORSNOP, D., PIENAAR, J.J., JÄRVINEN, E., CHELLAPERMAL, R., IGNATIUS, K., MAALICK, Z., CESNULYTE, V., RIPAMONTI, G., LABAN, T.L., SKRABALOVA, L., DU TOIT, M., VIRKKULA, A. & LAAKSO, L. 2013. Source region plume characterisation of the interior of South Africa, as measured at Welgegund. *Clean air journal*, 23(1):1-10.

BEUKES, J.P., VAN ZYL, P.G. & RAS, M. 2012. Treatment of Cr(VI)-containing wastes in the South African ferrochrome industry - a review of currently applied methods. *The Journal of the South African Institute of Mining and Metallurgy*, 112:413-418.

BOOYENS, W., VAN ZYL, P.G., BEUKES, J.P., RUIZ-JIMENEZ, J., KOOPERI, M., RIEKKOLA, M.-L., JOSIPOVIC, M., VENTER, A.D., JAARS, K., LAAKSO, L., VAKKARI, V., KULMALA, M. & PIENAAR, J.J. 2015. Size-resolved characterisation of organic compounds in atmospheric aerosols collected at Welgegund, South Africa. *Journal of Atmospheric Chemistry*, 72:43-64.

BOUROTTE, C., CURI-AMARANTE, A. P., FORTI, M. C., PEREIRA, L. A., BRAGA, A. L. & LOTUFO, P. A. 2007. Association between ionic composition of fine and coarse aerosol soluble

fraction and peak expiratory flow of asthmatic patients in Sao Paulo city (Brazil). *Atmospheric Environment*, 41(10):2036-2048.

BOUTRON, C., BARBANTE, C., HONG, S., ROSMAN, K., BOLSHOV, M., ADAMS, F., GABRIELLI, P., PLANE, J., HUR, S., FERRARI, C. & CESCON, P. 2011. Heavy Metals in Antarctic and Greenland Snow and Ice Cores: Man Induced Changes During the Last Millennia and Natural Variations During the Last Climatic Cycles. (*In* QUANTE, M., EBINGHAUS, R. & FLOSHER, G., *eds*. Persistent Pollution – Past, Present and Future. Geesthacht, Germany: Springer. p. 19-46.)

BRUNKE, E.-G., EBINGHAUS, R., KOCK, H.H., LABUSCHAGNE, C. & SLEMR, F. 2012. Emissions of mercury in southern Africa derived from long-term observations at Cape Point, South Africa. *Atmospheric Chemistry and Physics*, 12:7465–7474.

BRUNKE, E.-G., LABUSCHAGNE, C., EBINGHAUS, R., KOCK, H. H. & SLEMR, F. 2010. Gaseous elemental mercury depletion events observed at Cape Point during 2007–2008. *Atmospheric Chemistry and Physics*, 10:1121–1131.

BRUNKE, E.-G., LABUSCHAGNE, C., PARKER, B., SCHEEL, H. E. & WHITTLESTONE, S. 2004. Baseline airmass selection at Cape Point, South Africa: application of 222Rn and other filter criteria to CO2. *Atmospheric Environment*, 38(33):5693–5702.

CDC, Centers for Disease Control. 2015. Agency for Toxic Substances and Disease Registry. http://www.atsdr.cdc.gov/toxprofiles/index.asp Date of access: 14 July 2015.

CHOW, J.C. 1995. Measurement Methods to Determine Compliance with Ambient Air Quality Standards for Suspended Particles. *Journal of the Air & Waste Management Association*, 45(5):320-382.

CONNELL, D.W. 2005. Basic concepts of environmental chemistry. 2nd ed London: CRC Press. 480 p.

COWEY, A. 1994. Mining and metallurgy in South-Africa - a pictorial history. Randburg: Mintek 120 p.

CUI, H., FU, M., YU, S. & WANG, M.K. 2011. Reduction and removal of Cr(VI) from aqueous solutions using modified byproducts of beer production. *Journal of Hazardous Materials*, 186(2-3):1625-1631.

DENMEAD, O.T., LEUNING, R., GRIFFITH, D.W.T. & MEYER, C.P. 1999. Some Recent Developments in Trace Gas Flux Measurement Techniques. (*In* BOUWMAN, A.F., *ed*. Approaches to Scaling of Trace Gas Fluxes in Ecosystems. 24 ed. Elsevier Science. p. 69-84).

DIONEX. 2003. Determination of Hexavalent Chromium in Drinking Water Using Ion Chromatography. Sunnyvale, CA.

DIONEX. 2011. Sensitive Determination of Hexavalent Chromium in Drinking Water. Sunnyvale, CA.

DOCKERY, D.W. & POPE, C.A. 1994. Acute respiratory effects of particulate air pollution. *Annual Revision of Public Health*, 15:107-132.

DOCKERY, D. & POPE, A. 1996. Particles in our air: Concentrations and health effects. Cambridge: Harvard University Press. 259 p.

DOS SANTOS, M., GOMEZ, D., DAWIDOWSKI, L., GAUTIER, E. & SMICHOWSKI, P. 2009. Determination of water-soluble and insoluble compounds in size classified airborne particulate matter. *Microchemical Journal*, 91(1):133-139.

DREHER, K.L., JASKOT, R.H., LEHMANN, J.R., RICHARDS, J.H., MCGEE, J.K., GHIO, A.J. & COSTA, D.L. 1997. Soluble transition metals mediate residual oil fly ash induce acute lung injury. *Journal of Toxicology and Environmental Health*, 50(3):285–305.

DU PREEZ, S.P., BEUKES, J.P. & VAN ZYL, P.G. 2014. Cr(VI) Generation During Flaring of CO-Rich Off-Gas from Closed Ferrochromium Submerged Arc Furnaces. *Metallurgical and Materials Transactions*, 46(2):1002-1010.

EBINGHAUS, R., JENNINGS, S. G., SCHROEDER, W. H., BERG, T., DONAGHY, T., GUENTZEL, J., KENNY, C., KOCK, H. H., KVIETKUS, K., LANDING, W., MUHLECK, T., MUNTHE, J., PRESTBO, E. M., SCHNEEBERGER, D., SLEMR, F., SOMMAR, J., URBA, A., WALLSCHLAGER, D. & XIAO, Z. 1999. International field intercomparison measurements of atmospheric mercury species at Mace Head, Ireland. *Atmospheric Environment*, 33(18):3063–3073.

EBINGHAUS, R., KOCK, H.H., TEMME, C., EINAX, J. W., LOWE, A. G., RICHTER, A., BURROWS, J. P. & SCHROEDER, W. H. 2002. Antarctic springtime depletion of atmospheric mercury. *Environmental Science and Technology*, 36(6):5267-5276.

EEA. 2015. Air Qiality: Environment. http://ec.europa.eu/environment/air/quality/Date of access: 26 Aug 2015.

FENGER, J. 2009. Urban air pollution. (*In* HEWITT, C.N. & JACKSON, A.V., *eds*. Atmospheric Science for Environmental Scientists. Chichester, West Sussex: Wiley-Blackwell. p. 243-267.)

FISSEHA, R., DOMMEN, J., GUTZWILLER, L., WEINGARTNER, E., GYSEL, M., EMMENEGGER, C., KALBERER, M. & BALTENSPERGER, U. 2006. Seasonal and diurnal characteristics of water soluble inorganic compounds in the gas and aerosol phase in the Zurich area. *Atmospheric Chemistry and Physics*, 6:1895-1904.

FOMBA, K.,W., MULLER, K., VAN PINXTEREN, D. & HERRMANN, H. 2012. Aerosol size-resolved trace metal composition in remote northern tropical Atlantic marine environment: case study Cape Verde Islands. *Atmospheric Chemistry and Physics Discussions*, 12:29535-29569.

FORMENTI, P., CAQUINEAU, S., DESBOEUFS, K, KLAVER, A., CHEVAILLIER, S., JOURNET, E. & RAJOT, J.L. 2014. Mapping the physico-chemical properties of mineral dust in western Africa: mineralogical composition. *Atmospheric Chemistry and Physics*, 14:10663-10686.

FREIMAN, M. T. & PIKETH, S. J. 2002. Air transport into and out of the Industrial Highveld Region of South Africa. *Journal of Applied Meteorology*, 42:994–1002.

FU, X., FENG, X., QIU, G., SHANG, L. & ZHANG, H. 2011. Speciated atmospheric mercury and its potential source in Guiyang, China. *Atmospheric Environment*, 45(25):4205-4212.

GAD, C.S. 1989. Acute and chronic systematic chromium toxicity. *Science of the Total Environment*, 86(1-2):149–157.

GALLOWAY, J. N., THORNTON, J. D., NORTON, S. A., VOLCHOK, H. L. & MCLEAN, R. A. N. 1982. Trace-Metals in Atmospheric Deposition – a Review and Assessment. *Atmospheric Environment*, 16(7):1677–1700.

GARSTANG, M., TYSON, M., SWAP, R., EDWARDS, M., KALLBERG, P. & LINDESAY, J. A. 1996. Horizontal and vertical transport of air over southern Africa. *Journal of Geophysical Research*, 101(D19):23721–23736.

GHUDEA, S.D., VAN DER A, R.J., BEIGA, G., FADNAVISA, S. & POLADEA, S.D. 2009. Satellite derived trends in NO2 over the major global hotspot regions during the past decade and their inter-comparison. *Environmental Pollution*, 157(6):1873–1878.

GLASTONBURY, R.I., VAN DER MERWE, W., BEUKES, P.B., VAN ZYL, P.G., LACHMANN, G., STEENKAMP, C.J.H., DAWSON, N.F. & STEWART, H.M. 2010. Cr(VI) generation during sample preparation of solid samples - A chromite ore case study. *Water SA*, 36(1):105-110.

GRIFFIN, R.J., COCKER III, D.R., FLAGAN, R.C. & SEINFELD, J.H. 1999. Organic aerosol formation from the oxidation of biogenic hydrocarbons. *Journal of Geophysical Research*, 104(D3):3555-3567.

GRYTHE, H., STROM, J., Krejci, R., QUINN, P. & STOHL, A. 2014. A review of sea-spray aerosol source functions using a large global set of sea salt aerosol concentration measurements. *Atmospheric Chemistry and Physics*, 14:1277-1297.

HARRIS, P. 1999. On charcoal. *Interdisciplinary Science Reviews*, 24(4):301-306.

HARRISON, R. M., JONES, A. M. & LAWRENCE, R. G. 2004. Major component composition of PM10 and PM2.5 from roadside and urban background sites. *Atmospheric Environment*, 38:4531-4538.

HARTFORD, W.H. 1979. Chromium compounds. (*In* KIRK-OTHMER, *ed*. Encyclopedia of Chemical Technology, 3rd ed. New York: John Wiley & Sons. p. 82-120.)

HELLEN, H., KURONEN, P. & HAKOLA, H. 2012. Heated stainless steel tube for ozone removal in the ambient air measurements of mono- and sesquiterpenes. *Atmospheric Environment*, 57:35-40.

HENNIGAN, C. J., IZUMI, J., SULLIVAN, A.P., WEBER, R.J. & NENES, A. 2015. A critical evaluation of proxy methods used to estimate the acidity of atmospheric particles. *Atmospheric Chemistry and Physics*, 15:2775–2790.

HERING, S. & CASS, G. 1999. The Magnitude of Bias in the Measurement of PM2.5 Arising from Volatilization of Particulate Nitrate from Teflon Filters. *Journal of the Air & Waste Management Association*, 49(6):725-733.

HOBBS, P. V., SINHA, P., YOKELSON, R. J., CHRISTIAN, T. J., BLAKE, D. R., GAO, S., KIRCHSTETTER, T. W., NOVAKOV, T. & PILEWSKIE, P. 2003. Evolution of gases and particles from a savanna fire in South Africa. *Journal of geophysical research*, 108(D13):8485.

IARC. 1990. EVALUATION OF CARCINOGENIC RISKS TO HUMAS: Chromium, Nickel and Welding. Lyon, France: INTERNATIONAL AGENCY FOR RESEARCH ON CANCER.

IPCC. 2014. Climate Change 2014: Mitigation of Climate Change. Contribution of Working Group III to the Fifth Assessment Report of the Intergovernmental Panel on Climate Change.

JAARS, K., BEUKES, J.P., VAN ZYL, P.G., VENTER, A.D., JOSIPOVIC, M., PIENAAR, J.J., VAKKARI, V., AALTONEN, H., LAAKSO, H., KULMALA, M., TIITTA, P., GUENTHER, A.,

HELLÉN, H., LAAKSO, L. & HAKOLA, H. 2014. Ambient aromatic hydrocarbon measurements at Welgegund, South Africa. *Atmospheric Chemistry and Physics*, 14:7075–7089.

JACOBSON, M.Z. 2002. Atmospheric Pollution: History, science and regulation. Cambridge: Cambridge University Press. 412 p.

JACOBSON, M.C., HANSON, H.C., NOONE, K.J. & CHARLSON, R.J. 2000. Organic atmospheric aerosols: Review and state of the science. *Reviews of Geophysics*, 38(2):267-294.

KABIR, E., KIM, K., AHNA, J., HONGA, O. & SOHNB, J.R. 2009. Barbecue charcoal combustion as a potential source of aromatic volatile organic compounds and carbonyls. *Journal of Hazardous Materials*, 174(1-3):492–499.

KAISER, H. F. 1958. The varimax criterion for analytic rotation in factor analysis. *Psychometrika*, 23(3):187-200.

KANG, C., GUPTA, T., RUIZ, P.A., WOLFSON, J.M., FERGUSON, S.T., LAWRENCE, J.E., ROHR, A.C., GODLESKI, J. & KOUTRAKIS, P. 2010. Aged particles derived from emissions of coal-fired power plants: The TERESA field results. *Inhalation Toxicology*, 23:11-30.

KARTHIKEYAN, S. & BALASUBRAMANIAN, R. 2006. Determination of water-soluble inorganic and organic species in atmospheric fine particulate matter. *Microchemical Journal*, 82(1):49-55.

KASA, S. 2008. Industrial revolutions and environmental problems. *Confluence: Interdisciplinary Communications.* 2007/2008:70-75.

KASSEM, T.S. 2010. Kinetics and thermodynamic treatments of the reduction of hexavalent to trivalent chromium in presence of organic sulphide compounds. *Desalination*, 258(1-3):206-218.

KEATING, M.H., MAHAFFEY, K.R., SCHOENY, R., RICE, G.E., BULLOCK, O.R., AMBROSE, R.B., SWARTOUT, J. & NICHOLS, J.W. 1997. Mercury Study Report to Congress. Office of Air Quality Planning and Standards and Office of Research and Development.

KGABI, N.A. 2006. Monitoring the levels of toxic metals of atmospheric particulate matter in the Rustenburg district. Potchefstroom: NWU. (Dissertation – Ph.D.) 190 p.

KIM, J.G., DIXON, J.B., CHUSUEI, C.C. & DENG, Y. 2002. Oxidation of chromium(III) to (VI) by manganese dioxide. *Soil Science Society American Journal*, 66:306-315.

KLEPPER, M.R. & WYANT, D.G. 1957. Notes on the Geology of Uranium. Washington. 148 p.

KLEYNHANS, E.H. 2008. Spatial and temporal distribution of trace elements in aerosols in the Vaal triangle. Potchefstroom: NWU. (Dissertation – M.Sc.) 156 p.

KLEYNHANS, ELJ, BEUKES, JP, VAN ZYL, PG, KESTENS, PHI & LANGA, JM. 2012. Unique challenges of clay binders in a pelletised chromite pre-reduction process. *Minerals Engineering*, 34:55–62.

KLINE, J., HUEBERT, B., HOWELL, S., BLOMQUIST, B., ZHUANG, J., BERTRAM, T. & CARRILLO, J. 2004. Aerosol composition and size versus altitude measured from the C-130 during ACE-Asia. *Journal of Geophysical Research*, 109(D19):1-22.

KOULOURI, E., SAARIKOSKI, S., THEODOSI, C., MARKAKI, Z., GERASOPOULOS, E., KOUVARAKIS, G., MAKELA, T., HILLAMO, R. & MIHALOPOULOS, N. 2008. Chemical composition and sources of fine and coarse aerosol particles in the Eastern Mediterranean. *Atmospheric Environment*, 42(26):6542–6550.

KRUMMEL, E.M., GREGORY-EAVES, I., MACDONALD, R.W., KIMPE, L.E., DEMERS, M.J., SMOL, J.P., FINNEY, B. & BLAIS, J.M. 2005. Concentrations and fluxes of salmon-derived polychlorinated biphenyls (PCBs) in lake sediments. *Environmental Science & Technology*, 39(18):7020–7026.

KULKARNI, P., CHELLAM, S., FLANAGAN, J.B. & JAYANTY, R.K.M. 2007. Microwave digestion—ICP-MS for elemental analysis in ambient airborne fine particulate matter: Rare earth elements and validation. *Analytica Chimica Acta*, 599(2):170-176.

KULMALA, M., PIRJOLA, L. & MÄKELÄ, J.M. 2000. Stable sulphate clusters as a source of new atmospheric particles. *Nature*, 404:66-69.

KULMALA, M., VEHKAMAKI, H., PETAJA, T., DAL MASO, M., LAURI, A., KERMINEN, V.-M., BIRMILI, W. & MCMURRY, P. H. 2004. Formation and growth rates of ultrafine atmospheric particles: a review of observations. *Aerosol Science*, 35(2):143-176.

LADEN, F. SCHWARTZ, J., SPEIZER, F.E., & DOCKERY, D.W. 2006. Reduction in Fine Particulate Air Pollution and Mortality. *American Journal of Respiratory and Critical Care Medicine*, 173(6):667-672.

LAUDAL, D.L., PAVLISH, J.H., GRAVES, J. & STOCKDILL, D. 2000. Mercury mass balances: A case study of two North Dakota Power Plants. *Journal of the Air & Waste management Association*, 50(10):1798-1804.

LAU, X., TALBOT, R., CASTRO, M., PERRY, K. & LUKE, W. 2012. Seasonal and diurnal variations of atmospheric mercury across the US determined from AMNet monitoring data. *Atmospheric Chemistry and Physics*, 12:10569-10582.

LAWLER, M. J., FINLEY, B. D., KEENE, W. C., PSZENNY, A. A. P., READ, K. A., VON GLASOW, R. & SALTZMAN, E. S. 2009. Pollution-enhanced reactive chlorine chemistry in the eastern tropical Atlantic boundary layer. *Geophysical Research Letters*, 36(8):1-5.

LAWSON, D.R. & WINCHESTER, J.W. 1979. Sulfur, potassium, and phosphorus associations in aerosols from south American tropical rain forests. *Journal of Geophysical Research*, 84(C7):3723-3727.

LEANER, J. J., DABROWSKI, J. M., MASON, R. P., RESANE, T., RICHARDSON, M., GINSTER, M., GERICKE, G., PETERSEN, C. R., E., MASEKOAMENG, ASHTON, P. J. & MURRAY, K. 2009. Mercury emissions from point sources in South Africa. (*In* MASON, R. & PIRRONE, N., *eds*. Mercury Fate and Transport in the Global Atmosphere. Dordrecht: Springer. p. 113–130.)

LEE, R.G.M., COLEMAN, P., JONES, J.L., JONES, K.C. & LOHMANN, R. 2005. Emission Factors and Importance of PCDD/Fs, PCBs, PCNs, PAHs and PM10 from the Domestic Burning of Coal and Wood in the U.K. *Environmental Science and Technology*, 39(6):1436-1447.

LENSCHOW, D.H. 2003. Boundary Layer Processes Flux Measurements. (*In* POTTER, T.D. & COLMAN, B.R., *eds*. Handbook of Weather, Climate, and Water: Atmospheric Chemistry, Hydrology, and Societal Impacts. Hoboken, New Jersey: John Wiley & Sons Inc. p. 179-183.)

LEONARD, A. & LAUWERYS, R.R. 1980. Carcinogenicity and mutagenicity of chromium. *Mutation Research: Reviews in Genetic Toxicology*, 76(3):227–239.

LINDBERG, S., BULLOCK, R., EBINGHAUS, R., ENGSTROM, D., FENG, X., FITZGERALD, W., PIRRONE, N., PRESTBO, E. & SEIGNEUR, C. 2007. A synthesis of progress and uncertainties in attributing the sources of mercury in deposition. *Ambio: A Journal of the Human Envornment*, 36(1):19-33.

LIN, C.-J., PONGPRUEKSA, P., LINDBERG, S. E., PEHKONEN, S. O., BYUN, D. & JANG, C. 2006. Scientific uncertainties in atmospheric mercury models I: Model science evaluation. *Atmospheric Environment*, 40(16):2911– 2928.

LORENZO-SEVA, U. 2013. How to report the percentage of explained common variance in exploratory factor analysis. Tarragona.

LOURENS, A.S.M., BEUKES, J.P., VAN ZYL, P.G., FOURIE, G.D., BURGER, J.W., PIENAAR, J.J., READ, C.E. & JORDAAN, J.H. 2011. Spatial and Temporal assessment of Gaseous Pollutants in the Mpumalanga Highveld of South Africa. *South African Journal of Science*, 107(1/2):1-8.

LOURENS, A.S.M., BUTLER, T.M., BEUKES, J.P., VAN ZYL, P.G., BEIRLE, S. & WAGNER, T. 2012. Re-evaluating the NO2 hotspot over the South African Highveld. *South African Journal of Science*, 108(11/12):1-6.

MA, G. & GARBERS-CRAIG, A.M. 2006. A review on the characteristics, formation mechanisms and treatment processes of Cr(VI)-containing pyrometallurgical wastes. *The journal of the South African Institute of Mining and Metallurgy*, 106:753-763.

MARCONI, M., SFERLAZZO, D.M., BECAGLI, S., BOMMARITO, C., CALZOLAI, G., CHIARI, M, DI SARRA, A., GHEDINI, C., GÓMEZ-AMO, J.L., LUCARELLI, F., MELONI, D., MONTELEONE, F., NAVA, S., PACE, G., PIACENTINO, S., RUGI, F., SEVERI, M. & TRAVERSI, R Udisti, R. 2014. Saharan dust aerosol over the central Mediterranean Sea: PM10 chemical composition and concentration versus optical columnar measurements. *Atmospheric Chemistry and Physics*, 14:2039-2054.

MASEKOAMENG, K. E., LEANER, J. & DABROWSKI, J. 2010. Trends in anthropogenic mercury emissions estimated for South Africa during 2000-2006. *Atmospheric Environment*, 44(25):3007-3014.

MASHANYARE H.P. & GUEST, R.N. 1997. The recovery of ferrochrome from slag at Zimasco. *WMinerals Engineering*, 11:1253-1258.

MERGLER, D., ANDERSON, H. A., CHAN, L. H. M., MAHAFFEY, K. R., MURRAY, M., SAKAMOTO, M. & STERN, A. H. 2007. Methyl mercury exposure and health effects in humans: A worldwide concern. *Ambio: A Journal of the Human Environment*, 36(1)3-11.

MILLS, A.J. & FEY, M.V. 2003. Declining soil quality in South Africa: effects of land use on soil organic matter and surface crusting. *South African Journal of Science*, 99:429-436.

MKOMA, S.L., DA ROCHA, G.O. & DE ANDRADE, J.B. 2014. Determination of carboxylic acids and water-soluble inorganic ions by ion chromatography in atmospheric aerosols from Tanzania. *South African Journal of Chemistry*, 67:118-123.

MONNET, F. 2003. An Introduction to Anaerobic Digestion of Organic Wastes.

MOREL, F. M. M., MILLIGAN, A. J. & SAITO, M. A. 2003. Marine Bioinorganic Chemistry: The Role of Trace Metals in the Oceanic Cycles of Major Nutrients. (*In* HEINRICH, D. H. & KARL, K. T., *eds*. Treatise on Geochemistry. Pergamon: Oxford. p. 113-143.)

MOULI, P.C., MOHAN, S.V., V., Balaram, KUMAR, M.P. & S.J., Reddy. 2006. A study on trace elemental composition of atmospheric aerosols at a semi-arid urban site using ICP-MS technique. *Atmospheric Environment*, 40(1):136-146.

MUKHERJEE, A.B. 1998. Chromium in the environment of Finland. *Science of the Total Environment*, 217(1-2):9-19.

MUROZUMI, M., CHOW, T.J. & PATTERSON, C.C. 1969. Chemical concentration of pollutant lead aerosols, terrestrial dusts and sea salts in Greenland and Antarctic snow strata. *Geochimica et Cosmochimica Acta*, 33:1271–1294.

MURTHY, Y.R., TRIPATHY, S.K. & KUMAR, C.R. 2011. Chrome ore beneficiation challenges & opportunities - A review. *Minerals Engineering*, 24(5):375-380.

NEL, A. 2005. Air pollution-related illness: effects of particles. *Science*, 308(5723):804-806.

NEL, M.V., STRYDOM, C.A., SCHOBERT, H.H., BEUKES, J.P. & BUNT, J.R. 2011. Comparison of sintering and compressive strength tendencies of a model coal mineral mixture heat treated in inert and oxidising atmospheres. *Fuel Processing Technology*, 92(5):1042-1051.

NEMA: AQB. 2003. National Environmental Management: Air Quality Bill. Pretoria.

NIAGRU, J.O. 1998. Historical Perspectives. (*In* NIAGRU, J.O. & NIEBOER, E., *eds*. Chromium in the nature and human environments. NewYork: Wiley. p. 1-9.)

NRIAGU, J.O. 1989. A global assessment of natural sources of atmospheric trace metals. *Nature*, 338:47–49.

NRIAGU, J.O. 1990. The rise and fall of leaded gasoline. *Science of the Total Environment*, 92:13–28.

PACYNA, J.M. 1998. Source inventories for atmospheric trace metals. (*In* HARRISON, R.M. & VAN GRIEKEN, R.E., *eds*. Atmospheric Particles, IUPAC Series on Analytical and Physical Chemistry of Environmental Systems. Chichester, UK: JohnWiley. p. 385-42.)

PACYNA, J.M. & PACYNA, E.G. 2001. An assessment of global and regional emissions of trace metals to the atmosphere from anthropogenic sources worldwide. *Environmental Reviews*, 9(4):269-298.

PANICHEV, N., MABASA, W., NGOBENI, P., MANDIWANA, K. & PANICHEVA, S. 2008. The oxidation of Cr(III) to Cr(VI) in the environment by atmospheric oxygen during the bush fires. *Journal of Hazardous Materials*, 153(3):937-941.

PIERCE, J.R., WEISENSTEIN, D.K., HECKENDORN, P., PETER, T. & KEITH, D.W. 2010. Efficient formation of stratospheric aerosol for climate engineering by emission of condensible vapor from aircraft. *Geophysical Research Letters*, 37(18):1-5.

PLANCHON, F.A.M., BOUTRON, C.F., BARBANTE, C., COZZI, G., GASPARI, V., WOLFF, E.W., FERRARI, C.P. & CESCON, P. 2002. Changes in heavy metals in Antarctic snow from Coats Land since the mid-19th to the late-20th century. *Earth and Planetary Science Letters*, 200(1-2):207–222.

POLIDORI, A., CHEUNG, K.L., ARHAMI, M., DELFINO, R.J., SCHAUER, J.J. & SIOUTAS, C. 2009. Relationships between size-fractionated indoor and outdoor trace elements at four retirement communities in Southern California. *Atmospheric Chemistry and Physics*, 9:4521-4536.

POLISSAR, A.V., HOPKE, P.K., PAATERO, P., MALM, W.C. & SISLER, J.F. 1998. Atmospheric aerosol over Alaska 2: Elemental composition and sources. *Journal of Geophysical Research Discussions*, 103(D15):19045-19057.

POPE, C.A. & DOCKERY, D.W. 2006. Health effects of fine particulate air pollution: lines that connect. *Air & Waste Management Association*, 56(6):709–742.

POTGIETER, S.S., POTGIETER, J.H., PANICHEV, N. & PANICHEVA, S. 2003. Chromium determinations in cement. *Cement and Concrete Research*, 33(10):1589-1593.

PROCTOR, D.M., OTANI, J.M., FINLEY, B.L., PAUSTENBACH, D.J., BLAND, J.A., SPEIZER, N. & SARGENT, E.V. 2002. Is hexavalent chromium carcinogenic via ingestion? A weight-of-evidence review. *Journal of Toxicology and Environmental Health*, 65(10):701-746.

PUXBAUM, H., RENDL, J., ALLABASHI, R., OTTER, L. & SCHOLES, M.C. 2000. Mass balance of the atmospheric aerosol in a South African subtropical Savannah (Nylsvley, May 1997). *Journal of Geophysical Research*, 105(D16):20697-20706.

RAHMAN, M. & KIM, K. 2012. Release of offensive odorants from the combustion of barbecue charcoals. *Journal of Hazardous Materials*, 215– 216: 233– 242.

RAI, D., EARY, E.A. & ZACHARA, J.M. 1989. Environmental chemistry of chromium. *Science of the Total Environment*, 86(1-2):15–23.

REID, J. S. & HOBBS, P. V. 1998. Physical and optical properties of young smoke from individual biomass fires in Brazil. *Journal of Geophysical Research*, 103(32):32013–32030.

RICE, G.E., AMBROSE, R.B., BENJEY, W.G., CLARK, T., CLEVERLY, D.H., DURKEE, S., BULLOCK, O.R., SWARTOUT, J., KEATING, M.H., KILGROE, J.D., MAHAFFEY, K.R., NICHOLS, J.W. & SCHOENY, R. 1997. Fate and Transport of Mercury in the Environment. Office of Air Quality Planning & Standards and Office of Research and Development.

RIEKKOLA-VANHANEN, M. 1999. Finnish expert report on best available techniques in ferrochromium production. The Finnish Environment Institute, p.52.

ROGGE, W.F., HILDEMANN, L.M., MAZUREK, M.A., CASS, G.R. & SIMONEIT, B.R.T. 1991. Sources of Fine Organic Aerosol. 1. Charbroilers and Meat Cooking Operations. *Environmental Science & Technology*, 25(6):1112-1125.

SAMARA, C. & TSITOURIDOU, R. 2000. Fine and coarse ionic aerosol components in relation to wet and dry deposition. *Water, Air and Soil Pollution*, 120:71–88.

SCHAAP, M., SPINDLER, G., SCHULZ, M., ACKER, K., MAENHAUT, W., BERNER, A., WIEPRECHT, W., STREIT, N., MÜLLER, K., BRÜGGEMANN, E., CHI, X., PUTAUD, J. P., HITZENBERGER, R., PUXBAUM, H., BALTENSPERGER, U. & TEN BRINK, H. 2004. Artefacts in the sampling of nitrate studied in the "INTERCOMP" campaigns of EUROTRAC-AEROSOL. *Atmospheric Environment*, 38:6487-6496.

SCHEEPERS, P.T.J., HEUSSEN, G.A.H., PEER, P.G.M., VERBIST, K., ANZION, R. & WILLEMS, J. 208. Characterisation of exposure to total and hexavalent chromium of welders using biological monitoring. *Toxicology Letters*, 178(3):185-190.

SCHWARTZ, J., DOCKERY, D.W. & NEAS, L.M. 1996. Is daily mortality associated specifically with fine particles? *Journal of the Air & Waste Management Association*, 46(10):927-939.

SCHWARTZ, J., DOCKERY, D.W. & NEAS, L.M. 1996. Is Daily Mortality Associated Specifically with Fine Particles? *Journal of the Air & Waste Management Association*, 46(10):927-939.

SCHWELA, D., ZALI, O. & SCHWELA, P. 1997. Motor Vehicle Air Pollution: Public Health Impact and Control Measures. Geneva. 338 p.

SCOTT, G.M. & MDLULI, T.N. 2012. The Minamata Treaty / Protocol: Potential Implications for South Africa. *Clean Air Journal*, 22(2):17-19.

SEIGNEUR, C. & CONSTANTINOU, E. 1995. Chemical kinetic mechanism for atmospheric chromium. *Environmental Science and Technology*, 29(1):222-231.

SHANKER, A.K., CERVANTES, C., LOZA-TAVERA, H. & AVUDAINAYAGAM, S. 2005. Chromium toxicity in plants. *Environment International*, 31(5):739–753.

SIENFELD, J H & PANDIS, S N. 2006. Atmospheric chemistry and physics. New Jersey: John Wiley & Sons. 1225p.

SILVA, P.J., LIU, D.Y. & NOBLE, C.A.: Prather, K.A. 1999. Size and chemical characterization of individual particles resulting from biomass burning of local southern California species. *Environmental Science & Technology*, 33(18):3068-3076.

SLEMR, F., BRUNKE, E.-G., EBINGHAUS, R. & KUSS, J. 2011. Worldwide trend of atmospheric mercury since 1995. *Atmospheric Chemistry and Physics*, 11:4779–4787.

SLEMR, F., BRUNKE, E.-G., LABUSCHAGNE, C. & EBINGHAUS, R. 2008. Total gaseous mercury concentrations at the Cape Point GAW station and their seasonality. *Geophysical Research Letters*, 35(11):1-5.

SLEMR, F., BRUNKE, E.-G., WHITTLESTONE, S., ZAHOROWSKI, W., EBINGHAUS, R., KOCK, H. H. & LABUSCHAGNE, C. 2013. 222Rn-calibrated mercury fluxes from terrestrial surface of southern Africa. *Atmospheric Chemistry and Physics*, 13:6421-6428.

SOUTH AFRICA. 2009. National Environment Management: Air Quality Act, 2004 (ACT NO. 39 OF 2004). *Government gazette*, 32816: 24 Dec. Available: Department Environmental Affairs RSA. Date of access: 15 Oct. 2015.

SOUTH AFRICA. 2012. National Environmental Management: Air Quality Act, 2004 (ACT NO. 39 OF 2004) Declaration of the Waterberg National Priority Area. *Government gazette*, 35435: 15 Jun. Date of access: 15 Oct. 2015.

SOUTH AFRICA. 2012b. National Environmental Management: Air Quality Act, 2004 (ACT NO. 39 OF 2004) National ambient air quality standard for particulate matter with aerodynamic diameter less than 2.5 micro meters. Government Gazette: 35463, 29 June, pp.7-9.

SQUIZZATO, S., MASIOL, M.., BRUNELLI, A., PISTOLLATO, S., TARABOTTI, E., RAMPAZZO, G. & PAVONI, B. 2013. Factors determining the formation of secondary inorganic aerosol:a case study in the Po Valley (Italy). *Atmospheric Chemistry and Physics*, 13:1927–1939.

SUNDSTRÖM, A.-M., NIKANDROVA, A., ATLASKINA, K., NIEMINEN, T., VAKKARI, V., LAAKSO, L., BEUKES, J.P., AROLA, A., VAN ZYL, P.G., JOSIPOVIC, M., VENTER, A.D., JAARS, K., PIENAAR, J.J., PIKETH, S., WIEDENSOHLER, A., CHILOANE, E.K., DE LEEUW, G. & KULMALA, M. 2015. Characterization of satellite-based proxies for estimating nucleation mode particles over South Africa. *Atmospheric Chemistry and Physics*, 15:4983–4996.

SWAP, R.J., ANNEGARN, H.J., SUTTLES, J.T., KING, M.D., PLATNICK, S., PRIVETTE, J.L. & R.J., Scholes. 2003. Africa burning: A thematic analysis of the Southern African Regional Science Initiative (SAFARI 2000). *Journal of Geophysical Research*, 108(D13):8465.

TAKEMURA, T, NOZAWA, T, EMORI, S, NAKAJIMA, T Y & NAKAJIMA, T. 2005. Simulation of climate response to aerosol direct and indirect effects with aerosol transport-radiation model. *Journal of Geophysical Research*, 110(D2):1-16.

TEKRAN. 1998. Methyl Mercury in Water by Distillation, Aqueous Ethylation, Purge and Trap, and Cold Vapor Atomic Fluorescence Spectrometry. Washington. 51 p.

TELLOLI, C., MELAGUTI, A., MIRCEA, M., TASSINARI, R., VACCARO, C. & BERICO, M. 2014. Properties of agricultural aerosol released during wheat harvest threshing, plowing and sowing. *Journal of Environmental Sciences*, 26(9):1903-1912.

THURSTON, G. D., ITO, K., MAR, T., CHRISTENSEN, W. F., EATOUGH, D. J. & HENRY, R. C. 2005. Workgroup report: workshop on source apportionment of particulate matter health effects –intercomparison of results and implications. *Environmental Health Perspectives*, 113(12):1768-1774.

TIITTA, P., VAKKARI, V., JOSIPOVIC, M., CROTEAU, P., BEUKES, J.P., VAN ZYL, P.G., VENTER, A.D., JAARS, K., PIENAAR, J.J., NG, N.L., CANAGARATNA, M.R., JAYNE, J.T., KERMINEN, V.-M., KULMALA, M., LAAKSONEN, A., WORSNOP, D.R. & LAAKSO, L. 2014. Chemical composition, main sources and temporal variability of PM1 aerosols in southern African grassland. *Atmospheric Chemistry and Physics*, 14:1909-1927.

TRÜE, A. 2010. Environmental Mercury Monitoring in the South African Highveld Region. Pretoria: TUT. (Dissertation: M.Sc.) 99 p.

TURNER, J. & COLBECK, I. 2008. Environmental Chemistry of Aerosols. University of Essex: Blackwell Publishing. 268 p.

TYSON, P.D., GARSTANG, M. & SWAP, R. 1996. Large-Scale Recirculation of Air over Southern Africa. *Journal of Applied Meteorology*, 35(12):2218–2236.

USEPA. 2015. Summary of the Clean Air Act. http://www2.epa.gov/laws-regulations/summary-clean-air-act. Date of access: 26 Aug 2015.

VAKKARI, V., BEUKES, J.P., LAAKSO, H., MABASO, D., PIENAAR, J.J., KULMALA, M. & LAAKSO, L. 2013. Long-term observations of aerosol size distributions in semi-clean and polluted savannah in South Africa. *Atmospheric Chemistry and Physics*, 13:1751-1770.

VAKKARI, V., KERMINEN, V.-M., BEUKES, J.P., TIITTA, P., VAN ZYL, P.G., JOSIPOVIC, M., VENTER, A.D., JAARS, K., WORSNOP, D.R., KULMALA, M. & LAAKSO, L. 2014. Rapid changes in biomass burning aerosols by atmospheric oxidation. *Geophysical Research Letters*, 41:1-8.

VAKKARI, V., LAAKSO, H., KULMALA, M., LAAKSONEN, A., MABASO, D., MOLEFE, M., KGABI, N. & LAAKSO, L. 2011. New particle formation events in semi-clean South African savannah. *Atmospheric Chemistry and Physics*, 11:3333-3346.

VAN DER MERWE, W., BEUKES, J.P. & VAN ZYL, P.G. 2012. Cr(VI) formation during ozonation of Cr-containing materials in aqueous suspension - implications for water treatment. *Water SA*, 38(4):505-510.

VAN ZYL, P.G., BEUKES, J.P., DU TOIT, G., MABASO, D., HENDRIKS, J., VAKKARI, V., TIITTA, P., PIENAAR, J.J., KULMALA, M. & LAAKSO, L. 2014. Assessment of atmospheric trace metals in the western Bushveld Igneous Complex, South Africa. *South African Journal of Science*, 110(3/4):1-11.

VAN ZYL, P.G., J.P., Beukes, DU TOIT, G., MABASO, D., HENDRIKS, J., VAKKARI, V., TIITTA, P., PIENAAR, J.J., KULMALA, M. & LAAKSO, L. 2014. Assessment of atmospheric trace metals in the western Bushveld Igneous Complex, South Africa. *South African Journal of Scienc*e, 3/4(110):11.

VENTER, A.D., BEUKES, J.P., VAN ZYL, P.G., BRUNKE, E.-G., LABUSCHAGNE, C., SLEMR, F., EBINGHAUS, R. & KOCK, H. 2015. Statistical exploration of gaseous elemental mercury (GEM) measured at Cape Point from 2007 to 2011. *Atmospheric Chemistry and Physics*, 15:10271–10280.

VENTER, A.,D., JAARS, K., BOOYENS, W., BEUKES, J.,P., VAN ZYL, P.,G, JOSIPOVIC, M., HENDRIKS, J., VAKKARI, V., HELLÉN, H., HAKOLA, H., AALTONEN, H., RUIZ-JIMENEZ, J., RIEKKOLA, M-L. & LAAKSO, L. 2015. Plume characterisation of a typical South African braai. *South African Journal of Chemistry*, 68:181-194.

VENTER, A.D., VAKKARI, V., BEUKES, J.P., VAN ZYL, P.G., LAAKSO, H., MABASO, D., TIITTA, P., JOSIPOVIC, M., KULMALA, M., PIENAAR, J.J. & LAAKSO, L. 2012. An air quality assessment in the industrialized western Bushveld Igneous Complex, South Africa. *South African Journal of Science*, 108(9/10):1-10.

VENTER, A.D., VAN ZYL, P.G., BEUKES, J.P., JAARS, K., JOSIPOVIC, M., BOOYENS, W., HENDRIKS, J., VAKKARI, V. & LAAKSO, L. 2015. Measurement of atmospheric trace metals at a regional background site (Welgegund) in South Africa. In preparation for Atmospheric Chemistry and Physics Discussions

VOUTSA, D. & SAMARA, C. 2002. Labile and bioaccessible fractions of heavy metals in the airborne particulate matter from urban and industrial areas. *Atmospheric Environment*, 36(22):3583–3590.

WAGNER, N.J. 2001. Trace Elements in coal, their analysis and environmental impact. Sasolburg.

WAGNER, N.J. & LAPLANTE, A.R. 2005. The occurance of potentiallyu hazardous trace elements in five Highveld coals. *International Journal of Coal Geology*, 63(3-4):228-246.

WALL, S.M., JOHN, W. & ONDO, J.L. 1988. Measurement of aerosol size distributions for nitrate and major ionic species. *Atmospheric Environment*, 22(8):1649-1656.

WALNA, B., KURZYCA, I., BEDNORZ, E. & KOLENDOWICZ, L. 2013. Fluoride pollution of atmospheric precipitation and its relationship with air circulation and weather patterns (Wielkopolski National Park, Poland). *Environmental Monitoring and Assessment*, 185(7):5497–5514.

WHO. 2015. Air quality guidelines - global update 2005. http://www.who.int/phe/health_topics/outdoorair/outdoorair_aqg/en/ Date of access: 26 Aug 2015.

WILSON, D.L. & HAWTHORNE, A.R. 1987. Comparison of combustion pollutants from Charania briquettes, consumer barbecue briquettes, Pakistani mineral development corporation briquettes and Pakistani wood charcoal. Tennessee. US Department of Energy

WU, H.B. & CHAN, C.K. 2008. Effects of potassium nitrate on the solid phase transitions of ammonium nitrate particles. *Atmospheric Environment*, 42(2):313–322.

XIU, G., ZHANG, D., CHEN, J., HUANG, X., CHEN, Z., GUO, H. & PAN, J. 2004. Characterization of major water-soluble inorganic ions in size-fractionated particulate matters in Shanghai campus ambient air. *Atmospheric Environment*, 38(2):227-236.

YIN, J., ALLEN, A.G., HARRISON, R.M., JENNINGS, S.G., WRIGHT, E., FITZPATRICK, M., HEALY, T., BARRY, E., CEBURNIS, D. & MCCUSKER, D. 2005. Major component composition of urban PM10 and PM2.5 in Ireland. *Atmospheric Research,* 78(3-4):149-165.

YLI-JUUTI, T., NIEMINEN, T., HIRSIKKO, A., AALTO, P.P., ASMI, E., HORRAK, U., MANNINEN, H.E., PATOKOSKI, J., DAL MASO, M., PETAJA, T., RINNE, J., KULMALA, M. & RIIPINEN, I. 2011. Growth rates of nucleation mode particles in Hyytiälä during 2003–2009: variation with particle size, season, data analysis method and ambient conditions. *Atmospheric Chemistry and Physics*, 11:12865-12886.

YUE, D., HU, M., WU, Z., WANG, Z., GUO, S., WEHNER, B., NOWAK, A., ACHTERT, P., WIEDENSOHLER, A., JUNG, J., KIM, Y.J. & LIU, S. 2009. Characteristics of aerosol size distributions and new particle formation in the summer in Beijing. *Journal of Geophysical Research*, 114(D2):1-3.

ZHANG, Q.I., JIMENEZ, J.L., WORSNOP, D.R. & CANAGARATNA, M. 2007. A Case Study of Urban Particle Acidity and Its Influence on Secondary Organic Aerosol. *Environment science & technology*, 41(9):3213–3219.

ZHUANG, H., CHAN, C.K., FANG, M. & WEXLER, A.S. 1999. Size distribution of particulate sulfate, nitrate, and ammonium at a coastal site in Hong Kong. *Atmospheric Environment,* 33 (6):843-853.